SPATIO-TEMPORAL MECHANISMS OF MICROPLASTIC TRANSPORT IN RIVERS: FROM MOUNTAINS TO SEWAGE OUTFLOW

ANNA TUULIKKI KUKKOLA

A thesis submitted to the University of Birmingham for the degree of

DOCTOR OF PHILOSOPHY

School of Geography, Earth and Environmental Science

College of Life and Environmental Sciences

University of Birmingham

April 2023

UNIVERSITY OF
BIRMINGHAM

University of Birmingham Research Archive

e-theses repository

This unpublished thesis/dissertation is copyright of the author and/or third parties. The intellectual property rights of the author or third parties in respect of this work are as defined by The Copyright Designs and Patents Act 1988 or as modified by any successor legislation.

Any use made of information contained in this thesis/dissertation must be in accordance with that legislation and must be properly acknowledged. Further distribution or reproduction in any format is prohibited without the permission of the copyright holder.

Abstract

The spatio-temporal distributions of microplastic (MP) in three river systems affected differently by urbanization were investigated, with the aim of identifying key hydrological and source control effects on MP concentrations and MP loadings. The potential effects of MP on ecosystem health were assessed through a systematic literature review, which enabled recommendations for standardization of field and laboratory studies to be made, including using environmentally representative MP shapes and compositions and suggestion for harmonised toxicity endpoints across taxa. A new modified and faster MP identification method via fluorescent tagging with Nile Red was designed to facilitate fast and reliable MP identification and quantification in rivers and catchments that are affected by anthropogenic activities. This new method was applied to investigate how source and hydrological controls influence downstream transport of MP in remote mountainous catchments, downstream of sewage treatment works and to compare point and diffuse MP source activation across contrasting urban catchments. This research evidenced that human influences including water management can have substantial implications for MP load estimations and should be taken into consideration for quantification of catchment residence times of microplastics and river network contributions to the oceans. The results also highlight the need for MP sampling campaigns to give further consideration to how best to achieve more accurate MP sampling, recommendations for which include sampling of water diversions, and conducting pre-monitoring campaigns capturing flow regimens and possible MP fluctuations occurring during the day, especially at locations with varying flow regimen (such as downstream from sewage treatment works) to gain understanding of the minimum sample requirements to produce representative samples for that particular system. Furthermore, this thesis demonstrates that hydrological

catchment size may not be descriptive of the MP sources, as the effect of the catchment can be dominated by the presence of a single point source, such as a sewage treatment works, suggesting that water management can play a much more substantial role than typical hydrometeorological drivers within a catchment. For diffuse urban sources, the thesis demonstrates the importance of hydrometeorological events (e.g., rain events) as controls for MP source activation as well as their transport and connectivity to the river network, and the need for sampling across such events to increase understanding the impact of source activation on overall MP loadings.

Acknowledgements

I would like to extend my utmost gratitude for the Post Docs that I have had the pleasure to work with during my PhD journey. Particular thanks to Dr Holly Nel, Dr Uwe Schneidewind, Dr Andrew Chetwynd and Dr Jenn Drummond, who have taught me invaluable life and research skills, inside and outside of academia. Their support has enabled me to transition from an M.sc graduate into an early career scientist with more confidence and faith on what one can achieve in life.

I would also like to thank my partner, Maximilian Hughes, who has stood by me during the trials and tribulations of my journey and whose emotional support storage never wavered, despite the several historic events that this PhD degree and as a proxy, us, have lived through. I would also like to thank my parents for their financial and emotional support which enabled me to finalise the work and achieve the end goal.

Special thank you for my primary supervisors, Professor Stefan Krause and Professor Iseult Lynch, who has managed to keep me on track and guide me through an interesting journey, with a steep learning curve behind every corner. Without their expertise and practical guidance this PhD would never have been realised. I would also like to thank them for their patience, as supervising me has not always been an easy feat.

I would also like to thank everyone who has been involved in the sample collection and/or laboratory work, as without our laboratory technicians, everything stops working.

Table of Contents

Chapter 1: Introduction 1

1.1 Scientific rationale 1

1.2 Aims and Objectives 6

1.3 Layout of the thesis 6

1.4 References 11

Chapter 2: Methods 21

2.1 Density separation 21

2.2 Organic matter digestion 21

2.3 Fluorescence 22

2.4 Raman spectroscopy 23

2.6 Easy and accessible way to calibrate a fluorescence microscope and to create a microplastic identification key 27

Chapter 3: Nano and microplastic interactions with freshwater biota – Current knowledge, challenges and future solutions 48

3.1 Abstract 49

3.2 Introduction 50

3.3 Methods 54

3.4 Results 56

3.4.1 General results 56

3.4.2 Types of plastics 56

2.4.3 Sizes and morphology of plastics 57

3.4.4 Geographical spread 58

3.4.5 Trophic levels and biota groups 59

3.5 Discussion 60

3.5.1 General discussion 60

3.5.2 Challenges for future research 62

3.6 Conclusion 86

3.7 Acknowledgements 86

3.8 References 87

Chapter 4: Prevailing impacts of river management on microplastic transport in contrasting US streams requires rethinking of global microplastic flux estimations. 112

4.1 Abstract 113
4.2 Introduction 114
4.3 Materials and methods 117
4.3.1 Study region 117
4.3.2 Field data and sample collection 120
4.3.3 Sample analysis and QA/QC 121
4.3.4 Land cover, population density, and statistical analyses 122
4.3.5 MP loads and estimated concentrations in the absence of diversions 123
4.4 Results 124
4.4.1 Stream discharge 124
4.4.2 MP concentrations in surface water and streambed sediments 125
4.4.3 MP loads 127
4.4.4 Physical and chemical properties of MP 128
4.4.5 Land cover impacts on MP 129
4.5 Discussion 130
4.5.1 MP concentration in surface water and sediments 130
4.5.2 The effects of the mountain to plains transition and urbanization on MP concentrations and types 130
4.5.3 The effect of diversions on MP concentrations, loads, and downstream transport 133
4.5.4 Advantages of the load approach 137
4.6 Conclusion 139
4.7 Acknowledgments 139
4.8 References 140
Chapter 5: Are we timing it right? The impact of sampling frequency on microplastic load estimations downstream from a sewage treatment works. 148
5.1 Abstract 148
5.2 Introduction 149
5.3 Materials and methods 153
5.3.1 Study site 153
5.3.2 Field sampling 155
5.3.3 Laboratory analysis 158
5.3.4 QA/QC 160

5.3.5. Data analysis 161
5.4 Results 162
5.4.1 Variations in stream discharge 162
5.4.2 Variations in MP properties 164
5.4.3 Variations in MP concentrations 165
5.4.4 Variations in MP loading 168
5.4.5 MP relationships with stream hydrological parameters 171
5.5 Discussion 172
5.5.1 High variability in stream discharge linked to WWTP outflow 172
5.5.2 Stream characterisation requires temporally varied sampling 173
5.5.3 The range of MP loads is important for characterising downstream export dynamics 175
5.5.4 Implications and future research 177
5.6 References 179
Chapter 6: A tale of two catchments - what makes microplastic move? 189
6.1 Abstract 189
6.2 Introduction 190
6.3 Materials and methods 193
6.3.1 Study sites 193
6.3.2 Field sampling 195
6.3.3. Laboratory analysis 196
6.3.4 QA/QC 199
6.3.5 Data analysis 200
6.4 Results 201
6.4.1 MP concentration in water column and sediment 201
6.4.2 Physical properties of identified MP 203
6.4.3 Flow controls on MP concentrations 207
6.4.4 Impact of rain events 210
6.5 Discussion 210
6.5.1 MP concentrations exhibit urban signal at both sampled sites with distinct MP compositions 210
6.5.2 MP load controlled by source at EB and by source activation at BB 213
6.6. Conclusions 217

6.7 References 219
Chapter 7: Conclusions and discussion 230
APPENDIX 1 237
APPENDIX 2 248
APPENDIX 3 280
APPENDIX 4 297
APPENDIX 5 308

List of Figures

Figure 2.0 Graphical abstract 28

Figure 2.1. Schematic illustration of general effect for Pixel Brightness (PB) of each of the tested system settings.....32

Figure 2.2 Boxplot illustrating the different pixel brightness (BP) in arbitrary units (a.u).....34

Figure 2.3 Pixel brightness (PB) in arbitrary units (a.u) for tested samples under 32x magnification, light intensity of 12 and exposure time of 50 ms.....36

Figure 2.4 General part of the MP identification key that all MP had to adhere to.. 38

Figure 2.5 A schematic framework for the workflow described in this paper. 39

Figure 3.0 Graphical abstract 50

Figure 3.1. Conceptual model for MnP movements in the freshwater food web. Numbers (1-16) indicate that MnP interaction with this biotic group has been confirmed (Table S3.1).....52

Figure 3.2. Most common MnP plastic types reported across laboratory and field studies. 57

Figure 3.3. Relative abundance of studies per size class.....58

Figure 3.4. Number of laboratory studies per country, grouped via first and last authors of the studies and locations of the field sampling sites. 59

Figure 3.5. Number of published MnP interaction studies in freshwater biota groups.. 60

Figure 3.6. Potential principal and secondary toxicity endpoints for the four trophic levels.....76

Figure 4.0 Graphical abstract 114

Figure 4.1: Map of catchment areas indicating major land cover classes and sampling locations. 119

Figure 4.2: Discharge and precipitation during the sampling period in October 2019.. 120

Figure 4.3: Stream discharge (panels a-b), MP surface water concentrations [#MP L^{-1}] and estimated concentrations in the absence of diversions (panels c-d), and downstream profiles of MP loads [#MP s^{-1}] (panels e-f) for Boulder Creek and South Boulder Creek.. 125

Figure 4.4: MP concentration distribution in water. 127

Figure 4.5: MP Load (Yellow line), Diverted load (Dashed line) and Discharge (L s^{-1}) shown for a) Boulder Creek and b) South Boulder Creek.....134

Figure 5.0 Graphical abstract 148

Figure 5.1: Sampling location and the Barston sewage treatment works near Birmingham, UK.. 155

Figure 5.2: Variations in stream discharge (m^3 s^{-1}) 163

Figure 5.3. The percentage and number of identified polymers by composition for all of the positively identified plastic particles in this study, grouped by A) Fibres and B) Fragments. 165

Figure 5.4: MP concentration in surface water (MP L^{-1}). 167

Figure 5.5: MP loads as MP per hour (#MP h^{-1}). 170

Figure 5.6: Bar chart showing minimum and maximum ranges and mean MP load per hour.....171

Figure 6.1: Maps showing the sampling locations in the context of the United Kingdom 194

Figure 6.2: Schematic illustration of the sample preparation workflow. 197

Figure 6.3: Surface water concentrations [#MP L^{-1}] (panels a-b), Stream discharge [m^3 s^{-1}] (panels c-d), MP load per hour [#MP h^{-1}] (panels e-f) and MP concentration in sediments [#MP Kg^{-1}] 202

Figure 6.4. Surface water MP concentrations (MP L^{-1}) plotted against sediment MP concentrations (MP Kg^{-1}) for A) Eastcote Brook and B) Bourn Brook 203

Figure 6.5: Size distribution of fragments in surface water for A) Eastcote Brook (EB) and B) Bourn Brook (BB).....204

Figure 6.6: The size distribution of MP fragments recovered from sediment samples from A) Eastcote Brook (EB) and B) Bourn Brook (BB). 205

Figure 6.7: A) MP load per hour (MP h^{-1}) plotted against mean MP concentration in surface water.....209

Figure 6.8: MP load per hour…….209

Figure 7.1: Schematic figure presenting the thesis…….235

Figure S2.1: Plastic standards photographed under 32x magnification, Light intensity 12 and with 50 ms exposure time.. 241
Figure S2.2: False positives photographed under 32x magnification, light intensity 12 and 50 ms exposure time. 243
Figure S2.3: Identification key for fluorescent and non-fluorescent microplastic fibres.. 244
Figure S2.4: Identification key for microplastic spheres/beads. 244
Figure S2.5: Identification key for microplastic fragments including films.. 245
Figure S2.6: Photographs taken in bright field and fluorescent light modes showing features described in Figures above.. 246
Figure S4.1: The chemical composition of MP in A) water and B) sediments.. 289
Figure S5.1:15-minute interval hydrograph comparing reported WWTP outflow and the level of stream discharge at the sampling location reported in L s^{-1} 300
Figure S5.2. Outflow data for 15-minute intervals reported by Barston WWTP for the period of 14th of June – 20th of June 2021. Mean flow (green), maximum flow (purple) and minimum flow (blue).....301
Figure S5.3: The respective colours for A) 4-seasons, B) 8-weekly, C) Daily and D) 12-monthly sampling 302
Figure S5.4: The relative fraction and abundance of fragments and fibres for the 8-week sampling campaign 303
Figure S5.5: The size ranges for A) 12-monthly sampling, B) 8-weekly sampling and C) for sub-daily as a summary.. 304
Figure S5.6: The detailed breakdown of polymer types for 12-monthly sampling.....305
Figure S5.7: The coefficient variation of MP concentration means for all randomly chosen 3x1h, 5x1h and 10x1h combinations for each of the sub-daily sampling days.. 307
Figure S6.1: Schematic figure illustrating the spatial distribution of the sediment sample collection in relation to the river corridor, and flow velocity measurements.....308

Figure S6.2: The distribution of MP fibre sizes in surface waters at A) Eastcote brook (EB) and B) Bourn Brook (BB).....308
Figure S6.3: Distribution of the fibre colours in surface water from Eastcote Brook (EB) and Bourn Brook (BB).....309
Figure S6.4: Distribution of The Fragment colour breakdown in surface water from Eastcote Brook (EB) and Bourn Brook (BB).....310
Figure S6.5: The distribution of fragment colours in sediments from Eastcote Brook (EB) and Bourn Brook (BB).....310
Figure S6.6: The stream discharge ($m^3 s^{-1}$) plotted against MP concentration in surface water (MP L^{-1})..
.....311
Figure S6.7: The stream discharge ($m^3 s^{-1}$) plotted against MP concentration in sediments (MP Kg^{-1})...312
Figure S6.8: The average MP size plotted against discharge ($m^3 s^{-1}$) for A) in surface waters and B) in sediments.....313
Figure S6.9: The average stream velocity ($m s^{-1}$) plotted against MP concentration in surface water (MP L^{-1}).. 313
Figure S6.10: The average stream velocity ($m s^{-1}$) plotted against MP concentration in sediments (MP Kg^{-1}) 314

List of tables

Table 2.1 Results from FTIR analysis for the MP particles chosen by Researcher One for chemical analysis for identification of polymer-types.....42

Table 2.2: Results from Raman spectroscopy for MP particles chosen by Researcher Two for confirmatory chemical analysis of polymer type. 42

Table 3.1. Recommendations for field sampling that aims to understand the interplay between ingested MnP and environment. 67

Table 3.2. Recommendations for laboratory studies that aim to systematically understand the drivers and toxicological effects of MnP exposure. 70

Table 4.1 Microplastic (MP) total, diverted and cumulative loading rates for Boulder Creek (site IDs B1-B28.5) and South Boulder Creek (site IDs S1-S15). 138

Table S3.1: The laboratory and field based studies included in this review and the species identified to interact with nano,- and/or microplastics, the dominant shape of plastic used/found, dominant polymer type(s) and sizing method 249

Table S4.1. Hydrological and physical properties of sampling locations. 208

Table S4.2. Results for positive blank spiking experiment 286

Table S4.3. The land classification according to NLCD 2019 and the new classification.....287

Table S4.4. Spearman correlation coefficients and p values for microplastic particle size (maximum Feret length) and hydrological forcings. BC – Boulder Creek, SBC – South Boulder Creek. 291

Table S4.5. Spearman correlation coefficients and p values for microplastic counts in water and sediments with hydrological factors. BC – Boulder Creek, SBC – South Boulder Creek. 292

Table S5.1: Details on average microplastic (MP) concentration [MP L^{-1}] obtained from the triplicate samples, the stream discharge [m^3 s^{-1}] and MP loads [MP h^{-1}]. 297

List of abbreviations

°C - Degrees Celsius

% - Percentage

> - Greater than

< - Less than

~ - Approximately

˙OH - Hydroxyl radical

µm - Micrometres

µg – Micrograms

µS - Microsiemens

A - Area

a.u. - Arbitrary units

AChE - Acetylcholinesterase

ATR - Attenuated total reflection

aq – Aqueous

BF - Bright-field microscopy

BPA - Bisphenol A

CA - Cellulose acetate

$CaCl_2$ - Sodium chloride

CAT - Catalase gene

Chl-α - Chlorophyll-a

DLS - Dynamic light scattering

DI – Deionized

EC – Electrical conductivity

EPS - Expanded Polystyrene

Fe^{2+} - Ferrous ion

FT-IR - Fourier transform infrared

g - Grams

GC-MS - Gas chromatography-mass spectrometry

GFP - Green Fluorescent Protein

GI - Gastrointestinal

h - Hour

H_2O_2 - Hydrogen peroxide

H^+ - Proton

H_2O - Water

HDPE - High-density Polyethylene

HO^- - Hydroxide ion

HOO• - Hydroperoxyl radical

KOH - Potassium hydroxide

Kg - Kilograms

km - Kilometres

km^2 - Square kilometres

L - Litres

LD - Lethal dose

LDPE - Low density polyethylene

m - Meters

m^3 - Cubic meters

MDA - Malondialdehyde

mg - Milligrams

mL - Millilitres

mm - Millimetres

MnP - Micro and nanoscale plastics

MP – Microplastic

mW - Milliwatt

ms – Millisecond

n - Number

NaI - Sodium iodine

nm - Nanometers

NaOH – Sodium hydroxide

NLCD - National Land Cover Database (USGS)

NR- Nile Red

OM - Organic matter

PA - Polyamide

PA6 - Polyamide-6

PAM - Pulse Amplitude Modulation

PB - Pixel brightness

PHB - Polyhydroxybutyrate

PE- Polyethylene

PEST - Polyester

PET - Polyethylene terephthalate

PLA - Polylactic acid

PMMA - polymethyl methacrylate

PP- Polypropylene

PPCP - Pharmaceuticals and personal care product

PPT - Parts per thousand

PS - Polystyrene

PUR - Polyurethane

PVC - Polyvinyl chloride

ROS - Reactive oxygen species

Rpm - Rounds per minute

SD - Standard Deviation

SEM - Scanning electron microscopy

SMI - Sediment-Microplastic Isolation

SOD - Superoxide dismutase

TGA-FTIR-GCMS - Thermogravimetric analysis-Fourier transform infrared spectroscopy-gas chromatography-mass spectrometry

UK - United Kingdom

UV-VIS - Ultraviolet–visible

WWTP - Waste water treatment plant

W - Watt

$ZnCl_2$ - Zinc chloride

Chapter 1: Introduction

1.1 Scientific rationale

Since their mass production began over 100 years ago, synthetic polymers (commonly known as 'plastics') have found widespread use in a variety of industrial sectors, such as food and water packaging and medical and electronic equipment. Plastics are very lucrative for industry due to their versatility, durability, and low associated manufacturing costs (Andrady and Neal, 2009, Ryan, 2015). However, the same properties that have made plastic so cost-effective to use, also has led to the ubiquitous and persistent problem of plastic waste ending up in the global environment due to plastic waste mismanagement, as well as spillages and leakages (Law, 2017, Thompson et al., 2004, Geyer et al., 2017, Lebreton et al., 2017). The amount of mismanaged plastic waste has grown exponentially over the last decades, in parallel with the increased production and usage of plastics (Barnes et al., 2009, Geyer et al., 2017, Welden and Lusher, 2020). For example, Jambeck et al. (2015) estimated that up to 12.7 million metric tons of mismanaged plastic had entered global oceans in the year 2010 alone, while Lebreton and Andrady (2019) estimated an annual global input into the sea of up to 8.2 million metric tons of plastic waste.

A considerable proportion of the mismanaged plastic waste that can be found in the environment is classified as microplastics (MP), i.e., plastic particles less than 1 mm in size (Hartmann et al., 2019, Welden and Lusher, 2020). These particles can be considered either 'primary' or 'secondary', depending on their origin. Primary MP have been manufactured directly into specific size-range to fulfil a certain purpose (e.g., as fillers in cosmetics) (GESAMP, 2016),

while secondary MP originate from the breakdown of larger plastic items via chemical (hydrolysis/photolysis), physical, and/or biological degradation processes (Corcoran et al., 2009, Mateos-Cárdenas et al., 2020, Andrady and Neal, 2009, O'Brine and Thompson, 2010). The MP enter the environment either indirectly, when larger macroplastics degrade in the environment releasing MP, or are released directly from a multitude of point and non-point sources, such as road-runoff and waste water treatment plants (WWTP) (Waldschläger et al., 2020, Krause et al., 2021, Talbot and Chang, 2022). These MP have been identified as an contaminant of concern for both ecosystem and human health (Lambert and Wagner, 2018; Rochman et al., 2019), and their presence has been recorded in all environmental compartments globally (Allen et al., 2021; Cunningham et al., 2020; Kukkola et al., 2022; Luo et al., 2019; Mintenig et al., 2019; Mu et al., 2019; Padha et al., 2022; Zhang et al., 2021a; Zhou et al., 2020).

Historically, marine and coastal environments have been the main focus of MP research, with rivers being considered to represent a transport pathway for MP to the world's oceans, connecting terrestrial sources with the oceans (Lebreton et al., 2017; Meijer et al., 2021; Weiss et al., 2021). However, as the fate, transport and impact of MP in freshwater systems have gained increasing interest (Hu et al., 2020; Li et al., 2021; Napper et al., 2021; Talbot and Chang, 2022; Wang et al., 2021; Wong et al., 2020), it has become more clear that it is not only the world's oceans that acts as a final sink for MP, but rivers, with all their inherent complexity can act both as temporary and long-term sinks (Drummond et al., 2022; Frei et al., 2019; Weiss et al., 2021), as well as a MP source themselves before MP reaches the oceans (Hurley et al., 2018; Tibbetts et al., 2018; Weiss et al., 2021).

The factors that control MP transport and accumulation patterns in rivers are still not fully evident and several different factors can affect the transport and ultimate fate of MP. These can be the physical properties of the MP themselves (such as density and morphology) which have been suggested to be linked to where in water column and/or sediment the particles settle. Lighter density particles and elongated fibres have been suggested to stay afloat for longer and to be transported by the surface load rather than the bed load (Cowger et al., 2021; Kooi et al., 2021; Van Melkebeke et al., 2020; Waldschläger et al., 2022). However, what determines where MP will be deposited is much more nuanced than just the factor of their respective density: environmental factors and biological processes such as biofilm and heteroaggregate formation have also been reported to affect the settling rate of MP, especially of those of smaller size, not only in marine environments but also in freshwater, suggesting that smaller particles with higher surface-to-volume ratios might be deposited faster as a result of rapid biofilm colonization and the resulting increased density (Chen et al., 2019; Cunha et al., 2019; Fazey and Ryan, 2016; Miao et al., 2021; Van Melkebeke et al., 2020).

Besides the particle properties, there are several hydrological controls in rivers that need to be considered when assessing MP transport. These include physical aspects of the rivers such as river slope, elevation, flow velocity, discharge and sinuosity (the degree of meandering of a river), which all may affect the relative abundance and concentrations of MP in the water column, as well as their transport, accumulation and resuspension in sediments (Mani et al., 2015; Nyberg et al., 2023; Talbot and Chang, 2022; Vianello et al., 2013). To complicate the building of holistic predictions of the MP transport, evidence exists that their distribution is also linked to source proximity, specifically human activities (Talbot and Chang, 2022; Yin et al., 2021), as well as to

hydrometeorological incidents, such as floods and rain events that may decrease the MP concentration in the sediments due to remobilization, while increasing their abundance in the water column due to this remobilization and run-off from storm water (de Carvalho et al., 2022; Hitchcock, 2020; Hurley et al., 2018; Ockelford et al., 2020; Piñon-Colin et al., 2020). Chapters 4-6 explore these issues in greater detail. This heterogeneous dispersion also makes it more difficult to assess how, when and which freshwater biota are exposed to MP, making the local exposure risk assessments challenging to build.

The assessment of MP distribution in rivers is important, not only because MP can interact with freshwater organisms and communities in different ways including, through ingestion, with harmful consequences on organism (e.g., suffocation, inflammation of intestines) and ecosystem health (Sun et al., 2021, Anbumani and Kakkar, 2018), but they can also pose a threat for human health, due to pathogen transport and potential antimicrobial resistance gene transfer (Imran et al., 2019; Kaur et al., 2022; Yang et al., 2020), as well as potential contamination of food sources (e.g., De-la-Torre, 2020; Martinez-Tavera et al., 2021). However, in order to map the real risks that MP pose, freshwater ecotoxicology studies should reflect what is being observed in the field studies and vice versa, and further coordination is needed between the two realms – see Chapter 3 for a deeper evaluation of the disconnect between current laboratory and field studies.

In order to begin to assess the different mechanistic factors that may affect the MP transport in rivers, a standardized approach with harmonized sampling method needs to be applied in several hydrologically different settings globally (Talbot and Chang, 2022). This will enable data comparison between the studies and sites as well as enable more accurate MP transport models to be built, ultimately leading to better global risk assessments of MP in river environment which

requires an extensive baseline to be captured. This is where 100 Plastic Rivers project, of which this thesis is part of, offers unique solution. Its aim is to collect global dataset with a harmonized methodology to further the knowledge of global river MP concentrations, composition, and properties and how these might be related to catchment and river properties discussed above. As a part of the project, certain specific rivers were studied in more detail, to enable in-depth analysis on which hydrological and anthropogenic mechanisms drive the distribution and transport of MP within different river corridors and to what degree the described source and transport control mechanisms influence the often-reported high variability in spatial patterns of MP in surface water and sediments of rivers (Castañeda et al., 2014; Wong et al., 2020; Zhang et al., 2021b).

For the purpose of this thesis, three river systems from United States of America (USA) and United Kingdom (UK) were specifically selected, each with different perceived MP sources: a mountainous catchment with anthropogenically altered flow (Boulder Creek and South Boulder Creek as a paired comparison, located in Colorado, USA at front range of Rocky Mountains), a single point-source (Eastcote Brook, immediately downstream of a wastewater treatment plant, located in Hampton in Arden, UK) and a diffuse urban source (Bourn Brook. located near the University of Birmingham, UK). River selection was guided partly by the acknowledgment that, as anthropogenic activities affect large portions of rivers globally (up to 97% of rivers in Great Britain) (Grill et al., 2019; Jones et al., 2019), the effect that human activities has needs to be studied concurrently with the hydrological activation and transport mechanisms under different temporal scales if accurate predictions of MP fluxes to the oceans from rivers are to be generated. Enhanced understanding of these MP transport mechanisms will also lead to better informed risk assessments for local exposure and facilitate quantification of potential impacts in freshwater

ecosystems. To further advance the field of MP effect studies and to increase the coordination between the laboratory and field studies, this thesis also includes an in-depth review of the effects of micro and nanoplastics on freshwater biota, highlighting the difficulties that the field is facing and proposes solutions to overcome these.

1.2 Aims and Objectives

The work presented in this thesis aims to identify mechanisms that control MP spatial and temporal distribution and exposure in specific rivers and catchments that are affected by anthropogenic activities. The research objectives are:

1) To develop a robust, rapid and reproducible method for MP quantification and counting

2) To systematically compare the approaches taken in field and laboratory studies of MP incidence and effects, recommend standards and parameter selection for field and laboratory studies to enhance their alignment.

3) Investigate how urbanization and water management influences downstream transport of MP in a remote mountainous catchment.

4) Study the temporal distribution of MP downstream of a known point source (sewage treatment works), and to assess the effect of sampling frequency of annual load estimations.

5) Investigate how point and diffuse MP sources contribute to local exposure and explore the hydrological transport mechanisms related to each source.

1.3 Layout of the thesis

This thesis is structured so that after the general introduction laying out the objectives of the thesis (Chapter 1), the following chapter provides details of the methods applied (Chapter 2), as

well as describes the development and application of methodology for MP identification under fluorescence microscopy (objective 1). Chapter 3 is an in-depth literature review on the effects of micro and nanoplastics on freshwater biota and ecology (objective 2), which is followed by three research chapters focusing on the research objectives 3-5: Chapter 4 investigates the effect of human influence on the MP transport (objective 3), Chapter 5 evaluates the effectiveness of current "snapshot" sampling regimens (objective 4) and Chapter 6 identifies the key differences in MP transport mechanisms between point and non-point sources and the consequences for local exposures (objective 5).

Chapter 2

Methods development and methodologies for MP detection and quantification

This chapter describes the methods used in this research as well as describing a new methodology developed as a core part of this thesis for MP identification and quantification (counting) using a fluorescence microscope: the method provides an easy and accessible way to calibrate a fluorescence microscope and to apply a MP identification key to reduce false negatives and false positives while maximizing correctly identified MP.

This method relies on Nile Red staining of the MP which makes them fluoresce. To aid in MP identification, detection limits were established for nine common polymer types as well as for five natural substrates (potential false positives). A morphology specific identification key was created to facilitate reproducibility. This enabled fast pre-screening where only particles with fluorescence above the pre-set threshold were considered further for the visual identification under bright-field

(reducing the total number of particles to be considered). This sub-chapter was published in MethodsX (doi.org/10.1016/j.mex.2023.102053).

Chapter 3

Nano and microplastic interactions with freshwater biota – Current knowledge, challenges and future solutions.

This chapter summarizes the current understanding of nano- and MP movement, interaction, and potential effects on biota in freshwater environments from both field and laboratory studies, with the aim to identify the key challenges that the field faces and recommend approaches to overcome these issues and to improve harmonization. A literature review was conducted in Web of Science with a set topic search equation, focusing on MP and nanoplastics in freshwater systems. The results were divided into laboratory and field studies, with the metadata such as geographical location, plastic types, particle morphology, particle sizes, toxicity endpoints and species recorded. This chapter has been published in Environment International *(doi.org/10.1016/j.envint.2021.106504).*

Chapter 4:

Prevailing impacts of river management on microplastic transport in contrasting US

streams requires rethinking of global microplastic flux estimations.

This chapter aims to explore and quantify the potential controls on the observed spatial variability of MP, applying a paired-catchment approach in a remote mountainous area to characterize the down-stream evolution of MP in surface water and streambed sediment across Boulder Creek and South Boulder Creek, USA, exploring the relative effect of urbanization and revealing the

importance of source proximity and water management to MP concentration in comparison to hydrodynamic transport controls. This study was a collaborative study with the United States Geological Survey (USGS), who provided expertise and data on stream flow conditions and supported the sample collection from Boulder Creek and South Boulder Creek which was carried out by Ms. Danja Mews in collaboration with USGS.

Chapter 5:

Are we timing it right? The impact of sampling frequency on microplastic load estimations downstream from a sewage treatment works

This chapter aims to measure the temporal distribution of MP in the surface water downstream from a known point-source: Barston sewage treatment work in the UK, and how different sampling frequencies affects the annual MP load estimations. A nested sampling approach was used, with the lowest resolution reflecting four seasonal samples, the middle resolution being 12 monthly samples, and the highest resolutions being 8-weekly samples and 4-sub daily sampling regimens where samples were collected each hour for 12-hour periods. This chapter highlights the high variability of MP concentration in the sewage outflow, which was not directly correlated with the discharge, suggesting that snap-shot sampling at this site was not suitable as inputs for annual MP load estimation calculations, as depending on the time of the day at which the sampling was performed, an over or underestimation of 3.8 billion MP annually could arise if the single snap-shot sample happened to have been at one of the high or low loading events, respectively.

Chapter 6:

The tale of two catchments - what makes microplastic move?

This chapter aims to investigate how point and diffuse MP sources contribute to local exposure and explore the hydrological transport mechanisms related to each source type. The chapter highlights how hydrological catchment size may not be descriptive of the MP sources, as the effect of the catchment can be dominated by a single point source present, suggesting that water management can play a substantial role in MP pollution. It also highlights how urban diffuse sources might be activated due to hydrometeorological events (such as rain events), that will lead into these diffused sources to become periodically high MP pollution sources to the river catchments. It was determined that while MP load was unpredictable at the point source, it was much more predictable at the diffuse source, suggesting that water management and human influence can have unpredictable effects on MP loads downstream.

1.4 References

ALLEN, S., ALLEN, D., BALADIMA, F., PHOENIX, V. R., THOMAS, J. L., LE ROUX, G. & SONKE, J. E. 2021. Evidence of free tropospheric and long-range transport of microplastic at Pic du Midi Observatory. *Nature Communications,* 12**,** 7242.

ANDRADY, A. L. & NEAL, M. A. 2009. Applications and societal benefits of plastics. *Philosophical Transactions of the Royal Society B: Biological Sciences,* 364**,** 1977-1984.

BARNES, D. K. A., GALGANI, F., THOMPSON, R. C. & BARLAZ, M. 2009. Accumulation and fragmentation of plastic debris in global environments. *Philosophical Transactions of the Royal Society B: Biological Sciences,* 364**,** 1985-1998.

CASTAÑEDA, R. A., AVLIJAS, S., SIMARD, M. A. & RICCIARDI, A. 2014. Microplastic pollution in St. Lawrence River sediments. *Canadian Journal of Fisheries and Aquatic Sciences,* 71**,** 1767-1771.

CHEN, X., XIONG, X., JIANG, X., SHI, H. & WU, C. 2019. Sinking of floating plastic debris caused by biofilm development in a freshwater lake. *Chemosphere,* 222**,** 856-864.

CORCORAN, P. L., BIESINGER, M. C. & GRIFI, M. 2009. Plastics and beaches: A degrading relationship. *Marine Pollution Bulletin,* 58**,** 80-84.

COWGER, W., GRAY, A. B., GUILINGER, J. J., FONG, B. & WALDSCHLÄGER, K. 2021. Concentration Depth Profiles of Microplastic Particles in River Flow and Implications for Surface Sampling. *Environmental Science & Technology,* 55**,** 6032-6041.

CUNHA, C., FARIA, M., NOGUEIRA, N., FERREIRA, A. & CORDEIRO, N. 2019. Marine vs freshwater microalgae exopolymers as biosolutions to microplastics pollution. *Environmental Pollution,* 249**,** 372-380.

CUNNINGHAM, E. M., EHLERS, S. M., DICK, J. T. A., SIGWART, J. D., LINSE, K., DICK, J. J. & KIRIAKOULAKIS, K. 2020. High Abundances of Microplastic Pollution in Deep-Sea Sediments: Evidence from Antarctica and the Southern Ocean. *Environmental Science & Technology,* 54**,** 13661-13671.

DE-LA-TORRE, G. E. 2020. Microplastics: an emerging threat to food security and human health. *Journal of Food Science and Technology,* 57**,** 1601-1608.

DE CARVALHO, A. R., RIEM-GALLIANO, L., TER HALLE, A. & CUCHEROUSSET, J. 2022. Interactive effect of urbanization and flood in modulating microplastic pollution in rivers. *Environmental Pollution,* 309**,** 119760.

DRUMMOND, J. D., SCHNEIDEWIND, U., LI, A., HOELLEIN, T. J., KRAUSE, S. & PACKMAN, A. I. 2022. Microplastic accumulation in riverbed sediment via hyporheic exchange from headwaters to mainstems. *Science Advances,* 8**,** eabi9305.

FAZEY, F. M. C. & RYAN, P. G. 2016. Biofouling on buoyant marine plastics: An experimental study into the effect of size on surface longevity. *Environmental Pollution,* 210**,** 354-360.

FREI, S., PIEHL, S., GILFEDDER, B. S., LÖDER, M. G. J., KRUTZKE, J., WILHELM, L. & LAFORSCH, C. 2019. Occurence of microplastics in the hyporheic zone of rivers. *Scientific reports,* 9**,** 15256-15256.

GESAMP 2016. SOURCES, FATE AND EFFECTS OF MICROPLASTICS IN THE MARINE ENVIRONMENT: PART TWO OF A GLOBAL ASSESSMENT. *In:* KERSHAW P.J., A. R., C.M (ed.). GESAMP Working Group 40 2nd phase. London: IMO/FAO/UNESCO-IOC/UNIDO/WMO/IAEA/UN/UNEP/UNDP Joint Group of Experts on the Scientific Aspects of Marine Environmental Protection.

GEYER, R., JAMBECK, J. R. & LAW, K. L. 2017. Production, use, and fate of all plastics ever made. *Science Advances,* 3**,** e1700782.

GRILL, G., LEHNER, B., THIEME, M., GEENEN, B., TICKNER, D., ANTONELLI, F., BABU, S., BORRELLI, P., CHENG, L., CROCHETIERE, H., EHALT MACEDO, H., FILGUEIRAS, R., GOICHOT, M., HIGGINS, J., HOGAN, Z., LIP, B., MCCLAIN, M. E., MENG, J., MULLIGAN, M., NILSSON, C., OLDEN, J. D., OPPERMAN, J. J., PETRY, P., REIDY LIERMANN, C., SÁENZ, L., SALINAS-RODRÍGUEZ, S., SCHELLE, P., SCHMITT, R. J. P., SNIDER, J., TAN, F., TOCKNER, K., VALDUJO, P. H., VAN SOESBERGEN, A. & ZARFL, C. 2019. Mapping the world's free-flowing rivers. *Nature,* 569**,** 215-221.

HARTMANN, N. B., HÜFFER, T., THOMPSON, R. C., HASSELLÖV, M., VERSCHOOR, A., DAUGAARD, A. E., RIST, S., KARLSSON, T., BRENNHOLT, N., COLE, M., HERRLING, M. P., HESS, M. C., IVLEVA, N. P., LUSHER, A. L. & WAGNER, M. 2019. Are We Speaking the Same Language? Recommendations for a Definition and Categorization Framework for Plastic Debris. *Environmental Science & Technology,* 53**,** 1039-1047.

HITCHCOCK, J. N. 2020. Storm events as key moments of microplastic contamination in aquatic ecosystems. *Science of The Total Environment,* 734**,** 139436.

HU, D., ZHANG, Y. & SHEN, M. 2020. Investigation on microplastic pollution of Dongting Lake and its affiliated rivers. *Marine Pollution Bulletin,* 160**,** 111555.

HURLEY, R., WOODWARD, J. & ROTHWELL, J. J. 2018. Microplastic contamination of river beds significantly reduced by catchment-wide flooding. *Nature Geoscience,* 11**,** 251-257.

IMRAN, M., DAS, K. R. & NAIK, M. M. 2019. Co-selection of multi-antibiotic resistance in bacterial pathogens in metal and microplastic contaminated environments: An emerging health threat. *Chemosphere,* 215**,** 846-857.

JAMBECK, J. R., GEYER, R., WILCOX, C., SIEGLER, T. R., PERRYMAN, M., ANDRADY, A., NARAYAN, R. & LAW, K. L. 2015. Plastic waste inputs from land into the ocean. Science, 347, 768-771.

JONES, J., BÖRGER, L., TUMMERS, J., JONES, P., LUCAS, M., KERR, J., KEMP, P., BIZZI, S., CONSUEGRA, S., MARCELLO, L., VOWLES, A., BELLETTI, B., VERSPOOR, E., VAN DE BUND, W., GOUGH, P. & GARCIA DE LEANIZ, C. 2019. A comprehensive assessment of stream fragmentation in Great Britain. *Science of The Total Environment,* 673**,** 756-762.

KAUR, K., REDDY, S., BARATHE, P., OAK, U., SHRIRAM, V., KHARAT, S. S., GOVARTHANAN, M. & KUMAR, V. 2022. Microplastic-associated pathogens and antimicrobial resistance in environment. *Chemosphere,* 291**,** 133005.

KOOI, M., PRIMPKE, S., MINTENIG, S. M., LORENZ, C., GERDTS, G. & KOELMANS, A. A. 2021. Characterizing the multidimensionality of microplastics across environmental compartments. *Water Research,* 202**,** 117429.

KRAUSE, S., BARANOV, V., NEL, H. A., DRUMMOND, J. D., KUKKOLA, A., HOELLEIN, T., SAMBROOK SMITH, G. H., LEWANDOWSKI, J., BONET, B., PACKMAN, A. I., SADLER, J., INSHYNA, V., ALLEN, S., ALLEN, D., SIMON, L., MERMILLOD-BLONDIN, F. & LYNCH, I. 2021. Gathering at the top? Environmental controls of microplastic uptake and biomagnification in freshwater food webs. *Environmental Pollution,* 268**,** 115750.

KUKKOLA, A. T., SENIOR, G., MAES, T., SILBURN, B., BAKIR, A., KRÖGER, S. & MAYES, A. G. 2022. A large-scale study of microplastic abundance in sediment cores from the UK continental shelf and slope. *Marine Pollution Bulletin,* 178**,** 113554.

LAMBERT, S. & WAGNER, M. 2018. Microplastics Are Contaminants of Emerging Concern in Freshwater Environments: An Overview. *In:* WAGNER, M. & LAMBERT, S. (eds.) *Freshwater Microplastics : Emerging Environmental Contaminants?* Cham: Springer International Publishing.

LAW, K. L. 2017. Plastics in the Marine Environment. *Annual Review of Marine Science,* 9**,** 205-229.

LEBRETON, L. C. M., VAN DER ZWET, J., DAMSTEEG, J.-W., SLAT, B., ANDRADY, A. & REISSER, J. 2017. River plastic emissions to the world's oceans. *Nature Communications,* 8**,** 15611.

LI, Y., LIU, S., LIU, M., HUANG, W., CHEN, K., DING, Y., WU, F., KE, H., LOU, L., LIN, Y., ZHANG, M., LIU, F., WANG, C. & CAI, M. 2021. Mid-Level Riverine Outflow Matters: A Case of Microplastic Transport in the Jiulong River, China. *Frontiers in Marine Science,* 8.

LUO, W., SU, L., CRAIG, N. J., DU, F., WU, C. & SHI, H. 2019. Comparison of microplastic pollution in different water bodies from urban creeks to coastal waters. *Environmental Pollution,* 246**,** 174-182.

MANI, T., HAUK, A., WALTER, U. & BURKHARDT-HOLM, P. 2015. Microplastics profile along the Rhine River. *Scientific Reports,* 5**,** 17988.

MARTINEZ-TAVERA, E., DUARTE-MORO, A. M., SUJITHA, S. B., RODRIGUEZ-ESPINOSA, P. F., ROSANO-ORTEGA, G. & EXPÓSITO, N. 2021. Microplastics and

metal burdens in freshwater Tilapia (Oreochromis niloticus) of a metropolitan reservoir in Central Mexico: Potential threats for human health. *Chemosphere,* 266**,** 128968.

MATEOS-CÁRDENAS, A., O'HALLORAN, J., VAN PELT, F. N. A. M. & JANSEN, M. A. K. 2020. Rapid fragmentation of microplastics by the freshwater amphipod Gammarus duebeni (Lillj.). *Scientific Reports,* 10**,** 12799.

MEIJER, L. J., VAN EMMERIK, T., VAN DER ENT, R., SCHMIDT, C. & LEBRETON, L. 2021. More than 1000 rivers account for 80% of global riverine plastic emissions into the ocean. *Science Advances,* 7**,** eaaz5803.

MIAO, L., GAO, Y., ADYEL, T. M., HUO, Z., LIU, Z., WU, J. & HOU, J. 2021. Effects of biofilm colonization on the sinking of microplastics in three freshwater environments. *Journal of Hazardous Materials,* 413**,** 125370.

MINTENIG, S. M., LÖDER, M. G. J., PRIMPKE, S. & GERDTS, G. 2019. Low numbers of microplastics detected in drinking water from ground water sources. *Science of The Total Environment,* 648**,** 631-635.

MU, J., ZHANG, S., QU, L., JIN, F., FANG, C., MA, X., ZHANG, W. & WANG, J. 2019. Microplastics abundance and characteristics in surface waters from the Northwest Pacific, the Bering Sea, and the Chukchi Sea. *Marine Pollution Bulletin,* 143**,** 58-65.

NAPPER, I. E., BAROTH, A., BARRETT, A. C., BHOLA, S., CHOWDHURY, G. W., DAVIES, B. F. R., DUNCAN, E. M., KUMAR, S., NELMS, S. E., HASAN NILOY, M. N., NISHAT, B., MADDALENE, T., THOMPSON, R. C. & KOLDEWEY, H. 2021. The abundance and characteristics of microplastics in surface water in the transboundary Ganges River. *Environmental Pollution,* 274**,** 116348.

NYBERG, B., HARRIS, P. T., KANE, I. & MAES, T. 2023. Leaving a plastic legacy: Current and future scenarios for mismanaged plastic waste in rivers. *Science of The Total Environment,* 869**,** 161821.

O'BRINE, T. & THOMPSON, R. C. 2010. Degradation of plastic carrier bags in the marine environment. *Marine Pollution Bulletin,* 60**,** 2279-2283.

OCKELFORD, A., CUNDY, A. & EBDON, J. E. 2020. Storm Response of Fluvial Sedimentary Microplastics. *Scientific Reports,* 10**,** 1865.

PADHA, S., KUMAR, R., DHAR, A. & SHARMA, P. 2022. Microplastic pollution in mountain terrains and foothills: A review on source, extraction, and distribution of microplastics in remote areas. *Environmental Research,* 207**,** 112232.

PIÑON-COLIN, T. D. J., RODRIGUEZ-JIMENEZ, R., ROGEL-HERNANDEZ, E., ALVAREZ-ANDRADE, A. & WAKIDA, F. T. 2020. Microplastics in stormwater runoff in a semiarid region, Tijuana, Mexico. *Science of The Total Environment,* 704**,** 135411.

ROCHMAN, C. M., BROOKSON, C., BIKKER, J., DJURIC, N., EARN, A., BUCCI, K., ATHEY, S., HUNTINGTON, A., MCILWRAITH, H., MUNNO, K., DE FROND, H., KOLOMIJECA, A., ERDLE, L., GRBIC, J., BAYOUMI, M., BORRELLE, S. B., WU, T., SANTORO, S., WERBOWSKI, L. M., ZHU, X., GILES, R. K., HAMILTON, B. M., THAYSEN, C., KAURA, A., KLASIOS, N., EAD, L., KIM, J., SHERLOCK, C., HO, A. & HUNG, C. 2019. Rethinking microplastics as a diverse contaminant suite. *Environmental Toxicology and Chemistry,* 38**,** 703-711.

RYAN, P. G. 2015. A Brief History of Marine Litter Research. *In:* BERGMANN, M., GUTOW, L. & KLAGES, M. (eds.) *Marine Anthropogenic Litter.* Cham: Springer International Publishing.

TALBOT, R. & CHANG, H. 2022. Microplastics in freshwater: A global review of factors affecting spatial and temporal variations. *Environmental Pollution,* 292**,** 118393.

THOMPSON, R. C., OLSEN, Y., MITCHELL, R. P., DAVIS, A., ROWLAND, S. J., JOHN, A. W. G., MCGONIGLE, D. & RUSSELL, A. E. 2004. Lost at Sea: Where Is All the Plastic? *Science,* 304**,** 838-838.

TIBBETTS, J., KRAUSE, S., LYNCH, I. & SAMBROOK SMITH, G. H. 2018. Abundance, Distribution, and Drivers of Microplastic Contamination in Urban River Environments. *Water* [Online], 10.

VAN MELKEBEKE, M., JANSSEN, C. & DE MEESTER, S. 2020. Characteristics and Sinking Behavior of Typical Microplastics Including the Potential Effect of Biofouling: Implications for Remediation. *Environmental Science & Technology,* 54**,** 8668-8680.

VIANELLO, A., BOLDRIN, A., GUERRIERO, P., MOSCHINO, V., RELLA, R., STURARO, A. & DA ROS, L. 2013. Microplastic particles in sediments of Lagoon of Venice, Italy: First observations on occurrence, spatial patterns and identification. *Estuarine, Coastal and Shelf Science,* 130**,** 54-61.

WALDSCHLÄGER, K., BRÜCKNER, M. Z. M., CARNEY ALMROTH, B., HACKNEY, C. R., ADYEL, T. M., ALIMI, O. S., BELONTZ, S. L., COWGER, W., DOYLE, D., GRAY, A., KANE, I., KOOI, M., KRAMER, M., LECHTHALER, S., MICHIE, L., NORDAM, T., POHL, F., RUSSELL, C., THIT, A., UMAR, W., VALERO, D., VARRANI, A., WARRIER, A. K., WOODALL, L. C. & WU, N. 2022. Learning from natural sediments to tackle microplastics challenges: A multidisciplinary perspective. *Earth-Science Reviews,* 228**,** 104021.

WALDSCHLÄGER, K., LECHTHALER, S., STAUCH, G. & SCHÜTTRUMPF, H. 2020. The way of microplastic through the environment – Application of the source-pathway-receptor model (review). *Science of The Total Environment,* 713**,** 136584.

WANG, Z., ZHANG, Y., KANG, S., YANG, L., SHI, H., TRIPATHEE, L. & GAO, T. 2021. Research progresses of microplastic pollution in freshwater systems. *Science of The Total Environment,* 795**,** 148888.

WEISS, L., LUDWIG, W., HEUSSNER, S., CANALS, M., GHIGLIONE, J.-F., ESTOURNEL, C., CONSTANT, M. & KERHERVÉ, P. 2021. The missing ocean plastic sink: Gone with the rivers. *Science,* 373**,** 107-111.

WELDEN, N. A. & LUSHER, A. 2020. Chapter 9 - Microplastics: from origin to impacts. *In:* LETCHER, T. M. (ed.) *Plastic Waste and Recycling.* Academic Press.

WONG, G., LÖWEMARK, L. & KUNZ, A. 2020. Microplastic pollution of the Tamsui River and its tributaries in northern Taiwan: Spatial heterogeneity and correlation with precipitation. *Environmental Pollution,* 260**,** 113935.

YANG, Y., LIU, W., ZHANG, Z., GROSSART, H.-P. & GADD, G. M. 2020. Microplastics provide new microbial niches in aquatic environments. *Applied Microbiology and Biotechnology,* 104**,** 6501-6511.

YIN, K., WANG, D., ZHAO, H., WANG, Y., GUO, M., LIU, Y., LI, B. & XING, M. 2021. Microplastics pollution and risk assessment in water bodies of two nature reserves in Jilin Province: Correlation analysis with the degree of human activity. *Science of The Total Environment,* 799**,** 149390.

ZHANG, Y., GAO, T., KANG, S., ALLEN, S., LUO, X. & ALLEN, D. 2021a. Microplastics in glaciers of the Tibetan Plateau: Evidence for the long-range transport of microplastics. *Science of The Total Environment,* 758**,** 143634.

ZHANG, Z., DENG, C., DONG, L., LIU, L., LI, H., WU, J. & YE, C. 2021b. Microplastic pollution in the Yangtze River Basin: Heterogeneity of abundances and characteristics in different environments. *Environmental Pollution,* 287**,** 117580.

ZHOU, Y., WANG, J., ZOU, M., JIA, Z., ZHOU, S. & LI, Y. 2020. Microplastics in soils: A review of methods, occurrence, fate, transport, ecological and environmental risks. *Science of The Total Environment,* 748**,** 141368.

Chapter 2: Methods

2.1 Density separation

Identification of MP requires them to be isolated from the environmental matrix. A commonly deployed method for isolation of MP is density separation. This method relies on the density differences between plastics and the environmental sediments (e.g., 0.92 g/cm³ for polypropylene and 1.8 g/cm^3 for sand), which will allow the denser particles to sink and the lighter MP to float when suspended in a media with a specific density (Quinn et al., 2017). Saturated salt solutions, such as NaCl have frequently been used in the past (Reddy et al., 2006, Browne et al., 2010, Thompson et al., 2004b), but other salt solutions have been used as well. Some examples include NaI (Nuelle et al., 2014), $CaCl_2$ (Stolte et al., 2015) and $ZnCl_2$ (Imhof et al., 2016). $ZnCl_2$ was chosen for this study, as it can be made into a solution of density 1.5 g/cm³, which is heavy enough to float some of the denser plastics (e.g., polyvinyl chloride with density 1.38 g/cm^3), the resistance of common polymers to the solution and the relatively low risk for personnel handling the chemical. To facilitate the density separation, sediment MP extraction units were used (Coppock et al., 2017, Nel et al., 2019).

2.2 Organic matter digestion

If organic matter (OM) is present after density separation, this can interfere with MP identification. Therefore, it is important to remove any OM from the samples before the identification and counting of MP. This can involve different chemical and/or enzymatic treatments, which break down OM but do not affect the MP adversely (Dehaut et al., 2016, Cowger et al., 2020). Fenton's reagent has been chosen as the digestion method for the purpose of this study

due to its low impact on MP and successful use in similar riverine environments and in wastewater (Margenat, 2021, Tagg et al., 2017). Fenton's reagent works by using ferrous ion (Fe^{2+}) as a catalyst for the decomposition of hydrogen peroxide (H_2O_2) into two different oxygen-radical species and water, with the oxygen-radicals leading to oxidative degradation of OM (Gupta et al., 2016, Stasicka, 2011). The chemical reactions can be described as follows: 1) H_2O_2 oxidizes the iron(II) into iron(III), producing a hydroxyl radical ($^{\cdot}OH$) and a hydroxide ion (HO^-). 2) the iron(III) is reduced back to iron(II) while producing a hydroperoxyl radical ($HOO\bullet$) and a proton (H^+). The two half-reactions and the overall net reaction are presented below:

1) $Fe^{2+} + H_2O_2 \rightarrow Fe^{3+} + {}^{\cdot}OH + HO^-$

2) $Fe^{3+} + H_2O_2 \rightarrow Fe^{2+} + HOO\bullet + H+$

Net reaction: $2\ H_2O_2 \rightarrow HO\bullet + HOO\bullet + H_2O$

2.3 Fluorescence

Nile Red is a hydrophilic fluorophore, which sorbs to plastics due to their polarity, rendering the plastics fluorescent. The fluorescence is created when Nile Red absorbs shorter-wavelength light (excitation light), which excites the molecule to a higher energy level, and when it relaxes back to the ground state it releases the absorbed energy as a photon (emission light) (Marshall and Johnsen, 2017, Lichtman and Conchello, 2005, Lakowicz, 1999). This emission light will have lower energy than that of the excitation/absorption, resulting in the emitted photons being shifted towards the red spectrum (Marshall and Johnsen, 2017, Lichtman and Conchello, 2005, Lakowicz, 1999). This emitted light can then be observed with a microscope, when the excitation light is filtered out with a specific wavelength emission filter, coupled with a beam-splitter which reflects

excitation light towards the sample and emission light towards the eyepieces. This allows only the emission spectra to reach the eyepieces and to be observed by the researcher.

2.4 Raman spectroscopy

Raman spectroscopy is non-destructive chemical analysis method that is based on the Raman effect, where the interaction of a laser beam (light source) with the chemical bonds of the substrate of interest creates Raman scattering. Raman scattering is an optical process whereby light interacting with the sample produces scattered light, most of which most is emitted with a similar wavelength as the original beam, but a small fraction will exhibit lower energy (referred to as the Raman effect) the wavelength of which is directly related to the chemical bonds of the specimen (Wang and Evans, 2016, Dana et al., 2019). This scattered Raman light is collected using specific optical filters, which is then used to infer the chemical species and molecular structures of the material being studied (Omidi et al., 2017, Dana et al., 2019).

Due to specific chemical bonds and molecules having distinct Raman signal, this technique cand be used to identify the substance and polymer being studied. The obtained Raman spectra was compared to a reference Raman library containing spectra of known synthetic and natural polymers (open access: SLOPP, SLOPP-E and in-house built library) to assess whether the studied substance is MP. Fingerprint region of 650-1700 cm^{-1} was used and the spectra were exported into a custom Python script (Python 3.9) and using the Pandas and NumPy packages, peaks were matched to reference libraries using the Pearson correlation coefficient to determine whether studied substance was MP.

2.5 References

BROWNE, M. A., GALLOWAY, T. S. & THOMPSON, R. C. 2010. Spatial Patterns of Plastic Debris along Estuarine Shorelines. *Environmental Science & Technology,* 44**,** 3404-3409.

COPPOCK, R. L., COLE, M., LINDEQUE, P. K., QUEIRÓS, A. M. & GALLOWAY, T. S. 2017. A small-scale, portable method for extracting microplastics from marine sediments. *Environmental Pollution,* 230**,** 829-837.

COWGER, W., BOOTH, A. M., HAMILTON, B. M., THAYSEN, C., PRIMPKE, S., MUNNO, K., LUSHER, A. L., DEHAUT, A., VAZ, V. P. & LIBOIRON, M. 2020. Reporting guidelines to increase the reproducibility and comparability of research on microplastics. *Applied spectroscopy,* 74**,** 1066-1077.

DANA, C.-M., MICHAEL, S. & JUERGEN, P. 2019. Theoretical principles of Raman spectroscopy. *Physical Sciences Reviews,* 4.

DEHAUT, A., CASSONE, A.-L., FRÈRE, L., HERMABESSIERE, L., HIMBER, C., RINNERT, E., RIVIÈRE, G., LAMBERT, C., SOUDANT, P., HUVET, A., DUFLOS, G. & PAUL-PONT, I. 2016. Microplastics in seafood: Benchmark protocol for their extraction and characterization. *Environmental Pollution,* 215**,** 223-233.

GUPTA, P., LAKES, A. & DZIUBLA, T. 2016. Chapter One - A Free Radical Primer. *In:* DZIUBLA, T. & BUTTERFIELD, D. A. (eds.) *Oxidative Stress and Biomaterials.* Academic Press.

IMHOF, H. K., LAFORSCH, C., WIESHEU, A. C., SCHMID, J., ANGER, P. M., NIESSNER, R. & IVLEVA, N. P. 2016. Pigments and plastic in limnetic ecosystems: A qualitative and quantitative study on microparticles of different size classes. *Water Research,* 98**,** 64-74.

LAKOWICZ, J. R. 1999. Introduction to Fluorescence. *In:* LAKOWICZ, J. R. (ed.) *Principles of Fluorescence Spectroscopy.* Boston, MA: Springer US.

LICHTMAN, J. W. & CONCHELLO, J.-A. 2005. Fluorescence microscopy. *Nature Methods,* 2**,** 910-919.

LENZ, R., ENDERS, K., FISCHER, F., BRANDT, J., FISCHER, D. & LABRENZ, M. 2021. Measuring impacts of microplastic treatments via image recognition on immobilised particles below 100 µm. Microplastics and Nanoplastics, 1, 12

MARGENAT, H., NEL, H.A., STONEDAHL, S.H., KRAUSE, S., SABATER, F., DRUMMOND, J.D. 2021. Hydrologic controls on the accumulation of different sized microplastics in the streambed sediments downstream of a wastewater treatment plant (Catalonia, Spain). *Environmental Research Letters,* 16.

MARSHALL, J. & JOHNSEN, S. 2017. Fluorescence as a means of colour signal enhancement. *Philosophical Transactions of the Royal Society B: Biological Sciences,* 372**,** 20160335.

NEL, H., KRAUSE, S., SAMBROOK SMITH, G. H. & LYNCH, I. 2019. Simple yet effective modifications to the operation of the Sediment Isolation Microplastic unit to avoid polyvinyl chloride (PVC) contamination. *MethodsX,* 6**,** 2656-2661.

NUELLE, M.-T., DEKIFF, J. H., REMY, D. & FRIES, E. 2014. A new analytical approach for monitoring microplastics in marine sediments. *Environmental Pollution,* 184**,** 161-169.

OMIDI, M., FATEHINYA, A., FARAHANI, M., AKBARI, Z., SHAHMORADI, S., YAZDIAN, F., TAHRIRI, M., MOHARAMZADEH, K., TAYEBI, L. & VASHAEE, D. 2017. 7 -

Characterization of biomaterials. *In:* TAYEBI, L. & MOHARAMZADEH, K. (eds.) *Biomaterials for Oral and Dental Tissue Engineering.* Woodhead Publishing.

QUINN, B., MURPHY, F. & EWINS, C. 2017. Validation of density separation for the rapid recovery of microplastics from sediment. *Analytical Methods,* 9**,** 1491-1498.

REDDY, M. S., SHAIK, B., ADIMURTHY, S. & RAMACHANDRAIAH, G. 2006. Description of the small plastics fragments in marine sediments along the Alang-Sosiya ship-breaking yard, India. *Estuarine, Coastal and Shelf Science,* 68**,** 656-660.

STASICKA, Z. 2011. Chapter 7 - Transition metal complexes as solar photocatalysts in the environment: A short review of recent development. *In:* ELDIK, R. V. & STOCHEL, G. (eds.) *Advances in Inorganic Chemistry.* Academic Press.

STOLTE, A., FORSTER, S., GERDTS, G. & SCHUBERT, H. 2015. Microplastic concentrations in beach sediments along the German Baltic coast. *Marine Pollution Bulletin,* 99**,** 216-229.

TAGG, A. S., HARRISON, J. P., JU-NAM, Y., SAPP, M., BRADLEY, E. L., SINCLAIR, C. J. & OJEDA, J. J. 2017. Fenton's reagent for the rapid and efficient isolation of microplastics from wastewater. *Chemical Communications,* 53**,** 372-375.

THOMPSON, R. C., OLSON, Y., MITCHELL, R. P., DAVIS, A., ROWLAND, S. J., JOHN, A. W. G., MCGONIGLE, D. & RUSSELL, A. E. 2004. Lost at Sea: Where Is All the Plastic? *Science,* 304**,** 838.

WANG, H. & EVANS, C. L. 2016. Chapter 11 - Coherent Raman Scattering Microscopy in Dermatological Imaging. *In:* HAMBLIN, M. R., AVCI, P. & GUPTA, G. K. (eds.) *Imaging in Dermatology.* Boston: Academic Press.

2.6 Easy and accessible way to calibrate a fluorescence microscope and to create a microplastic identification key

Anna Kukkola[a]*, *Stefan Krause*[a, b,c], *Yasmin Yonan* [a,∫], *Liam Kelleher*[a,b], *Uwe Schneidewind*[a], *Gregory H Sambrook Smith*[a], *Holly Nel*[a,↓], *Iseult Lynch*[a, b]

[a] *School of Geography, Earth and Environmental Sciences,* University of Birmingham, Edgbaston, Birmingham B15 2TT, United Kingdom

[b] *Institute for Global Innovation, University of Birmingham, Edgbaston, Birmingham B15 2TT, United Kingdom*

[c] LEHNA- Laboratoire d'ecologie des hydrosystemes naturels et anthropises, University of Lyon, Darwin C & Forel, 3-6 Rue Raphaël Dubois, 69622 Villeurbanne, France.

∫ Current affiliation: *School of Geography, Geology and the Environment, The University of Leicester, University Road, Leicester, LE1 7RH, United Kingdom*

↓ Current affiliation: *Centre for Environment, Fisheries and Aquaculture, Pakefield Road, Lowestoft, Suffolk NR33 0HT, United Kingdom*

***This sub-chapter has been published in MethodsX:**

https://doi.org/10.1016/j.mex.2023.102053

2.6.1 Abstract

We present here a technique for setting up detection limits on any fluorescent microscope in conjunction with the fluorophore Nile Red for microplastic (MP) identification. Our method also describes a rigorous morphology-specific identification key for MP to reduce subjectivity between researchers. The detection limits were established for nine common polymer types and five natural substrates which could result in false-positive signals when using Nile Red for MP identification. This method was then applied to real freshwater samples and identified particles were validated with micro-FTIR or Raman spectroscopy. This approach may reduce subjectivity in MP identification and counting and enhances transparency, repeatability and harmonization within MP research community.

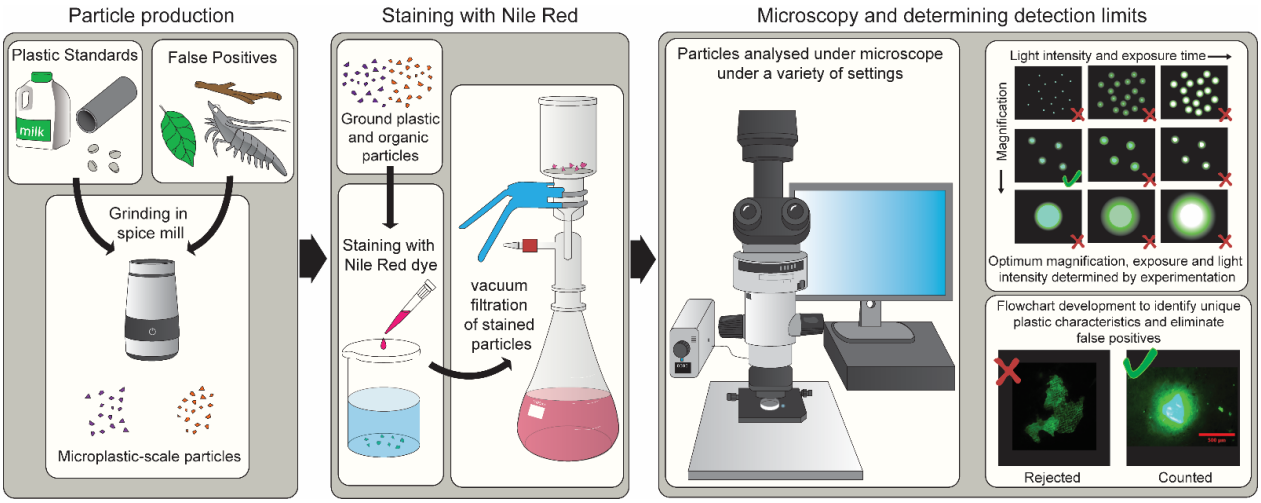


Figure 2.0 Graphical abstract

2.6.2 Method detail

2.6.2.1 Background

In MP research, a common method for MP extraction/fractionation is density separation, frequently carried out using saturated salt solutions (Nabi et al., 2022) followed by visual identification under bright-field microscopy (Löder and Gerdts, 2015, Shim et al., 2017). Relying on visual identification is still a very popular technique as analytical approaches such as FT-IR and/or Raman spectroscopy or similar chemical verification methods are not widely accessible and are time consuming and very data intensive (Nel et al., 2021c). Visual identification, however, is highly subjective, as it depends on individual understanding of how MP appears under the light microscope (often based on colour and shape). Visual identification has also been criticized for being imprecise for smaller MP particles, especially for sizes below 200 μm (Lenz et al., 2015, Song et al., 2015, Löder and Gerdts, 2015, Nel et al., 2019). This has led to calls to create reproducible methods that are universally accessible globally. Nile Red staining, a method where samples are stained with fluorescent dye, has been suggested to overcome some of these limitations, as it can be applied at low-cost and is widely accessible (Shruti et al., 2022, Shim et al., 2016, Nel et al., 2021a, Lv et al., 2019, Maes et al., 2017, Kukkola et al., 2022).

However, this method also has its limitations. Nel et al. (2021a) showed that not everything that had fluorescence should be counted as MP, as Nile Red can also stain organic matter (OM) present in the samples, which can result in some particles being falsely identified as plastics (Stanton et al., 2019a, Nel et al., 2021a). To overcome this, Nel et al. (2021a) investigated the pixel brightness of various plastic polymers and natural substrates before and after Nile Red staining. This allowed a suitable particle brightness (detection limit) to be determined, whereby only

particles above this specific threshold would be counted, which would allow detection of MP while simultaneously reducing inclusion of false positives.

To set up a fluorescence detection limit, which is optimized for MP identification, every microscope used for counting and identifying MP must be calibrated. This is because each fluorescence microscope has unique fluorescence intensity/brightness for a specific combination of optical filter(s), light source, detector, and camera (Nel et al., 2021a). To establish these limits for a specific microscope system, several different settings need to be trialled with known plastic types, as well as some common natural materials (e.g., wood, leaves etc.) that may be present in the samples. This paper provides a guideline for how this calibration process can be carried out, and contributes towards the standardization of MP identification using Nile Red.

Furthermore, to aid reproducibility and transparency we developed easy-to-use identification keys within our research group for use with Nile Red staining. The first key relies on the fluorescence detection limit as a pre-screening for particles of interest to determine which ones should be considered further, thereby considerably shortening the overall time spent on analysing a filter. It then requires the operator to inspect particles above the set fluorescence detection limit under bright-field microscopy and uses morphology specific keys to quantify the different forms present in the sample. The detection limits coupled with the identification keys result in higher detection comparability between individual researchers in terms of MP count numbers as well as their morphological categorization. This type of identification/decision tree has been used previously in MP literature for bright-field microscopy and is considered an example of best practice (e.g., Lusher et al., 2020). Here, we take the next step and combine fluorescence and visual observation to create a quick and robust identification method for MP identification.

2.6.2.2 Establishing microplastic detection limits

To establish MP detection limits in Nile Red supported fluorescent microscopy, thirteen different synthetic polymer types, including polylactic acid (PLA), polyvinyl chloride (PVC), expanded polystyrene (EPS), two types of high-density polyethylene (HDPE), polyamide-6 (PA6), polyethylene (PE), polyethylene terephthalate (PET), three types of polypropylene (PP) and two types of polystyrene (PS), were selected as exemplar materials (PlasticsEurope, 2022). Polymer composition was confirmed using thermogravimetric analysis-Fourier transform infrared spectroscopy-gas chromatography-mass spectrometry TGA-FTIR-GCMS (Nel et al., 2021b). All plastics were ground down with a spice mill and size fractions between 63 µm - 400 µm were kept after sieving with stainless steel sieves, to represent environmental MP. Five substrates commonly present in environmental samples were also included as examples of potential false positives. These were wood (twigs), dead leaves (maple and birch), chitosan (chitin) and sand.

Plastic (n=13) and natural substrate (n=5) samples were placed individually into clean glass beakers each with 20 mL of deionized (DI) water and subsequently left to stain with Nile Red at a concentration of 5 µg mL^{-1} for an hour at about 21 °C. Each beaker was gently agitated every 10 minutes to ensure equivalent staining. Samples were then vacuum-filtered onto Whatmann GF/D glass fibre filters and oven dried for 24 h at 50 °C before imaging. No organic matter digestion was carried out.

Imaging was carried out in green fluorescence mode using a macro zoom microscope (Olympus MVX-ZB10) equipped with a 1 x 0.25 N objective (MVPLAPO 1X, Olympus) and a U-M49002XL GFP (Green Fluorescent Protein) filter cube (excitation filter: 470/40 nm, dichroic mirror: 495 nm high pass, emission filter: 525/50 nm) with a 130 W mercury apo lamp (U-

HGLGPS, Olympus) as light source. Filters were photographed with a DP74 colour camera. Fifteen particles on each filter were imaged with each of the following five settings (Figure 2.1), (i) 20x magnification; Light intensity 12 (2xLi12) and 25 (2xLi25), with 50 ms exposure time, (ii) 50x magnification; Light intensity 12 (5xLi12) and 25 (5xLi25), with 50 ms exposure time, and additionally (iii) 32x magnification; Light intensity 12 (3.2xLi12), with 50 ms exposure time. Fifteen individual particles were imaged per sample type (plastic and false positive type) and each particle was measured for their median green pixel brightness (PB) in arbitrary units (a.u) across their longest Feret diameter using the *CellSens* software under each of the above settings.

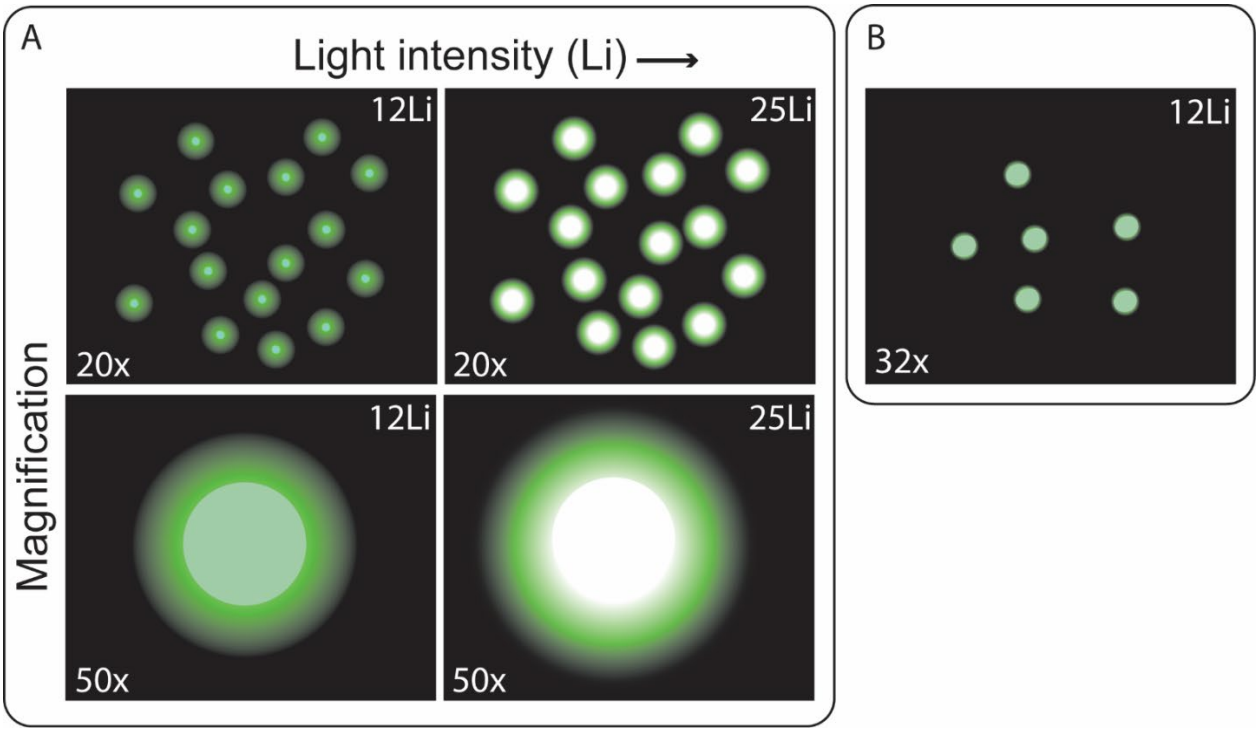


Figure 2.1. Schematic illustration of general effect for Pixel Brightness (PB) of each of the tested system settings. A) panel shows 20x magnification (top row); Light intensity 12 (2xLi12) and 25 (2xLi25), with 50 ms exposure time and 50x magnification (bottom row); Light intensity 12

(5xLi12) and 25 (5xLi25), with 50 ms exposure time. B) 32x magnification; Light intensity 12 (3.2xLi12), with 50 ms exposure time.

Statistical analysis was performed using Rstudio software (Integrated Development for R. Rstudio, PBC, Boston, MA; R Core Team 2021) to evaluate the effects of magnification and light intensity on the PB of the MP and natural substrates. Wilcoxon Rank Sum tests with multiple comparisons were performed with PB as the dependent variable and light intensity and magnification as independent variables in order to determine whether the PB of a given sample type changed significantly depending on the settings used.

The results of the Wilcoxon Rank Sum analyses are presented in the Appendix 1, but overall, higher magnification and higher light intensity both show an increase in the PB of the detected MP, apart from HDPE_2, PP_3 and PS_2 which had high PB regardless of the chosen magnification or light intensity. For PA6, light intensity increased PB significantly, but magnification seemed to have a negligible effect. Conversely, light intensity had no significant impact on the PB of HDPE_1, whereas magnification did. Only for PET did MP both magnification and light intensity have a significant effect on PB. PET and PVC had the lowest PB, regardless of the magnification used or light intensity settings. Overall, it was impossible to identify a clear statistical trend for the most favourable settings for the microscope in relation to light intensity and magnification. Instead, the descriptive statistics were calculated for each sample type and used to identify the lowest PB cut-off limit by comparing the mean PB value and the lower limit of the 95% confidence interval for each of the five settings, to identify a PB limit as the threshold above which over 90% of all the measured MP particles would be identified. The results are shown in a boxplot (Figure 2.2A).

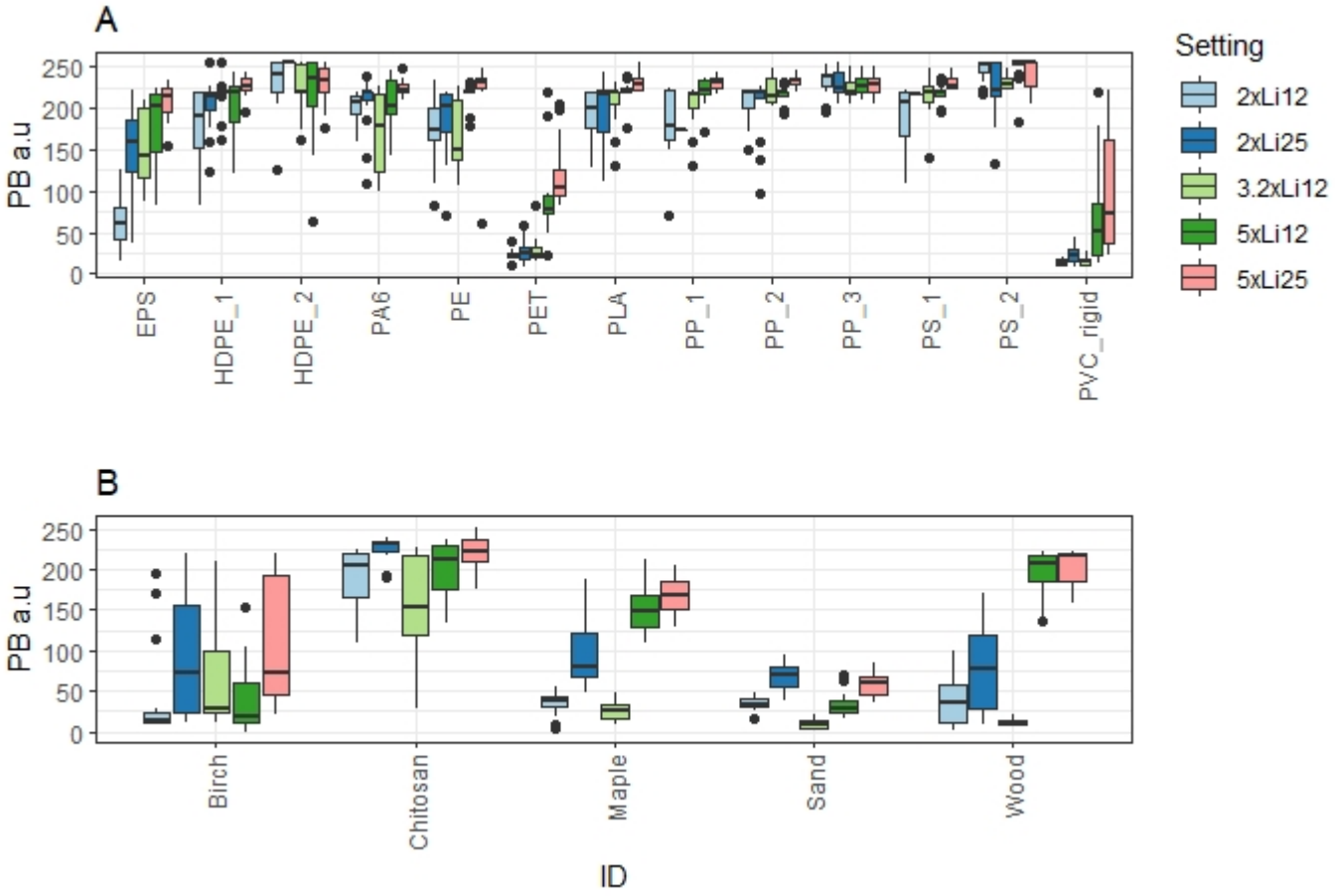


Figure 2.2 Boxplot illustrating the different pixel brightness (BP) in arbitrary units (a.u) results for A) thirteen different plastic types and B) for the five false positive substrates under different magnification, light intensity, exposure time, and image acquisition settings. The black central line in each boxplot indicates the median and whiskers indicate the inter quantile range (25 - 75%). Settings were as follows: 2xLi12) 20x magnification with light intensity 12 and 50 ms exposure time, 2xLi25) 20x magnification with light intensity 25 and 50 ms exposure time, 3.2xLi12) 32x magnification, light intensity 12, and 50 ms exposure time, 5xLi12) 50x magnification, light intensity 12 and 50 ms exposure time and 5xLi25), 50x magnification, light intensity 25 with 50 ms exposure time.

The most promising settings for imaging of the MP were the higher magnification (50x) and light intensity 12 or 25. With these settings, 90% of all MP particles (including PET and PVC) were detectable at a PB limit of 130 a.u. However, imaging of the five natural substrate sample types revealed that choosing this higher magnification (x50) leads to a higher inclusion of false positives, including wood litter (Figure 2.2B), which may be abundant in environmental samples, suggesting that lower (32x magnification) should be used.

Another setting that performed well was 32x magnification under light intensity 12 with 50 ms exposure time (Figure 2.2A & 2.2B, Appendix 1: Figures S2.1 & S2.2). This setting allowed us to identify 97.5% of plastics (excluding PET and PVC) while only 22.3% of false positives were detectable above the threshold of 100 a.u (Figure 2.2). From the detected false positives all were either chitosan or birch, substrate types that are easy to identify as false positives if the identification key described below is used, due to their internal structures. This led to adoption of 100 a.u as our fluorescence intensity threshold, whereby particles and fibres exhibiting intensity higher than this should be considered further for MP identification with the identification keys described below.

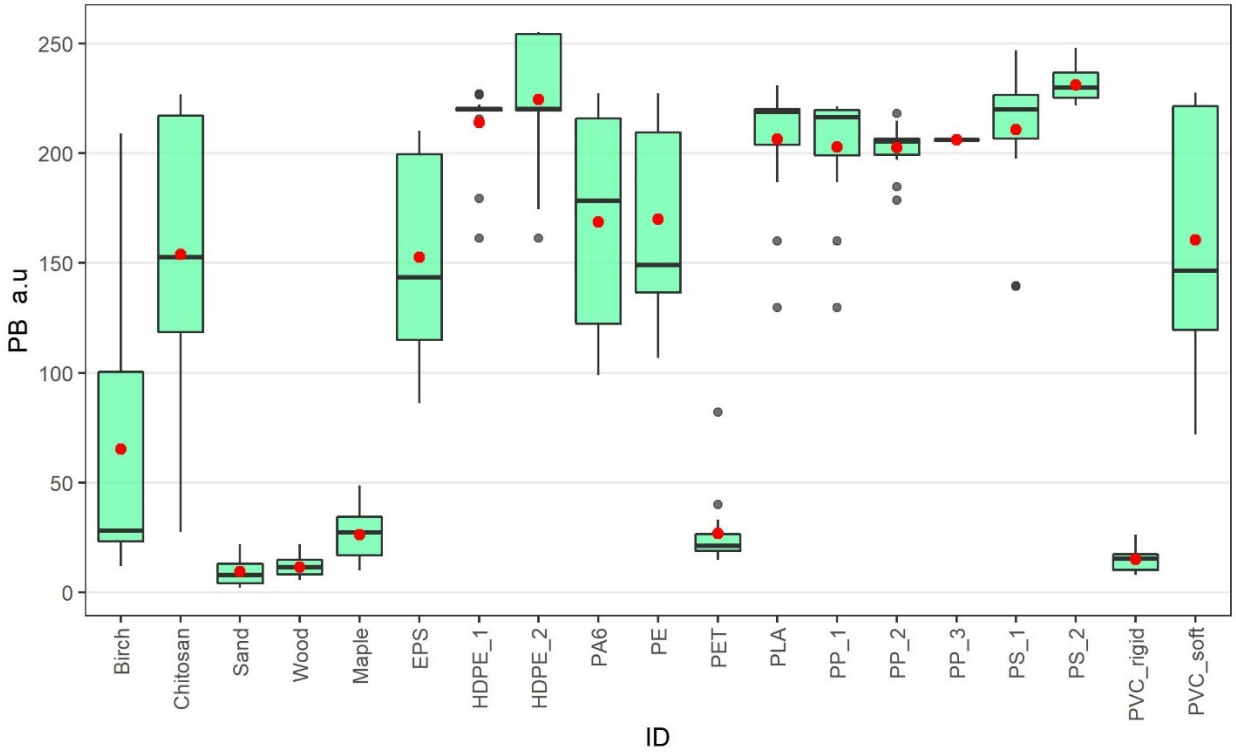


Figure 2.3 Pixel brightness (PB) in arbitrary units (a.u) for tested samples under 32x magnification, light intensity of 12 and exposure time of 50 ms. The black line indicates the median, and red dots represent mean values for measured PB, while black dots show outliers.

The rigid PVC sample tested seemed to stain relatively poorly with Nile Red. To better understand this, we tested another type of PVC. Plasticized, soft PVC tubing was cut into smaller pieces, ground, and the steps above were repeated with the chosen settings (32x magnification, light intensity 12 and 50 ms exposure). Our results show that soft PVC was easily detectible with fluorescent microscopy, as the mean PB value was 160 a.u. and 87% of all particles were found to be fluorescent above the set 100 a.u. limit (Figure 2.3). We hypothesize that the poor and uneven staining of the rigid PVC was due to its high crystalline melting temperature and/or colorants used

in products containing this plastic type (Wang et al., 2021, Nel et al., 2021a). It is recommended that further research should focus on improving our understanding of how Nile Red reacts with different polymer surfaces.

2.6.3 Microplastic identification key

To ensure that clear steps were taken to improve reproducibility and to increase transparency, an identification key was created to be used in conjunction with the fluorescence detection limit of 100 a.u set above by the researchers in our facility. It is presented here and, in the Appendix 1, as an example for the research community with the aim to enhance reproducibility and repeatability in the future.

The key comprises four parts, a general part that describes an overall decision on whether a certain particle should be considered further (Figure 2.4), and three morphology-specific identification keys to be applied in bright-field mode, which can be found from the Appendix 1: fibres (Appendix 1: Figure S2.3), spheres/beads (Appendix 1: Figure S2.4) and fragments, which includes films (Appendix 1: Figure S2.5). Building this extra layer into the identification key to account for morphology adds to the quantification accuracy. Some examples of particles identified in natural samples using the identification key are also included in the images presented in Appendix 1: Figure S2.6 in order to illustrate some of the descriptions provided.

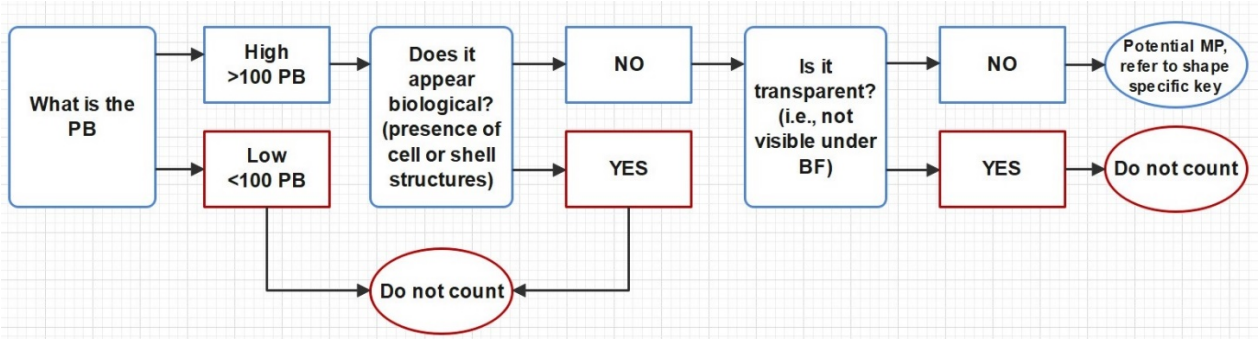


Figure 2.4 General part of the MP identification key that all MP had to adhere to. Note: 'is it transparent' refers in this context to a highly fluorescent particle without any visible biological structure, which becomes essentially invisible for the researcher under Bright-field, making positive identification impossible (PB – pixel brightness, BF – Bright-field microscopy, MP - Microplastic).

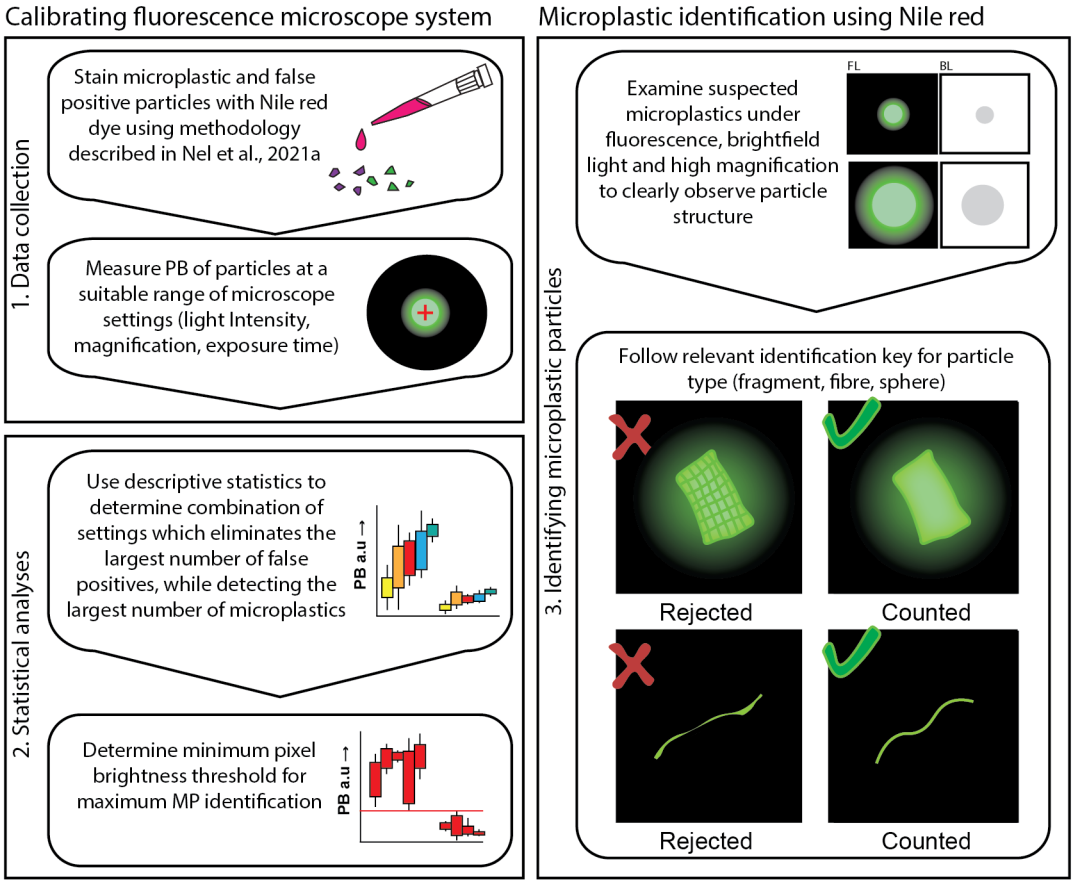


Figure 2.5 A schematic framework for the workflow described in this paper. 1) Data collection for the calibration of the fluorescence microscope, 2) Use of statistical analysis to identify a suitable threshold whereby most of the MP will be detected and most of false positives will not. 3) Use the determined pixel brightness (PB) threshold for pre-screening of particles of interest and develop/adjust existing MP identification key(s) to reduce false positive detection, e.g., of biological entities

2.6.4 Method application to freshwater samples

To evaluate the ease with which the identification key and fluorescence detection limits can be applied to quantification of MP extracted from freshwater samples by different researchers, two independent researchers working on two separate environmental sample sets were asked to apply

the fluorescence detection limits set here, as well as the MP identification key detailed above. Both researchers underwent training for a day on the microscope, after which they proceeded with counting and identifying putative MP in riverbed sediment and water samples according to the method set above. The sequence of the method was: 1) screen the filter under fluorescence mode for particles with light intensity above 100 a.u.; 2) follow the identification keys for any particle above 100 a.u to rule out false positives and confidently identify any MP; and 3) screen the filter for fibres only under bright-field mode and use the fibre key for assessment of any fibres detected. The first researcher had five riverbed sediment samples and the second researcher had five river surface water samples. A minimum of 25% of all the particles identified according to this method were then further analysed for their chemical make-up.

The first researcher was asked to pick roughly 30% of putative MP fibres and fragments from the five filters that were sampled and extracted from riverbed sediment. In total, this amounted to 18 out of 78 identified potential MP. These were then filtered onto 25 mm silver membranes and analysed with a Bruker Hyperion 2000 microscope, coupled with a Vertex 70 FT-IR spectrometer at the University of East Anglia (UK). The 20 × Ge-tipped ATR lens was used for spectral acquisition and identities were assigned by spectral searching in a Bruker polymers database (Details see SI Kukkola et al., 2022). Hit quality Index was set to minimum 60%, but peak position was prioritised over peak intensity. In total the researcher picked nine fibres and nine fragments. One particle and one fibre got lost during transfer onto the silver filter(s), leaving eight fibres and eight fragments available for analysis. The identification results are shown in Table 2.1 below.

Researcher Two was similarly asked to pick roughly 30% of particles that they had identified as MP according to this method (in total 25 particles out of 98 particles). These were transferred

onto anodiscs (Whatman, 25 mm diameter, 0.2 µm pore size) for Raman spectroscopy. A Renishaw InVia Qontor Raman microscope equipped with a 785 nm laser was used for chemical verification. The objective used was 10 x with slit width 65 µm, 1200 l/mm, spatial resolution < 1µm and a spectral resolution < 1 cm^{-1}, laser intensity 10% of the system (approximately 15 mW). 10 accumulations of 1 s exposures were repeated three times per particle. Spectral pre-processing for baseline and signal smoothing were implemented in Spectragryph v1.2.15.1 (Munno et al., 2020), using the advanced baseline function (coarseness = 10 and offset = 0) and the advanced smoothing function (Savitsky-Golay filter with window = 10 and order = 3). The processed spectra were then matched using the Pearson correlation coefficient for the fingerprint region to the reference libraries SLOPP, SLOPP-E (Munno et al., 2020) and in-house built reference libraries. The results are shown in Table 2.2.

Of the nine putative MP fragments picked by the first researcher, eight were identified as MP (four PE, four PP) while one particle was lost during processing. From the nine fibres, again one particle was lost, while six were identified as plastics (four PA, one PE, one PET), one as cellulose and one fibre was unclassified. For the putative MP picked by the second researcher, from thirteen selected fragments, all thirteen were identified as plastic (four PE, four PET, five PA) with three more particles showing up in the Raman analysis as unclassified while for the twelve selected fibres, eight were identified as plastic (seven PET, one polyester (PEST)), one particle was lost and three were unclassified. For our examples, we see that based on the fluorescence limit and the identification key, between 70 and 100% of the selected particles were validated to be MP with FTIR or Raman spectroscopy. This suggests that our method combining well-established fluorescence limits with a rigorous identification key is generally reliable. Any excess particles picked up during Raman spectroscopy are, in our example, probably organic material transferred

to the anodiscs along with the MP. However, full-filter scanning with Raman spectroscopy on the original GF/D filters would have taken excessively long and future research should focus on how Raman spectroscopy can be used in fluorescence mode, to aid in the selection of particles for chemical analysis. Researcher Two was also able to select PVC and PEST (not originally tested for) following the above method, leading us to the conclusion that our method although simple is rather robust.

Table 2.1: Results from FTIR analysis for the MP particles chosen by Researcher One for chemical analysis for identification of polymer-types.

	PE	***PP***	***PA***	***PET***	***lost***	***Weak spectrum***	***Cellulose (Possible synthetic)***	***sum***	***Plastic ID***
Fibre (n=9)	**1**	**0**	**4**	**1**	**1**	**1**	**1**	**9**	**6**
Fragment (n=9)	**4**	**4**	**0**	**0**	**1**	**0**	**0**	**9**	**8**

Table 2.2: Results from Raman spectroscopy for MP particles chosen by Researcher Two for confirmatory chemical analysis of polymer type.

Morphology & Number picked	***PP***	***PET***	***PVC***	***PEST***	***PE***	***Unclassified/burnt***	***sum***	***Plastic ID***
Fibre (n=12)	**0**	**7**	**0**	**1**	**0**	**3**	**11**	**8**
Fragment (n=13)	**4**	**4**	**5**	**0**	**0**	**3**	**16**	**13**

2.6.5 Additional information

These results clearly highlight that a fluorescence detection limit of 100 a.u was efficient in identifying up to 90% of plastic particles. However, even when the detection limits are set some false positives do still occur, and it has been reported that Nile Red does not stain some synthetic fibres well (Prata et al., 2019, Galvão et al., 2023). This implies that while Nile Red is valuable for choosing particles for further screening, it needs to be coupled with methodological visual identification/verification in order to eliminate naturally occurring particles. This can take the form of an identification key with different types of visual cues to determine if something should be counted as MP or not. For example, as suggested by Galvão et al., 2023, some natural fibres, such as cotton and linen, may stain with Nile Red. However, the occurrence of these natural fibres as false positives can be easily countered when fibres are inspected further: natural fibres typically exhibit distinct morphology, such as being internally segmented or twisted around themselves (ribbon-like) (Stanton et al., 2019b, Murphy et al., 2016). It is also suggested herein that in order to counter the potential for false negatives, such as synthetic fibres whose presence may be missed due to poor staining, as a last step the filter will be scanned under bright-field following the identification key established for fibres. Decision/identification keys can facilitate transparency in the MP research community and add to the reproducibility of results. The identification key that was created based on relevant literature (MARI, 2017, Lusher et al., 2020, Hidalgo-Ruz et al., 2012, Stanton et al., 2019b, Zhu et al., 2019) and the expertise and of University of Birmingham researchers is demonstrated in the Appendix 1 as an example.

The results presented here indicate that the pre-set MP selection criteria, which rely not only on the fluorescence detection limit, but also consider morphological cues via the identification key,

provide a reliable, fast, and transparent tool for MP identification. We propose this approach to be implemented for the MP community, as it can lead to more reproducible and consistent results. It should be noted that each new fluorescence system/microscope requires individual calibration to determine its optimal detection limits, as described above. Re-analysis of older samples might also be beneficial, as in many cases there has been over-identification of fibres at the expense of fragments and other shapes, which the identification-tree presented here also helps to overcome. The overall workflow for setting fluorescence detection limits and how to use identification key is presented in Figure 2.5.

2.6.6 Acknowledgements

Funding from The Leverhulme Trust via the "PlasticRivers" - The fate and transport of microplastics in rivers (RPG-2017-377) project is gratefully acknowledged. U.S. was supported by funding from the German Research Foundation (DFG – grant number 403826296), and Y.Y by the NERC-funded International Freshwater Microplastics Network (Grant number: NE/T004533/1). The authors extend their gratitude to Professor Dr. Andrew Mayes for his insight, knowledge and help with FTIR**.**

2.6.8 References

GALVÃO, L. S., FERREIRA, R. R., FERNANDES, E. M. S., CORREIA, C. A., VALERA, T. S., DOS SANTOS ROSA, D. & WIEBECK, H. 2023. Analysis of selective fluorescence for the characterization of microplastic fibres: Use of a Nile Red-based analytical method to compare between natural and synthetic fibres. *Journal of Hazardous Materials,* 443**,** 130217.

HIDALGO-RUZ, V., GUTOW, L., THOMPSON, R. C. & THIEL, M. 2012. Microplastics in the Marine Environment: A Review of the Methods Used for Identification and Quantification. *Environmental Science & Technology,* 46**,** 3060-3075.

KUKKOLA, A. T., SENIOR, G., MAES, T., SILBURN, B., BAKIR, A., KRÖGER, S. & MAYES, A. G. 2022. A large-scale study of microplastic abundance in sediment cores from the UK continental shelf and slope. *Marine Pollution Bulletin,* 178**,** 113554.

LENZ, R., ENDERS, K., STEDMON, C. A., MACKENZIE, D. M. A. & NIELSEN, T. G. 2015. A critical assessment of visual identification of marine microplastic using Raman spectroscopy for analysis improvement. *Marine Pollution Bulletin,* 100**,** 82-91.

LÖDER, M. G. J. & GERDTS, G. 2015. Methodology Used for the Detection and Identification of Microplastics—A Critical Appraisal. *In:* BERGMANN, M., GUTOW, L. & KLAGES, M. (eds.) *Marine Anthropogenic Litter.* Cham: Springer International Publishing.

LUSHER, A. L., BRÅTE, I. L. N., MUNNO, K., HURLEY, R. R. & WELDEN, N. A. 2020. Is It or Isn't It: The Importance of Visual Classification in Microplastic Characterization. *Applied Spectroscopy,* 74**,** 1139-1153.

LV, L., QU, J., YU, Z., CHEN, D., ZHOU, C., HONG, P., SUN, S. & LI, C. 2019. A simple method for detecting and quantifying microplastics utilizing fluorescent dyes - Safranine T, fluorescein isophosphate, Nile red based on thermal expansion and contraction property. *Environmental Pollution,* 255**,** 113283.

MAES, T., JESSOP, R., WELLNER, N., HAUPT, K. & MAYES, A. G. 2017. A rapid-screening approach to detect and quantify microplastics based on fluorescent tagging with Nile Red. *Scientific Reports,* 7**,** 44501.

MARI. 2017. *Guide to microplastic identification* [Online]. Available: Retrieved from; https://www.ccb.se/documents/Postkod2017/Mtg050317/Guide%20to%20Microplastic%20Identification_MERI.pdf [Accessed].

MUNNO, K., DE FROND, H., O'DONNELL, B. & ROCHMAN, C. M. 2020. Increasing the Accessibility for Characterizing Microplastics: Introducing New Application-Based and Spectral Libraries of Plastic Particles (SLoPP and SLoPP-E). *Analytical Chemistry,* 92**,** 2443-2451.

MURPHY, F., EWINS, C., CARBONNIER, F. & QUINN, B. 2016. Wastewater Treatment Works (WwTW) as a Source of Microplastics in the Aquatic Environment. *Environmental Science & Technology,* 50**,** 5800-5808.

NABI, I., BACHA, A.-U.-R. & ZHANG, L. 2022. A review on microplastics separation techniques from environmental media. *Journal of Cleaner Production,* 337**,** 130458.

NEL, H. A., CHETWYND, A. J., KELLEHER, L., LYNCH, I., MANSFIELD, I., MARGENAT, H., ONOJA, S., GOLDBERG OPPENHEIMER, P., SAMBROOK SMITH, G. H. & KRAUSE, S. 2021a. Detection limits are central to improve reporting standards when using Nile red for microplastic quantification. *Chemosphere,* 263**,** 127953.

NEL, H. A., CHETWYND, A. J., KELLY, C. A., STARK, C., VALSAMI-JONES, E., KRAUSE, S. & LYNCH, I. 2021b. An Untargeted Thermogravimetric Analysis-Fourier Transform Infrared-Gas Chromatography-Mass Spectrometry Approach for Plastic Polymer Identification. *Environmental Science & Technology,* 55**,** 8721-8729.

NEL, H. A., DALU, T., WASSERMAN, R. J. & HEAN, J. W. 2019. Colour and size influences plastic microbead underestimation, regardless of sediment grain size. *Science of The Total Environment,* 655**,** 567-570.

NEL, H. A., NAIDOO, T., AKINDELE, E. O., NHIWATIWA, T., FADARE, O. O. & KRAUSE, S. 2021c. Collaboration and infrastructure is needed to develop an African perspective on micro(nano)plastic pollution. *Environmental Research Letters,* 16**,** 021002.

PLASTICSEUROPE 2022. Plastics - The facts 2021.

PRATA, J. C., REIS, V., MATOS, J. T. V., DA COSTA, J. P., DUARTE, A. C. & ROCHA-SANTOS, T. 2019. A new approach for routine quantification of microplastics using Nile Red and automated software (MP-VAT). *Science of The Total Environment,* 690**,** 1277-1283.

SHIM, W. J., HONG, S. H. & EO, S. E. 2017. Identification methods in microplastic analysis: a review. *Analytical Methods,* 9**,** 1384-1391.

SHIM, W. J., SONG, Y. K., HONG, S. H. & JANG, M. 2016. Identification and quantification of microplastics using Nile Red staining. *Marine Pollution Bulletin,* 113**,** 469-476.

SHRUTI, V. C., PÉREZ-GUEVARA, F., ROY, P. D. & KUTRALAM-MUNIASAMY, G. 2022. Analyzing microplastics with Nile Red: Emerging trends, challenges, and prospects. *Journal of Hazardous Materials,* 423**,** 127171.

SONG, Y. K., HONG, S. H., JANG, M., HAN, G. M., RANI, M., LEE, J. & SHIM, W. J. 2015. A comparison of microscopic and spectroscopic identification methods for analysis of microplastics in environmental samples. *Marine Pollution Bulletin,* 93**,** 202-209.

STANTON, T., JOHNSON, M., NATHANAIL, P., GOMES, R. L., NEEDHAM, T. & BURSON, A. 2019a. Exploring the Efficacy of Nile Red in Microplastic Quantification: A Costaining Approach. *Environmental Science & Technology Letters,* 6**,** 606-611.

STANTON, T., JOHNSON, M., NATHANAIL, P., MACNAUGHTAN, W. & GOMES, R. L. 2019b. Freshwater and airborne textile fibre populations are dominated by 'natural', not microplastic, fibres. *Science of The Total Environment,* 666**,** 377-389.

WANG, C., JIANG, L., LIU, R., HE, M., CUI, X. & WANG, C. 2021. Comprehensive assessment of factors influencing Nile red staining: Eliciting solutions for efficient microplastics analysis. *Marine Pollution Bulletin,* 171**,** 112698.

ZHU, X., NGUYEN, B., YOU, J. B., KARAKOLIS, E., SINTON, D. & ROCHMAN, C. 2019. Identification of Microfibres in the Environment Using Multiple Lines of Evidence. *Environmental Science & Technology,* 53**,** 11877-11887.

Chapter 3: Nano and microplastic interactions with freshwater biota – Current knowledge, challenges and future solutions

Anna Kukkola,[a*] Stefan Krause, [a, b, c] Iseult Lynch, [a, c] Gregory H. Sambrook Smith, [a] Holly Nel [a]

[a] School of Geography, Earth and Environmental Sciences, University of Birmingham B15 2TT, Birmingham, United Kingdom.

[b] LEHNA- Laboratoire d'ecologie des hydrosystemes naturels et anthropises, University of Lyon, Darwin C & Forel, 3-6 Rue Raphaël Dubois, 69622 Villeurbanne, France.

[c] Institute of Global Innovation, University of Birmingham B15 2SA, Birmingham. United Kingdom.

***This chapter has been published in Environment International:**

https://doi.org/10.1016/j.envint.2021.106504

3.1 Abstract

Current understanding of nano- and microplastic movement, propagation and potential effects on biota in freshwater environments is developing rapidly. Still, there are significant disconnects in the integration of knowledge derived from laboratory and field studies. This review synthesizes the current understanding of nano- and microplastic impacts on freshwater biota from field studies and combines it with the more mechanistic insights derived from laboratory studies. Several discrepancies between the field and laboratory studies, impacting progress in process understanding, were identified including that the most prevalent plastic morphologies found in the field (fibres) are not those used in most of the laboratory studies (particles). Solutions to overcome these disparities are proposed to aid comparability of future studies. For example, environmental sampling and separation of biota into its constituents is encouraged when conducting field studies to map microplastic uptake preferences. In laboratory studies, recommendations include performing toxicity studies to systematically test possible factors affecting toxicity of nano- and microplastics, including morphology, chemical makeup (e.g., additives) and effects of plastic size. Consideration should be given to environmentally relevant exposure factors in laboratory studies, such as realistic exposure medium and effects of plastic ageing. Furthermore, based on this comprehensive review recommendations of principal toxicity endpoints for each of the main trophic levels (microbes, primary producers, primary consumers and secondary consumers) that should be reported to make toxicity studies more comparable in the future are given.

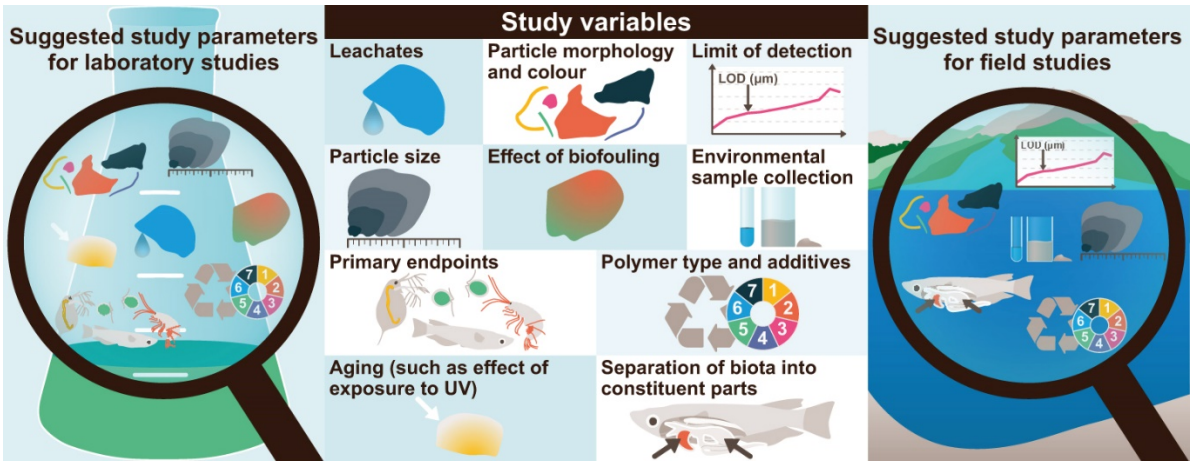


Figure 3.0 Graphical abstract

3.2 Introduction

Plastic pollution in the world's oceans is a widely reported issue (Cózar et al., 2014, Geyer et al., 2017, Jambeck et al., 2015). Besides the visible macroplastic, there is also concern surrounding smaller plastics, such as microplastics (dimension less than 5 mm) (Arthur et al., 2009, GESAMP, 2016, Thompson et al., 2004a), and nanoplastics (despite some ongoing debate in the literature generally considered less than 1000 nm). These micro and nanoscale plastics are referred to hereafter as MnP, unless specifically only micro or nanoplastics are discussed. MnP can be either directly designed and produced for this specific size-range (primary), or result from breakdown of macroscale plastic into smaller pieces (secondary) due to physical, photochemical and/or biological degradation (Corcoran et al., 2009, Dawson et al., 2018, Mateos-Cárdenas et al., 2020, O'Brine and Thompson, 2010, Zbyszewski et al., 2014).

To date, a vast majority of plastic research has focused on marine and coastal environments (Desforges et al., 2014, Kanhai et al., 2017, Lusher et al., 2015, Munari et al., 2017, Van

Cauwenberghe et al., 2015, Woodall et al., 2014) with the transport, fate and impact of plastics in freshwater systems only recently gaining attention (Li et al., 2018, Krause et al., 2021). This is likely driven by the increasing realization that lakes and rivers are not merely conduits transporting MnP from terrestrial sources to the marine environment, but also have the potential to act as temporary/long-term sinks (Hurley et al., 2018, Luo et al., 2019b). There is, thus, a risk that MnP may cause detrimental effects to freshwater ecosystems.

Microplastics have been found in the surface waters and sediments of both rivers and lakes (Eerkes-Medrano et al., 2015, Li et al., 2018, Tibbetts et al., 2018). They can enter freshwater systems via various pathways, such as outfall from waste water treatment plants (WWTP) (Murphy et al., 2016), or through surface runoff (Corradini et al., 2019, Kole et al., 2017, Liu et al., 2019a). Microplastics can also find their way into freshwater systems through transport via air and accumulate as dry or wet deposits (Allen et al., 2019, Dris et al., 2017, Dris et al., 2016). Although the extent of our knowledge is not the same for nanoplastics, due to extraction (sampling) and detection limitations, it is suspected that nanoplastics are present everywhere that microplastics are, and may follow similar transport and fate pathways to those of microplastics (Wang et al., 2021).

MnP interaction and/or ingestion and their effects have been documented for a variety of freshwater biota, such as algae, zooplankton, fish and birds (Faure et al., 2015, Sadler et al., 2019, Wu et al., 2019) (Figure 3.1).

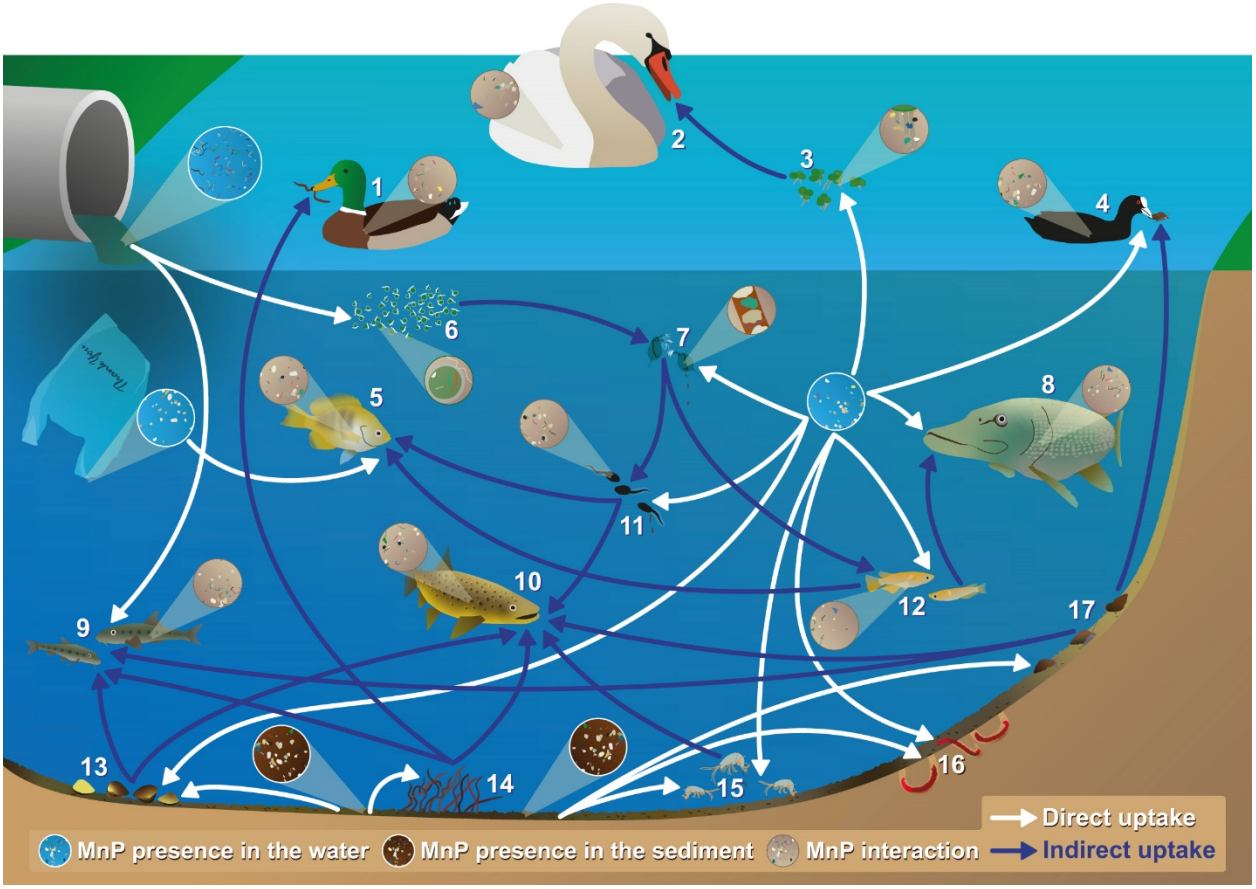


Figure 3.1. Conceptual model for MnP movements in the freshwater food web. Numbers (1-16) indicate that MnP interaction with this biotic group has been confirmed (Table S3.1). Species in the figure: 1) *Anas platyrhynchos,* 2) *Cygnus olor,* 3) *Lemna minor,* 4) *Fulica atra,* 5) *Lepomis macrochirus,* 6) *Chlorella vulgaris,* 7) *Daphnia magna,* 8) *Esox lucius,* 9) *Gobio gobio,* 10) *Squalius cephalus,* 11) *Microhyla ornate,* 12) *Alburnus alburnus* 13) *Dreissena polymorpha,* 14) *Tubifex tubifex,* 15) *Gammarus pulex and* 16) *Chironomus spp.*

There is some initial evidence of pollutant transfer from MnP to organisms (Coffin et al., 2019, Rochman et al., 2013, Wardrop et al., 2016). However, it is still debated whether MnP can be considered an environmentally relevant pathway for sorbed pollutants (Hartmann et al., 2017,

Koelmans, 2015, Koelmans et al., 2016). Nevertheless, MnP could be toxic to biota in their own right through physical effects, such as slowed egestion times (Au et al., 2015, Shang et al., 2020), that could lead to clogging or damage of intestinal tracts (Lei et al., 2018). This, together with the realization that MnPs are omnipresent in freshwater systems, has led to an expansion of interaction and toxicity studies in freshwater organisms. However, this research field is still in its infancy and potential entry points, uptake mechanisms, and fate for MnP in biota and consequently into food-webs have not yet been clearly established (Krause et al., 2021, Wong et al., 2020). In particular, analytical methods to quantify MnP burden are still being optimized for environmental matrices (Hartmann et al., 2019) and biological tissues (Wagner et al., 2017). There are also questions regarding how well laboratory studies reflect field data and vice versa. This review aims to provide a pathway forward whereby harmonization between field and laboratory studies is discussed. This extensive review of over 76 field and 164 laboratory studies also aims to find commonalities amongst published literature that may support future studies by providing a solid baseline against which to design and implement future experimental and sampling campaigns, thereby maximizing their increased comparability and utility for risk assessment. Therefore, a comprehensive synthesis of current research on MnP interactions with freshwater biota was performed to:

1. Identify freshwater species shown to be capable of interacting with MnP in the field and the laboratory at the different trophic levels;
2. Establish potential patterns in the freshwater MnP literature including types of plastics found/used, geographical context and the physical characteristics of the MnP assessed;
3. Identify key areas for increased alignment of laboratory and field research, to facilitate risk assessment, and the priority challenges for future research, for which we propose solutions.

3.3 Methods

A comprehensive literature review was carried out using Web of Science with the following topic search equation:

TS=(((microplastic OR nanoplastic*) AND (freshwater OR lake OR river)) AND (ingestion OR abundance OR occurrence OR content OR quantity OR feeding OR contamination OR gut OR intestines OR gastrointestinal OR bioaccumulation OR bioavailability OR uptake OR organism*))*

Publications for the period 2011 and 2020 have been included in this review. Studies were analysed using the following four criteria: 1) Original study (reviews were excluded), 2) Focus on freshwater ecosystems (salinity less than 0.5% or 0.5 ppt), 3) Report results showing an interaction between MnP and freshwater organisms, and 4) Quantifies or uses plastics less than 5 mm in diameter (Arthur et al., 2009, GESAMP, 2016, Thompson et al., 2004a). The initial search yielded 878 matches from which 656 articles were excluded due to not conforming with the criteria set above. An additional 18 articles met the criteria for inclusion after citation analysis was carried out for the studies included from the first step, bringing the total number of journal articles reviewed for this synthesis to 240 (Appendix 2: Table S3.1).

The studies were divided into field or laboratory based research. Studies were also grouped into: algae, vascular plants, microbes, cladocerans (separated from the rest of crustaceans, due to high occurrence in the literature), crustaceans, gastropods, dipterans, bivalves, annelids, amphibians, fish, birds, and others. These biota groups were then organized into the following four trophic levels:

1. Microbes

2. Primary producers (algae, vascular plants)

3. Primary consumers (cladocerans, crustaceans, gastropods, dipterans, bivalves, annelids and others)

4. Secondary consumers (amphibians, fish, and birds)

From each of these trophic levels the following were identified; 1) species studied, 2) physical (i.e., size, morphology, colour) and chemical (i.e., plastic type) characteristics of the MnP identified (field) or used (laboratory) and 3) methodologies (characterization and toxicity endpoints) used. Toxic effects were included in the context of identifying potential endpoints that could be used for baseline studies, but were not extensively reviewed, as this topic has been covered previously (e.g.,Anbumani and Kakkar, 2018, Triebskorn et al., 2019, Prokić et al., 2019) and was considered to be out of the scope of this study.

Size was divided into two separate categories: microplastics (1 - 5000 μm) and nanoplastics (less than 1000 nm). Morphology of plastics was assigned into three main categories; a) fibres, b) particles (that encapsulated both spheres and granules due to lack of morphology characterization in several studies) and c) fragments.

To identify any regional hotspots of MnP research, the origin of laboratory studies was assessed according to the locations of the first and last author's facilities/addresses, while field studies had their respective sampling location(s) recorded independently of the author's respective locations.

3.4 Results

3.4.1 General results

From the 240 studies, 76 (~32%) field studies and 164 (~68%) laboratory studies were identified (Appendix 2: Table S3.1).

3.4.2 Types of plastics

Polyethylene (PE) was the most common plastic type found in field studies, followed by polypropylene (PP), polyethylene terephthalate (PET), polyamide (PA) and polystyrene (PS), as shown in Figure 3.2. 'Not given' was the largest group in field studies, highlighting the lack of chemical verification tools used, with forty-two percent of studies not including polymer identification. In laboratory studies, the most frequently used plastic was PS, followed by PE, 'others', PP and PET. Here also, several papers used a commercial microplastic for which no compositional information was available (grouped as "other"), reducing the utility of the data for risk assessment.

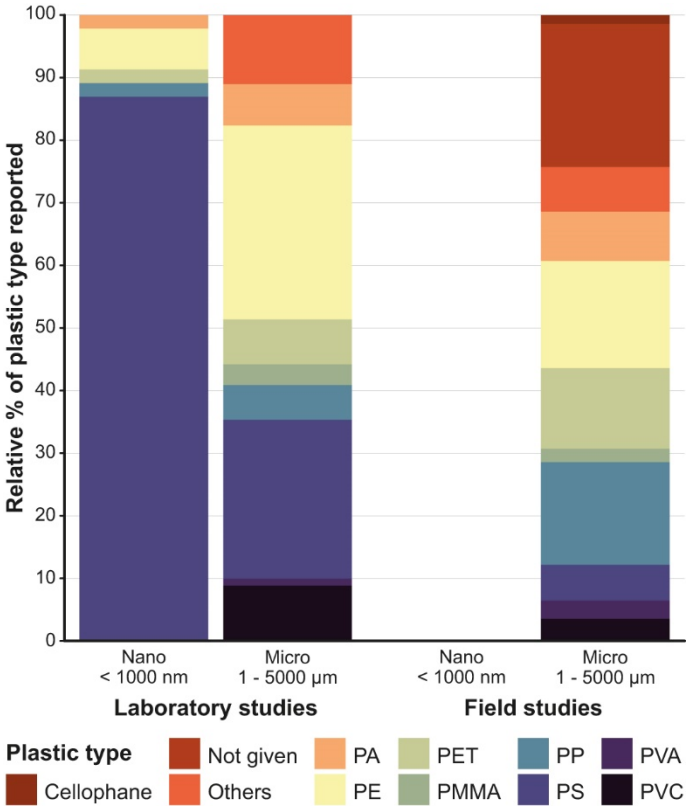


Figure 3.2. Most common MnP plastic types reported across laboratory and field studies.

2.4.3 Sizes and morphology of plastics

Most of the studies fell into the size range of microplastics, with reports on nanoplastics being absent from field studies. Twenty-six percent of field studies did not report the respective size of the observed plastics (Figure 3.3), while laboratory studies included size by stating the commercial size range and in some instances provided additional size characterization information, via techniques such as dynamic light scattering (DLS) and/or scanning electron microscopy (SEM).

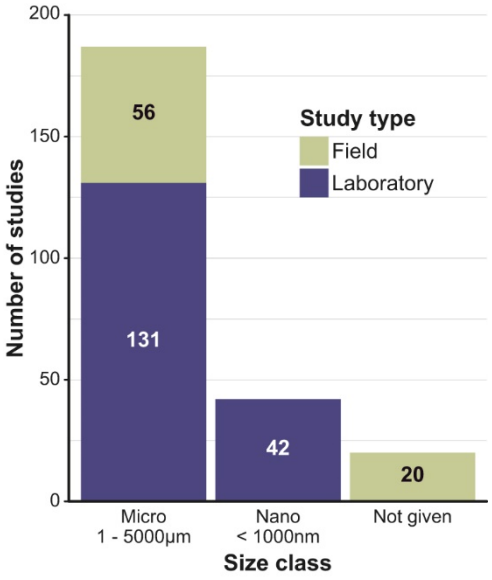


Figure 3.3. Relative abundance of studies per size class. Note that studies that included MnP from different size classes were counted as separate studies for the purpose of this figure.

The most prevalent morphology reported in field studies, where this information was available, was fibres (76.5%). However, particles were the most abundant morphology used (76.2%) in laboratory settings, with fibres used in eight studies (4.8%).

3.4.4 Geographical spread

Analysis of the spatial distribution identified some clear geographical hotspots for MnP research. The majority of laboratory studies originated from China (n=43), North America (n=20) and Europe (Germany (n=22), Italy (n=11) and UK (n=11)) as shown in Figure 3.4. This spread in laboratory studies is matched by patterns identified in the sampling locations of field studies, that were clustered in Europe (n=22), North America (n=14) and China (n=15).

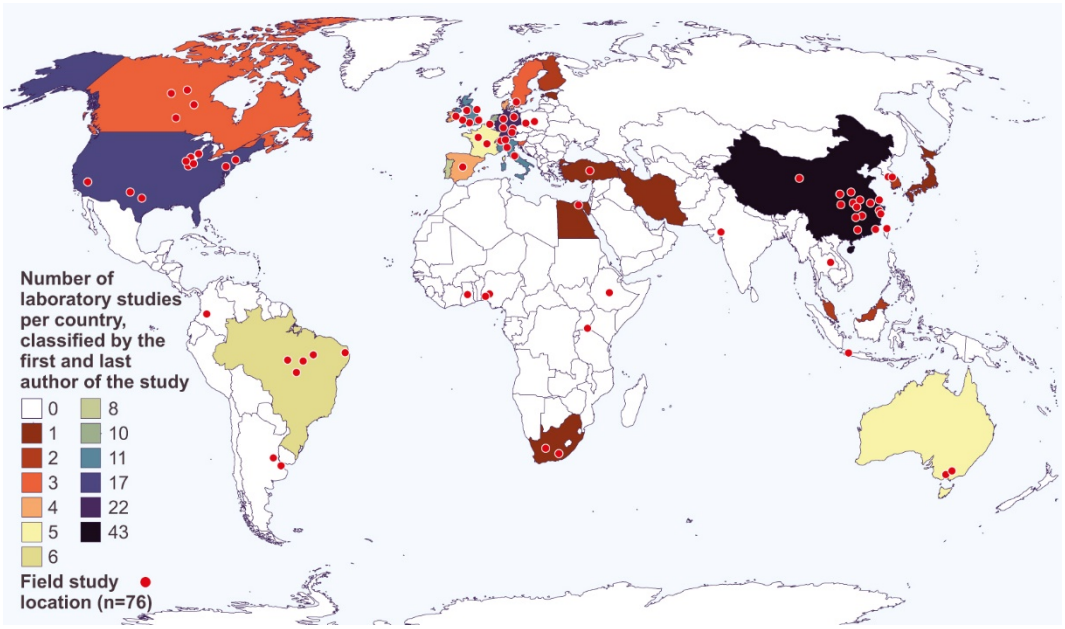


Figure 3.4. Number of laboratory studies per country, grouped via first and last authors of the studies and locations of the field sampling sites.

3.4.5 Trophic levels and biota groups

From the four trophic levels including thirteen biota groups defined above, fish were the most studied (n=90) making up ~59% of field studies and ~27% of laboratory studies. This was followed by cladocerans (n=43), which were all laboratory studies (Figure 3.5).

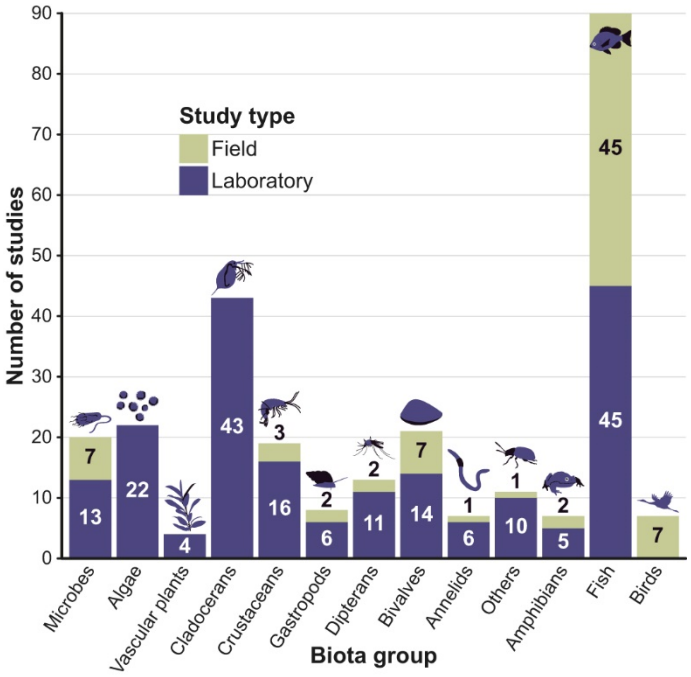


Figure 3.5. Number of published MnP interaction studies in freshwater biota groups. Note that one field study and some laboratory studies included more than one biota group and each species is counted separately for this figure.

3.5 Discussion

3.5.1 General discussion

The major plastic types used in laboratory settings and found in biota loosely follow the trends in global plastic production. According to PlasticsEurope (2020), the major plastics manufactured in 2019 were PE (29.8%), PP (19.4%), polyvinyl chloride (PVC) (10%), polyurethane (PUR) (7.9%), PET (7.9%) and PS (6.2%). A similar trend was observed in field studies (Figure 3.2), with PE and PP being the most common plastic types identified from the field samples, while the most common plastics used in laboratory studies were PS, followed by PE, PP and PET. Although most common plastic types are well represented in laboratory studies, it is recommended to extend

laboratory effect testing to more diverse range of plastic types. Special consideration should be given to those identified in biota from field studies, such as PA and cellophane, as the current trend favours certain plastic types and makes results difficult to compare.

Regional hotspots for laboratory and field research were found to largely overlap (Figure 2.4). Critically, Asian (apart from China) and African systems appear under-represented despite many of these regions, such as, South and Southeast Asia, having been identified as being amongst the most plastic polluted areas globally (Jambeck et al., 2015, Lebreton et al., 2017). The identified lack of field studies in these areas is therefore of concern, as this impedes our holistic understanding regarding global MnP pollution and its impacts on biota. Furthermore, the total number of field studies is still relatively low (n=76), when compared to laboratory studies. More observations are thus required, especially in highly polluted and under-represented regions, such as parts of Southeast Asia and Africa (Nel et al., 2021b).

There was a clear predisposition towards laboratory studies in all biotic groups, with the exception of fish and birds (Figure 3.5). Studying higher trophic level organisms in laboratory settings can pose ethical challenges, as well as being time consuming, which can partly explain this trend. From all biotic groups, fish were the most studied. Fish represent one of the largest classes of Animalia in freshwater systems and can stretch over several trophic levels and feeding guilds. As they are generally higher up in the food chain and have commercial importance and health implications for humans via consumption, it is logical that studies on MnP ingestion have focused on this group. However, more studies are required across the different biotic groups to map out the occurrence of MnPs in the field and to identify their potential ecosystem-level effects. In addition to more field studies, we identified three key challenges that freshwater MnP research is currently

facing, described below, along with proposed solutions to overcome them, which have also been summarized into Tables 3.1 and 3.2.

3.5.2 Challenges for future research

3.5.2.1 Challenge 1: The mismatch between field and laboratory studies

In order to predict effects of MnP on biota and freshwater ecosystems, exposure scenarios used in the laboratory should reflect real environmental conditions as closely as possible. Here, we explore the mismatch between field and laboratory studies and suggest solutions to close this gap.

Fibres were the most prominent microplastic morphology identified across taxa in field studies. This trend potentially reflects the relative abundance of fibres in the environment, as fibres are commonly identified in freshwater studies (Dris et al., 2015, Luo et al., 2019b, Wang et al., 2017). There appears to be a relationship between microplastic load within sediment and water, and microplastic burden within biota (Akindele et al., 2019, Li et al., 2020a, Lv et al., 2019, Nel et al., 2018, Su et al., 2018, Su et al., 2016, Yan et al., 2019). For example, Lv et al. (2019) found that the microplastic composition was similar between the crayfish *Procambarus 62zteca 62* and surrounding sediments, with fibres prevalent in both. Furthermore, Su et al. (2018) found that the microplastic load in bivalves at the Yangtze River basin was significantly dependent on both water and sediment microplastic contamination. In contrast, Su et al. (2016) reported that the microplastic load in bivalves was negatively correlated with the contamination in surrounding sediments. However, with only a handful of studies collecting data on MnP contamination from all compartments, this relationship remains inconclusive.

The prevalence of fibres could also be an indication of preferential consumption by certain biotic groups, especially in fish (Collard et al., 2019). There is evidence from laboratory studies

that visually orientated fish actively forage on MnP resembling their prey items (Roch et al., 2020). Indeed, Yuan et al. (2019) noted that the proportion of white fibres in goldfish from Poyang Lake, China, was higher than that found in the surrounding environment, which could indicate confusion with prey species, such as mosquito larvae or zooplankton. This is further supported by McNeish et al. (2018) where microplastic colours varied in surface water collected within the tributaries of Lake Michigan, (USA), which was not reflected in the fish who preferentially ingested blue and transparent fibres. Hurley et al. (2017) reported an absence of microbeads in the freshwater worm *Tubifex tubifex*, even though they were found in the surrounding sediment. Similarly, Schessl et al. (2019) reported an absence of microbeads in bivalves *Dreissena polymorpha* and *D. bugensis* despite their presence in the environment. Drivers of this apparent preferential uptake remain unknown; possibilities include size, morphology, biofouling and/or plastic type. Laboratory studies have begun focusing on this question, with Li et al. (2019) stating that uptake of plastic fibres in bivalves was related to the elastic modulus, i.e., "softness" of the plastic type. It is essential to test these possible drivers in laboratory settings.

An alternative explanation may be that fibres are accumulating in the gastrointestinal (GI) tracts of biota due to their elongated shape. There is some initial support for this hypothesis; the only two field studies that separated the individual fish into different parts (i.e., stomach, muscle, gills and liver), reported different microplastic morphologies present in the various regions. For example, Collard et al. (2018) indicated that in field conditions PS and PE fragments ranging from 147 to 567 µm appeared to translocate into the livers of European chubs *Squalius cephalus* after ingestion, while fibres were prevalent in the stomach. Similarly, Garcia et al. (2021) reported microplastic films being more prevalent in gut tissues of *Prochilodus magdalenae* and *Pimelodus*

grosskopfii whereas fragments were more prevalent in muscle and gills. Microfibre retention in the gut was also observed by Au et al. (2015) in a laboratory study, where PP fibres remained in the gut of the crustacean *Hyalella 64zteca* for longer than natural food and/or PE particles. This offers some initial support for the hypothesis that fibres could be retained in the gut for a longer duration. However, more research is needed targeting gut retention times of fibres.

The apparent dominance of fibres in field samples could also be a result of overestimation due to methodological bias in the applied analytical approach. For example, 31 out of 69 field studies (excluding studies on microbes) did not use any chemical verification tools and relied solely on visual identification and/or a hot needle test to confirm the presence of plastics. It is plausible that during the visual identification, the larger, less ambiguous fibres are more readily identified compared to other morphologies. The lack of chemical verification means that the identified fibres could also be natural or cotton fibres. Moreover, only six of the analysed papers stated clearly the lower size detection limit (Domogalla-Urbansky et al., 2019, Park et al., 2020, Roch et al., 2019, Winkler et al., 2020, Xiong et al., 2018, Yuan et al., 2019). This raises questions about the 'non-detected' fraction, and underestimation of smaller plastics could lead to overestimation of the pervasiveness of more easily identified fibres.

In order for the research community to address these challenges, there is a need to improve the extraction of MnP from field biotic samples: Firstly, relying on visual identification solely should be minimized, as this can discriminate against smaller MnP which are more difficult to identify. The use of tagging methods, such as fluorescent dyes, for example, Nile Red (Erni-Cassola et al., 2017, Maes et al., 2017, Nel et al., 2021a, Shim et al., 2016) that can reduce visual bias, should be explored (Table 3.1). Researchers are encouraged to refer to the reporting guideline

checklist and quality criteria published by Cowger et al. (2020), Collard et al. (2019) and Hermsen et al. (2018). Secondly, the lower detection limit (where putative MnP can be confidently identified) should always be reported in order to facilitate comparability between studies (Table 3.1).

Thirdly, where applicable (e.g., fish), it is important to separate the biota samples into different parts, such as brain, muscle, liver and gut (Table 3.1), which can give more specific information on where MnP are found and any preferential distributions (Collard et al., 2018, Garcia et al., 2021). More studies including this step are required, as there is contrasting evidence on tissue translocation (Collard et al., 2017, Elizalde-Velázquez et al., 2020, Jovanović et al., 2018, Zeytin et al., 2020, Zitouni et al., 2020) and disagreement exists particularly regarding the size fractions that are capable of translocating into tissues (as reviewed by Triebskorn et al. 2019). In the field of nanomedicine, it is generally accepted that endocytosis pathways are limited to particle sizes up to 5 µm (Kou et al., 2013, Zhang et al., 2009), raising questions regarding any potential mechanisms for translocation of larger items. It is plausible that bigger fragments (> 20 µm) could be methodological artefacts or contamination from processing of the samples, if not enough rigor is applied. However, granuloma formation has been proposed as a potential entry pathway for MnP into muscle tissue (Zeytin et al., 2020).

Digestion should be carried out for each separate body part, with the same digestive method, such as KOH (Karami et al., 2017a, Thiele et al., 2019), followed by the extraction step and chemical analysis (such as $ZnCl_2$ separation followed by Fourier-transform infrared (FT-IR) or Raman spectroscopy), and where possible 50% of putative MnP should be analysed (Hermsen et al., 2018) (Table 3.1). Extra care should be taken to reduce any false-positives, such as dislocation

or introduction of particles and/or fragments during dissection and rigorous control measures should be in place.

Fourthly, to fully address the possibility of the selective uptake of MnPs and to examine which factors in the immediate environment drive their ingestion, environmental samples (water column and sediment) should always be collected and analysed to characterize the sizes, morphologies, colours, and types of MnPs present (Table 3.1). The digestion, extraction and chemical analysis methods used for the environmental samples should match as closely as possible to those used for biota, in order to reduce any methodological bias. This would inform on the possible drivers of fibre uptake and would aid in the prioritization of plastics for laboratory exposure experiments.

Despite fibres being the most common morphology reported in the field, this is not reflected in laboratory studies, which most commonly employed particles. Only 8 out of 164 laboratory studies used fibres in MnP interaction studies (Appendix 2: Table S3.1), and only six studied their effects, from which all reported negative effects on the test species. For example, decreased growth was seen in the crustacean *H. azteca* and planarian *Dugesia japonica* exposed to 20 - 75 µm PP fibres (Au et al., 2015) and ~30 µm PET fibres (Gambino et al., 2020) and the freshwater flea *Daphnia magna* showed increased mortality rates when exposed to 60 - 1400 µm PET fibres (Jemec et al., 2016).

The type and origin of fibres used in these studies also varied. For example, Au et al. (2015) used aged PP marine rope. Jemec et al. (2016) used milled PET fabrics and Gambino et al. (2020) produced PET fibres in their laboratory. Evidence suggests that additives may influence toxicity (Boyle et al., 2020, Capolupo et al., 2020), therefore the same plastic type from different

commercial sources/products may further confound results, especially if information about chemical composition and additive content is not given. However, all fibres studied to date, regardless of the source, have shown negative effects on biota. It is clear, however, that there are not enough studies focusing on the effects of fibres and their leachates to build a full picture of their deleterious effects, and more systematic testing of different plastic fibre types (such as PET fibres in different lengths and colours) on multiple biota groups in needed.

The respective size classes found/used in field and laboratory studies also differed (Figure 3.3). The absence of nanoplastics in field data can be attributed to the current challenges in sample collection, extraction and quantification methods (Nguyen et al., 2019, Schwaferts et al., 2019). These smaller plastics should, however, be the focus of future research, as it is predicted that smaller plastics are more numeric, both in the environment and in biota (Roch et al., 2019, Triebskorn et al., 2019).

Table 3.1. Recommendations for field sampling that aims to understand the interplay between ingested MnP and environment.

Recommendations	
Collection of field samples in conjunction with biota samples	Sediment and water samples (background concentrations needed for assessment of potential biomagnification)
Separation of organism into its constituents	Stomach, muscle, liver and brain when applicable (i.e., fish) and quantification of MnP load in each

Usage of relevant digestion method	KOH, NaOH or similar. Match to that used for environmental samples
Identification methods	Tagging methods, such as fluorescent dyes, Chemical identification, such as FT-IR, Raman spectroscopy or GC-MS (50% of putative MnP)
Recording physical characteristics of MnP	Colour (where possible), morphology and size
Reporting	Lowest detection limit and internalised dose, as follows; number mg^{-1} tissue, mg mg^{-1} tissue and items $individual^{-1}$
Method development	To enable nanoplastic identification from the field samples

3.5.2.2. Challenge 2: Baseline studies comparing physical and chemical characteristics of MnPs and their effects on toxicity

To fully understand and map the effects of different MnP, a shift towards systematic reporting of MnP morphology, chemical makeup and size under specific exposure conditions, is needed to allow correlation of properties with potential toxic effects. Here, we introduce four major factors that could affect the MnP toxicity, each of which needs to be separately and systematically tested. Special attention should be given to realistic environmental exposure scenarios in terms of

exposure medium and the presence/absence of natural compounds, as well as the impact of aging of the MnP compared to effects of pristine MnP

i. Morphology

Plastic fibres have been reported to be more harmful than other tested morphologies (i.e., particles). For example, Au et al. (2015) reported that acute exposure to PP fibres (20 - 75 μm at 45 fibres mL^{-1}) reduced the growth rate of crustacean *H. azteca* in a dose dependent manner whereas exposure to PE particles (10 - 27 μm at 1 $x10^5$ particles mL^{-1}) did not. In this case it is difficult to determine whether the morphology or the chemical characteristics were causing the deleterious effect of PP as no control with similar morphologies were carried out. Ziajahromi et al. (2017) reported a lower LC_{50} (lethal concentration required to kill 50% of test population) value in *Ceriodaphnia dubia* for PET fibres (280 ± 50 μm at 5 $x10^{-4}$ mg mL^{-1} or 13 fibres mL^{-1}) than for PE particles (1 - 4 μm at 1 $x10^{-3}$ or 74 particles mL^{-1}). This, however, does not translate directly into fibrous MnP being more deleterious, as morphology along with any additives and plasticizers, total surface area and particle number differences may have confounded these results. It is also plausible that mode of exposure, i.e., how biota are exposed to MnP, could affect the harmfulness. For example, exposure of *C. dubia* to PET fibres resulted in more severe effects on body size and neonate numbers than exposure to PE particles despite having no fibres in their guts (Ziajahromi et al., 2017), suggesting that fibres caused physical harm but not via ingestion. Thus, the mode of exposure can play an important role in determining the effects of MnPs and should be taken into consideration in the study design (see iv. Environmental factors).

In order to fully address to what degree, the plastic morphology may impact toxicity, tests using the same/similar parent plastic with different morphologies must be carried out (Table 3.2), and the

observed effects must be differentiated by physical versus chemical damage where possible (direct and indirect effect). Use of computational image descriptors for shape, such as circulatory, convexity and main elongation, which can be determined with transmission electron microscopy (Varsou et al., 2020), may provide an useful approach to normalize between different morphologies and enable direct comparison of non-spherical morphologies.

Table 3.2. Recommendations for laboratory studies that aim to systematically understand the drivers and toxicological effects of MnP exposure.

Recommendations	
Morphology	Carry out exposures with similar parent plastic but different morphology (i.e., fragments, fibres, and spheres)
Chemical composition	1) Identify chemical fingerprint: e.g., colourants, plasticisers 2) Wash a sub-set of parent plastic for toxicity assessment of leachates 3) Avoid usage of proprietary polymers whose composition is unknown
Size	1) Systematic testing of similar parent plastic in different sizes e.g., PS 1 µm, 5 µm and 10 µm, match exposure dose by surface area, mass and MnP number

Exposure	1) Environmental considerations i.e., always provide food, consider the presence of organic matter, natural medium and mode of exposure etc. 2) Aging of the plastic i.e., Pristine vs aged (natural or laboratory aged) 3) Abundance i.e., Inclusion of lower concentrations with life-time exposure 3) Duration i.e., Extended monitoring periods and consider depuration steps
Endpoints	1) Microbes i) Principal endpoints: taxon richness ii) secondary endpoints: species specific preference for plastic type 2) Primary producers i) Principal endpoints: photosynthetic activity and growth ii) Secondary endpoints: gene regulations and stress responses 3) Primary consumers i) Principal endpoints: growth and mortality ii) Secondary endpoints: reproduction and multigenerational studies 4) Secondary consumers i) Principal endpoints: growth, mortality and reproduction

	ii) Secondary endpoints: behavioural changes, AChE and oxidative stress

ii. Chemical composition

MnPs found in nature consist of a complex mixture of monomers, plasticizers, colorants and other additives (OECD, 2014b). Therefore, to fully understand the effects of MnP, it is not sufficient to report and identify the different parent plastic types only (Figure 3.2), but also their chemical make-up, including additives, such as plasticizers, flame-retardants and colorants. Different MnP leachates have shown different degrees of effect on the freshwater algae *Raphidocelis subcapitata* (Capolupo et al., 2020), while the leachate from PVC was more toxic to zebrafish *Danio rerio* larvae than the plastic fragments themselves (Boyle et al., 2020). Similar leaching of additives (such as Bisphenol A) has been demonstrated in simulated gut conditions of marine biota (Coffin et al., 2019). As this leaching of additives could affect the observed toxicity, there is a need to differentiate between the toxicity of parent plastic and any specific additives. For example, routine washing of a sub-set of the parent plastic should be carried out to remove leachable additives, followed by parallel testing of the pristine and washed MnP and the leachate (Table 3.2), as this may shed important light into the exact drivers of any observed toxicity. The use of commercial polymers, where the composition is unknown should be discouraged in toxicity testing, and complete chemical mapping should be carried out for plastics used in the experiments. If this is not possible, the composition should be identified as a minimum to the level of parent

polymer/copolymer. Typical equipment used to identify parent plastic type includes equipment like FT-IR, Raman spectroscopy or similar. Identification of the additives could be carried out using equipment like gas chromatography–mass spectrometry (GC-MS), which would also be useful to extend emerging databases on plastic additives and spectra (Munno et al., 2020) and to correlate specific plastic sources with specific combination of additives that may prove diagnostic.

iii. MnP size

It has been shown in marine settings that plastic size can play an important role in MnP toxicity (Jeong et al., 2016, Lee et al., 2013). Similar size-dependent effects have been observed in freshwater species, for example, Lei et al. (2018) found that mortality of nematodes was related to the size of PS MnP (1.0 μm were less lethal than 0.1 or 5.0 μm). Similarly, the effect of PE MnP in dipterans *Chironomus riparius* and *C. tepperi* was more pronounced with decreasing particle sizes (Silva et al., 2019a, Ziajahromi et al., 2018).

It has also been observed that nanoplastics had a higher toxicity than microplastics in the freshwater flea *D. magna* (Ma et al., 2016). This higher toxicity could be related to nanoplastics ability to cross cell-walls and accumulate in sites such as the egg-yolk sacs of water flea, the gills, gut and liver of zebrafish, and the digestive gland of the bivalve *Elliptio complanata* (Auclair et al., 2020, Brandts et al., 2020, Chae et al., 2018, Lu et al., 2016, Parenti et al., 2019). Indeed, size dependent toxicity needs to be systematically tested using similar parent plastic type (Table 3.2).

iv. Environmental exposure considerations

To fully address the drivers behind MnP toxicity, all potential contributing factors i.e., morphology, composition and size, needs to be addressed in a proper environmentally relevant context (Table 3.2). Here, much can be learned from the nanomaterials eco-toxicological field,

where formation of an eco-corona, biofouling and ageing of the materials are increasingly recognized as being essential to realistic exposure and hazard assessment studies (Ellis et al., 2020, Nasser et al., 2020). It is important to realize that aging of plastics and other mechanisms such as adsorption of organic matter may affect the physical properties of the plastics. For example, growth inhibition of freshwater algae *Scenedemus subspicatus* and *Chlamydomonas reinhardtii* were found to be greater when exposed to aged or weathered rather than pristine plastics (Baudrimont et al., 2020, Wang et al., 2020b). Furthermore, Liu et al. (2019b) found that when zebrafish were co-exposed to1 μg L^{-1} and 1 mg L^{-1} of nano-sized PS (50 - 100 nm) and fulvic and humic acid, the reactive oxygen species (ROS) levels were stimulated synergistically. In contrast, the presence of these natural acidic organic polymers reduced the ROS level in freshwater algae *Scenedesmus obliquus*, suggesting that the presence of natural compounds in the medium affects MnP toxicity (Liu et al., 2019c, Liu et al., 2019b). Furthermore, Ziajahromi et al. (2018) reported that PE particles (10 - 27 μm) reduced the toxicity of the insecticide bifenthrin to Diptera *C. tepperi* in synthetic water but not in river water, indicating that consideration should be given to more realistic exposure media and their effects on toxicity. As discussed previously, mode of exposure might also play a key role; for example *C. tepperi* exposed to PE in sediment (500 particles Kg^{-1}) showed increased mortality (Ziajahromi et al., 2018), while exposure in water (1600 particles L^{-1}) showed no effect (Ziajahromi et al., 2019), indicating that how biota is exposed needs to be accounted for when planning experiments, and consideration should be given to whether this reflects environmentally realistic modes of exposure.

It is also important to understand how laboratory exposure concentrations compare with those observed in the environment. However, this can be problematic, as reported units for laboratory

and field studies varied. Exposure concentrations in laboratory studies were often mass per volume (mg L^{-1}) but reporting also MnP number and surface area might be more informative. Conversely, field studies reported mg individual^{-1}, or more often item individual^{-1}, making it difficult to compare the results between the two. In laboratory studies, it is common to use concentrations that span the expected effect threshold to ensure that an effect will be observed. Indeed, it is not uncommon to see arguably unrealistic exposure concentrations (De Felice et al., 2019, Li et al., 2020c) in laboratory studies. It is difficult, however, to predict what can be considered as 'environmentally relevant' concentrations, as there is uncertainty regarding the abundance of smaller MnP in the environment and occurrence of bigger microplastics varies with location(Li et al., 2018). Furthermore, the units used to report environmental concentrations are often item m^{-3} (water) and item Kg^{-1} (sediment), making it hard to relate directly to laboratory exposures which tend to report units as mass volume^{-1}. Regardless, it is imperative for the scientific community to expand the toxicity testing into lower exposure doses (such as MnP concentrations of 100 items L^{-1}) (Triebskorn et al., 2019) with extended exposure time scales to cover life-time and/or multiple generations (Table 3.2). For example, Kelpsiene et al. (2020) showed that when *D. magna* was exposed to 0.32 mg L^{-1} of 26 or 62 nm PS over its full life-time, increased mortality became obvious, which was not previously reported in acute 24 hour exposures to 400 mg L^{-1} (Mattsson et al., 2017) .

3.5.2.3 Challenge 3: Harmonization of endpoints reported for each trophic level

To facilitate inter-comparability of MnP toxicity data, common principal endpoints need to be identified for each trophic level, which should be included in each study as minimum. Here, potential principal endpoints for the four trophic levels identified in this paper (Figure 3.6, Table

3.2) are introduced, including justification for why these endpoints should be included in future studies.

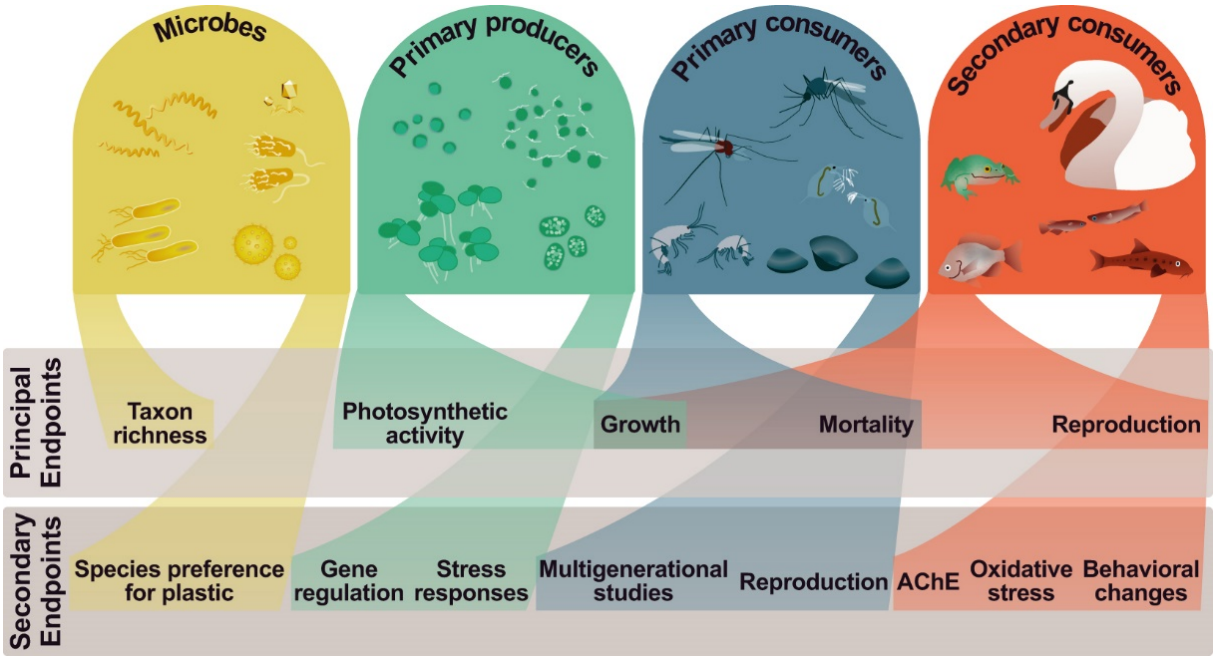


Figure 3.6. Potential principal and secondary toxicity endpoints for the four trophic levels.

i. Microbes

For microbes, the taxon richness, and its possible changes when in contact with different plastic types is the most important reporting requirement. There is evidence that MnP can act as a favourable substrate for specific microbial communities (Hoellein et al., 2017, Kettner et al., 2019, Li et al., 2020b, McCormick et al., 2014, McCormick et al., 2016). For example, McCormick et al. (2014), McCormick et al. (2016) and Kettner et al. (2019) found a lower species richness on microplastic surfaces when compared to the surrounding environment. This is further supported by Parrish & Fahrenfeld (2019) and by Kelly et al. (2020) who demonstrated that PE and PS particles (125 - 500 µm) and fragments (0.25 - 0.5 mm) exhibited distinct microbial communities

irrespective of the source water. Common human pathogens, such as arcobacters (Gong et al., 2019, Kettner et al., 2019, McCormick et al., 2014, McCormick et al., 2016) frequently colonize plastics, and certain antibiotic resistant genes can be aligned with presence of microplastics (Ram and Kumar, 2020, Wang et al., 2020a), thus the likelihood of MnP acting as transport medium cannot be negated. Hoellein et al. (2017) suggested that this preference was enhanced closer to a WWTP and diluted further downstream. Studying taxon richness and specifying any potential preferential colonization needs to be tested with different plastic types in order to fully address these interactions and their consequences.

ii. Primary producers

Photosynthetic activity was one of the most common endpoints measured when assessing effects on primary producers (19 out of 26 studies). 3 out of 4 studies on vascular-plant, duckweed, included this endpoint. From these, all reported no significant effect, even at high exposure concentrations, such as 5 $x10^4$ PE particles mL^{-1} (Mateos-Cárdenas et al., 2019). Photosynthetic activity was measured as chlorophyll-a (Chl-α) content with fluorometry (Mateos-Cárdenas et al., 2019) and as chlorophyll pigment content with UV-VIS spectroscopy (Dovidat et al., 2020, Kalčíková et al., 2017). Contrary to this, the majority of studies showed a significant effect of MnP on algal photosynthetic activity. Sjollema et al. (2016) measured the photosynthetic activity in *C. vulgaris* with Pulse Amplitude Modulation (PAM) fluorometer after exposure to high concentrations of PS particles (500 nm at 2.5 $x10^{-2}$, mg mL^{-1}) and found no conclusive impact. Interestingly, four other studies on cyanobacteria and freshwater algae *Microcystis aeruginosa*, *S. obliquus* and *C. reinhardtii* exposed to high PS particle concentrations in similar size-ranges (50 nm at 3.4 $x10^{-3}$ mg mL^{-1} , 200 nm at 0.01 mg and 0.02 mg mL^{-1}, 70 nm at 0.1 mg mL^{-1} and 300 -

600 nm at 0.1 mg mL^{-1}) showed decreased Chl-α content when measured with UV-VIS spectroscopy (Besseling et al., 2014, Feng et al., 2020, Zhang et al., 2018) and with a portable plant efficiency analyser (Li et al., 2020c). Conversion between mass and particle numbers was not possible in these cases and it is possible that the observed effects are related to the MnP sizes and concentrations or are species specific. The difference in method should not affect the outcome parameter (efficiency of photosynthetic activity), as UV-VIS Spectroscopy (Lichtenthaler, 1987) and fluorometry can both be used to estimate the chlorophyll content of plants(Maxwell and Johnson, 2000). In order to obtain baseline data, experiments with different plastic types with specific sizes and concentration ranges should be repeated on different species of algae. Photosynthetic activity appears to be a universally used endpoint for MnP toxicity tests and should continue being used to aid future comparability of studies.

Another common toxicity endpoint included for primary producers is growth (OECD, 2006, OECD, 2011, OECD, 2014a) which is relatively easy to measure. Only 2 out of 4 vascular-plant based studies reported an inhibitory effect on root growth of *Lemna minor* or *Spirodela polyrhiza* duckweeds. Although all MnP used in these studies adhered to the roots and leaves, it was only the larger PE particles (71.30 ± 34.29 μm, 96.00 ± 69.99 μm and 180.5 ± 118.7 μm) extracted from facewash that showed a statistically significant inhibitory effect on the root length of *L. minor* (Kalčíková et al., 2017, Kalčíková et al., 2020). Leachate effects were accounted for, suggesting that the microplastics themselves caused some type of physical inhibitory effect at all tested concentrations (0.01, 0.05, and 0.1 mg mL^{-1}) (Kalčíková et al., 2017). This effect could be due to the MnP size or morphology, as the other MnP tested; PE (10 - 45 μm at 5 $x10^4$ particles mL^{-1}) (Mateos-Cárdenas et al., 2019) and PS (50 and 500 nm at 1 $x10^6$ particles mL^{-1}) (Dovidat et al.,

2020) had more regular morphology, whereas the PE extracted from facewash was highly irregular. More studies are required with growth as a unifying endpoint, so that the effect of morphology and plastic type can be explored, and clear comparisons made to establish what MnP features affect growth.

8 out of 15 studies on freshwater algae measuring growth, reported a clear inhibitory effect after exposure to MnP. For instance, effects were induced by PS particles (70 nm at 1 mg mL^{-1} and 500 nm at 0.05 mg mL^{-1}) on *S. obliquus* and *C. vulgaris,* (Besseling et al., 2014, Tunali et al., 2020), by a mix of polymethyl methacrylate (PMMA) and PS fragments (< 250 µm at 1.25 $x10^{-2}$ mg and 0.125 mg mL^{-1}) on *Scenedesmus sp* and *Microcystis panniformis (Cunha et al., 2019)* and by polyurethane (PUR) foam fragments (3mm at 1.6 mg mL^{-1}) and its leachates on *C. vulgaris (Luo et al., 2019a)*.

Lagarde et al. (2016) reported decreased growth of the algae *C. reinhardtii* after exposure to PP fragments (400 < 1000 µm at 100 mg *no volume reported*), but only after 78 days. This, in conjunction with results from Mao et al. (2018), who reported that initial growth inhibition of *Chlorella pyrenoidosa* exposed to PS particles (0.1 µm at 0.01, 0.05 and 0.1 mg mL^{-1}), was countered after 22 days with biomass showing recovery, indicating some degree of organism adaptability. This strongly suggests that longer exposure times are required when assessing the impacts of MnP on algal communities, as negative effects seen at short exposure times might decrease in intensity over time or vice versa.

It is thus suggested that growth measured as length of roots and leaves for plants and as algae biomass and/or cell densities should be included as principal endpoint. Other endpoints such as stress responses and gene regulation should be included, where feasible, as explorative variables.

This minimum toxicity endpoint reporting will help to ensure that meta-analysis can be carried out in the future, leading to deeper understanding of MnP toxicity and the characteristics responsible.

iii. Primary consumers

Mortality is a common endpoint, determined often as the LC_{50} (lethal concentration required to kill 50% of test population) or LD_{50} (lethal dose required to kill 50% of the test population). Most studies reported mortality if it occurred, or used alternative indirect mortality endpoints, such as immobilization for cladecorans to estimate EC_{50} (half maximal effective concentration, which is halfway between baseline and maximum observed effect) (OECD, 2004). Where mortality was reported, higher exposures seemed to be more lethal. For example, some studies reported little to no mortality in *D. magna.* when exposed to PS particles (51 nm at 0.1mg mL^{-1} and 1 µm at 1.25 $x10^{-4}$ mg mL^{-1}) (Chae et al., 2018, De Felice et al., 2019), whereas, some PS exposures with similar size ranges did induce mortality (52 nm at 50 mg mL^{-1} and 100 nm at 0.0863 mg mL^{-1}) (Mattsson et al., 2017, Reynolds et al., 2019). Another discrepancy was observed in the case of the crustacean *H. azteca,* whereby Panko et al. (2013) reported no mortality after exposure to tire and road wear fragments (< 150 µm at 1 $x10^{4}$ mg Kg^{-1}) over 41 days, while Khan et al. (2019) observed mortality of *H. azteca* when exposed to tire rubber alone (< 500 µm at 3426 fragments mL^{-1}) over 21 days. Here, the differences between mode of exposure, the rubber types, associated additives and/or the road mixture could affect toxicity. It is noted, that in order to better understand the toxicity mechanisms, food should always be provided, so that effects of starvation would not be confused with those arising from the exposure (Aljaibachi et al., 2020). Furthermore, mortality should always be recorded and if no mortality is observed, this should be clearly stated.

Growth as an endpoint can reveal differences in toxicity of plastic types and aid comparisons between biotic groups. For example, the crustacean *Gammarus pulex* showed a significant reduction in growth when exposed to PS fragments (20 - 500 μm at 10% of sediment) despite feeding activity not being affected (Redondo-Hasselerharm et al., 2018). Reduction in growth was also observed in *G. fossarum,* by Straub et al. (2017), when exposed to PMMA and polyhydroxybutyrate (PHB) fragments (32 - 63 μm, 63 - 125 μm, and 125 - 250 μm at 1 $x10^5$ fragments $individual^{-1}$), despite no effects on feeding rates. However, *G. pulex* did not exhibit growth inhibition when exposed to car tire rubber of similar size and concentration (66 μm at 10% of sediment), despite retention times higher than for PS particles(Redondo-Hasselerharm et al., 2018). Similarly Panko et al. (2013) reported only slight non-statistically significant inhibition in growth of Diptera *Chironomus dilutus* exposed to tire and road wear fragments < 150 μm at 1 $x10^4$ mg Kg^{-1} while *C. riparius* and *C. tepperi,* were effected when exposed to PE (32 - 63 μm at 1259 mg Kg^{-1} 63 - 250 μm and 125 - 500 μm at 1 $x10^4$ mg Kg^{-1}) (Silva et al., 2019b) and PE (1 - 4, 10 - 27, 43 - 54 and 100 - 126 μm each at 500 particles Kg^{-1}) (Ziajahromi et al., 2018). However, whether the car tire and road wear fragments are less toxic than other MnP, such as PS, PE, PMMA and PHB remains inconclusive. For example, Panko et al. (2013) reported no effect on growth of the crustacean *H. azteca* exposed to tire and road wear fragments of size < 150 μm at 1 $x10^4$ mg Kg^{-1} while Khan et al. (2019) observed negative effects on growth in *H. azteca* when exposed to tire rubber of size < 500 μm at 3.426 $x10^3$ fragments mL^{-1}. The difference observed could be driven by either the road pavement, rubber types and associated specific mixture of additives and/or size, dose and/or mode of exposure, suggesting that more systematic studies are needed to determine the specific drivers of toxicity. To ensure comparability of effects across plastic types and species,

growth, measured as weight and length or biomass should be included as an endpoint for primary consumers. This will aid further meta-analysis and species sensitivity analysis in the future.

Besides inclusion of the primary endpoints mentioned above, it is crucial that the exposure times of primary producers will be extended. For example, the duration of exposure in *D. magna* and other cladocerans species is usually 48 hours for acute, and 21 days for chronic toxicity tests, according to OECD guidelines. However, it has been reported that some acute toxic effects (such as immobilization) of *D. magna* and *D. pulex* are not always obvious after 48 hours (Jaikumar et al., 2018, Rehse et al., 2016), and life-time exposures have revealed higher toxicity than that at 24 hour exposure (Kelpsiene et al., 2020), suggesting that acute exposure should be extended to at least 72 hours. Indeed, the OECD toxicity test guidelines are currently being revised for use with nanoparticles (Nasser and Lynch, 2019).

A secondary endpoint for primary consumers should be reproduction and where possible, multigenerational studies should be carried out. This is required to improve our understanding on population level effects. For example, three studies using non-disclosed proprietary type polymer from Cospheric LLC (1 - 5 μm), which measured reproduction capacity in cladocerans *Daphnia spp.* all reported negative effects (Jaikumar et al., 2019, Ogonowski et al., 2016, Pacheco et al., 2018). In addition, Felten et al. (2020), showed that PE 1 - 4 μm at 1 $x10^{-3}$ mg mL^{-1} had a negative effect on reproduction of *D. magna* while a transgenerational study by Martins and Guilhermino (2018) showed that *D. magna* went extinct in just two generations after exposure to Cospheric LLC (1 - 5 μm). It is clear that these specific MnP can have population level effects on cladocerans, and this type of systematic testing is required on other types of plastics and species. Furthermore, multigenerational studies should be a considered for primary consumers, as otherwise the

population level effects may be overlooked (Martins and Guilhermino, 2018). Most primary producers have a short life-cycle, making them ideal for this type of work.

Including these two principal toxicity parameters (growth and mortality) into each primary consumer MnP study is imperative. Considerations should be given to inclusion of secondary endpoints (reproduction and multigenerational studies). Other, especially sub-lethal parameters, such as enzyme activities for oxidative stress or immune response (Li et al., 2020d, Scopetani et al., 2020), should also be explored, to expand our understanding of MnP toxicity and their modes of action.

iv. Secondary consumers

For secondary consumers, similar principal endpoints as for primary consumers should be included (growth, mortality, and reproduction). However, as secondary consumers develop much slower than primary consumers, it is not always possible to include all three principal endpoints in one study, and therefore a combination of any two principal endpoints is acceptable. Still, as only one study from the reviewed literature reported increased mortality of adult zebrafish exposed to PP particles (~70 μm at 0.01 mg mL^{-1}) (Lei et al., 2018), further sub-lethal endpoints should be included. Effects observed in secondary consumers include changes in histopathology, gene expression and behaviour (Chae et al., 2018, Lei et al., 2018, Limonta et al., 2019, Oliveira et al., 2013, Rochman et al., 2017, Wen et al., 2018). Therefore, for secondary endpoints we recommend assessment of behavioural changes (e.g., predatory performance or distance swam), acetylcholinesterase (AChE) activity, which is an important enzyme that catalyses the breakdown of acetylcholine (neurotransmitter), or measures of oxidative stress, namely ROS or CAT (catalase

gene) and SOD (superoxide dismutase). One or more of these endpoints are encouraged to be included in future studies, to increase inter-comparability.

Behavioural changes can be used as a measure of sub-lethal effect in biota. This can be recorded using video combined with imaging software such as ImageJ (Chae et al., 2018, Critchell and Hoogenboom, 2018, da Costa Araújo et al., 2020) or more sophisticated tools and programs that have been designed for behavioural tracking of fish, such as DanioVision and EthoLog (Chen et al., 2017, Ottoni, 2000, Pedersen et al., 2020). For example, Chae et al. (2018) found that locomotive activity of two fish species, rice fish *Oryzias sinensis* and dark chub *Zacco temminckii,* were affected by PS particles (51 nm at 5 $x10^{-3}$ mg mL^{-1}). It was also reported that the livers of *Z. temminckii* showed abnormal histological patterns. Wen et al. (2018) similarly found that predatory performance of discus fish *Symphysodon aequifasciatus* declined following exposure to PE particles (70 - 88 μm at 2 $x10^{-4}$ mg mL^{-1}). This study also reported sub-lethal effects, such as a decrease in activity of enzymes AChE and Trypsin. It should be noted that these types of behavioural parameters (such as predatory performance or distance swam) cannot explain the underlying mode of action, however, it can offer important insight into MnP effects and is encouraged to be monitored where possible.

Neurotransmitter AChE decreased in 5 out of 6 studies assessed in this review, indicating neurotoxicity for the tested plastic types (PE and PS). PE was found to affect juvenile discus fish *S. aequifasciatus* (PE 70 - 88 μm at 2 $x10^{-4}$ mg mL^{-1}) and streaked prochilod *Prochilodus lineatus* (PE 10 - 90 μm at 2 $x10^{-5}$ mg mL^{-1}) (Roda et al., 2020, Wen et al., 2018). Two separate studies on juveniles of the common goby *Pomatoschistus microps,* reported similar effects on AChE when exposed to PE (1 - 5 μm at 1.84 $x10^{-5}$ mg mL^{-1} and 1.84 $x10^{-4}$ mg mL^{-1}) (Fonte et al., 2016, Oliveira

et al., 2013). PS 0.1 μm also decreased AChE in red tilapia *Oreochromis niloticus* at exposure concentrations of 1 $x10^{-6}$, 1 $x10^{-5}$ and 1 $x10^{-4}$ mg mL^{-1} (Ding et al., 2018). Only low density polyethylene (LDPE) (~10.9 μm) at exposure concentrations of 5 $x10^{-6}$, 5 $x10^{-5}$, and 5 $x10^{-4}$ mg mL^{-1} showed no effect on AChE mRNA levels of zebrafish larvae (Karami et al., 2017b). The duration of exposure is unlikely to explain these differences, as the studies that showed effects on AChE ranged from 96 hours to 31 days and the study of Karami et al. (2017b) exposed the larvae for 20 days, which falls within the range above. Whether the observed effect on AChE levels was species specific, related to the age of exposed fish, and/or plastic type is unclear. Inclusion of this endpoint where possible will facilitate assessment of possible neurotoxicity of different plastic types in different species.

Another important sub-lethal endpoint for secondary consumers is oxidative stress, which can lead to tissue damage and disrupt cellular functions (Valavanidis et al., 2006). There is already evidence that some MnP can induce oxidative stress in secondary consumers. For example, CAT gene, that is related to presence of oxidative stress, was upregulated in zebrafish after exposure to PS particles (1 μm, 5 μm and 70 nm) at 1 $x10^{-3}$ mg mL^{-1} (Qiang and Cheng, 2019), 2 $x10^{-4}$ or 2 $x10^{-3}$ mg mL^{-1} (Lu et al., 2016). However, we recommend that more than one parameter for oxidative stress should be measured, as this can give an indication of whether biota can form protective action against ROS. For example, Parenti et al. (2019) showed that while PS (0.5 μm at 1 $x10^{-3}$ mg mL^{-1}) induced activity of SOD it did not induce ROS. This could indicate that high SOD activity in zebrafish could protect it from excessive ROS. This is supported by a study on red tilapia *O. niloticus* exposed to 1 $x10^{-6}$,1 $x10^{-5}$, and 1 $x10^{-4}$ mg mL^{-1} PS particles (0.1 μm), where particles induced SOD but did not affect malondialdehyde (MDA), suggesting a similar protective

mechanism against oxidative damage (Ding et al., 2018). Furthermore, 5 $x10^{-6}$, 5 $x10^{-5}$, or 5 $x10^{-4}$ mg mL^{-1} LDPE (~10.9 μm) did not increase CAT in zebrafish, but decreased its concentration over the exposure period (Karami et al., 2017b). More studies capturing this endpoint in the future will enable further inferences on the effects of MnP type, morphology and size. It is also noteworthy that when zebrafish were co-exposed to 1 $x10^{-6}$ mg mL^{-1} and 1 $x10^{-3}$ mg mL^{-1} nano-sized PS (50 - 100 nm) and to fulvic and humic acid, the ROS levels were synergistically affected (Liu et al., 2019c) indicating that natural conditions, such as organic matter should be considered further when conducting toxicity tests.

3.6 Conclusion

The synthesis of the reviewed research revealed evidence of a significant mismatch between field and laboratory studies, highlighting a significant gap in our knowledge on how the most common morphology of MnP might affect freshwater species. Further, there is lack of systematic testing on different factors that may affect MnP toxicity, such as different morphologies, plastic types and sizes, including their leachates. This review has outlined some of the key recommendations and reporting guidelines for field and laboratory studies, with the goal of increasing inter-comparability across studies and trophic levels. It is imperative that baseline studies on the parameters suggested in this review are systematically undertaken. Only by gathering this type of data, can a full meta-analysis and comprehension of the effects of MnP on freshwater ecosystems can produced.

3.7 Acknowledgements

The authors would like to extend their gratitude towards Chantal Jackson and Dr. Giulio Curioni for their assistance with the graphics and figures, and the three anonymous reviewers and the editor

for their critical reading of the manuscript and insightful suggestions that led to the improvement of the manuscript. SK and IL are supported by the Institute of Global Innovation at Birmingham University.

Funding: This work was supported by the Leverhulme Trust grant “PlasticRivers”- The fate and transport of microplastics in rivers (RPG-2017-377).

3.8 References

AKINDELE, E. O., EHLERS, S. M. & KOOP, J. H. E. 2019. First empirical study of freshwater microplastics in West Africa using gastropods from Nigeria as bioindicators. *Limnologica,* 78**,** 125708.

ALJAIBACHI, R., LAIRD, W. B., STEVENS, F. & CALLAGHAN, A. 2020. Impacts of polystyrene microplastics on Daphnia magna: A laboratory and a mesocosm study. *Science of The Total Environment,* 705**,** 135800.

ALLEN, S., ALLEN, D., PHOENIX, V. R., LE ROUX, G., DURÁNTEZ JIMÉNEZ, P., SIMONNEAU, A., BINET, S. & GALOP, D. 2019. Atmospheric transport and deposition of microplastics in a remote mountain catchment. *Nature Geoscience,* 12**,** 339-344.

ANBUMANI, S. & KAKKAR, P. 2018. Ecotoxicological effects of microplastics on biota: a review. *Environmental Science and Pollution Research,* 25**,** 14373-14396.

ARTHUR, C., BAKER, J. & BAMFORD, H. 2009. Proceedings of the International Research Workshop on the Occurrence, Effects and Fate of Microplastic Marine Debris. *NOAA Technical Memorandum NOS-OR&R-30*.

AU, S. Y., BRUCE, T. F., BRIDGES, W. C. & KLAINE, S. J. 2015. Responses of Hyalella azteca to acute and chronic microplastic exposures. *Environmental Toxicology and Chemistry,* 34**,** 2564-2572.

AUCLAIR, J., PEYROT, C., WILKINSON, K. J. & GAGNÉ, F. 2020. Biophysical effects of polystyrene nanoparticles on Elliptio complanata mussels. *Environmental Science and Pollution Research,* 27**,** 25093-25102.

BAUDRIMONT, M., ARINI, A., GUÉGAN, C., VENEL, Z., GIGAULT, J., PEDRONO, B., PRUNIER, J., MAURICE, L., TER HALLE, A. & FEURTET-MAZEL, A. 2020. Ecotoxicity of polyethylene nanoplastics from the North Atlantic oceanic gyre on freshwater and marine organisms (microalgae and filter-feeding bivalves). *Environmental Science and Pollution Research,* 27**,** 3746-3755.

BESSELING, E., WANG, B., LÜRLING, M. & KOELMANS, A. A. 2014. Nanoplastic affects growth of S. obliquus and reproduction of D. magna. *Environ Sci Technol,* 48**,** 12336-43.

BOYLE, D., CATARINO, A. I., CLARK, N. J. & HENRY, T. B. 2020. Polyvinyl chloride (PVC) plastic fragments release Pb additives that are bioavailable in zebrafish. *Environmental Pollution,* 263**,** 114422.

BRANDTS, I., GARCIA-ORDOÑEZ, M., TORT, L., TELES, M. & ROHER, N. 2020. Polystyrene nanoplastics accumulate in ZFL cell lysosomes and in zebrafish larvae after acute exposure, inducing a synergistic immune response in vitro without affecting larval survival in vivo. *Environmental Science: Nano,* 7**,** 2410-2422.

BROWNE, M. A., GALLOWAY, T. S. & THOMPSON, R. C. 2010. Spatial Patterns of Plastic Debris along Estuarine Shorelines. *Environmental Science & Technology,* 44**,** 3404-3409.

CAPOLUPO, M., SØRENSEN, L., JAYASENA, K. D. R., BOOTH, A. M. & FABBRI, E. 2020. Chemical composition and ecotoxicity of plastic and car tire rubber leachates to aquatic organisms. *Water Res,* 169**,** 115270.

CHAE, Y., KIM, D., KIM, S. W. & AN, Y.-J. 2018. Trophic transfer and individual impact of nano-sized polystyrene in a four-species freshwater food chain. *Scientific Reports,* 8**,** 284.

CHEN, Q., GUNDLACH, M., YANG, S., JIANG, J., VELKI, M., YIN, D. & HOLLERT, H. 2017. Quantitative investigation of the mechanisms of microplastics and nanoplastics toward zebrafish larvae locomotor activity. *Sci Total Environ,* 584-585**,** 1022-1031.

COFFIN, S., HUANG, G.-Y., LEE, I. & SCHLENK, D. 2019. Fish and Seabird Gut Conditions Enhance Desorption of Estrogenic Chemicals from Commonly-Ingested Plastic Items. *Environmental Science & Technology,* 53**,** 4588-4599.

COLLARD, F., GASPERI, J., GABRIELSEN, G. W. & TASSIN, B. 2019. Plastic Particle Ingestion by Wild Freshwater Fish: A Critical Review. *Environmental Science & Technology,* 53**,** 12974-12988.

COLLARD, F., GASPERI, J., GILBERT, B., EPPE, G., AZIMI, S., ROCHER, V. & TASSIN, B. 2018. Anthropogenic particles in the stomach contents and liver of the freshwater fish Squalius cephalus. *Science of The Total Environment,* 643**,** 1257-1264.

COLLARD, F., GILBERT, B., COMPÈRE, P., EPPE, G., DAS, K., JAUNIAUX, T. & PARMENTIER, E. 2017. Microplastics in livers of European anchovies (Engraulis encrasicolus, L.). *Environmental Pollution,* 229**,** 1000-1005.

COPPOCK, R. L., COLE, M., LINDEQUE, P. K., QUEIRÓS, A. M. & GALLOWAY, T. S. 2017. A small-scale, portable method for extracting microplastics from marine sediments. *Environmental Pollution,* 230**,** 829-837.

CORCORAN, P. L., BIESINGER, M. C. & GRIFI, M. 2009. Plastics and beaches: A degrading relationship. *Marine Pollution Bulletin,* 58**,** 80-84.

CORRADINI, F., MEZA, P., EGUILUZ, R., CASADO, F., HUERTA-LWANGA, E. & GEISSEN, V. 2019. Evidence of microplastic accumulation in agricultural soils from sewage sludge disposal. *Science of The Total Environment,* 671**,** 411-420.

COWGER, W., BOOTH, A. M., HAMILTON, B. M., THAYSEN, C., PRIMPKE, S., MUNNO, K., LUSHER, A. L., DEHAUT, A., VAZ, V. P. & LIBOIRON, M. 2020. Reporting guidelines to

increase the reproducibility and comparability of research on microplastics. *Applied spectroscopy,* 74**,** 1066-1077.

CÓZAR, A., ECHEVARRÍA, F., GONZÁLEZ-GORDILLO, J. I., IRIGOIEN, X., ÚBEDA, B., HERNÁNDEZ-LEÓN, S., PALMA, Á. T., NAVARRO, S., GARCÍA-DE-LOMAS, J., RUIZ, A., FERNÁNDEZ-DE-PUELLES, M. L. & DUARTE, C. M. 2014. Plastic debris in the open ocean. *Proceedings of the National Academy of Sciences,* 111**,** 10239-10244.

CRITCHELL, K. & HOOGENBOOM, M. O. 2018. Effects of microplastic exposure on the body condition and behaviour of planktivorous reef fish (Acanthochromis polyacanthus). *PLOS ONE,* 13**,** e0193308.

CUNHA, C., FARIA, M., NOGUEIRA, N., FERREIRA, A. & CORDEIRO, N. 2019. Marine vs freshwater microalgae exopolymers as biosolutions to microplastics pollution. *Environmental Pollution,* 249**,** 372-380.

DA COSTA ARAÚJO, A. P., DE ANDRADE VIEIRA, J. E. & MALAFAIA, G. 2020. Toxicity and trophic transfer of polyethylene microplastics from Poecilia reticulata to Danio rerio. *Science of The Total Environment,* 742**,** 140217.

DANA, C.-M., MICHAEL, S. & JUERGEN, P. 2019. Theoretical principles of Raman spectroscopy. *Physical Sciences Reviews,* 4.

DAWSON, A. L., KAWAGUCHI, S., KING, C. K., TOWNSEND, K. A., KING, R., HUSTON, W. M. & BENGTSON NASH, S. M. 2018. Turning microplastics into nanoplastics through digestive fragmentation by Antarctic krill. *Nature Communications,* 9**,** 1001.

DE FELICE, B., SABATINI, V., ANTENUCCI, S., GATTONI, G., SANTO, N., BACCHETTA, R., ORTENZI, M. A. & PAROLINI, M. 2019. Polystyrene microplastics ingestion induced behavioral effects to the cladoceran Daphnia magna. *Chemosphere,* 231**,** 423-431.

DEHAUT, A., CASSONE, A.-L., FRÈRE, L., HERMABESSIERE, L., HIMBER, C., RINNERT, E., RIVIÈRE, G., LAMBERT, C., SOUDANT, P., HUVET, A., DUFLOS, G. & PAUL-PONT, I.

2016. Microplastics in seafood: Benchmark protocol for their extraction and characterization. *Environmental Pollution,* 215**,** 223-233.

DESFORGES, J.-P. W., GALBRAITH, M., DANGERFIELD, N. & ROSS, P. S. 2014. Widespread distribution of microplastics in subsurface seawater in the NE Pacific Ocean. *Marine Pollution Bulletin,* 79**,** 94-99.

DING, J., ZHANG, S., RAZANAJATOVO, R. M., ZOU, H. & ZHU, W. 2018. Accumulation, tissue distribution, and biochemical effects of polystyrene microplastics in the freshwater fish red tilapia (Oreochromis niloticus). *Environmental Pollution,* 238**,** 1-9.

DOMOGALLA-URBANSKY, J., ANGER, P. M., FERLING, H., RAGER, F., WIESHEU, A. C., NIESSNER, R., IVLEVA, N. P. & SCHWAIGER, J. 2019. Raman microspectroscopic identification of microplastic particles in freshwater bivalves (Unio pictorum) exposed to sewage treatment plant effluents under different exposure scenarios. *Environ Sci Pollut Res Int,* 26**,** 2007-2012.

DOVIDAT, L. C., BRINKMANN, B. W., VIJVER, M. G. & BOSKER, T. 2020. Plastic particles adsorb to the roots of freshwater vascular plant Spirodela polyrhiza but do not impair growth. *Limnology and Oceanography Letters,* 5**,** 37-45.

DRIS, R., GASPERI, J., MIRANDE, C., MANDIN, C., GUERROUACHE, M., LANGLOIS, V. & TASSIN, B. 2017. A first overview of textile fibres, including microplastics, in indoor and outdoor environments. *Environmental Pollution,* 221**,** 453-458.

DRIS, R., GASPERI, J., ROCHER, V., SAAD, M., RENAULT, N. & TASSIN, B. 2015. Microplastic contamination in an urban area: a case study in Greater Paris. *Environmental Chemistry,* 12**,** 592-599.

DRIS, R., GASPERI, J., SAAD, M., MIRANDE, C. & TASSIN, B. 2016. Synthetic fibres in atmospheric fallout: A source of microplastics in the environment? *Marine Pollution Bulletin,* 104**,** 290-293.

EERKES-MEDRANO, D., THOMPSON, R. C. & ALDRIDGE, D. C. 2015. Microplastics in freshwater systems: A review of the emerging threats, identification of knowledge gaps and prioritisation of research needs. *Water Research,* 75**,** 63-82.

ELIZALDE-VELÁZQUEZ, A., CARCANO, A. M., CRAGO, J., GREEN, M. J., SHAH, S. A. & CAÑAS-CARRELL, J. E. 2020. Translocation, trophic transfer, accumulation and depuration of polystyrene microplastics in Daphnia magna and Pimephales promelas. *Environmental Pollution,* 259**,** 113937.

ELLIS, L.-J. A., VALSAMI-JONES, E. & LYNCH, I. 2020. Exposure medium and particle ageing moderate the toxicological effects of nanomaterials to Daphnia magna over multiple generations: a case for standard test review? *Environmental Science: Nano,* 7**,** 1136-1149.

ERNI-CASSOLA, G., GIBSON, M. I., THOMPSON, R. C. & CHRISTIE-OLEZA, J. A. 2017. Lost, but Found with Nile Red: A Novel Method for Detecting and Quantifying Small Microplastics (1 mm to 20 μm) in Environmental Samples. *Environmental Science & Technology,* 51**,** 13641-13648.

FAURE, F., DEMARS, C., WIESER, O., KUNZ, M. & DE ALENCASTRO, L. F. 2015. Plastic pollution in Swiss surface waters: nature and concentrations, interaction with pollutants. *Environmental Chemistry,* 12**,** 582-591.

FELTEN, V., TOUMI, H., MASFARAUD, J.-F., BILLOIR, E., CAMARA, B. I. & FÉRARD, J.-F. 2020. Microplastics enhance Daphnia magna sensitivity to the pyrethroid insecticide deltamethrin: Effects on life history traits. Science of The Total Environment, 714, 136567.

FENG, L.-J., SUN, X.-D., ZHU, F.-P., FENG, Y., DUAN, J.-L., XIAO, F., LI, X.-Y., SHI, Y., WANG, Q., SUN, J.-W., LIU, X.-Y., LIU, J.-Q., ZHOU, L.-L., WANG, S.-G., DING, Z., TIAN, H., GALLOWAY, T. S. & YUAN, X.-Z. 2020. Nanoplastics Promote Microcystin Synthesis and Release from Cyanobacterial Microcystis aeruginosa. *Environmental Science & Technology,* 54**,** 3386-3394.

FONTE, E., FERREIRA, P. & GUILHERMINO, L. 2016. Temperature rise and microplastics interact with the toxicity of the antibiotic cefalexin to juveniles of the common goby (Pomatoschistus microps):

Post-exposure predatory behaviour, acetylcholinesterase activity and lipid peroxidation. *Aquat Toxicol,* 180**,** 173-185.

GAMBINO, G., FALLENI, A., NIGRO, M., SALVETTI, A., CECCHETTINI, A., IPPOLITO, C., GUIDI, P. & ROSSI, L. 2020. Dynamics of interaction and effects of microplastics on planarian tissue regeneration and cellular homeostasis. Aquatic Toxicology, 218, 105354.

GARCIA, A. G., SUÁREZ, D. C., LI, J. & ROTCHELL, J. M. 2021. A comparison of microplastic contamination in freshwater fish from natural and farmed sources. *Environ Sci Pollut Res Int,* 28**,** 14488-14497.

GESAMP 2016. SOURCES, FATE AND EFFECTS OF MICROPLASTICS IN THE MARINE ENVIRONMENT: PART TWO OF A GLOBAL ASSESSMENT. *In:* KERSHAW P.J., A. R., C.M (ed.). GESAMP Working Group 40 2nd phase. London: IMO/FAO/UNESCO-IOC/UNIDO/WMO/IAEA/UN/UNEP/UNDP Joint Group of Experts on the Scientific Aspects of Marine Environmental Protection.

GEYER, R., JAMBECK, J. R. & LAW, K. L. 2017. Production, use, and fate of all plastics ever made. *Science Advances,* 3**,** e1700782.

GONG, M., YANG, G., ZHUANG, L. & ZENG, E. Y. 2019. Microbial biofilm formation and community structure on low-density polyethylene microparticles in lake water microcosms. *Environmental Pollution,* 252**,** 94-102.

GUPTA, P., LAKES, A. & DZIUBLA, T. 2016. Chapter One - A Free Radical Primer. *In:* DZIUBLA, T. & BUTTERFIELD, D. A. (eds.) *Oxidative Stress and Biomaterials.* Academic Press.

HARTMANN, N. B., HÜFFER, T., THOMPSON, R. C., HASSELLÖV, M., VERSCHOOR, A., DAUGAARD, A. E., RIST, S., KARLSSON, T., BRENNHOLT, N., COLE, M., HERRLING, M. P., HESS, M. C., IVLEVA, N. P., LUSHER, A. L. & WAGNER, M. 2019. Are We Speaking the Same Language? Recommendations for a Definition and Categorization Framework for Plastic Debris. *Environmental Science & Technology,* 53**,** 1039-1047.

HARTMANN, N. B., RIST, S., BODIN, J., JENSEN, L. H., SCHMIDT, S. N., MAYER, P., MEIBOM, A. & BAUN, A. 2017. Microplastics as vectors for environmental contaminants: Exploring sorption, desorption, and transfer to biota. *Integrated Environmental Assessment and Management,* 13**,** 488-493.

HERMSEN, E., MINTENIG, S. M., BESSELING, E. & KOELMANS, A. A. 2018. Quality Criteria for the Analysis of Microplastic in Biota Samples: A Critical Review. *Environmental Science & Technology,* 52**,** 10230-10240.

HOELLEIN, T. J., MCCORMICK, A. R., HITTIE, J., LONDON, M. G., SCOTT, J. W. & KELLY, J. J. 2017. Longitudinal patterns of microplastic concentration and bacterial assemblages in surface and benthic habitats of an urban river. *Freshwater Science,* 36**,** 491-507.

HURLEY, R., WOODWARD, J. & ROTHWELL, J. J. 2018. Microplastic contamination of river beds significantly reduced by catchment-wide flooding. *Nature Geoscience,* 11**,** 251-257.

HURLEY, R. R., WOODWARD, J. C. & ROTHWELL, J. J. 2017. Ingestion of Microplastics by Freshwater Tubifex Worms. Environmental Science & Technology, 51, 12844-12851.

IMHOF, H. K., LAFORSCH, C., WIESHEU, A. C., SCHMID, J., ANGER, P. M., NIESSNER, R. & IVLEVA, N. P. 2016. Pigments and plastic in limnetic ecosystems: A qualitative and quantitative study on microparticles of different size classes. *Water Research,* 98**,** 64-74.

JAIKUMAR, G., BAAS, J., BRUN, N. R., VIJVER, M. G. & BOSKER, T. 2018. Acute sensitivity of three Cladoceran species to different types of microplastics in combination with thermal stress. *Environmental Pollution,* 239**,** 733-740.

JAIKUMAR, G., BRUN, N. R., VIJVER, M. G. & BOSKER, T. 2019. Reproductive toxicity of primary and secondary microplastics to three cladocerans during chronic exposure. *Environmental Pollution,* 249**,** 638-646.

JAMBECK, J. R., GEYER, R., WILCOX, C., SIEGLER, T. R., PERRYMAN, M., ANDRADY, A., NARAYAN, R. & LAW, K. L. 2015. Plastic waste inputs from land into the ocean. *Science,* 347**,** 768-771.

JEMEC, A., HORVAT, P., KUNEJ, U., BELE, M. & KRŽAN, A. 2016. Uptake and effects of microplastic textile fibres on freshwater crustacean Daphnia magna. *Environmental Pollution,* 219**,** 201-209.

JEONG, C.-B., WON, E.-J., KANG, H.-M., LEE, M.-C., HWANG, D.-S., HWANG, U.-K., ZHOU, B., SOUISSI, S., LEE, S.-J. & LEE, J.-S. 2016. Microplastic Size-Dependent Toxicity, Oxidative Stress Induction, and p-JNK and p-p38 Activation in the Monogonont Rotifer (Brachionus koreanus). *Environmental Science & Technology,* 50**,** 8849-8857.

JOVANOVIĆ, B., GÖKDAĞ, K., GÜVEN, O., EMRE, Y., WHITLEY, E. M. & KIDEYS, A. E. 2018. Virgin microplastics are not causing imminent harm to fish after dietary exposure. *Marine Pollution Bulletin,* 130**,** 123-131.

KALČÍKOVÁ, G., SKALAR, T., MAROLT, G. & JEMEC KOKALJ, A. 2020. An environmental concentration of aged microplastics with adsorbed silver significantly affects aquatic organisms. *Water Research,* 175**,** 115644.

KALČÍKOVÁ, G., ŽGAJNAR GOTVAJN, A., KLADNIK, A. & JEMEC, A. 2017. Impact of polyethylene microbeads on the floating freshwater plant duckweed Lemna minor. *Environmental Pollution,* 230**,** 1108-1115.

KANHAI, L. D. K., OFFICER, R., LYASHEVSKA, O., THOMPSON, R. C. & O'CONNOR, I. 2017. Microplastic abundance, distribution and composition along a latitudinal gradient in the Atlantic Ocean. *Marine Pollution Bulletin,* 115**,** 307-314.

KARAMI, A., GOLIESKARDI, A., CHOO, C. K., ROMANO, N., HO, Y. B. & SALAMATINIA, B. 2017a. A high-performance protocol for extraction of microplastics in fish. *Science of The Total Environment,* 578**,** 485-494.

KARAMI, A., GROMAN, D. B., WILSON, S. P., ISMAIL, P. & NEELA, V. K. 2017b. Biomarker responses in zebrafish (Danio rerio) larvae exposed to pristine low-density polyethylene fragments. *Environmental Pollution,* 223**,** 466-475.

KELPSIENE, E., TORSTENSSON, O., EKVALL, M. T., HANSSON, L.-A. & CEDERVALL, T. 2020. Long-term exposure to nanoplastics reduces life-time in Daphnia magna. *Scientific Reports,* 10**,** 5979.

KELLY, J. J., LONDON, M. G., OFORJI, N., OGUNSOLA, A. & HOELLEIN, T. J. 2020. Microplastic selects for convergent microbiomes from distinct riverine sources. Freshwater Science, 39, 281-291.

KETTNER, M. T., OBERBECKMANN, S., LABRENZ, M. & GROSSART, H.-P. 2019. The Eukaryotic Life on Microplastics in Brackish Ecosystems. *Frontiers in Microbiology,* 10.

KHAN, F. R., HALLE, L. L. & PALMQVIST, A. 2019. Acute and long-term toxicity of micronized car tire wear particles to Hyalella azteca. Aquatic Toxicology, 213, 105216.

KOELMANS, A. A. 2015. Modeling the Role of Microplastics in Bioaccumulation of Organic Chemicals to Marine Aquatic Organisms. A Critical Review. *In:* BERGMANN, M., GUTOW, L. & KLAGES, M. (eds.) *Marine Anthropogenic Litter.* Cham: Springer International Publishing.

KOELMANS, A. A., BAKIR, A., BURTON, G. A. & JANSSEN, C. R. 2016. Microplastic as a Vector for Chemicals in the Aquatic Environment: Critical Review and Model-Supported Reinterpretation of Empirical Studies. *Environmental Science & Technology,* 50**,** 3315-3326.

KOLE, P. J., LÖHR, A. J., VAN BELLEGHEM, F. G. A. J. & RAGAS, A. M. J. 2017. Wear and Tear of Tires: A Stealthy Source of Microplastics in the Environment. *International Journal of Environmental Research and Public Health* [Online], 14.

KOU, L., SUN, J., ZHAI, Y. & HE, Z. 2013. The endocytosis and intracellular fate of nanomedicines: Implication for rational design. *Asian Journal of Pharmaceutical Sciences,* 8**,** 1-10.

KRAUSE, S., BARANOV, V., NEL, H. A., DRUMMOND, J. D., KUKKOLA, A., HOELLEIN, T., SAMBROOK SMITH, G. H., LEWANDOWSKI, J., BONET, B., PACKMAN, A. I., SADLER, J., INSHYNA, V., ALLEN, S., ALLEN, D., SIMON, L., MERMILLOD-BLONDIN, F. & LYNCH, I. 2021. Gathering at the top? Environmental controls of microplastic uptake and biomagnification in freshwater food webs. *Environmental Pollution,* 268**,** 115750.

MCNEISH, R. E., KIM, L. H., BARRETT, H. A., MASON, S. A., KELLY, J. J. & HOELLEIN, T. J. 2018. Microplastic in riverine fish is connected to species traits. Scientific Reports, 8, 11639

LAGARDE, F., OLIVIER, O., ZANELLA, M., DANIEL, P., HIARD, S. & CARUSO, A. 2016. Microplastic interactions with freshwater microalgae: Hetero-aggregation and changes in plastic density appear strongly dependent on polymer type. Environmental Pollution, 215, 331-339.

LAKOWICZ, J. R. 1999. Introduction to Fluorescence. *In:* LAKOWICZ, J. R. (ed.) *Principles of Fluorescence Spectroscopy.* Boston, MA: Springer US.

LEBRETON, L. C. M., VAN DER ZWET, J., DAMSTEEG, J.-W., SLAT, B., ANDRADY, A. & REISSER, J. 2017. River plastic emissions to the world's oceans. *Nature Communications,* 8**,** 15611.

LEE, K.-W., SHIM, W. J., KWON, O. Y. & KANG, J.-H. 2013. Size-Dependent Effects of Micro Polystyrene Particles in the Marine Copepod Tigriopus japonicus. *Environmental Science & Technology,* 47**,** 11278-11283.

LI, L., SU, L., CAI, H., ROCHMAN, C. M., LI, Q., KOLANDHASAMY, P., PENG, J. & SHI, H. 2019. The uptake of microfibres by freshwater Asian clams (Corbicula fluminea) varies based upon physicochemical properties. Chemosphere, 221, 107-114.

LEI, L., WU, S., LU, S., LIU, M., SONG, Y., FU, Z., SHI, H., RALEY-SUSMAN, K. M. & HE, D. 2018. Microplastic particles cause intestinal damage and other adverse effects in zebrafish Danio rerio and nematode Caenorhabditis elegans. *Science of The Total Environment,* 619-620**,** 1-8.

LI, B., SU, L., ZHANG, H., DENG, H., CHEN, Q. & SHI, H. 2020a. Microplastics in fishes and their living environments surrounding a plastic production area. *Science of The Total Environment,* 727**,** 138662.

LI, C., GAN, Y., DONG, J., FANG, J., CHEN, H., QUAN, Q. & LIU, J. 2020b. Impact of microplastics on microbial community in sediments of the Huangjinxia Reservoir—water source of a water diversion project in western China. *Chemosphere,* 253**,** 126740.

LI, J., LIU, H. & PAUL CHEN, J. 2018. Microplastics in freshwater systems: A review on occurrence, environmental effects, and methods for microplastics detection. *Water Research,* 137**,** 362-374.

LI, S., WANG, P., ZHANG, C., ZHOU, X., YIN, Z., HU, T., HU, D., LIU, C. & ZHU, L. 2020c. Influence of polystyrene microplastics on the growth, photosynthetic efficiency and aggregation of freshwater microalgae Chlamydomonas reinhardtii. *Science of The Total Environment,* 714**,** 136767.

LI, Y., LIU, Z., LI, M., JIANG, Q., WU, D., HUANG, Y., JIAO, Y., ZHANG, M. & ZHAO, Y. 2020d. Effects of nanoplastics on antioxidant and immune enzyme activities and related gene expression in juvenile Macrobrachium nipponense. *Journal of Hazardous Materials,* 398**,** 122990.

LICHTENTHALER, H. K. 1987. [34] Chlorophylls and carotenoids: Pigments of photosynthetic biomembranes. *Methods in Enzymology.* Academic Press.

LICHTMAN, J. W. & CONCHELLO, J.-A. 2005. Fluorescence microscopy. *Nature Methods,* 2**,** 910-919.

LIMONTA, G., MANCIA, A., BENKHALQUI, A., BERTOLUCCI, C., ABELLI, L., FOSSI, M. C. & PANTI, C. 2019. Microplastics induce transcriptional changes, immune response and behavioral alterations in adult zebrafish. *Scientific Reports,* 9**,** 15775.

LIU, K., WU, T., WANG, X., SONG, Z., ZONG, C., WEI, N. & LI, D. 2019a. Consistent Transport of Terrestrial Microplastics to the Ocean through Atmosphere. *Environmental Science & Technology,* 53**,** 10612-10619.

LIU, Y., WANG, Z., WANG, S., FANG, H., YE, N. & WANG, D. 2019b. Ecotoxicological effects on Scenedesmus obliquus and Danio rerio Co-exposed to polystyrene nano-plastic particles and natural acidic organic polymer. *Environ Toxicol Pharmacol,* 67**,** 21-28.

LIU, Y., WANG, Z., WANG, S., FANG, H., YE, N. & WANG, D. 2019c. Ecotoxicological effects on Scenedesmus obliquus and Danio rerio Co-exposed to polystyrene nano-plastic particles and natural acidic organic polymer. *Environmental Toxicology and Pharmacology,* 67**,** 21-28.

LU, Y., ZHANG, Y., DENG, Y., JIANG, W., ZHAO, Y., GENG, J., DING, L. & REN, H. 2016. Uptake and Accumulation of Polystyrene Microplastics in Zebrafish (Danio rerio) and Toxic Effects in Liver. *Environmental Science & Technology,* 50**,** 4054-4060.

LUO, H., XIANG, Y., HE, D., LI, Y., ZHAO, Y., WANG, S. & PAN, X. 2019a. Leaching behavior of fluorescent additives from microplastics and the toxicity of leachate to Chlorella vulgaris. *Science of The Total Environment,* 678**,** 1-9.

LUO, W., SU, L., CRAIG, N. J., DU, F., WU, C. & SHI, H. 2019b. Comparison of microplastic pollution in different water bodies from urban creeks to coastal waters. *Environmental Pollution,* 246**,** 174-182.

LUSHER, A. L., TIRELLI, V., O'CONNOR, I. & OFFICER, R. 2015. Microplastics in Arctic polar waters: the first reported values of particles in surface and sub-surface samples. *Scientific Reports,* 5**,** 14947.

LV, L., QU, J., YU, Z., CHEN, D., ZHOU, C., HONG, P., SUN, S. & LI, C. 2019. A simple method for detecting and quantifying microplastics utilizing fluorescent dyes - Safranine T, fluorescein isophosphate, Nile red based on thermal expansion and contraction property. *Environmental Pollution,* 255**,** 113283.

MA, Y., HUANG, A., CAO, S., SUN, F., WANG, L., GUO, H. & JI, R. 2016. Effects of nanoplastics and microplastics on toxicity, bioaccumulation, and environmental fate of phenanthrene in fresh water. *Environ Pollut,* 219**,** 166-173.

MAES, T., VAN DER MEULEN, M. D., DEVRIESE, L. I., LESLIE, H. A., HUVET, A., FRÈRE, L., ROBBENS, J. & VETHAAK, A. D. 2017. Microplastics Baseline Surveys at the Water Surface and in Sediments of the North-East Atlantic. *Frontiers in Marine Science,* 4.

MARGENAT, H., NEL, H.A., STONEDAHL, S.H., KRAUSE, S., SABATER, F., DRUMMOND, J.D. 2021. Hydrologic controls on the accumulation of different sized microplastics in the streambed sediments downstream of a wastewater treatment plant (Catalonia, Spain). *Environmental Research Letters,* 16.

MARSHALL, J. & JOHNSEN, S. 2017. Fluorescence as a means of colour signal enhancement. *Philosophical Transactions of the Royal Society B: Biological Sciences,* 372**,** 20160335.

MARTINS, A. & GUILHERMINO, L. 2018. Transgenerational effects and recovery of microplastics exposure in model populations of the freshwater cladoceran Daphnia magna Straus. *Science of The Total Environment,* 631-632**,** 421-428.

MATEOS-CÁRDENAS, A., O'HALLORAN, J., VAN PELT, F. N. A. M. & JANSEN, M. A. K. 2020. Rapid fragmentation of microplastics by the freshwater amphipod Gammarus duebeni (Lillj.). *Scientific Reports,* 10**,** 12799.

MATEOS-CÁRDENAS, A., SCOTT, D. T., SEITMAGANBETOVA, G., FRANK N.A.M, V. P., JOHN, O. H. & MARCEL A.K, J. 2019. Polyethylene microplastics adhere to Lemna minor (L.), yet have no effects on plant growth or feeding by Gammarus duebeni (Lillj.). *Science of The Total Environment,* 689**,** 413-421.

MATTSSON, K., JOHNSON, E. V., MALMENDAL, A., LINSE, S., HANSSON, L.-A. & CEDERVALL, T. 2017. Brain damage and behavioural disorders in fish induced by plastic nanoparticles delivered through the food chain. *Scientific Reports,* 7**,** 11452.

MAXWELL, K. & JOHNSON, G. N. 2000. Chlorophyll fluorescence—a practical guide. *Journal of Experimental Botany,* 51**,** 659-668.

MCCORMICK, A., HOELLEIN, T. J., MASON, S. A., SCHLUEP, J. & KELLY, J. J. 2014. Microplastic is an Abundant and Distinct Microbial Habitat in an Urban River. *Environmental Science & Technology,* 48**,** 11863-11871.

MCCORMICK, A. R., HOELLEIN, T. J., LONDON, M. G., HITTIE, J., SCOTT, J. W. & KELLY, J. J. 2016. Microplastic in surface waters of urban rivers: concentration, sources, and associated bacterial assemblages. *Ecosphere,* 7**,** e01556.

MUNARI, C., INFANTINI, V., SCOPONI, M., RASTELLI, E., CORINALDESI, C. & MISTRI, M. 2017. Microplastics in the sediments of Terra Nova Bay (Ross Sea, Antarctica). *Marine Pollution Bulletin,* 122**,** 161-165.

MUNNO, K., DE FROND, H., O'DONNELL, B. & ROCHMAN, C. M. 2020. Increasing the Accessibility for Characterizing Microplastics: Introducing New Application-Based and Spectral Libraries of Plastic Particles (SLoPP and SLoPP-E). *Analytical Chemistry,* 92**,** 2443-2451.

MURPHY, F., EWINS, C., CARBONNIER, F. & QUINN, B. 2016. Wastewater Treatment Works (WwTW) as a Source of Microplastics in the Aquatic Environment. *Environmental Science & Technology,* 50**,** 5800-5808.

NASSER, F., CONSTANTINOU, J. & LYNCH, I. 2020. Nanomaterials in the Environment Acquire an "Eco-Corona" Impacting their Toxicity to Daphnia Magna—a Call for Updating Toxicity Testing Policies. *PROTEOMICS,* 20**,** 1800412.

NASSER, F. & LYNCH, I. 2019. Updating traditional regulatory tests for use with novel materials: Nanomaterial toxicity testing with Daphnia magna. *Safety Science,* 118**,** 497-504.

NEL, H., KRAUSE, S., SAMBROOK SMITH, G. H. & LYNCH, I. 2019. Simple yet effective modifications to the operation of the Sediment Isolation Microplastic unit to avoid polyvinyl chloride (PVC) contamination. *MethodsX,* 6**,** 2656-2661.

NEL, H. A., CHETWYND, A. J., KELLEHER, L., LYNCH, I., MANSFIELD, I., MARGENAT, H., ONOJA, S., GOLDBERG OPPENHEIMER, P., SAMBROOK SMITH, G. H. & KRAUSE, S.

2021a. Detection limits are central to improve reporting standards when using Nile red for microplastic quantification. *Chemosphere,* 263**,** 127953.

NEL, H. A., DALU, T. & WASSERMAN, R. J. 2018. Sinks and sources: Assessing microplastic abundance in river sediment and deposit feeders in an Austral temperate urban river system. *Science of The Total Environment,* 612**,** 950-956.

NEL, H. A., NAIDOO, T., AKINDELE, E. O., NHIWATIWA, T., FADARE, O. O. & KRAUSE, S. 2021b. Collaboration and infrastructure is needed to develop an African perspective on micro(nano)plastic pollution. *Environmental Research Letters,* 16**,** 021002.

NGUYEN, B., CLAVEAU-MALLET, D., HERNANDEZ, L. M., XU, E. G., FARNER, J. M. & TUFENKJI, N. 2019. Separation and Analysis of Microplastics and Nanoplastics in Complex Environmental Samples. *Accounts of Chemical Research,* 52**,** 858-866.

NUELLE, M.-T., DEKIFF, J. H., REMY, D. & FRIES, E. 2014. A new analytical approach for monitoring microplastics in marine sediments. *Environmental Pollution,* 184**,** 161-169.

O'BRINE, T. & THOMPSON, R. C. 2010. Degradation of plastic carrier bags in the marine environment. *Marine Pollution Bulletin,* 60**,** 2279-2283.

OECD (2004), Test No. 202: Daphnia sp. Acute Immobilisation Test, OECD Guidelines for the Testing of Chemicals, Section 2, OECD Publishing, Paris, https://doi.org/10.1787/9789264069947-en.

OECD (2006), Test No. 221: Lemna sp. Growth Inhibition Test, OECD Guidelines for the Testing of Chemicals, Section 2, OECD Publishing, Paris, https://doi.org/10.1787/9789264016194-en.

OECD (2011), Test No. 201: Freshwater Alga and Cyanobacteria, Growth Inhibition Test, OECD Guidelines for the Testing of Chemicals, Section 2, OECD Publishing, Paris, https://doi.org/10.1787/9789264069923-en.

OECD (2014b), Test No. 239: Water-Sediment Myriophyllum Spicatum Toxicity Test, OECD Guidelines for the Testing of Chemicals, Section 2, OECD Publishing, Paris,

https://doi.org/10.1787/9789264224155-en.OECD 239: Water-sediment Myriophyllum spicatum toxicity test.

OECD (2014), Plastic Additives, Series on Emission Scenario Documents, No. 3, OECD Publishing, Paris, https://doi.org/10.1787/9789264221291-en.

OGONOWSKI, M., SCHÜR, C., JARSÉN, Å. & GOROKHOVA, E. 2016. The Effects of Natural and Anthropogenic Microparticles on Individual Fitness in Daphnia magna. *PLOS ONE,* 11**,** e0155063.

OLIVEIRA, M., RIBEIRO, A., HYLLAND, K. & GUILHERMINO, L. 2013. Single and combined effects of microplastics and pyrene on juveniles (0+ group) of the common goby Pomatoschistus microps (Teleostei, Gobiidae). *Ecological Indicators,* 34**,** 641-647.

OMIDI, M., FATEHINYA, A., FARAHANI, M., AKBARI, Z., SHAHMORADI, S., YAZDIAN, F., TAHRIRI, M., MOHARAMZADEH, K., TAYEBI, L. & VASHAEE, D. 2017. 7 - Characterization of biomaterials. *In:* TAYEBI, L. & MOHARAMZADEH, K. (eds.) *Biomaterials for Oral and Dental Tissue Engineering.* Woodhead Publishing.

OTTONI, E. B. 2000. EthoLog 2.2: A tool for the transcription and timing of behavior observation sessions. *Behavior Research Methods, Instruments, & Computers,* 32**,** 446-449.

PACHECO, A., MARTINS, A. & GUILHERMINO, L. 2018. Toxicological interactions induced by chronic exposure to gold nanoparticles and microplastics mixtures in Daphnia magna. *Science of The Total Environment,* 628-629**,** 474-483.

PARENTI, C. C., GHILARDI, A., DELLA TORRE, C., MAGNI, S., DEL GIACCO, L. & BINELLI, A. 2019. Evaluation of the infiltration of polystyrene nanobeads in zebrafish embryo tissues after short-term exposure and the related biochemical and behavioural effects. *Environmental Pollution,* 254**,** 112947.

PARK, T.-J., LEE, S.-H., LEE, M.-S., LEE, J.-K., LEE, S.-H. & ZOH, K.-D. 2020. Occurrence of microplastics in the Han River and riverine fish in South Korea. *Science of The Total Environment,* 708**,** 134535.

PEDERSEN, A. F., MEYER, D. N., PETRIV, A.-M. V., SOTO, A. L., SHIELDS, J. N., AKEMANN, C., BAKER, B. B., TSOU, W.-L., ZHANG, Y. & BAKER, T. R. 2020. Nanoplastics impact the zebrafish (Danio rerio) transcriptome: Associated developmental and neurobehavioral consequences. *Environmental Pollution,* 266**,** 115090.

PLASTICSEUROPE. Plastics - the Facts 2020. Retrieved from; https://www.plasticseurope.org/en/resources/market-data.

PROKIĆ, M. D., RADOVANOVIĆ, T. B., GAVRIĆ, J. P. & FAGGIO, C. 2019. Ecotoxicological effects of microplastics: Examination of biomarkers, current state and future perspectives. *TrAC Trends in Analytical Chemistry,* 111**,** 37-46.

QIANG, L. & CHENG, J. 2019. Exposure to microplastics decreases swimming competence in larval zebrafish (Danio rerio). *Ecotoxicology and Environmental Safety,* 176**,** 226-233.

QUINN, B., MURPHY, F. & EWINS, C. 2017. Validation of density separation for the rapid recovery of microplastics from sediment. *Analytical Methods,* 9**,** 1491-1498.

RAM, B. & KUMAR, M. 2020. Correlation appraisal of antibiotic resistance with fecal, metal and microplastic contamination in a tropical Indian river, lakes and sewage. *npj Clean Water,* 3**,** 3.

REDDY, M. S., SHAIK, B., ADIMURTHY, S. & RAMACHANDRAIAH, G. 2006. Description of the small plastics fragments in marine sediments along the Alang-Sosiya ship-breaking yard, India. *Estuarine, Coastal and Shelf Science,* 68**,** 656-660.

REDONDO-HASSELERHARM, P. E., FALAHUDIN, D., PEETERS, E. T. H. M. & KOELMANS, A. A. 2018. Microplastic Effect Thresholds for Freshwater Benthic Macroinvertebrates. *Environmental Science & Technology,* 52**,** 2278-2286.

REHSE, S., KLOAS, W. & ZARFL, C. 2016. Short-term exposure with high concentrations of pristine microplastic particles leads to immobilisation of Daphnia magna. *Chemosphere,* 153**,** 91-99.

REYNOLDS, A., GILTRAP, M. & CHAMBERS, G. 2019. Evaluation of non-invasive toxicological analysis of nano-polystyrene in relative in vivo conditions to D. magna. *Environmental Science: Nano,* 6**,** 2832-2849.

ROCH, S., FRIEDRICH, C. & BRINKER, A. 2020. Uptake routes of microplastics in fishes: practical and theoretical approaches to test existing theories. *Scientific Reports,* 10**,** 3896.

ROCH, S., WALTER, T., ITTNER, L. D., FRIEDRICH, C. & BRINKER, A. 2019. A systematic study of the microplastic burden in freshwater fishes of south-western Germany - Are we searching at the right scale? *Science of The Total Environment,* 689**,** 1001-1011.

ROCHMAN, C. M., HOH, E., KUROBE, T. & TEH, S. J. 2013. Ingested plastic transfers hazardous chemicals to fish and induces hepatic stress. *Scientific Reports,* 3**,** 3263.

ROCHMAN, C. M., PARNIS, J. M., BROWNE, M. A., SERRATO, S., REINER, E. J., ROBSON, M., YOUNG, T., DIAMOND, M. L. & TEH, S. J. 2017. Direct and indirect effects of different types of microplastics on freshwater prey (Corbicula fluminea) and their predator (Acipenser transmontanus). *PLOS ONE,* 12**,** e0187664.

RODA, J. F. B., LAUER, M. M., RISSO, W. E. & BUENO DOS REIS MARTINEZ, C. 2020. Microplastics and copper effects on the neotropical teleost Prochilodus lineatus: Is there any interaction? *Comparative Biochemistry and Physiology Part A: Molecular & Integrative Physiology,* 242**,** 110659.

SADLER, D. E., BRUNNER, F. S. & PLAISTOW, S. J. 2019. Temperature and clone-dependent effects of microplastics on immunity and life history in Daphnia magna. *Environmental Pollution,* 255**,** 113178.

SCHESSL, M., JOHNS, C. & ASHPOLE, S. L. 2019. Microbeads in Sediment, Dreissenid Mussels, and Anurans in the Littoral Zone of the Upper St. Lawrence River, New York. Pollution, 5, 41-52.

SCHWAFERTS, C., NIESSNER, R., ELSNER, M. & IVLEVA, N. P. 2019. Methods for the analysis of submicrometer- and nanoplastic particles in the environment. *TrAC Trends in Analytical Chemistry,* 112**,** 52-65.

SCOPETANI, C., ESTERHUIZEN, M., CINCINELLI, A. & PFLUGMACHER, S. 2020. Microplastics Exposure Causes Negligible Effects on the Oxidative Response Enzymes Glutathione Reductase and Peroxidase in the Oligochaete Tubifex tubifex. *Toxics* [Online], 8.

SHANG, X., LU, J., FENG, C., YING, Y., HE, Y., FANG, S., LIN, Y., DAHLGREN, R. & JU, J. 2020. Microplastic (1 and 5 μm) exposure disturbs lifespan and intestine function in the nematode Caenorhabditis elegans. *Science of The Total Environment,* 705**,** 135837.

SHIM, W. J., SONG, Y. K., HONG, S. H. & JANG, M. 2016. Identification and quantification of microplastics using Nile Red staining. *Marine Pollution Bulletin,* 113**,** 469-476.

SILVA, C. J. M., SILVA, A. L. P., GRAVATO, C. & PESTANA, J. L. T. 2019a. Ingestion of small-sized and irregularly shaped polyethylene microplastics affect Chironomus riparius life-history traits. *Sci Total Environ,* 672**,** 862-868.

SILVA, C. J. M., SILVA, A. L. P., GRAVATO, C. & PESTANA, J. L. T. 2019b. Ingestion of small-sized and irregularly shaped polyethylene microplastics affect Chironomus riparius life-history traits. *Science of The Total Environment,* 672**,** 862-868.

SJOLLEMA, S. B., REDONDO-HASSELERHARM, P., LESLIE, H. A., KRAAK, M. H. S. & VETHAAK, A. D. 2016. Do plastic particles affect microalgal photosynthesis and growth? Aquatic Toxicology, 170, 259-261.

STASICKA, Z. 2011. Chapter 7 - Transition metal complexes as solar photocatalysts in the environment: A short review of recent development. *In:* ELDIK, R. V. & STOCHEL, G. (eds.) *Advances in Inorganic Chemistry.* Academic Press.

STOLTE, A., FORSTER, S., GERDTS, G. & SCHUBERT, H. 2015. Microplastic concentrations in beach sediments along the German Baltic coast. *Marine Pollution Bulletin,* 99**,** 216-229.

SU, L., CAI, H., KOLANDHASAMY, P., WU, C., ROCHMAN, C. M. & SHI, H. 2018. Using the Asian clam as an indicator of microplastic pollution in freshwater ecosystems. *Environmental Pollution,* 234**,** 347-355.

SU, L., XUE, Y., LI, L., YANG, D., KOLANDHASAMY, P., LI, D. & SHI, H. 2016. Microplastics in Taihu Lake, China. *Environmental Pollution,* 216**,** 711-719.

TAGG, A. S., HARRISON, J. P., JU-NAM, Y., SAPP, M., BRADLEY, E. L., SINCLAIR, C. J. & OJEDA, J. J. 2017. Fenton's reagent for the rapid and efficient isolation of microplastics from wastewater. *Chemical Communications,* 53**,** 372-375.

THIELE, C. J., HUDSON, M. D. & RUSSELL, A. E. 2019. Evaluation of existing methods to extract microplastics from bivalve tissue: Adapted KOH digestion protocol improves filtration at single-digit pore size. *Marine Pollution Bulletin,* 142**,** 384-393.

THOMPSON, R. C., OLSEN, Y., MITCHELL, R. P., DAVIS, A., ROWLAND, S. J., JOHN, A. W. G., MCGONIGLE, D. & RUSSELL, A. E. 2004a. Lost at Sea: Where Is All the Plastic? *Science,* 304**,** 838-838.

THOMPSON, R. C., OLSON, Y., MITCHELL, R. P., DAVIS, A., ROWLAND, S. J., JOHN, A. W. G., MCGONIGLE, D. & RUSSELL, A. E. 2004b. Lost at Sea: Where Is All the Plastic? *Science,* 304**,** 838.

TIBBETTS, J., KRAUSE, S., LYNCH, I. & SAMBROOK SMITH, G. H. 2018. Abundance, Distribution, and Drivers of Microplastic Contamination in Urban River Environments. *Water,* 10**,** 1597.

TRIEBSKORN, R., BRAUNBECK, T., GRUMMT, T., HANSLIK, L., HUPPERTSBERG, S., JEKEL, M., KNEPPER, T. P., KRAIS, S., MÜLLER, Y. K., PITTROFF, M., RUHL, A. S., SCHMIEG, H., SCHÜR, C., STROBEL, C., WAGNER, M., ZUMBÜLTE, N. & KÖHLER, H.-R. 2019. Relevance of nano- and microplastics for freshwater ecosystems: A critical review. *TrAC Trends in Analytical Chemistry,* 110**,** 375-392.

TUNALI, M., UZOEFUNA, E. N., TUNALI, M. M. & YENIGUN, O. 2020. Effect of microplastics and microplastic-metal combinations on growth and chlorophyll a concentration of Chlorella vulgaris. *Science of The Total Environment,* 743**,** 140479.

VALAVANIDIS, A., VLAHOGIANNI, T., DASSENAKIS, M. & SCOULLOS, M. 2006. Molecular biomarkers of oxidative stress in aquatic organisms in relation to toxic environmental pollutants. *Ecotoxicol Environ Saf,* 64**,** 178-89.

VAN CAUWENBERGHE, L., DEVRIESE, L., GALGANI, F., ROBBENS, J. & JANSSEN, C. R. 2015. Microplastics in sediments: A review of techniques, occurrence and effects. *Marine Environmental Research,* 111**,** 5-17.

VARSOU, D. D., AFANTITIS, A., TSOUMANIS, A., PAPADIAMANTIS, A., VALSAMI-JONES, E., LYNCH, I. & MELAGRAKI, G. 2020. Zeta-Potential Read-Across Model Utilizing Nanodescriptors Extracted via the NanoXtract Image Analysis Tool Available on the Enalos Nanoinformatics Cloud Platform. *Small,* 16**,** e1906588.

WAGNER, J., WANG, Z.-M., GHOSAL, S., ROCHMAN, C., GASSEL, M. & WALL, S. 2017. Novel method for the extraction and identification of microplastics in ocean trawl and fish gut matrices. *Analytical Methods,* 9**,** 1479-1490.

WANG, H. & EVANS, C. L. 2016. Chapter 11 - Coherent Raman Scattering Microscopy in Dermatological Imaging. *In:* HAMBLIN, M. R., AVCI, P. & GUPTA, G. K. (eds.) *Imaging in Dermatology.* Boston: Academic Press.

WANG, J., QIN, X., GUO, J., JIA, W., WANG, Q., ZHANG, M. & HUANG, Y. 2020a. Evidence of selective enrichment of bacterial assemblages and antibiotic resistant genes by microplastics in urban rivers. *Water Research,* 183**,** 116113.

WANG, L., WU, W.-M., BOLAN, N. S., TSANG, D. C. W., LI, Y., QIN, M. & HOU, D. 2021. Environmental fate, toxicity and risk management strategies of nanoplastics in the environment: Current status and future perspectives. *Journal of hazardous materials,* 401**,** 123415-123415.

WANG, Q., WANGJIN, X., ZHANG, Y., WANG, N., WANG, Y., MENG, G. & CHEN, Y. 2020b. The toxicity of virgin and UV-aged PVC microplastics on the growth of freshwater algae Chlamydomonas reinhardtii. *Science of The Total Environment,* 749**,** 141603.

WANG, W., NDUNGU, A. W., LI, Z. & WANG, J. 2017. Microplastics pollution in inland freshwaters of China: A case study in urban surface waters of Wuhan, China. *Science of The Total Environment,* 575**,** 1369-1374.

WARDROP, P., SHIMETA, J., NUGEGODA, D., MORRISON, P. D., MIRANDA, A., TANG, M. & CLARKE, B. O. 2016. Chemical Pollutants Sorbed to Ingested Microbeads from Personal Care Products Accumulate in Fish. *Environmental Science & Technology,* 50**,** 4037-4044.

WEN, B., ZHANG, N., JIN, S.-R., CHEN, Z.-Z., GAO, J.-Z., LIU, Y., LIU, H.-P. & XU, Z. 2018. Microplastics have a more profound impact than elevated temperatures on the predatory performance, digestion and energy metabolism of an Amazonian cichlid. *Aquatic Toxicology,* 195**,** 67-76.

WINKLER, A., NESSI, A., ANTONIOLI, D., LAUS, M., SANTO, N., PAROLINI, M. & TREMOLADA, P. 2020. Occurrence of microplastics in pellets from the common kingfisher (Alcedo atthis) along the Ticino River, North Italy. *Environmental Science and Pollution Research,* 27**,** 41731-41739.

WONG, G., LÖWEMARK, L. & KUNZ, A. 2020. Microplastic pollution of the Tamsui River and its tributaries in northern Taiwan: Spatial heterogeneity and correlation with precipitation. *Environmental Pollution,* 260**,** 113935.

WOODALL, L. C., SANCHEZ-VIDAL, A., CANALS, M., PATERSON, G. L. J., COPPOCK, R., SLEIGHT, V., CALAFAT, A., ROGERS, A. D., NARAYANASWAMY, B. E. & THOMPSON, R. C. 2014. The deep sea is a major sink for microplastic debris. *Royal Society Open Science,* 1**,** 140317.

WU, Y., GUO, P., ZHANG, X., ZHANG, Y., XIE, S. & DENG, J. 2019. Effect of microplastics exposure on the photosynthesis system of freshwater algae. *Journal of Hazardous Materials,* 374**,** 219-227.

XIONG, X., ZHANG, K., CHEN, X., SHI, H., LUO, Z. & WU, C. 2018. Sources and distribution of microplastics in China's largest inland lake – Qinghai Lake. *Environmental Pollution,* 235**,** 899-906.

YAN, M., NIE, H., XU, K., HE, Y., HU, Y., HUANG, Y. & WANG, J. 2019. Microplastic abundance, distribution and composition in the Pearl River along Guangzhou city and Pearl River estuary, China. *Chemosphere,* 217**,** 879-886.

YUAN, W., LIU, X., WANG, W., DI, M. & WANG, J. 2019. Microplastic abundance, distribution and composition in water, sediments, and wild fish from Poyang Lake, China. *Ecotoxicology and Environmental Safety,* 170**,** 180-187.

ZBYSZEWSKI, M., CORCORAN, P. L. & HOCKIN, A. 2014. Comparison of the distribution and degradation of plastic debris along shorelines of the Great Lakes, North America. *Journal of Great Lakes Research,* 40**,** 288-299.

ZEYTIN, S., WAGNER, G., MACKAY-ROBERTS, N., GERDTS, G., SCHUIRMANN, E., KLOCKMANN, S. & SLATER, M. 2020. Quantifying microplastic translocation from feed to the fillet in European sea bass Dicentrarchus labrax. *Mar Pollut Bull,* 156**,** 111210.

ZHANG, Q., QU, Q., LU, T., KE, M., ZHU, Y., ZHANG, M., ZHANG, Z., DU, B., PAN, X., SUN, L. & QIAN, H. 2018. The combined toxicity effect of nanoplastics and glyphosate on Microcystis aeruginosa growth. *Environmental Pollution,* 243**,** 1106-1112.

ZHANG, S., LI, J., LYKOTRAFITIS, G., BAO, G. & SURESH, S. 2009. Size-Dependent Endocytosis of Nanoparticles. *Advanced Materials,* 21**,** 419-424.

ZIAJAHROMI, S., KUMAR, A., NEALE, P. A. & LEUSCH, F. D. L. 2017. Impact of Microplastic Beads and Fibres on Waterflea (Ceriodaphnia dubia) Survival, Growth, and Reproduction: Implications of Single and Mixture Exposures. *Environmental Science & Technology,* 51**,** 13397-13406.

ZIAJAHROMI, S., KUMAR, A., NEALE, P. A. & LEUSCH, F. D. L. 2018b. Environmentally relevant concentrations of polyethylene microplastics negatively impact the survival, growth and emergence of sediment-dwelling invertebrates. *Environmental Pollution,* 236**,** 425-431.

ZIAJAHROMI, S., KUMAR, A., NEALE, P. A. & LEUSCH, F. D. L. 2019. Effects of polyethylene microplastics on the acute toxicity of a synthetic pyrethroid to midge larvae (Chironomus tepperi) in synthetic and river water. *Science of The Total Environment,* 671**,** 971-975.

ZITOUNI, N., BOUSSERRHINE, N., BELBEKHOUCHE, S., MISSAWI, O., ALPHONSE, V., BOUGHATASS, I. & BANNI, M. 2020. First report on the presence of small microplastics (≤ 3 μm) in tissue of the commercial fish Serranus scriba (Linnaeus. 1758) from Tunisian coasts and associated cellular alterations. *Environmental Pollution,* 263**,** 114576.

Chapter 4: Prevailing impacts of river management on microplastic transport in contrasting US streams requires rethinking of global microplastic flux estimations.

Anna Kukkola[a], Uwe Schneidewind[a], Liam Kelleher[a], Greg Sambrook Smith[a], Holly Astrid Nel[b], Iseult Lynch[a,d] and Stefan Krause[a,c,d]

[a] School of Geography, Earth and Environmental Sciences, University of Birmingham, Edgbaston, Birmingham B15 2TT, United Kingdom

[b] Centre for Environment, Fisheries and Aquaculture, Pakefield Road, Lowestoft, Suffolk NR33 0HT, United Kingdom

[c] LEHNA- Laboratoire d'ecologie des hydrosystemes naturels et anthropises, University of Lyon, Darwin C & Forel, 3-6 Rue Raphaël Dubois, 69622 Villeurbanne, France.

[d] Institute of Global Innovation, University of Birmingham B15 2SA, Birmingham. United Kingdom.

***This chapter has been published in Water Research**

https://doi.org/10.1016/j.watres.2023.120112

4.1 Abstract

While microplastic inputs into rivers are assumed to be correlated with anthropogenic activities and to accumulate towards the sea, the impacts of water management on downstream microplastic transport are largely unexplored. A comparative study of microplastic abundance in Boulder Creek (BC), and its less urbanized tributary South Boulder Creek (SBC), (Colorado USA), characterized the downstream evolution of microplastics in surface water and sediments, evaluating the effects of urbanization and flow diversions on the up-to-downstream profiles of microplastic concentrations and loads. Water and sediment samples were collected from 21 locations along both rivers and microplastic properties determined by fluorescence microscopy and Raman spectroscopy. The degree of catchment urbanization affected microplastic patterns, as evidenced by greater water and sediment concentrations and loads at BC than the less densely populated SBC, which is consistent with the differences in the degree of urbanization between both catchments. Microplastic removal through flow diversions was quantified, showing that water diversions removed over 500 MP particles per second from the river, and caused stepwise reductions of downstream loads at abstraction points. This redistribution of microplastics back into the catchment needs to be considered in large scale models quantifying plastic fate and transport to the oceans.

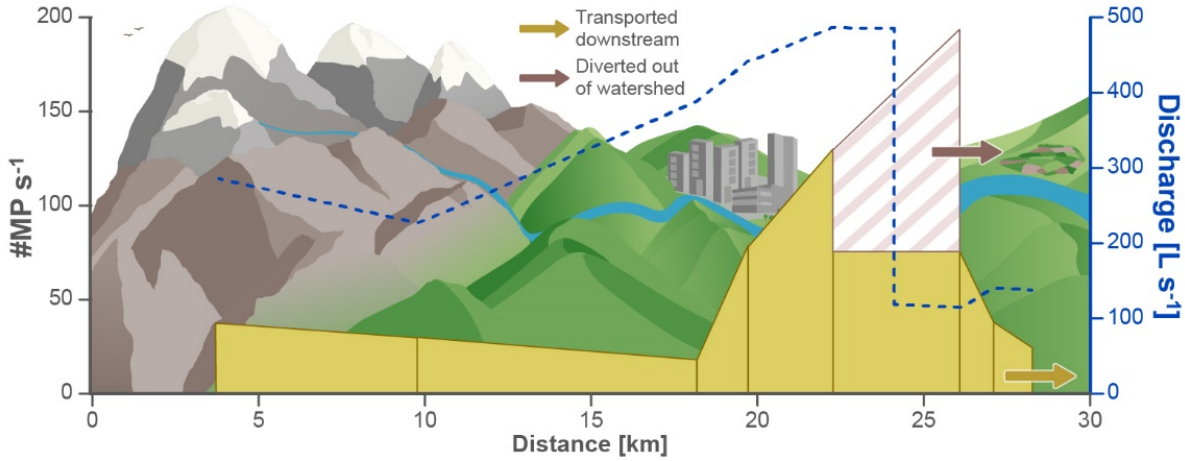


Figure 4.0 Graphical abstract

4.2 Introduction

Microplastics (plastic particles <1 mm) (Hartmann et al., 2019) (herein referred to as MP) are considered to be contaminants of concern (Lambert and Wagner, 2018) and are omnipresent in all environmental compartments on a global scale (e.g.,Bian et al., 2022; Kukkola et al., 2022; Samandra et al., 2022; Zhang et al., 2021). Despite MPs having been the focus of intense research efforts, their sources, environmental entry points, transport mechanisms and resulting distribution in the environment have yet to be fully understood.

It has been demonstrated that rivers represent major MP transport pathways to the oceans (Lebreton et al., 2017; Meijer et al., 2021), but can also act as long-term sinks (Drummond et al., 2020; Drummond et al., 2022; Margenat, 2021). Additionally, MP in riverine environments may undergo major physio-chemical transformation processes (Krause et al., 2021; McGivney et al., 2020) and interact with the diverse community of freshwater organisms with potentially

detrimental effects on species and ecosystem health (e.g., causing external and intestinal damage and suffocation) (Anbumani and Kakkar, 2018; Kukkola et al., 2021).

To fully assess the risks that MP pose to river environments and their ecosystem services, it is crucial to understand how MP are distributed within river corridors and how they get transported and potentially accumulated in river networks (Krause et al., 2021). Previous research has highlighted the existence of substantial spatial variability in MP in surface water and sediment in a wide range of river systems (e.g., Castañeda et al., 2014; Wong et al., 2020). However, it is less well-established which processes control this spatial variability. A better understanding of these processes is a requirement for more accurate predictions of the full extent to which rivers contribute to global plastic fluxes into the oceans and for site-specific risk assessments. Additionally, flux information needs to be coupled with estimates of MP residence times, to assess local exposure and potential impacts on freshwater ecosystems.

Previous research has aimed to identify how population density and specifically, the location of potential point and diffuse sources of mismanaged plastic waste influence the spatial distribution of MP. Consequently, land use/land cover has been linked to MP concentrations and distribution in rivers (Grbić et al., 2020; Wang et al., 2021), and global scale estimates of terrestrial plastic pollution and resulting riverine contributions to the oceans have predicted pollution hotspots to occur in densely populated urban areas with poor waste management systems (Ferraz et al., 2020; Lebreton et al., 2019; Lebreton et al., 2017; Meijer et al., 2021). However, a clear correlation between the degree of urbanization and MP concentration could often not be established (see Talbot and Chang, 2022; Tibbetts et al., 2018).

There is growing awareness that, in addition to the spatial distribution of sources, the environmental fate of MP is strongly determined by their transport, dispersal and potential deposition and storage along river networks (de Carvalho et al., 2021; Margenat, 2021; Tibbetts et al., 2018). Flow conditions may strongly affect MP deposition behaviour and residence time in the hyporheic zone (Drummond et al., 2020; Drummond et al., 2022). Current model predictions of riverine contributions to MP in the world's oceans show discrepancies ranging over several orders of magnitude (Lebreton et al., 2017; Schmidt et al., 2017). Current models use only relatively coarse spatial information of river discharge, if included at all (Siegfried et al., 2017; Uzun et al., 2022; van Wijnen et al., 2019). Very few studies have investigated the change in MP concentrations in relation to the hydrological regime and the characteristic flow and transport behaviour of the respective river systems (Campanale et al., 2020; Wagner et al., 2019). A general assumption of existing large scale plastic transport models is a downstream convergence of particle fluxes along the river network. There is a severe lack of understanding of the impact of river water management schemes (e.g., water diversion for irrigation and drinking water), on MP distribution, fate, and transport in river corridors, despite the majority of rivers globally now being regulated in their flow (Barbarossa et al., 2020; Baumgartner et al., 2022). It is therefore imperative to analyse and quantify the combined impacts of MP source distributions, and their transport in river networks under the influence of anthropogenically altered flow and transport conditions, in order to aid model predictions.

Here, we present a comparative field study that applies a paired-catchment approach to quantify the spatial distribution of MP in two neighbouring catchments (South Boulder Creek and Boulder Creek, Colorado, USA) with different degrees of urbanization. This study (i) characterizes

the downstream evolution of MP concentration and associated particle properties in surface water and streambed sediments, (ii) identifies MP source areas using spatial profiles of stream load (the product of concentration and stream discharge), (iii) evaluates the effects of a) the mountain to plains transition and b) urbanization, and (iv) quantifies the degree to which flow diversions affect MP concentrations, loads, and downstream transport.

4.3 Materials and methods

4.3.1 Study region

Boulder Creek (BC) and its tributary South Boulder Creek (SBC) (Colorado, USA) are part of the wider Boulder Creek Watershed, which extends over 1160 km^2 and is located in the Front Range of the Rocky Mountains, east of the Continental Divide. Both catchments cover diverse geographical and hydro-geomorphological conditions along a rural-urban gradient and differ significantly in catchment-wide and near-stream land cover patterns (Figure 4.1).

Both streams flow northeast from their mountainous headwaters that originate at the Continental Divide (elevations >4100 m) and through canyons (upstream sampling locations B1 and S1 are ~2400 m) before they reach the plains (sampling locations B12 and S6, elevation <1800 m), and eventually confluence at the eastern edge of the city of Boulder near sampling point B33 (Figure 4.1). Ultimately these waters drain into the Mississippi River and the Gulf of Mexico, in over 2300 km distance. The BC catchment is more urbanized (12% upstream of confluence with SBC) than SBC (3.9% upstream of confluence with BC). Both are characterized by a high forest cover (BC 73% and SBC 84%). The catchment areas for BC and SBC upstream of their confluence are 405 km^2 and 342 km^2 respectively, with a total catchment size of 790 km^2 at point B34 (Figure 4.1). The sampled river sections cover 36.7 km flow length of BC and 27.7 km of SBC. Over these

sections, river slope varies between 0.003 m/m (B34) and 0.040 m/m (B9) for BC and 0.005 m/m (S9) and 0.085 (S1) for SBC while average sinuosity is 1.31 (BC) and 1.39 (SBC), respectively, indicating a comparable, and generally low degree of meandering.

Like for many river systems in the western United States, water management plays a large role in both streams (Murphy, 2006). Mountain reservoirs are used to store large volumes of water generated during spring snowmelt, and this water is subsequently diverted out of the catchments for municipal and agricultural use through a system of canals. As such, stream discharge decreases in downstream direction for long periods of the year.

The BC study reach begins approximately 4 km downstream of Barker Reservoir, which receives water from the surrounding catchment, a relatively undeveloped area to the east of the Continental Divide. Water released from Barker Reservoir travels down Boulder Canyon, entering the City of Boulder near sampling location B12 (Figure 4.1). The primary diversion affecting stream discharge during this study is located downstream of sample location B19, where more than half of the discharge is diverted away from BC at certain times of year.

The SBC study reach begins approximately 1.5 km downstream of Gross Reservoir which receives much of its water from the underground Moffatt Tunnel that transports water from west of the Continental Divide to the eastern side. Most of the water leaving Gross Reservoir is diverted out of SBC downstream of sampling location S1, supplying water to Denver city. SBC flows through the small town of Eldorado Springs before entering the plains downstream of sample location S6. A second major diversion active during the study period is located downstream of site S13, resulting in additional decreases in stream discharge.

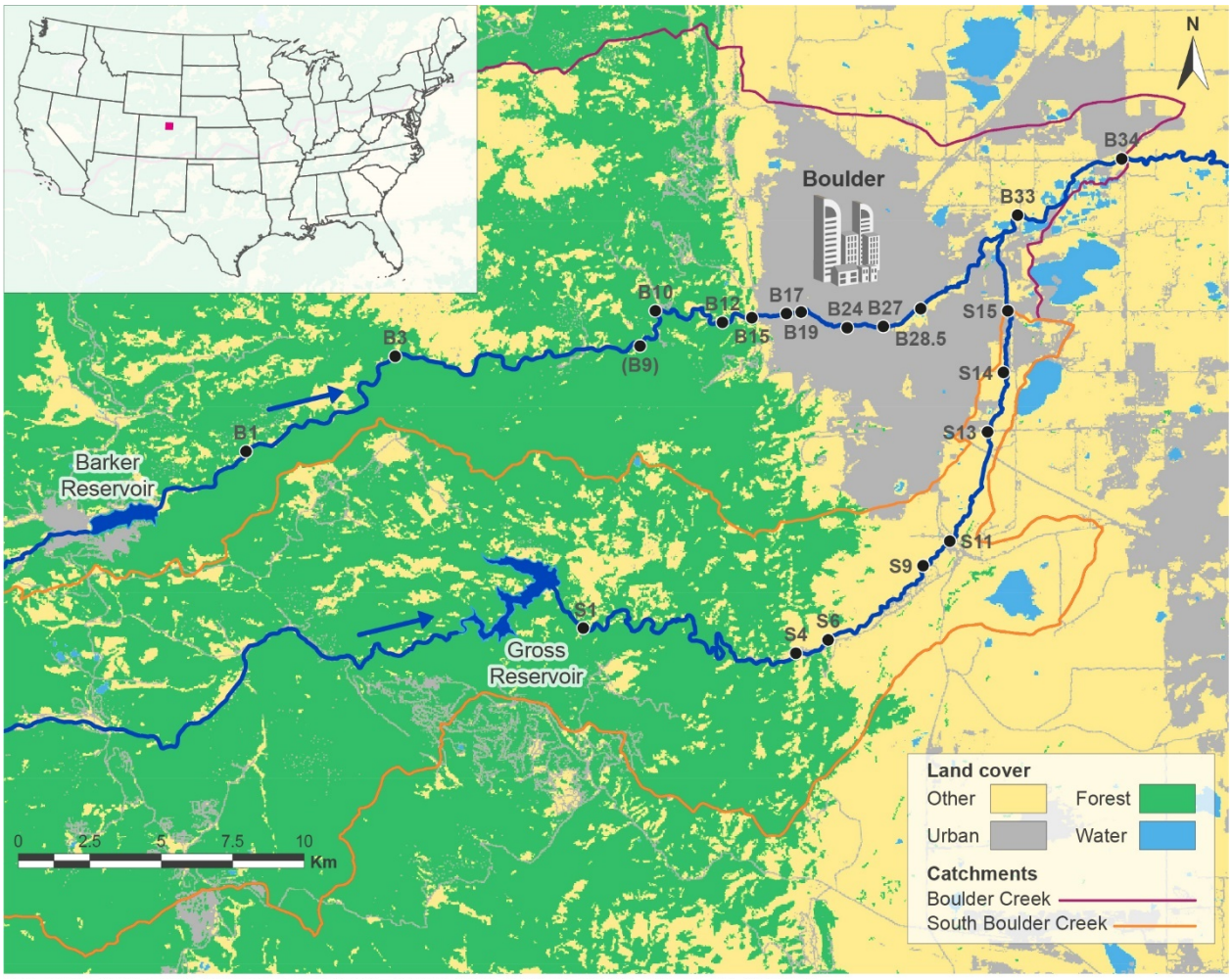


Figure 4.1: Map of catchment areas indicating major land cover classes and sampling locations (black dots) along Boulder Creek (B1-34) and South Boulder Creek (S1-15), Colorado, USA. Blue arrows indicate flow direction and orange and pink lines the extent of SBC and BC catchment areas, respectively. Coordinates of each sampling location are provided in Table S4.1. Land cover class "Other" includes perennial ice/snow, barren land, grassland, shrub/scrub, cultivated crops, and pastry-hay.

4.3.2 Field data and sample collection

Surface water and sediment samples were collected from thirteen locations within BC and eight sites within SBC (as a subset of a longer-term study that includes additional sample locations (Runkel et al., 2022). Sampling took place October 14-18, 2019, during steady low-flow conditions, which are typical in the research area for the period between October and March. The relatively steady flow conditions during the sampling period were confirmed by stream discharge records from gauging stations BOCOROCO (~18.5 km downstream from Barker Reservoir, sampling location B9) and BOCELSCO (~0.7 km downstream from the major diversion located between S1 and S4) (Figure 4.2).

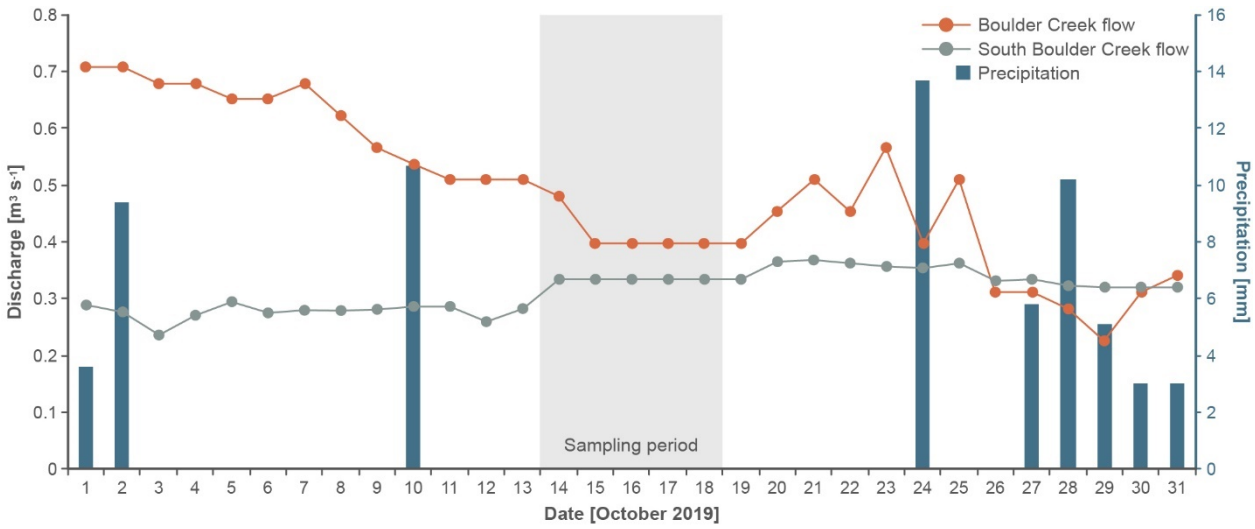


Figure 4.2: Discharge and precipitation during the sampling period in October 2019. Discharge data are from the Colorado Division of Water Resources gauges BOCOROCO near Orodell, CO (B9 Figure 4.1) and BOCELSCO near Eldorado Springs, CO (https://www.dwr.state.co.us). Precipitation data are for the National Oceanic and Atmospheric Administration Physical Sciences Laboratory, located at 39.99271N, -105.2652W (Wetherbee et al., 2021).

At each sampling site, 50 L of surface water was collected from the centre of the stream and water column, and filtered through a 63 µm nylon mesh, from which contents were then transferred into a precleaned 20 mL glass vial using deionized (DI) water. Sediment was collected from both streambanks just above the water line using a metal spoon. A composite sediment sample from three spots (within a radius of about 1 m) was collected and stored in a clean glass jar, giving a final sample mass of 60 - 90 g per streambank. All samples (N_{water} = 21 and $N_{sediment}$ = 42) were stored at room temperature and transported to the University of Birmingham, UK for analysis at the end of the sampling period. Data collected at each sampling point comprised geographic coordinates, stream depth, cross-sectional area, velocity, and discharge as measured by Acoustic Doppler Velocimetry (Appendix 3: Table S4.1).

4.3.3 Sample analysis and QA/QC

Sediment samples were extracted using sediment-MP isolation (SMI) units in accordance with Nel et al., (2020), and water samples as described in Appendix 3: S4.1 MP extraction. After extraction, organic matter (OM) was digested using Fenton reagent, which after the samples were stained with Nile Red as described in Appendix 3: S4.1. Samples were analysed with fluorescence microscopy as described in Kukkola et al., (2023) and in Appendix 3: S4.2. Polymer identification by confocal Raman spectroscopy was employed for roughly 44% of all putative MP (in total 206 particles). The procedure and spectra acquisition parameters are described in Appendix 3: S4.3. Field background samples, laboratory blanks and positive blanks were collected and analysed as described in Appendix 3: S4.4. For the purposes of this study, MP measurements in counts per litre are hereinafter referred to as concentrations.

4.3.4 Land cover, population density, and statistical analyses

To understand how MP concentrations vary in relation to catchment area and the percent of urban land cover, each sub-catchment (defined as the drainage area discharging towards each sampling location) was delineated with the USGS program StreamStats v4.6.2 (https://streamstats.usgs.gov) and exported into ArcMap 10.7.1. Population density per sub-catchment for 2019 was obtained from the Colorado State Demography Office (https://demography.dola.colorado.gov) and land cover classes for sub-catchments were determined utilizing the National Land Cover Database (Multi-Resolution Land Characteristics Consortium; https://www.mrlc.gov/viewer/) NLCD 2019 dataset which contains official land cover data for the USA (2019) with a resolution of 30 x 30 m. The 20 landcover classes from the NLCD data set were reclassified into nine general categories (see Appendix 3, section S5).

To analyse potential local land cover impacts on observed MP concentrations, a 500 m circular buffer (A=0.79 km^2) was created around each sampling site in ArcMap, to aid identification of possible local source effects, as compared to the sub-catchment wide approach. To study effects in sub-catchments, the area per land cover class was normalized to the respective sub-catchment area. All data was assessed for normality using a Shapiro-Wilk Test. Spearman's rank coefficient was used to determine correlations between MP concentrations and urban land cover and population density, because MP data followed a non-normal distribution.

To evaluate any variation in MP concentrations in water and sediment between and within the two streams, Mann-Whitney U and Kruskal-Wallis tests were applied. Spearman's rank coefficient was used to assess correlation direction and strength for MP concentration and size

(measured as longest length) and hydrological parameters. All statistical analyses were carried out in RStudio (R Core Team 2022) with a significant threshold of $\alpha = 0.05$.

4.3.5 MP loads and estimated concentrations in the absence of diversions

Contributions of MP from the sub-catchments discharging to each segment of the study reaches (i.e., the distance between sampling locations) were quantified using spatial profiles of the stream MP loads (Table 4.1), developed by summing the observed load at each location (the product of stream discharge and concentration) and the load that had been diverted out of the system (the product of the diverted stream discharge and the concentration at the nearest upstream site). Profiles of cumulative load were calculated by summing all positive changes in instream load, while keeping the cumulative load constant when the instream load decreased (Kimball et al., 2002; Runkel et al., 2013). Stream segments with increases in cumulative load thus represent source areas, with each source area contributing a percentage to the overall load:

$$percent\ contribution\ = 100 \times \frac{(L_d - L_u)}{(L_b - L_t)} \quad (1)$$

where $\boldsymbol{L}$ is the cumulative load, $\boldsymbol{d}$ and $\boldsymbol{u}$ denote the cumulative load at the downstream and upstream ends of a stream segment, while $\boldsymbol{b}$ and $\boldsymbol{t}$ denote the cumulative load at the bottom and top of the study reach.

Loading rates (change in load per km) were also calculated for individual segments (between sampling points) and for the entire study reach as:

$$Loading\ rate\ = \frac{\Delta\ load}{distance} \quad (2)$$

where Δ ***load*** is the change in load for the segment or study reach ($\boldsymbol{L_d - L_u}$ or $\boldsymbol{L_b - L_t}$) and distance equals the length of the segment or study reach (Table 4.1). Three sampling points were excluded from the loading analysis due to unsteady flow conditions during sampling (B15, B17 and B19). Two additional BC sites located below the confluence of BC and SBC (B33, B34) were also excluded as they couldn't contribute to the comparison of the two study reaches. These downstream sites are omitted from our discussion of the results presented in Sections 4.3.1 and 4.3.3.

Both study reaches have water diversions which decrease stream discharge. Sampling locations downstream of these diversions will have a smaller volume of water than they would in the absence of diversions, and consequently the impact of a given source area and loading rate will be exacerbated with less dilution occurring due to reduced discharge. These impacts can be formally quantified by estimating the MP concentrations that would be observed in the absence of diversions. MP water concentrations in the absence of diversions are calculated by summing the observed and diverted loads and dividing by the sum of the observed and diverted stream discharge.

4.4 Results

4.4.1 Stream discharge

Stream discharge measured during the sampling period ranged from 0.12 $m^3\ s^{-1}$ (B24) to 0.50 $m^3\ s^{-1}$ (B12) for BC (Figure 4.3a) and from 0.06 $m^3\ s^{-1}$ (S14) to 2.48 $m^3\ s^{-1}$ (S1) for SBC (Figure 4.3b). Several flow diversions were active during the sampling event, with the major diversion on BC diverting 87% of the stream discharge at B19 away from BC (0.43 $m^3\ s^{-1}$). For the SBC study reach, 95% of the stream discharge at S1 (2.35 $m^3\ s^{-1}$) was diverted for use by the city of Denver and 79% of the remaining stream discharge at S13 (0.24 $m^3\ s^{-1}$) was diverted out of the channel.

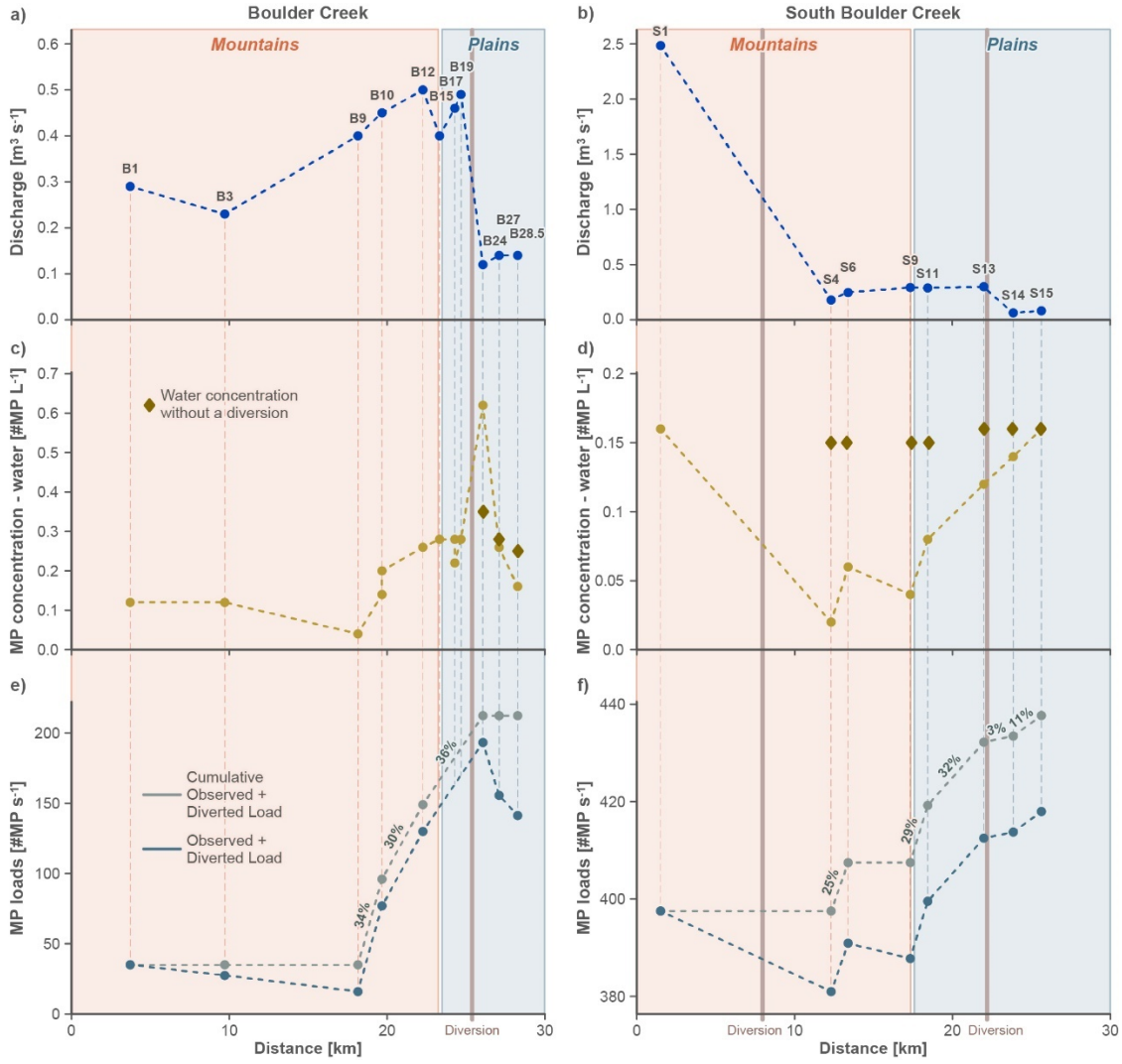


Figure 4.3: Stream discharge (panels a-b), MP surface water concentrations [#MP L^{-1}] and estimated concentrations in the absence of diversions (panels c-d), and downstream profiles of MP loads [#MP s^{-1}] (panels e-f) for Boulder Creek and South Boulder Creek. Note replicate samples collected at B10 and B17 (panel c).

4.4.2 MP concentrations in surface water and streambed sediments

MP were detected in all surface water and sediment samples across the studied sites (Figure 4.4). Mean surface water MP concentrations for BC were 0.22 MP L^{-1} (± 0.14 standard deviation

(SD)), ranging between 0.08 MP L^{-1} (B9) and 0.62 MP L^{-1} (B24). For SBC, mean MP concentrations were 0.09 MP L^{-1} (± 0.05 SD) with a range between 0.02 MP L^{-1} (S4) and 0.16 MP L^{-1} (S1). A Mann-Whitney U test confirmed that the difference in surface water MP concentration was significant (p = 0.0163) between the two streams. Streambed sediments for BC had a mean dry-weight MP concentration of 186 MP kg^{-1} (± 80 MP SD), ranging between 114 MP kg^{-1} (B3) and 342 MP kg^{-1} (B24). For SBC the mean sediment MP concentrations were 142 MP kg^{-1} (± 55 MP SD), ranging from 98 MP kg^{-1} (S1) to 224 MP kg^{-1} (S13). Mann-Whitney Test indicated that the difference in sediment concentration was non-significant (p = 0.0912).

MP concentrations at BC surface water remained relatively low in the mountainous upstream reach (B1-B9, Figure 4.4) and exhibited an initial increase at B10, where urbanization begins. The MP concentrations remained fairly consistent in the stream reach between B10 and B27, with the exception of a hotspot at B24. The sediment concentrations generally displayed a non-significant increasing trend downstream, with peaks between sites B12 and B24 (Figure 4.4), B12 being where BC emerges from Boulder Canyon at the city margins of Boulder, while B24 is located at the eastern edge of a high-density urban area where the highest surface water concentration was also observed.

The highest surface water MP concentrations at SBC were recorded at the most upstream site (S1) and the most downstream site (S15) (0.16 MP L^{-1}); the highest MP concentrations in SBC sediment were recorded at site S13. Surface water concentrations in SBC exhibited a linear positive relationship with distance downstream of the first major diversion (site S1 excluded; R_s = .964, p = 1.85×10^{-5}), with increasing concentrations downstream. No relationship was observed between distance from source and MP concentration in sediments (Figure 4.4).

No correlation was found between stream discharge and the size of MP either in surface water or sediments at BC; however, a moderate positive correlation was found between discharge and size of MP in surface water at SBC (Appendix 3: Table S4.4). There was no correlation between discharge and MP concentration in water or sediments (Appendix 3: Table S4.5). No correlation was found between river velocity or slope and MP concentration in surface water or sediments (Appendix 3: Table S4.5).

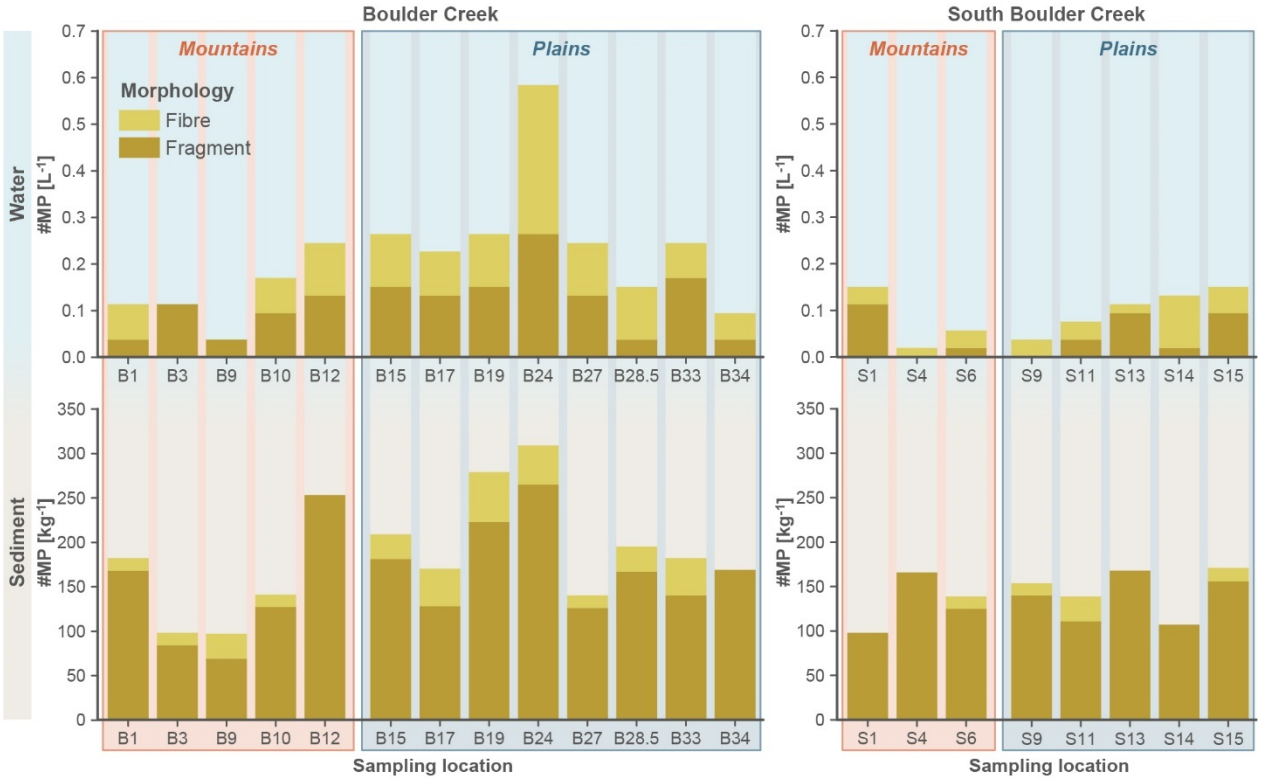


Figure 4.4: MP concentration distribution in water (top panel) and sediments (bottom panel) of Boulder Creek (left) and South Boulder Creek (right).

4.4.3 MP loads

The average stream MP load for BC was 97 MP s^{-1}, with a range between 16 MP s^{-1} (B9) and 193 MP s^{-1} (B24) (Figure 4.3e). The stream MP load for BC declines from B1 (35 MP s^{-1}) to

B9 (16 MP s^{-1}), after which it steadily increases to its maximum of 193 MP s^{-1} at B24. MP load then decreases in the last two stream segments (B27 and B28.5), to 141 MP s^{-1} (Figure 4.3e).

The average stream load for SBC was 400 MP s^{-1}, with a range between 381 MP s^{-1} (S4) and 418 MP s^{-1} (S15) (Figure 4.3f). The MP stream load drops between sites S1 and S4, after which it generally increases to its maximum value at the end of the study reach (S15, Figure 4.3f). As will be discussed in detail in Section 4.4.4, most of the stream load is diverted out of the SBC catchment near the head of the study reach.

Average study-reach loading rates were 7.2 and 1.7 MP s^{-1} km^{-1} for BC and SBC, respectively. MP loading in BC is dominated by contributions to the three stream segments ending at B10, B12, and B24 (percent contributions of 34, 30, and 36% respectively; Figure 4.3e). MP loading at SBC had major contributions at S6 (25%), S11 (29%), S13 (32%), and S15 (11%) (Figure 4.3f).

4.4.4 Physical and chemical properties of MP

For BC surface water, fragments amounted to 51.7% and fibres to 48.3% of the total MP detected (Figure 4.4). Similarly, for SBC surface water, 51.3% of total MP were fragments and 48.7% fibres. No spheres were detected in water samples from either stream. A clear colour dominated fragments and a blue colour dominated fibres in both streams. In the BC sediments, mostly fragments were present (87%), while fibres (12%) and spheres (1%) played a minor role (Appendix 3: Figure S4.3). For SBC the percentage of fragments (93%) was slightly larger while fibres only amounted to 7%. In sediments from both streams, most fragments were a clear colour while most fibres were black. In total, 206 putative MP (44% of total) were subjected to Raman spectroscopy analysis from which 86% were positively identified as plastics, with the most

common polymer type in surface water being polyester (50%) and in sediment being polyethylene terephthalate (36%, for details see Appendix 3: S4.6).

4.4.5 Land cover impacts on MP

A Mann Whitney U test indicated a statistically significant difference in urban land cover between BC and SBC upstream of their confluence (U = 84, p = 0.0001). When assessing the relationship of urban land cover within sub-catchments to MP concentrations, no correlation was found in water or sediments for BC. However, at SBC, a very strong correlation was found in surface water (site S1 excluded; R_s = .964, p < 0.001), with no trend evident in the sediments (SBC Rs -.047, p = 0.910). Besides urbanization, no significant correlations were found for other land cover types for SBC. MP concentrations in surface water were positively correlated with forest cover (Rs .643, p = 0.0241) for BC, but negatively for SBC (Rs -.658, p = 0.075). This is likely related to forest cover in BC increasing downstream to the confluence but decreasing downstream at SBC. MP concentrations in surface water and sediment were not correlated with the total catchment area (BC_{water} Rs = 0.275 p = 0.391, BC_{sed} Rs 0.322 p = 0.222, SBC_{water} Rs 0.395 p = 0.332 SBC_{sed} Rs 0.476 p = 0.232).

The analysis of land cover impacts in the immediate 500 m buffer around each sampling location revealed a strong positive correlation between surface water MP concentration and urban cover at BC (Rs.793, p = 0.025), and at SBC if the most upstream sampling point (S1) was excluded from the analysis (Rs_{withS1}.299, p = 0.4713, $Rs_{withoutS1}$.828, p = 0.023). For sediments, no significant correlation was identified for BC (Rs .508, p = 0.075) while for SBC the moderate correlation found was not statistically significant (Rs .547, p = 0.16). None of the other land cover types had any correlation to MP concentrations for BC or SBC.

4.5 Discussion

4.5.1 MP concentration in surface water and sediments

The more urbanized BC (0.22 MP L^{-1}, > 63 μm) had higher MP concentrations in surface water than SBC (0.09 MP L^{-1}), but both streams could be considered to have relatively low MP contamination present and our findings are similar to other studies in rivers of comparable properties (remote, mountainous) (Bian et al., 2022; Dalmau-Soler et al., 2021; Ferraz et al., 2020) and orders of magnitude lower than those reported from lowland rivers, such as canals in Suzhou city, China (8 - 40 MP L^{-1}) (> 20 μm) or Amsterdam, Netherlands (48-187 MP L^{-1}) (> 10μm) (Jin et al., 2022; Leslie et al., 2017). Similarly, BC had higher sediment MP concentrations (186 MP kg^{-1}) than SBC (142 MP kg^{-1}), but these are in line with those previously reported from remote areas, such as from the rivers of the Tibetan Plateau, (50 - 195 MP kg^{-1} > 20μm) (Jiang et al., 2019) and from Dafeng River, China, (0.0 - 50.3 MP kg^{-1} > 20 μm) (Liu et al., 2021).

4.5.2 The effects of the mountain to plains transition and urbanization on MP concentrations and types

Surface water and sediment MP concentrations increase in the downstream direction for both BC and SBC, with downstream trends being particularly clear in surface water (Figure 4.4). This is consistent with previous studies: six rivers located at a mountain-foothill transition area in the Chin Ling - Wei River Plain, China, had concentrations of 2.57 ± 0.14 MP L^{-1} (> 75 μm) in the mountainous areas, with increasing concentrations downstream (up to 20.40 ± 0.43 MP L^{-1}) (Bian et al., 2022). Similarly, in the Llobregat River, Spain, no MP (> 20 μm) were reported from headwater locations, but concentrations increased downstream to 3.60 MP L^{-1} (Dalmau-Soler et al., 2021). This type of downstream change has previously been attributed to increasing population,

urbanization, and anthropogenic activity, typically present along the flow length(s) of rivers (de Carvalho et al., 2021; Yuan et al., 2022). These trends therefore suggest a linkage between MP concentration and urbanization, given the increase in urbanization with distance downstream that has been documented in both our catchments. This linkage is further illuminated by the sub-catchment analysis. A positive relationship was detected for MP concentration and degree of urbanization in sub-catchments of SBC downstream of S1. Though this relationship was not found for the sub-catchments of BC, the effect of urbanization was evident in both surface water and sediments, with a clear increase of MP concentrations at B10 where the stream emerges from Boulder Canyon and enters the urban area (Figure 4.4). This increase is maintained downstream of B10, with relatively consistent MP concentrations through the highly urbanized area (B10-B27). The effect of urbanization was further supported by assessment of the immediate 0.79 km^2 buffer around sampling points, as this revealed a significant local impact of urbanization in surface water for both BC and SBC (S1 was excluded as an outlier), indicating that proximity to the source and human activities is a critical factor in driving MP concentration in this riverine environment.

Although data from both streams suggests a linkage between MP concentration and urbanization, the effect of urbanization can be further elucidated by directly comparing the two streams. Urban land cover in the BC catchment is approximately 3.1 times greater than that of SBC (Section 4.3.1), and the higher degree of urbanization in BC may be responsible for the higher surface water and sediment MP concentrations (Section 4.3.2). Further, the MP loading rate for the BC study reach is 4.2 times higher than for SBC (Section 4.3.3), in close agreement with the urban land cover ratio (3:1) and the ratio of loading rates for inorganic constituents considered in the larger study that coincided with this research (Runkel et al., 2022).

Sub-catchment contributions of MP to the receiving streams are formally quantified by the loading analysis. For the case of BC, three consecutive stream segments represent the dominant MP sources, with each contributing approximately one third of the MP load (B10-B24; Figure 4.3e, Section 4.4.3). The sub-reach encompassing these segments begins upstream of the City of Boulder, suggesting the presence of a margin around the urban area that is affected by the more populated area: i.e., access to numerous mountain homes and recreational activities is provided by a heavily travelled highway in the lower part of Boulder Canyon. The lower parts of this sub-reach are within the city proper, and water and sediment concentrations at its terminus are the highest concentrations observed in this study (B24, Section 4.3.2).

At SBC, higher sub-catchment contributions include S1 at the head of the study reach and stream segments downstream of Eldorado Springs. Although the surface water concentration at S1 is high relative to other SBC sites, S1 is not in an urban area and its concentration is lower than at the urban sites in BC (Figure 4.4). The high MP concentration observed at S1 is likely attributable to its proximity to Gross Reservoir, where potential sources include recreational activities, water diverted from west of the continental divide, and a nearby road. Though atmospheric deposition has been reported previously for this study area and adjacent Upper Colorado area (Reynolds et al., 2022; Wetherbee et al., 2019), the contribution to MP concentration is expected to remain equal at all sites, and is not believed to be the driving cause of the relatively high MP concentrations at S4.1. All stream segments downstream of Eldorado Springs contribute to the MP load, except for the segment ending at S9 (Figure 4.3f). This loading may also be associated with urban activities, with potential sources being areas such as Eldorado Springs, low-density housing upstream of S11, and highways and roads that cross SBC as it enters the plains.

4.5.3 The effect of diversions on MP concentrations, loads, and downstream transport

The magnitude of flow diversions from BC and SBC results in large quantities of MP being removed from each catchment, despite the relatively low surface water concentrations observed in both streams. The diversion downstream of B19 removes ~90% of the water (Section 4.4.1) and an equivalent percentage of surface water MP from BC (a removal of 119 MP s^{-1}: Figure 4.5). Similarly, the diversion below S1 removes ~95% of the water and MP (a removal of 376 MP s^{-1}) from SBC, while the second diversion removes ~80% of the remaining water and MP (removing 29 MP s^{-1}, Figure 4.5). While many studies thus far have considered rivers as dendritic conveyor belts where plastics particle fluxes are converging along the transport from land to ocean with certain MP retention times (Hurley et al., 2018; Ockelford et al., 2020), this study's quantitative load analysis suggests that water management may have a significant impact on MP fate, and the MP flux delivered to the ocean. The eventual fate of diverted MP depends on the diverted water's use. Water used as a source of municipal drinking water may result in the sequestration of MP, given the effectiveness of water treatment plants that remove 80-93% of MP (> 20 mm) from potable water supplies (Dalmau-Soler et al., 2021; Shen et al., 2020). In contrast, water diverted for agricultural purposes re-routs and disperses MP to the wider terrestrial environment, and these particles may be flushed back into streams in the long term.

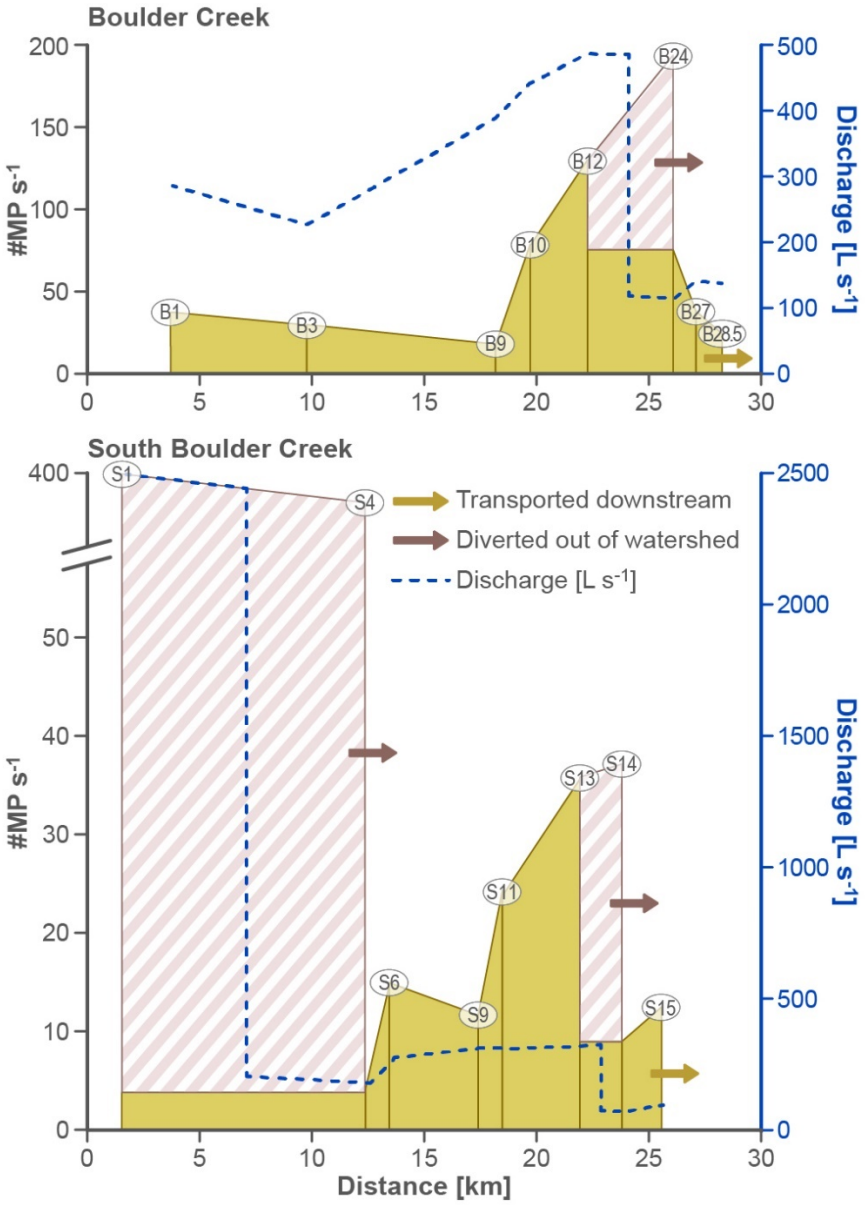


Figure 4.5: MP Load (Yellow line), Diverted load (Dashed line) and Discharge (L s^{-1}) shown for a) Boulder Creek and b) South Boulder Creek.

Diversions may also have a large impact on MP concentration, fate, and transport in the downstream portions of these managed systems. Estimated MP water concentrations are calculated for sampling locations downstream of large diversions (Section 4.3.5) and are shown in Figure 4.3

c-d and Table 4.1. An example of this effect is B24, the site with the highest MP concentration recorded in this study. B24 is the first sampling location downstream of the large diversion on BC, and its concentration is roughly double that of all other BC locations, despite having a percent contribution to the total load that is comparable to the stream segments above the diversion and a loading rate that is lower (Table 4.1). This disconnect is explained by the large magnitude of the diversion; the estimated concentration at B24 in the absence of the diversion is similar to that of nearby sites and what appears to be an outlier is just an artifact of the flow regime. A second example of this effect is the large diversion on SBC below S1. With the diversion in place, most of the MP mass is diverted out of the system and what remains in the stream is more easily diluted by waters in the undeveloped portions of the SBC canyon. In the absence of this diversion, MP concentrations at the downstream locations would have the concentration signature of S1, as this large volume of water (and large amount of MP mass) would be relatively unaffected by the sources downstream (Figure 4.3d).

Diversions also alter the hydrodynamic conditions of the downstream reach, potentially changing the fate of the MP traveling in the water column. In the case considered here, the diversion on BC causes a dramatic decrease in stream velocity, with a median velocity below the diversion (0.14 m s^{-1}, B24-B28.5) that is roughly half the velocity above the diversion (0.26 m s^{-1}, B1-B19; Appendix 3: Table S4.1). This decrease in velocity increases MP residence time in the stream segment, potentially resulting in increased settling of MP mass to the streambed. In addition, median stream depth decreases below the diversion (0.2 m, B24-B28.5; median 0.3 m, B1-B19), increasing the probability that MP will settle and become entrained in the streambed. The effects of these changes are evident in the loading analysis, with instream loads decreasing in two of the

three segments below the diversion (B27 and B28.5, Figure 4.3e). This additional loss of MP mass may be attributable to increased settling and retention in the streambed.

In summary, little focus has been given previously to how water management activities affect MP transport downstream, and the effects have not been incorporated into global models to date. The total diverted load within this system was as high as 524 MP s^{-1}, within 3.05 m^3 s^{-1}, or 171.8 MP per m^3, which is a significant finding given that the present study was conducted in a relatively remote mountain watershed over a short spatial scale. It has been estimated that in the year 2012, 241 km^3 of water was diverted for the purpose of agriculture in North America alone, and 2670 km^3 globally (Frenken, 2012). Using the value from this study (171.8 MP m^3), an estimated 41.39×10^{12} MP particles > 63 μm are redistributed to the terrestrial environment in North America and as many as 4.59×10^{14} (or 459 trillion) MP globally. However, as the numbers for diverted MP used here are only representative of this relatively remote and clean system, this is likely a gross underestimation of the global total, as higher MP concentrations have been reported in lower order streams (up to 25.5 ± 3.5 MP L^{-1} in the Maozhou River) (Kumar et al., 2021; Wu et al., 2020). This implies that diversions located in more polluted systems will unavoidably carry and re-distribute more MP than estimated here, none of which has been integrated into global or regional MP models. In 2020, ~693 million m^3 per capita of surface water was diverted globally for purposes of irrigation, industrial processes, and potable water (OECD, 2022), which has not been accounted for in any of the current global models. The models may therefore overestimate the total amount of MP flowing into oceans and simultaneously underestimate the quantity ending up in terrestrial ecosystems due to this re-distribution.

4.5.4 Advantages of the load approach

The application of a loading analysis developed for metal contamination (Kimball et al., 2002; Runkel et al., 2013) to an assessment of MP results in several advances in understanding the concentration and fate of this contaminant in streams and rivers. First, stream discharge measurements made at each sampling location allow for the development of longitudinal loading profiles (Figure 4.3e-f) that are in turn used to identify MP sources in a quantitative manner (Table 4.1). This identification, based on MP load, cannot be done using concentration data alone. In the case of metal contamination from mining, the identified stream segments are further investigated to pinpoint specific inflows responsible for the mass loading (e.g., tributary inflows, small springs and/or groundwater). This follow-up activity is more complicated for MP, due to potential contributions from atmospheric transport (Wetherbee et al., 2019; Brahney et al., 2020; Sun et al., 2022), a mechanism that is not a factor in the studies of metal loading upon which this work is based. As such, additional techniques may be needed to further elucidate MP sources. Second, the loading analysis allows for the identification of potential removal mechanisms, such as settling from the water column to the streambed. Third, our detailed analysis of the effects of diversions would not be possible without the quantitative loading approach. As shown here, the reduction in water volume due to diversions can result in a higher relative concentration of MP at a site, and locations with seemingly high concentrations can be erroneously considered hotspots if only concentration data is considered. Our analysis does in fact identify the site with the highest concentration as a hotspot (site B24, Section 4.4.3), but the associated percent contribution, loading rate (Table 4.1), and concentration in the absence of diversions (Figure 4.3c) indicate that this stream segment is no different from the stream segments immediately upstream. This suggests that some recorded hotspots in the literature may not be the result of increased input, but rather the

result of water diversions upstream of the sampling site. This finding could also have profound implications on studies of freshwater organisms, as these sudden changes in water volume could lead to higher local exposure, a factor that should be considered when assessing ecosystem health.

Table 4.2. Microplastic (MP) total, diverted and cumulative loading rates for Boulder Creek (site IDs B1-B28.5) and South Boulder Creek (site IDs S1-S15).

Site ID	*Distance from reservoir [m]*	*Stream Discharge [L s^{-1}]*	*Total Diverted stream flow [L s^{-1}]*	*Surface water MP concentration [MP L^{-1}]*	*Observed (Obs) load [MP s^{1}]*	*Total Diverted (Div.) load [MP s^{-1}]*	*Obs + Div [MP s^{-1}]*	*Cumulative Obs + Div. load [MP s^{-1}]*	*Percent Contribution [%]*	*Loading rate [MP s^{-1} km^{-1}]*	*No Div. Conc [MP L^{-1}]*
B1	3719	292	0	0.12	35	0	35	35			0.12
B3	9711	230	0	0.12	28	0	28	35			0.12
B9	18150	399	0	0.04	16	0	16	35			0.04
B10	19676	453	0	0.17	77	0	77	96	34%	40	0.17
B12	22266	500	0	0.26	130	0	130	149	30%	20	0.26
B24	26073	119	426	0.62	74	119	193	212	36%	17	0.35
B27	27097	140	426	0.26	36	119	156	212			0.28
B28.5	28272	138	426	0.16	22	119	141	212			0.25
S1	1515	2485	0	0.16	398	0	398	398			0.16
S4	12319	179	2418	0.02	4	377	381	398			0.15
S6	13354	248	2350	0.06	15	376	391	407	25%	10	0.15
S9	17352	293	2350	0.04	12	376	388	407			0.15
S11	18454	288	2361	0.08	23	376	400	419	29%	11	0.15
S13	21952	300	2361	0.12	36	376	413	432	32%	4	0.16
S14	23848	63	2598	0.14	9	405	414	433	3%	1	0.16
S15	25630	81	2598	0.16	13	405	418	438	11%	2	0.16

4.6 Conclusion

Our research revealed profound links between the degree of urbanization and MP concentrations, even in the investigated mountainous streams. More importantly, it highlighted the crucial role of water diversions on MP concentrations and loads, with over 500 MP s^{-1} or 171.8 MP per m^3 being re-distributed from the stream network into the catchment and beyond due to diversions. Clearly, these findings highlight the importance of understanding river catchments as complex systems, rather than the dendritic model through which MP only converge downstream which underlies most existing models for the simulation of global plastic fluxes from terrestrial compartments to the ocean. Our findings demonstrate that we are only beginning to uncover the true complexity of how rivers contribute to global MP flows, and that anthropogenic impacts on water management practice such as river diversions can have substantial impact on MP fate and transport.

4.7 Acknowledgments

Funding from The Leverhulme Trust via the “PlasticRivers” - The fate and transport of MP in rivers (RPG-2017-377) project is gratefully acknowledged. S.K. was supported by the Royal Society under Fellowship INF\R2\212060 while U.S. was supported by funding from the German Research Foundation (DFG – grant number 403826296). The authors extend their gratitude towards Chantal Jackson for assistance with the graphic designs. MP samples were collected by Danja Mewes with assistance from Ron Antweiler, Mac Jones, Alex Nolan, Tanya Petach, and Ted Stets. R.R. and S.M. are supported by the U.S. Geological Survey’s Ecosystem Mission Area (Climate Research & Development and Environmental Health Programs)

4.8 References

ANBUMANI, S. & KAKKAR, P. 2018. Ecotoxicological effects of microplastics on biota: a review. Environmental Science and Pollution Research, 25, 14373-14396.

BARBAROSSA, V., SCHMITT, R. J. P., HUIJBREGTS, M. A. J., ZARFL, C., KING, H. & SCHIPPER, A. M. 2020. Impacts of current and future large dams on the geographic range connectivity of freshwater fish worldwide. Proceedings of the National Academy of Sciences, 117, 3648-3655.

BAUMGARTNER, L. J., MARSDEN, T., DUFFY, D., HORTA, A. & NING, N. 2022. Optimizing efforts to restore aquatic ecosystem connectivity requires thinking beyond large dams. Environmental Research Letters, 17, 014008.

BIAN, P., LIU, Y., ZHAO, K., HU, Y., ZHANG, J., KANG, L. & SHEN, W. 2022. Spatial variability of microplastic pollution on surface of rivers in a mountain-plain transitional area: A case study in the Chin Ling-Wei River Plain, China. Ecotoxicology and Environmental Safety, 232, 113298.

CAMPANALE, C., STOCK, F., MASSARELLI, C., KOCHLEUS, C., BAGNUOLO, G., REIFFERSCHEID, G. & URICCHIO, V. F. 2020. Microplastics and their possible sources: The example of Ofanto river in southeast Italy. Environmental Pollution, 258, 113284.

CASTAÑEDA, R. A., AVLIJAS, S., SIMARD, M. A. & RICCIARDI, A. 2014. Microplastic pollution in St. Lawrence River sediments. Canadian Journal of Fisheries and Aquatic Sciences, 71, 1767-1771.

DALMAU-SOLER, J., BALLESTEROS-CANO, R., BOLEDA, M. R., PARAIRA, M., FERRER, N. & LACORTE, S. 2021. Microplastics from headwaters to tap water: occurrence and removal in a drinking water treatment plant in Barcelona Metropolitan area (Catalonia, NE Spain). Environmental Science and Pollution Research, 28, 59462-59472.

DE CARVALHO, A. R., GARCIA, F., RIEM-GALLIANO, L., TUDESQUE, L., ALBIGNAC, M., TER HALLE, A. & CUCHEROUSSET, J. 2021. Urbanization and hydrological conditions drive the spatial and temporal variability of microplastic pollution in the Garonne River. Science of The Total Environment, 769, 144479.

DRUMMOND, J. D., NEL, H. A., PACKMAN, A. I. & KRAUSE, S. 2020. Significance of Hyporheic Exchange for Predicting Microplastic Fate in Rivers. Environmental Science & Technology Letters, 7, 727-732.

DRUMMOND, J. D., SCHNEIDEWIND, U., LI, A., HOELLEIN, T. J., KRAUSE, S. & PACKMAN, A. I. 2022. Microplastic accumulation in riverbed sediment via hyporheic exchange from headwaters to mainstems. Science Advances, 8, eabi9305.

FERRAZ, M., BAUER, A. L., VALIATI, V. H. & SCHULZ, U. H. 2020. Microplastic Concentrations in Raw and Drinking Water in the Sinos River, Southern Brazil. Water, 12, 3115.

FRENKEN, K. A. G., V. 2012. Irrigation water requirement and water withdrawal by country. In: NATIONS, F.-T. F. A. A. O. O. T. U. (ed.).

GRBIĆ, J., HELM, P., ATHEY, S. & ROCHMAN, C. M. 2020. Microplastics entering northwestern Lake Ontario are diverse and linked to urban sources. Water Research, 174, 115623.

HARTMANN, N. B., HÜFFER, T., THOMPSON, R. C., HASSELLÖV, M., VERSCHOOR, A., DAUGAARD, A. E., RIST, S., KARLSSON, T., BRENNHOLT, N., COLE, M., HERRLING, M. P., HESS, M. C., IVLEVA, N. P., LUSHER, A. L. & WAGNER, M. 2019. Are We Speaking the Same Language? Recommendations for a Definition and Categorization Framework for Plastic Debris. Environmental Science & Technology, 53, 1039-1047.

HURLEY, R., WOODWARD, J. & ROTHWELL, J. J. 2018. Microplastic contamination of river beds significantly reduced by catchment-wide flooding. Nature Geoscience, 11, 251-257.

JIANG, C., YIN, L., LI, Z., WEN, X., LUO, X., HU, S., YANG, H., LONG, Y., DENG, B., HUANG, L. & LIU, Y. 2019. Microplastic pollution in the rivers of the Tibet Plateau. Environmental Pollution, 249, 91-98.

JIN, X., FU, X., LU, W. & WANG, H. 2022. Fugitive release and influencing factors of microplastics in urbanized watersheds: A case study of the central area of Suzhou City. Science of The Total Environment, 837, 155653.

KIMBALL, B. A., RUNKEL, R. L., WALTON-DAY, K. & BENCALA, K. E. 2002. Assessment of metal loads in watersheds affected by acid mine drainage by using tracer injection and synoptic sampling: Cement Creek, Colorado, USA. Applied Geochemistry, 17, 1183-1207.

KRAUSE, S., BARANOV, V., NEL, H. A., DRUMMOND, J. D., KUKKOLA, A., HOELLEIN, T., SAMBROOK SMITH, G. H., LEWANDOWSKI, J., BONET, B., PACKMAN, A. I., SADLER, J., INSHYNA, V., ALLEN, S., ALLEN, D., SIMON, L., MERMILLOD-BLONDIN, F. & LYNCH, I. 2021. Gathering at the top? Environmental controls of microplastic uptake and biomagnification in freshwater food webs. Environmental Pollution, 268, 115750.

KUKKOLA, A., KRAUSE, S., LYNCH, I., SAMBROOK SMITH, G. H. & NEL, H. 2021. Nano and microplastic interactions with freshwater biota – Current knowledge, challenges and future solutions. Environment International, 152, 106504.

KUKKOLA, A., KRAUSE, S., YONAN, Y., KELLEHER, L., SCHNEIDEWIND, U., SMITH, G. H. S., NEL, H. & LYNCH, I. 2023. Easy and accessible way to calibrate a fluorescence microscope and to create a microplastic identification key. MethodsX, 10, 102053.

KUKKOLA, A. T., SENIOR, G., MAES, T., SILBURN, B., BAKIR, A., KRÖGER, S. & MAYES, A. G. 2022. A large-scale study of microplastic abundance in sediment cores from the UK continental shelf and slope. Marine Pollution Bulletin, 178, 113554.

KUMAR, R., SHARMA, P., MANNA, C. & JAIN, M. 2021. Abundance, interaction, ingestion, ecological concerns, and mitigation policies of microplastic pollution in riverine ecosystem: A review. Science of The Total Environment, 782, 146695.

LAMBERT, S. & WAGNER, M. 2018. Microplastics Are Contaminants of Emerging Concern in Freshwater Environments: An Overview. In: WAGNER, M. & LAMBERT, S. (eds.) Freshwater Microplastics : Emerging Environmental Contaminants? Cham: Springer International Publishing.

LEBRETON, L., EGGER, M. & SLAT, B. 2019. A global mass budget for positively buoyant macroplastic debris in the ocean. Scientific Reports, 9, 12922.

LEBRETON, L. C. M., VAN DER ZWET, J., DAMSTEEG, J.-W., SLAT, B., ANDRADY, A. & REISSER, J. 2017. River plastic emissions to the world's oceans. Nature Communications, 8, 15611.

LESLIE, H. A., BRANDSMA, S. H., VAN VELZEN, M. J. M. & VETHAAK, A. D. 2017. Microplastics en route: Field measurements in the Dutch river delta and Amsterdam canals, wastewater treatment plants, North Sea sediments and biota. Environment International, 101, 133-142.

LIU, S., CHEN, H., WANG, J., SU, L., WANG, X., ZHU, J. & LAN, W. 2021. The distribution of microplastics in water, sediment, and fish of the Dafeng River, a remote river in China. Ecotoxicology and Environmental Safety, 228, 113009.

MARGENAT, H., NEL, H.A., STONEDAHL, S.H., KRAUSE, S., SABATER, F., DRUMMOND, J.D. 2021. Hydrologic controls on the accumulation of different sized microplastics in the streambed sediments downstream of a wastewater treatment plant (Catalonia, Spain). Environmental Research Letters, 16.

MCGIVNEY, E., CEDERHOLM, L., BARTH, A., HAKKARAINEN, M., HAMACHER-BARTH, E., OGONOWSKI, M. & GOROKHOVA, E. 2020. Rapid Physicochemical Changes in Microplastic Induced by Biofilm Formation. Frontiers in Bioengineering and Biotechnology, 8.

MEIJER, L. J., VAN EMMERIK, T., VAN DER ENT, R., SCHMIDT, C. & LEBRETON, L. 2021. More than 1000 rivers account for 80% of global riverine plastic emissions into the ocean. Science Advances, 7, eaaz5803.

MURPHY, S. F. 2006. State of the Watershed: Water Quality of Boulder Creek, Colorado: U.S. Geological Survey Circular. 1284, 34p.

OCKELFORD, A., CUNDY, A. & EBDON, J. E. 2020. Storm Response of Fluvial Sedimentary Microplastics. Scientific Reports, 10, 1865.

OECD. 2022. Freshwater abstractions (million m3) [Online]. Available: https://stats.oecd.org/Index.aspx?DataSetCode=WATER_ABSTRACT [Accessed].

REYNOLDS, R. L., GOLDSTEIN, H. L., KOKALY, R. F. & DERRY, J. 2022. Microplastic particles in dust-on-snow, Upper Colorado River Basin, Colorado Rocky Mountains, 2013–16. Open-File Report. Reston, VA.

RUNKEL, R. L., WALTON-DAY, K., KIMBALL, B. A., VERPLANCK, P. L. & NIMICK, D. A. 2013. Estimating instream constituent loads using replicate synoptic sampling, Peru Creek, Colorado. Journal of Hydrology, 489, 26-41.

SAMANDRA, S., JOHNSTON, J. M., JAEGER, J. E., SYMONS, B., XIE, S., CURRELL, M., ELLIS, A. V. & CLARKE, B. O. 2022. Microplastic contamination of an unconfined groundwater aquifer in Victoria, Australia. Science of The Total Environment, 802, 149727.

SCHMIDT, C., KRAUTH, T. & WAGNER, S. 2017. Export of Plastic Debris by Rivers into the Sea. Environmental Science & Technology, 51, 12246-12253.

SHEN, M., SONG, B., ZHU, Y., ZENG, G., ZHANG, Y., YANG, Y., WEN, X., CHEN, M. & YI, H. 2020. Removal of microplastics via drinking water treatment: Current knowledge and future directions. Chemosphere, 251, 126612.

SIEGFRIED, M., KOELMANS, A. A., BESSELING, E. & KROEZE, C. 2017. Export of microplastics from land to sea. A modelling approach. Water Research, 127, 249-257.

SUN, J., PENG, Z., ZHU, Z.-R., FU, W., DAI, X. & NI, B.-J. 2022. The atmospheric microplastics deposition contributes to microplastic pollution in urban waters. Water Research, 225, 119116.

TALBOT, R. & CHANG, H. 2022. Microplastics in freshwater: A global review of factors affecting spatial and temporal variations. Environmental Pollution, 292, 118393.

TIBBETTS, J., KRAUSE, S., LYNCH, I. & SAMBROOK SMITH, G. H. 2018. Abundance, Distribution, and Drivers of Microplastic Contamination in Urban River Environments. Water, 10, 1597.

UZUN, P., FARAZANDE, S. & GUVEN, B. 2022. Mathematical modeling of microplastic abundance, distribution, and transport in water environments: A review. Chemosphere, 288, 132517.

VAN WIJNEN, J., RAGAS, A. M. J. & KROEZE, C. 2019. Modelling global river export of microplastics to the marine environment: Sources and future trends. Science of The Total Environment, 673, 392-401.

WAGNER, S., KLÖCKNER, P., STIER, B., RÖMER, M., SEIWERT, B., REEMTSMA, T. & SCHMIDT, C. 2019. Relationship between Discharge and River Plastic Concentrations in a Rural and an Urban Catchment. Environ Sci Technol, 53, 10082-10091.

WANG, T., WANG, J., LEI, Q., ZHAO, Y., WANG, L., WANG, X. & ZHANG, W. 2021. Microplastic pollution in sophisticated urban river systems: Combined influence of land-use types and physicochemical characteristics. Environmental Pollution, 287, 117604.

WETHERBEE, G. A., BALDWIN, A. K. & RANVILLE, J. F. 2019. It is raining plastic. Open-File Report. Reston, VA.

WETHERBEE, G. A., MURPHY, S.F., REPERT, D.A., HEINDEL, R.C., AND LIETHEN, E.A 2021. Chemical analyses and precipitation depth data for wet deposition samples collected as part

of the National Atmospheric Deposition Program in the Colorado Front Range, 2017-2019. In: RELEASE, U. S. G. S. D. (ed.).

WONG, G., LÖWEMARK, L. & KUNZ, A. 2020. Microplastic pollution of the Tamsui River and its tributaries in northern Taiwan: Spatial heterogeneity and correlation with precipitation. Environmental Pollution, 260, 113935.

WU, P., TANG, Y., DANG, M., WANG, S., JIN, H., LIU, Y., JING, H., ZHENG, C., YI, S. & CAI, Z. 2020. Spatial-temporal distribution of microplastics in surface water and sediments of Maozhou River within Guangdong-Hong Kong-Macao Greater Bay Area. Science of The Total Environment, 717, 135187.

YUAN, W., CHRISTIE-OLEZA, J. A., XU, E. G., LI, J., ZHANG, H., WANG, W., LIN, L., ZHANG, W. & YANG, Y. 2022. Environmental fate of microplastics in the world's third-largest river: Basin-wide investigation and microplastic community analysis. Water Research, 210, 118002.

ZHANG, Y., GAO, T., KANG, S., ALLEN, S., LUO, X. & ALLEN, D. 2021. Microplastics in glaciers of the Tibetan Plateau: Evidence for the long-range transport of microplastics. Science of The Total Environment, 758, 143634.

Chapter 5: Are we timing it right? The impact of sampling frequency on microplastic load estimations downstream from a sewage treatment works.

Anna Kukkola[a], Uwe Schneidewind[a], Lee Haverson[a], Liam Kelleher[a,c], Jennifer Drummond[a], Greg Sambrook Smith[a], Iseult Lynch[a,c] and Stefan Krause[a,b,c]

[a] School of Geography, Earth and Environmental Sciences, University of Birmingham, Edgbaston, Birmingham B15 2TT, United Kingdom

[b] LEHNA- Laboratoire d'ecologie des hydrosystemes naturels et anthropises, University of Lyon, Darwin C & Forel, 3-6 Rue Raphaël Dubois, 69622 Villeurbanne, France.

[c] Institute of Global Innovation, University of Birmingham B15 2SA, Birmingham. United Kingdom

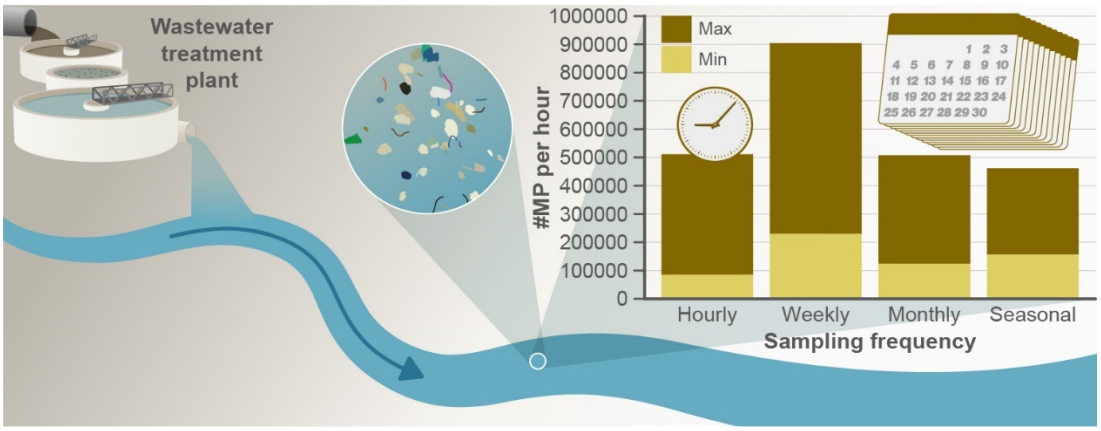


Figure 5.0 Graphical abstract

5.1 Abstract

Wastewater and sewage treatment works (WWTPs) have been described as a significant source of microplastic particle (MP) input into the aquatic environment. However, the impact of treated effluent on the temporal variability of riverine MP concentrations and MP loads downstream of WWTPs remains unclear. Here, the impact of the frequency of surface water

sampling on identified MP concentrations and load estimates were studied downstream of an WWTP which was identified as the major input source of MP to the stream. Fluorescent microscopy and Raman spectroscopy were used to quantify MP concentrations and identify polymer types, respectively. It was found that while MP concentrations could fluctuate within an hour over an order of magnitude, the relative composition of the polymer types remained largely unchanged. MP concentration was not correlated to the discharge at the site and temporal variability in MP loads was driven by MP concentration and/or discharge alone or simultaneously. This led to high uncertainty if the annual MP load would have been calculated by using a snap-shot MP concentration and annual discharge. These results highlight the importance of a mechanistic understanding of the hydrodynamic forcings of MP transport processes in a given river system, in order to determine the dynamics of MP concentration and load ranges and quantify the downstream transport. We recommend pre-monitoring reconnaissance campaigns to be conducted to characterise the system, mainly to identify relevant flow pattern, the optimal sampling frequency and duration to ensure representative sampling and thus more accurate predictions of trends and patterns on larger scale.

5.2 Introduction

Microplastics (MP) are small plastic particles (< 1mm) (Hartmann et al., 2019) that originate from the breakdown of larger plastic items via (photo)chemical, physical, and/or biological degradation (Corcoran et al., 2009; Mateos-Cárdenas et al., 2020), or are purposely generated directly at this specific size range (e.g., for use in cosmetics). They have been abundantly found in all aquatic environments, from the deep sea to the Arctic, including rivers (Bergmann et al., 2022; Bian et al., 2022; Bigalke et al., 2022; Ferreira et al., 2022; Kelleher et al., 2023; Kukkola

et al., 2022) and have been classified as a contaminant of concern (Lambert and Wagner, 2018) because of their negative environmental impacts and public health risk (Blackburn and Green, 2022; Yuan et al., 2022). Early evidence suggests that MP can adsorb a range of environmental pollutants, including heavy metals or persistent organic pollutants (POPs), which may transfer into organisms after MP ingestion with the potential for biomagnification (Besseling et al., 2013; Brennecke et al., 2016; Mato et al., 2001; Wang et al., 2018). Further, MP host distinct microbial communities in freshwater, in comparison to their immediate surroundings, with seemingly more favourable potential for growth for known human pathogens, such as Arcobacter, which may pose an additional threat to humans and to ecosystem health (Kukkola et al., 2021; Yang et al., 2020). As rivers provide many ecosystem services for humans, such as water supply and tourism (Böck et al., 2018; Vári et al., 2022), understanding the sources, transport, and fate of MP is imperative to the study of rivers, especially as it has been shown that rivers not only transport MP towards the ocean but have the potential themselves to retain a significant portion of the MP for extended times (Drummond et al., 2020; Drummond et al., 2022; Krause et al., 2021; Margenat, 2021).

Wastewater treatment plants and sewage treatment works (henceforth referred to as WWTPs) have frequently been reported as a major source of MP inputs to freshwater systems, despite removal efficiencies of > 90% for particles > 100 µm (Carr et al., 2016; Liu et al., 2021; Mani et al., 2015; Murphy et al., 2016; Sun et al., 2019; Wu et al., 2022). A recent review focussing on 38 different STWs across 11 countries estimated that the average daily MP emission from a typical WWTP is 5.00×10^5 - 1.39×10^{10} MP, depending on the treatment plant type (Liu et al., 2021). In Germany WWTPs are estimated to emit up to 7×10^{12} MP (size >10 µm) annually (Schmidt et al., 2020), with similar estimates found for Australia (8.06×10^9 to 4.85×10^{10} MP,

size > 25 μm) (Ziajahromi et al., 2021). However, these annual load calculations are usually based on extrapolations from snap-shot sampling (i.e., single, or limited numbers of time points) that provide sparse and non-targeted data on MP concentrations which are then upscaled by combining them with daily or average annual discharge information (Liu et al., 2021, Ziajahromi et al., 2021). While such studies provide a first estimate of MP concentrations downstream of WWTPs, our knowledge on how MP concentrations and loads vary over time, for example, due to seasonal or daily changes in discharge or because of variations in MP release patterns in WWTP effluent, remains severely limited.

To date only few studies have focused on establishing the temporal variability of MP in the effluent from WWTPs. Some studies have been investigating the seasonal variations of MP emissions from WWTP over the course of a year, limiting their analysis to four or five seasonal sampling occasions (Conley et al., 2019; Mak et al., 2020). The longest studies of WWTP outflow with respect to MP currently seem to be less than twelve consecutive months, with one study including weekly grab sampling of 30 L over nine months, as well as grab sampling of 100 L and 24-hour composite samples over four months (Ben-David et al., 2021). Other studies sampled bi-weekly for three months or roughly every two months over a ten-month period (Blair et al., 2019; Lares et al., 2018). Data on changes in MP concentrations downstream of WWTPs within one day are even more limited. For example, Watkins et al., (2019) obtained high-resolution data deploying a Neuston net for 10 minutes every 3h over a 2-day period at a set location downstream of an WWTP in Six Mile Creek and Fall Creek (NY USA), while Ruffell et al., 2021 collected one 24-h composite sample Canterbury region, New Zealand bi-monthly. The previous studies observed no significant difference in effluent treatment efficiency nor MP concentrations in outflows of WWTP

plants (Ruffell et al., 2021; Watkins et al., 2019). However, Watkins et al. (2019) reported higher MP concentrations during the dry low-flow conditions at Six Mile Creek and Fall Creek (NY, USA), hinting at potential hydrological control mechanism on the MP loading during periods of reduced dilution.

This lack of combined long-term and high-frequency observations of MP concentrations hampers our understanding of the (drivers of) potential temporal changes of MP fluxes (loads) downstream of WWTPs, especially in cases where the WWTP effluent is not strongly diluted by upstream river water but constitutes a major or even the main local MP source. With the short-to-long-term variations of MP concentrations downstream of a major WWTP point sources not having been established yet, it currently remains largely unclear which frequencies of observations carry the highest information content which would enable more accurate predictions of MP loads affecting downstream ecosystems and public health. There is therefore a requirement for higher resolution data, including assessment of short-term variability at locations where fluxes or MP inputs may vary within hours, as well as assessment of variability at daily, seasonal, and annual time scales. Integrating such multi-frequency knowledge will ultimately lead to better understanding of MP loading changes that are driven by less frequent and more irregular hydrodynamical changes. Additionally, representative sampling is a major prerequisite to be able to accurately estimate local downstream MP export as well as global plastic budgets, and to improve existing or develop new transport models that consider temporal aspects of downstream MP transport on regional and global scales (Miller et al., 2021; Weiss et al., 2021). Therefore, a more robust understanding of how MP surface water concentrations downstream of WWTPs can

potentially vary in time and to what degree this variability can be best captured by different frequencies of collecting samples is warranted.

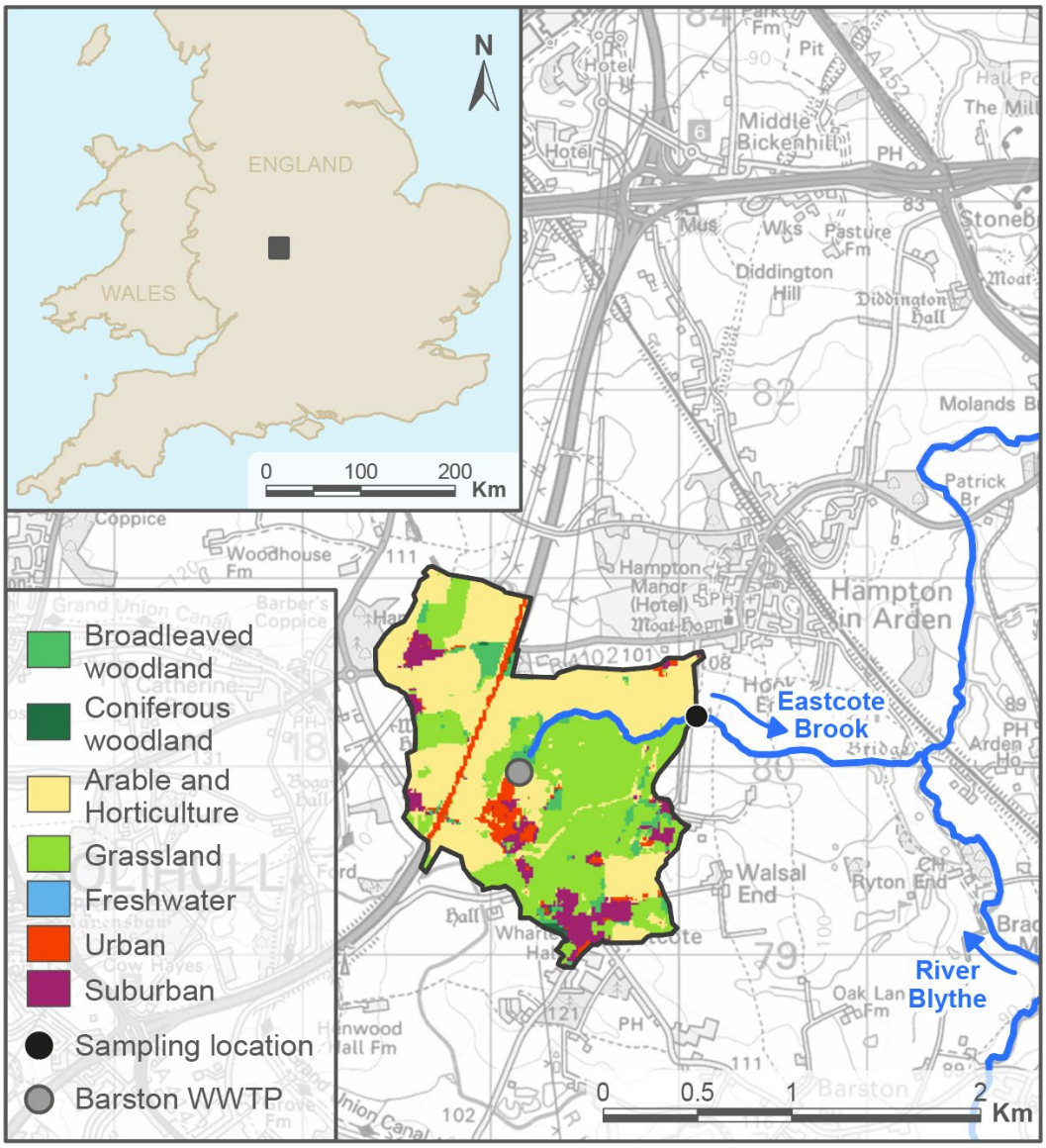
Here, we present time-dependent MP concentration data and analyse MP loads in the Eastcote Brook, UK, downstream of a WWTP. The WWTP effluent constitutes the only discharge source of the brook at the sampling location and is therefore assumed to be its major MP source, which allowed us to: i) quantify short-to-long term variability in MP concentration and load in a river with a known point source; ii) evaluate the impact of hydrological controls (discharge) on downstream MP transport, and iii) study the influence of different sampling frequencies (seasonal, monthly, weekly, and sub-daily) on identified MP concentration and load estimates from a single point-source. We discuss potential limitations associated estimating annual MP fluxes based on extrapolations from snap-shot sampling that is frequently being used in the literature. We will therefore establish to what degree current approaches carried out by multiplying snap-shot MP concentrations with mean annual discharge data are sufficient for capturing the broad range of MP loads and concentrations found in dynamic rivers with a major local point source, and whether in such environments, MP surface water sampling campaigns need to be planned according to the pattern and timescales of MP variability.

5.3 Materials and methods

5.3.1 Study site

The study site (latitude: 52.419714, longitude: -1.704480) is a small tributary of the River Blythe called Eastcote Brook, with a drainage area of 2.06 km^2. It is located east of Birmingham near Hampton-in-Arden (UK), in an agricultural area (Figure 5.1). The River Blythe later flows into the River Tame and then the River Trent, ultimately draining into the North Sea. The Eastcote

Brook originates at Barston WWTP in a previous osier bed and no flow exists upstream of the WWTP (confirmed by the WWTP operator and suggested by the hydrograph in Appendix 4: Figure S1). Barston WWTP is a sewage treatment plant equipped with a tertiary treatment system and sand filtration operated by Severn Trent Plc and serves a population of ~62,500. Influent water arrives from urbanised regions of South Birmingham and Coleshill. The WWTP includes a storm treatment stream (395 L s^{-1} Full Flow to Treatment), inlet screens, grit removal, followed by a proprietary treatment system NEREDA, Ferric dosing and a Mecana cloth filter. The sampling site was located approximately 800 m downstream of the WWTP.



© Crown Copyright and database rights 2023 Ordnance Survey (100025252)

Figure 5.1: Sampling location (black dot) and the Barston WWTP (grey dot) near Birmingham, United Kingdom. The arrows indicate stream flow direction.

5.3.2 Field sampling

A sampling that temporally nested different sampling intervals and durations was conducted over the course of one year (between April 1st 2021 and March 31st 2022) and consisted of four

seasonal (April 30th, July 26th, October 28th, January 26th), 12 monthly (collected in the last week of each month in general), and eight weekly sampling dates (2021 June 2nd, 8th, 15th, 22nd and July 2nd 9th 15th and 26th). Additionally, a high-frequency campaign over 12 hours on each of four days was conducted, with 1-hour interval sampling sub-daily, comprising two weekdays (Tuesday and Wednesday, 15th & 16th June 2021) and two weekend days (Saturday and Sunday, 19th & 20th June 2021). All samples, with the exception of sub-daily samples, were consistently collected between 9 am and 11 am in an attempt to reduce any potential time-dependent fluctuation related to the operations of the WWTP. On the sampling dates 15th, 16th, 19th and 20th of June 2021, the surface water samples were collected every hour between 9 am and 8 pm, resulting in twelve hourly samples for each of the four sampling days. The four seasonal samples from the 12-monthly sampling were selected to reflect a common practise, whereby snap-shots are used to describe and upscale what is happening in a system at a given time to encompass the whole annual cycle. The last weeks of June and July 2021 were selected from the 8-weekly samples to represent the respective monthly sample, as monthly samples were all collected at the end of a month.

During each sampling, 50 L of surface water was collected from the centre of the river, from the upper 20 cm of the water column using a 2 L jug and filtered in-situ through a 63 µm nylon mesh, from which the contents were then backwashed into 20 mL borosilicate glass vials using deionised (DI) water. All samples were collected in triplicate, which were treated separately. The volume of water collected was based on results of a pilot study and was chosen to provide a balance between capturing the inherit heterogeneity of the MP concentration and preventing clogging of the mesh with organic matter while achieving time sensitive sampling. All samples collected in

this study (n=204) were stored in a cooler and transported immediately after collection to the University of Birmingham where they were stored in a cold dark room at 6°C before processing.

Additional parameters measured *in situ* included stream flow velocity and electrical conductivity (EC). Flow velocity was obtained using a Sensa-RC2 (Aqua Data Services Ltd) electromagnetic velocity meter, from a predetermined and marked cross-section of the stream. For each 30 cm subsection (beginning at 0, marking the start of the bank), depth measurements were taken at the middle of the section and coupled with the average velocity measurement (averaged over 15 s) that was obtained by moving the velocity meter steadily up and down the water column between 20 and 80% of the stream depth. The total stream discharge was then calculated as follows:

$$Q_{tot} = \sum Q_x = v_x \times b_x \times d_x$$

where, Q_{tot} is the total cross-sectional discharge ($m^3\ s^{-1}$), which is the sum of all sub-sectional discharges Q_x, where x indicates the sub-section, v is the flow velocity ($m\ s^{-1}$), b is sub-section width (m), and d is the sub-section depth (m). The electrical conductivity (EC) was monitored continuously using a Solinst level logger. The minimum, maximum, and mean WWTP effluent discharge was provided in 15 min interval data ($L\ s^{-1}$) for the period between 15th and 20th June 2021 by Severn Trent Plc, the Barston WWTP operating company and is shown in Figure S2. This data was used to confirm the relationship between the WWTP discharge and the stream discharge of the Eastcote Brook as the main drainage structure of the WWTP.

5.3.3 Laboratory analysis

5.3.3.1 Sample Preparation, digestion, and staining

MP collected as described in section 5.3.2 were extracted from the surface water samples following the methods and protocol described by Kukkola et al., (2023b/Chapter 4) and Nel et al., (2019). Briefly, each of the water samples were extracted by pouring the contents of the 20 mL vials onto a 63 µm sieve, after which the vials were rinsed several times (≥ 3 times) with DI-water into the sieve to ensure that all the contents of the vials were removed. Chemical wet peroxide oxidation was used to digest organic matter (OM) at a ratio of 1:10 (Margenat, 2021). 20 mL 30% H_2O_2 was used to backwash the contents of the sieve into 250 mL beakers, before adding 2 mL Fe^{2+} (aq) (0.05 M) as a catalyst. Samples were covered with loose aluminium foil lids, allowing for any heat/gas to escape to prevent any pressure developing, while avoiding airborne contamination, and then left for at least 24 hours at ambient room temperature to allow degradation of the OM.

For Nile Red staining, the oxidised samples were first decanted through 63 µm sieves and backwashed into beakers with DI-water. A stock solution of 1 mg mL^{-1} Nile Red was added to bring the sample to 5 µg mL^{-1} Nile Red and left covered on an orbital shaker at 105 rpm (Grant-bio, PSU-20i) to stain for one hour. The samples were then filtered via a glass vacuum-filtration system onto glass-fibre GF/D filters (Whatman, diameter 47 mm, pore size 2.7 µm) and rinsed with DI-water. Yellow goggles and UV-light were used to inspect the beaker and the funnel to ensure all visible particles had been removed. The filters were transferred into pre-labelled clean PP Petri dishes and dried for 24 hours at 50 °C. Storage in PP petri dishes were not expected to have any effect on the MP identification, as any possible contamination introduced from petri dishes would not have been stained with Nile Red and thus would not be counted.

5.3.3.2 Microscopy and MP identification

Each filter was observed under fluorescence mode with a Macro zoom microscope (Olympus MVX-ZB10) with the settings described in the Appendix 4: S5.1 and further discussed in Kukkola et al., (2023a). Measurements for fluorescence intensity and photographs were taken with a DP74 colour camera using the CellSens Software (Olympus). A set threshold of 100 fluorescence a.u. (arbitrary units) was used to select particles of interest under magnification of 32x for further consideration. Each putative MP was then observed further under bright-field (using a ring light, with 45 LED bulbs), with magnification of 63x (as suggested in Kukkola et al., 2023a) and had to comply with pre-set selection criteria via an identification key (Kukkola et al., 2023a).

5.3.3.3 Chemical characterisation of MP

For polymer identification, confocal Raman spectroscopy was employed. For each sampling event, a minimum of 40% (n = 729) of counted MP was analysed. These particles were transferred into clean glass vials with filtered DI-water (2.7 µm) with fine tweezers before being filtered onto Whatman Anodiscs (diameter 25 mm, pore size 0.2 µm) for further analysis. A Renishaw InVia Qontor Raman microscope equipped with a 785 nm laser was used for polymer identification with the detailed configuration provided in the Appendix 4 (SI5.2) and further discussed in Kelleher et al. (2023). For spectral matching, the fingerprint region of 650-1700 cm^{-1} was assessed for prominent peaks. The spectral peaks were exported into a custom Python script (Python 3.9) and using the Pandas and Numpy packages, peaks were matched to reference libraries using the Pearson correlation coefficient. The spectral library consisted of the SLOPP, SLOPP-E (Munno et al., 2020) and in-house built reference libraries.

5.3.4 QA/QC

Field background samples (n = 12) were collected using pre-cleaned glass jars that were left open by the stream bank to identify any possible air deposition for the duration of the water sampling. To account for any contamination from the researchers conducting the sampling, sample handling and processing, fibre samples from personnel's clothing were taken (n = 2). Researchers wore the same outer layer for each field visit throughout the sampling campaign, and any fibres matching the physical properties of the respective clothing fibres were excluded from the analysis.

All solutions used were pre-filtered onto GF/D (2.7 μm) glass-fibre filters. All GF/D filters were burnt off at 500 °C for 5 hours prior use. All working surfaces were cleaned prior to and after sample handling with filtered 70% ethanol. Equipment was cleaned with detergent and rinsed with DI-water before and between usage. Glassware was used where feasible, and beakers were placed in a sonification bath (GT sonic-D9) for 10 min for further cleaning. Personnel wore 100% cotton laboratory coats and only cotton/wool clothes were allowed in the laboratory. Nitril gloves were worn when handling samples and aluminium foil was used to cover samples during procedures. Two procedural blanks were run for each extraction batch (n_{total} = 20) using DI-water and were analysed following the same criteria as for the samples.

From the 12 field background samples, three contained one clear fragment, indicating that air deposition or potential contamination was minimal at the site. In the 20 laboratory blanks, only one fragment and one black fibre (not on the same day nor filter) were found. These were not deducted from the final counts, as no black fibres with an identical diameter and properties were found from the filters processed the same day and the additional laboratory blanks for the same batch indicated

no contamination. It was concluded that based on that evidence, levels of contamination appear to be negligible and extremely random.

5.3.5. Data analysis

Normality of all data was assessed with a Shapiro-Wilk's test and non-parametric tests were applied where data was not normally distributed. To evaluate whether MP size (measured as longest length) or MP concentration correlated with the average stream flow velocity (taken as the average of the three 30 cm mid-sections, which covered the stream segment where surface water samples were collected), stream total discharge or EC, the non-parametric Spearman rank coefficient (Rs) was used to assess direction and strength of any correlation.

To compare MP concentrations between sampling occasions within temporal scales (4-season, 12-montlhy, 8-weekly and 4-sub-daily), Kruskal-Wallis tests were applied, followed by Dunn-test with the Benjamini-Hochberg Procedure to reduce false discovery rates. In order to assess whether any of the hourly triplicates collected during the four 12-hour sampling frequency campaign were significantly different from the total daily mean, an Unpaired Two-Samples Wilcoxon Test was carried out.

Student's T-test was applied to assess the statistical significance of differences between MP concentrations, stream discharge and EC between weekdays and weekend days. Statistical analyses were carried out within RStudio (RStudio, Inc. R Core Team 2022). The significance threshold was set to $\alpha = 0.05$. All values for MP concentrations are reported with mean and standard deviation (SD).

The MP loads were calculated as $L = C_t Q_{tot,t}$,

where L is load (MP s^{-1}), C is the concentration of MP in the surface water (MP L^{-1}), Q is the discharge (m^3 s^{-1}) and t is the time/date of the measurement. MP concentration was scaled to MP per m^3. For hourly load the L is adjusted by multiplying with 60 (seconds to minute) and the product multiplied with 60 (minutes to an hour). Though this calculation assumes homogeneous MP distribution for the whole river cross section, it is likely that different MP concentrations would have been found from different sub-sections with different flow properties and/or depths (Cowger et al., 2021). For the sake of simplicity, no modelling was applied here to correct for these parameters, and the loading rates presented in this study should be taken with some caveats.

5.4 Results

5.4.1 Variations in stream discharge

Within the present study, the stream discharge downstream of the outflow of the WWTP was characterised by high temporal variability (Appendix 4: Figure S5.1). The discharge from the WWTP varied in a broad diurnal cycle, peaking twice a day at approximately 9.30 am and 9.30 pm (Appendix 4: Figure S5.2). However, within this daily wastewater release cycle, the variability between the minimum and maximum discharge varied between 30 and 200 L s^{-1}, sometimes within only 15 minutes, underlining the high fluctuations in WWTP outflow.

The stream discharge observed for the four seasonal samples ranged between 0.16 (26th July 2021) - 0.31 m^3 s^{-1} (30th April 2021), with the highest discharge occurring in spring and the lowest during the summer (Figure 5.2A). The variation of stream discharge obtained from the 12 monthly sampling dates ranged between 0.15 (18th August 2021) and 0.38 m^3 s^{-1} (23rd March 2022), revealing a less clear seasonal pattern (Figure 5.2B). The weekly measured stream discharge ranged from 0.16 (26th July 2021) – 0.39 m^3 s^{-1} (08th June 2021). The sub-daily measurements revealed

high variability in stream discharge, with rapid changes of as much as 0.20 $m^3 s^{-1}$ within just one hour (Figure 5.2D). T-test results suggested that the observed higher discharge during the two weekend-days as compared to the two-weekdays was statistically significant ($t(46) = -4.32$, $p < 0.001$). For further details see Appendix 4: Table S5.1.

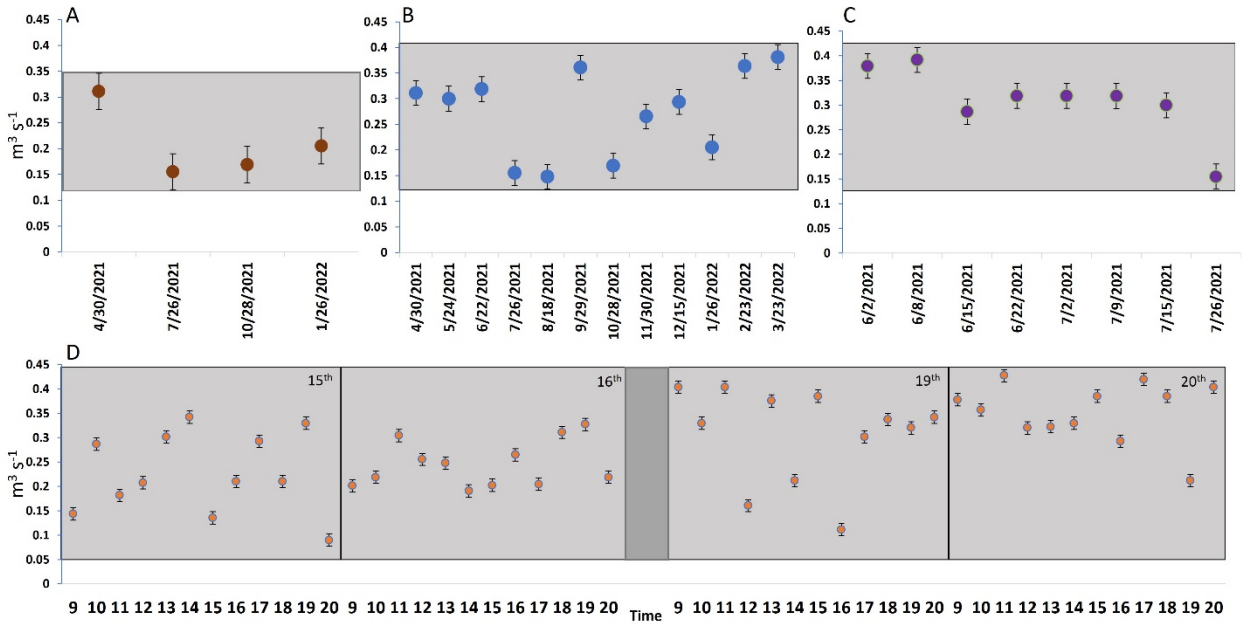


Figure 5.2: Variations in stream discharge ($m^3 s^{-1}$) based on: A) 4-seasonal samples (April 30th, July 26th, October 28th, January 26th), B) 12 monthly samples (collected in the last 2 weeks of each month), C) 8 weekly samples (2021, June 2nd, 8th, 15th, 22nd and July 2nd, 9th, 15th and 26th) and D) 4 days with sub-daily 12-hour interval sampling, with two weekdays (Tuesday and Wednesday, 15th & 16th June 2021) and two weekend days (Saturday and Sunday 19th & 20th June 2021). Grey background indicates the extent of the range for each sampling frequency and black error bars show the standard error.

5.4.2 Variations in MP properties

MP were identified in all samples collected throughout the observation period. Overall, clear/colourless was the most frequently assigned colour-type category recorded (46.3% of total) and stained/pink was the second most dominant category (21.7%), followed by black (9.7% which were exclusively fibres) and white (5.0%). The colour composition of different MP did not correlate with the sampling frequency (Appendix 4: Figure S5.3).

Fragments represented the dominant morphology type of observed MP (73.2%) with 26.5% being fibres and only 0.3% spheres. A similar composition of MP morphologies was observed for the 4 seasonal, 12 monthly and sub-daily samples, however, the eight weekly samples revealed a change in the relative abundance of fibres from the end of June towards the end of July. The relative proportion of fibres increased from 30% on 22nd of June to 57% on 15th and 26th of July (Appendix 4: Figure S5.4).

According to a Kruskal-Wallis test, no significant difference in MP sizes amongst different sampling frequencies was found. The average MP size of fragments for all samples was 283.8 µm and 1378 µm for fibres (for details of the size distribution see Appendix 4: Figure S5.5).

From the particles identified as MP and picked for chemical identification (n = 729), 88.75% were confirmed as plastics. For fibres, acrylic represented the dominant polymer category across the sampling regimens, followed by nylon, polylactic acid (PLA), polyethylene (PE) and polystyrene (PS) (Figure 5.3). For fragments, acrylic was the dominant polymer type across all sampling regimens, and was followed by PLA, polyethylene terephthalate (PET), PS and PE (for detailed breakdown of polymers by sampling campaign, see Appendix 4: Figure S5.6).

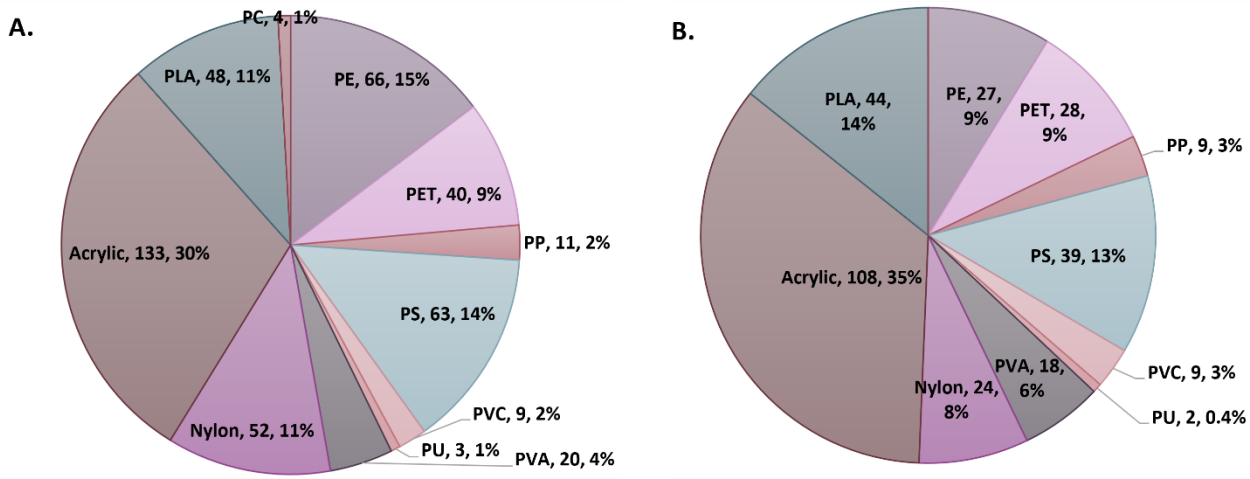


Figure 5.3. The percentage and number of identified polymers by composition for all of the positively identified MP particles in this study, grouped by A) Fibres and B) Fragments.

5.4.3 Variations in MP concentrations

Mean MP concentrations and the ranges observed during the seasonal sampling were compared to results obtained from the 12-monthly, 8-weekly, and sub-daily sampling campaigns to determine the influence of MP sampling frequency on the characterisation of the dynamics of stream concentrations and loads.

The 4-season sampling showed a significant difference in MP concentrations between the four seasons (Chi squared = 9.842, p = 0.019), with the highest concentration recorded during summer on 26th of July 2021 (0.55 MP L^{-1}) and lowest in spring on 30th of April 2021 (0.14 MP L^{-1}) (Figure 5.4A). The mean MP concentration for this sampling frequency was 0.307 ± 0.153 MP L^{-1}.

For the one year long monthly sampling period, the range of observed MP concentrations was similar to the seasonal sampling: between 0.14 and 0.55 MP L^{-1} (Figure 5.4B) with a mean of 0.244 ± 0.104 MP L^{-1}. The biggest difference in the monthly sampling was found between July and

April as well as December sampling times (Chi squared = 22.386, p = 0.021). For the 8-weekly sampling period, MP concentrations ranged between 0.20 and 0.63 MP L^{-1} (Figure 5.4C), with a mean of 0.371 ± 0.146 MP L^{-1}. A small increase during the weekly sampling was observed between June and July, with the highest mean MP concentration recorded on 15th July 2021. This was significantly higher than MP concentrations observed on June 2nd, June 8th, June 22nd, and July 2nd (Chi squared = 19.2, p = 0.007).

With the sampling frequency increasing to the sub-daily sampling, high variability was observed between the days and the hours sampled. In general, the average MP concentration seemed to increase between 9-10 am and between 7-8 pm (Figure 5.4D), but no other trends were identified. When the total mean of the day(s) was considered, there was no significant difference between the four days (Chi-squared = 4.77, p = 0.189) and the average MP concentration were 0.228 ± 0.055 (15th June), 0.197 ± 0.053 (16th June), 0.239 ± 0.053 (19th June) and 0.197 ± 0.041 MP L^{-1} (20th June). The mean for the four days was 0.216 ± 0.054 MP L^{-1}. According to a T-test there was also no significant difference between the MP concentrations on weekdays and the weekend (t(142) = -0.399, p = 0.689).

To assess how the MP concentrations determined based on hourly samples differed from those derived based on the entire 12-hour mean on the four sub-daily sampling days, the mean of each hour was compared to the mean of the whole day. On the 15th June, only one hour provided concentrations that were significantly different from the daily mean (4pm, p = 0.018). On the 16th June, two hours were slightly significantly different from the daily mean (4pm, p = 0.067 and 8pm, p = 0.067). For the 19th June, only 1 hour was marginally different from the daily mean (3pm, p =

0.080) and for the 20th June there was one significantly different (2pm, p = 0.040) and three slightly significant (11am, p = 0.079, 1pm, p = 0.055 and 5pm, p = 0.070) from the daily mean.

There was a significant difference between MP concentration of different sampling frequencies (Chi squared = 47.2, p = 0.040), with the pairwise post-hoc Dunn test suggesting that this was only significant between 8-weekly and sub-daily sampling frequency (p = 0.014).

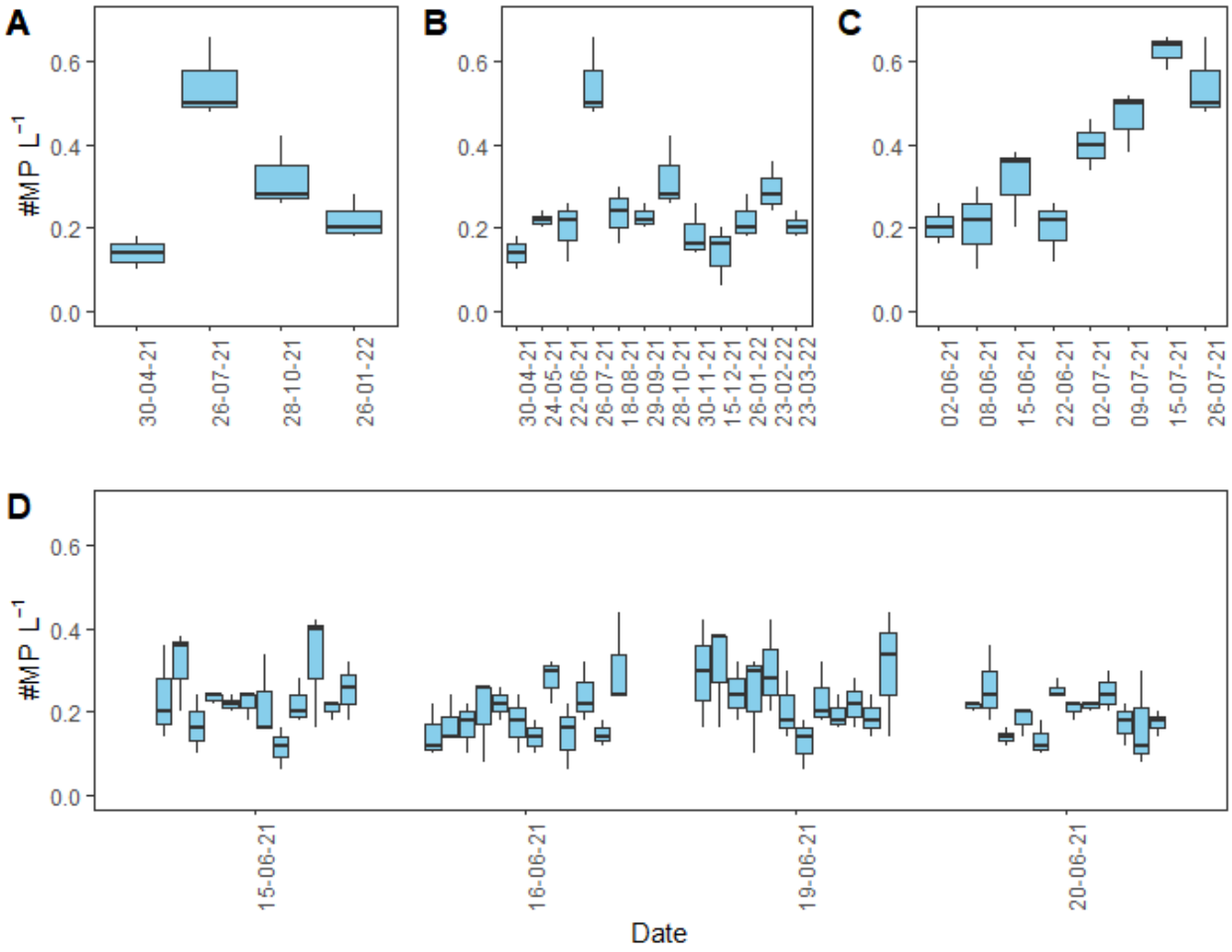


Figure 5.4: MP concentration in surface water (MP L^{-1}) as obtained from: A) seasonal sampling (4-seasons), B) monthly sampling (12-months), C) weekly sampling (8-weeks) and D) sub-daily sampling (12 hourly intervals over 4 separate days).

5.4.4 Variations in MP loading

The average MP load (MP h^{-1}) determined through the different sampling frequencies was not significantly different statistically (chi-squared = 66.874, p = 0.378). However, the observed range between minimum and maximum MP load became wider with different sampling frequencies, revealing high variability being present within MP loads (Figure 5.5).

The average MP load for the 4-season sampling regimen was 204,818 MP h^{-1} with the highest load occurring during the summer 305,136 MP h^{-1} (Figure 5.5). Seasonal sampling revealed the tightest range of all the sampling frequencies with the minimum load being 156,719 and the maximum load being 305,136 MP h^{-1} (Figure 5.6).

The average MP load identified based on the 12-month sampling regimen was 224,897 MP h^{-1} with a range between 124,183 and 384,076 MP h^{-1} for different months. This range was wider than that identified by seasonal sampling, suggesting that the seasonal sampling did reveal less of the actual variability in MP loads occurring over the year. Some of the largest identified loads coincided with the highest stream discharges, although the month of July (26th July 2021) was characterised by a high load despite a relatively low stream discharge (0.16 m^3 s^{-1}) (Figure 5.5, Figure 5.2).

The average MP load determined by the 8-week long weekly sampling was 387,542 MP per h^{-1} with a range between 229,409 MP h^{-1} and 675,677 MP h^{-1}. Here again, the range identified

by weekly sampling was wider than that revealed by the 4-season or the 12-month sampling regimens. The weekly sampling furthermore revealed an increasing trend of MP loads for the first three weeks of July (Figure 5.6), with values clearly above the annual average during these three weeks (Figure 5.5).

The highest (sub-daily) sampling frequency revealed even higher fluctuation in MP loads, with one order of magnitude differences being observed within a single day (15th of June) (Figure 5.5). For the weekdays, the range of MP loads on the 15th of June varied between 85,691 and 323,365 MP h^{-1} with an average of 186,598 MP h^{-1} and for the 16th of June the range of observed MP loads was between 101,806 and 273,200 with an average of 175,745 MP h^{-1}. For the weekend, the range of the MP loads on the 19th of June was between 93,343 and 425,931, with an average load of 267,197 MP h^{-1}. On the 20th of June the MP load ranged between 127,082 and 382,574 with an average of 251,232 h^{-1}. The sub-daily sampling also suggested that the weekdays (15th and 16th June) were characterised by lower MP loads, (average 186,598 MP per h^{-1} on the 15th June, and 175,745 MP per h^{-1} on the 16th June) than weekend days (267,197 MP per h^{-1} on 19th June and 251,232 MP per h^{-1} on 20th June), ($t(46) = 3.212$, $p = 0.002$).

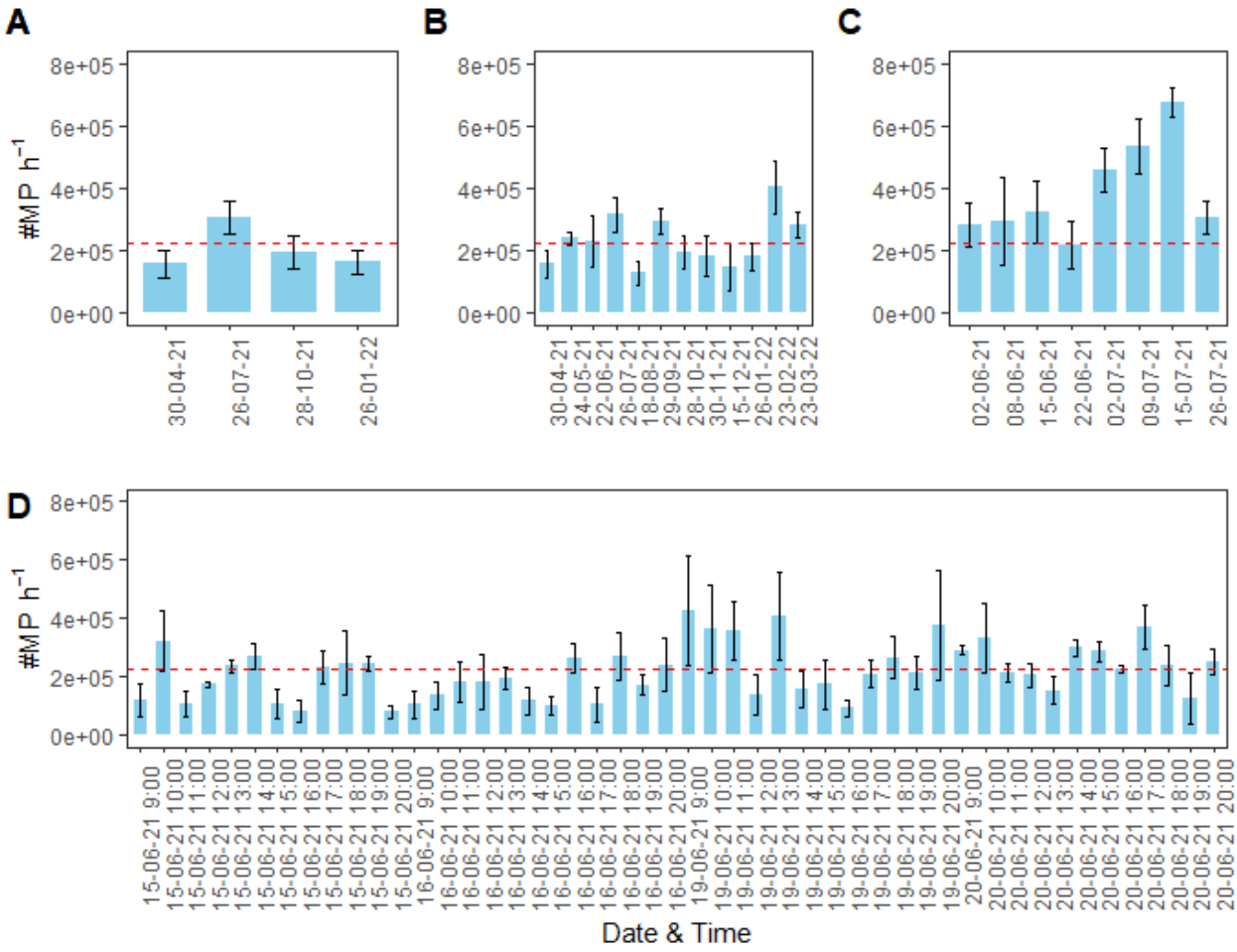


Figure 5.5: MP loads as MP per hour (#MP h^{-1}) for: A) seasonal (4-seasons), B) monthly (12-months), C) weekly (8-week period in June-July 2021) and D) sub-daily sampling (hourly for the 15th, 16th, 19th and 20th June 2021), the error bars represent the standard deviation of the triplicate samples and the dashed line shows annual mean calculated based on the 12-monthly sampling (224,897 MP h^{-1})

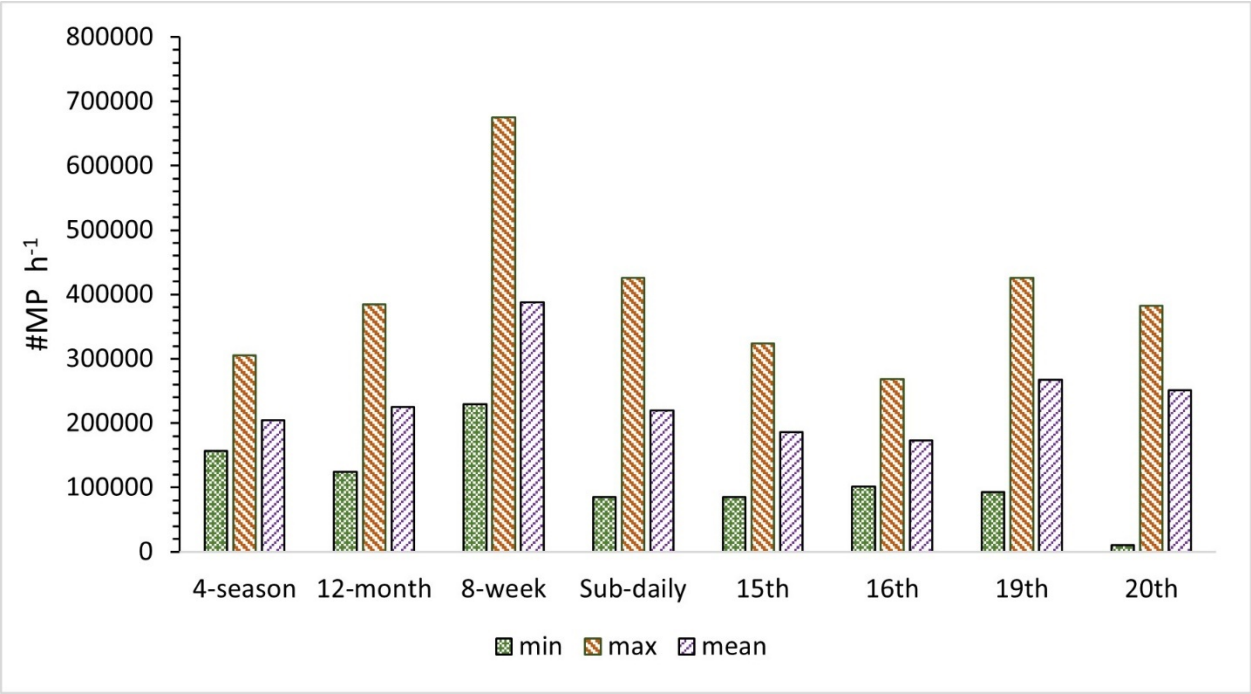


Figure 5.6: Bar chart showing minimum and maximum ranges and mean MP load per hour for the different sampling regimens. Green bars on show minimum, orange in the middle maximum and purple the mean load. Note that sub-daily has been also depicted as individual days (15th, 16th, 19th and 20th of June).

5.4.5 MP relationships with stream hydrological parameters

Microplastic concentrations were compared to stream hydrological parameters in order to assess relationships that indicate source or transport controls of the observed MP dynamics. Stream electrical conductivity (EC, measured in µS/cm) as a potential indicator of the concentration of released wastewater exhibited no clear seasonal trend but was negatively correlated with the stream discharge at the times of sampling ($Rs = -.35$, $p < 0.001$). However, EC was not correlated with MP concentrations ($Rs = .01$, $p = 0.862$). The stream discharge was not correlated with the observed MP concentration ($Rs = -.257$, $p = 0.418$) or recorded MP sizes ($Rs = .10$, $p < 0.001$). Flow velocity

did not correlate with MP concentration in the stream either (Rs = -.10, p = 0.555), nor with MP sizes spectra (Rs_{vel} = .08, p = 0.002).

5.5 Discussion

5.5.1 High variability in stream discharge linked to WWTP outflow

The highly variable stream discharge observed at the field site could be attributed to the fluctuating WWTP outflow, with difference of minimum and maximum discharge within 15 min being as high as 200 L s^{-1}. This type of discharge variation isn't unusual in particular in highly responsive headwater streams and similar variability in flow regimes can be found in other urban as well as more natural streams. Depending on the specific catchment conditions, variability in stream flow can be driven by shorter term weather events, human influence (such as water management) or seasonal variability (e.g., snowmelt) (Bookhagen and Burbank, 2010, Gribovszki et al., 2010). Our results highlight the impact of stream flow variability on the differences in calculated MP loads, underlining the importance of adequately covering representative MP sampling for different flow conditions. This includes consideration of existing flow dynamic data/conditions and pre-existing mechanistic system understanding should inform decisions about any MP sampling design.

The present study allowed for a first assessment of the variability of MP during a variety of sampling regimens to answer the question of MP concentration consistency and site representation based on different sampling frequencies. This particular study site provided a unique opportunity to observe the variation in MP concentrations downstream of a known point source in absence of any other major sources of MP or discharge that could have caused interference with the MP signal. The MP counts obtained here (0.244 ± 0.104 MP L^{-1}, > 63 µm) were slightly lower than previously

reported from other waste water influenced sites in studies with similar limit of detection (e.g., 0.59 ± 0.22 MP L^{-1} (> 50 µm) (Yang et al., 2019), 2.5 ± 0.3 MP L^{-1} (> 63 µm) (Magni et al., 2019) and 1.97 ± 0.05 MP L^{-1} (> 20 µm) (Ben-David et al., 2021). Some of these differences could be related to the size cut-off limit, as smaller MP are more abundant than larger ones (Ben-David et al., 2021), while some of the differences could also be related to the specific WWTP type, as removal efficiencies have been reported to vary between treatment types and WWTP operation (Cristaldi et al., 2020, Iyare et al., 2020). Another potential factor explaining the differences to previous studies could be that the sampling location in this study 800 m downstream from the outflow point, contrary to previous studies that sampled directly at the source of the outflow. While no additional MP sources were present in that section, MP transport and potential accumulation could have been affected by several different transport and sedimentation processes (e.g., settling, burial, hyporheic exchange, resuspension, bedload transport etc.), causing the respective MP concentration to decrease (Waldschläger et al., 2022, Drummond et al., 2020).

5.5.2 Stream characterisation requires temporally varied sampling

Snap-shot sampling as it is carried out in most freshwater MP studies provides insights into the specific status of an investigated system at a given time and location. Our results reveal that for conditions as the single source dominated study site, seasonal and even monthly or weekly sampling regimes may be insufficient to capture a representative range of MP concentrations. Seasonally, MP concentrations appeared to be highest in July when considering only seasonal or monthly sampling intervals (Figure 5.5). Analysis of weekly sampling indicated a slow increase of MP concentrations from June towards the end of July (Figure 5.5), However, even higher frequency sampling (sub-daily) suggested that this trend could have been observed by pure chance rather than

being a true increase: despite the sampling taking place consistently between 9 am - 11 am, the sub-daily data suggested that MP concentrations at the field site could fluctuate by as much as five times for samples collected only one hour apart. This highlights the risk of misinterpretations when generalising from the seasonal or monthly sampling results alone and regardless of the consistent sampling time. The large variability in MP concentrations observed throughout the day may have huge implications for load estimations, source evaluation and most importantly the effect that this has on MP transport downstream. Similar sub-daily variation has been reported previously from wastewater effluent where 3h intervals were analysed (Talvitie et al., 2017). The MP concentrations fluctuated during one day with an order of magnitude, however, as only one day was sampled, it is impossible to draw any conclusions, whether any re-occurring trends would be present (Talvitie et al., 2017). Similar behaviour has previously been described for pharmaceuticals and personal care products and other micro-contaminants, which were characterised by high heterogeneity and considerable short-term variations in pollutant loads at sewage outflows (Ort et al., 2010a, Ort et al., 2010b, Johnson et al., 2008). To further the complexity of the sampling, the MP concentrations measured here were not correlated with the stream discharge, average flow velocity or EC, suggesting that the MP concentrations were unlikely to be solely controlled by release of concentrated effluent discharge from the WWTP. Furthermore, the MP polymer composition did not vary significantly, regardless of the sampling frequency, suggesting that the type of MP output from the WWTP is temporally consistent. It is possible that MP concentration changes were at least in parts controlled by variability in WWTP operation and the treatments plant's efficiency to remove MP from effluent or reflect differences in the input concentration of MP. Further studies analysing the impacts of WWTP plant operations on variability in effluent MP concentrations as

well as temporal variability in MP inputs into WTP could help to provide better understanding of the driving mechanisms of MP dynamics downstream dominant pollution sources.

5.5.3 The range of MP loads is important for characterising downstream export dynamics

Interestingly, the average MP load calculated based on the different sampling frequencies remained remarkably similar throughout the observation period. The range of identified MP loads was larger for higher sampling frequencies. This variability in calculated MP loading was a consequence of a combination of the high variability observed in both the MP concentration and stream discharge, with the range of both parameters increasing with higher sampling frequency. Discharge and MP concentrations were not correlated within the field site. Different mechanisms affected the MP load at different times in this system: load could be driven by discharge and/or MP concentration. For instance, during the 8-week frequency sampling, the July MP concentrations were all high (Figure 5.4). However, the MP load was high for only the first three weeks (Figure 5.6) and dropped on the last week of July (26th July 2021). This was despite the MP concentration being the second highest for this sampling frequency (0.55 MP L^{-1}). This example highlights the interactions of the two governing mechanisms working in the investigated stream system: for the first three weeks of July the MP concentrations were the main driver for MP loading and during the last week of July the MP load was mainly controlled by stream discharge. As the 26th of July 2021 was also a datapoint that was pre-chosen to represent the summer season for the 4-season frequency, by chance, this would have led to an interpretation of summer having a lower MP loading than other seasons. This high variability between individual days highlights that the choice of an individual date as being representative for an entire season comes with large uncertainties

and it is imperative to capture the discharge at the sampling time in order to fully realise the dynamics of the study system.

Sewage outflow is often branded as a continuous 'hotspot' for MP pollution at local scale (Yaseen et al., 2022, Bretas Alvim et al., 2020) and typically annual MP load estimates are based on the multiplication of annual discharge with observed MP concentrations at a given sampling time (e.g.,Carr et al., 2016, Murphy et al., 2016, Gies et al., 2018, Mintenig et al., 2017). Here, based on the load calculation of different sampling regimes presented in section 5.4.4, we show MP loads ranging from 85,691 MP h^{-1} up to 675,677 MP h^{-1} (Figure 5.7). The changes in the range of MP loads over the 12-hour period of hourly sampling suggests that depending on the time of the day when sampling occurred, the annual load estimation based on a snapshot multiplied by the annual discharge could, in this specific system, result in over or underestimation of MP loads by up to 3.8 billion MP. The rapid changes in MP loading throughout the day suggest that rather than acting as a continuous MP release, the WWTP outflow creates MP pulses at the site, with different loads of MP being transported downstream at different times. Furthermore, the observed rapid changes in MP loads will not only have local scale effects but will also have wider implications in the rest of the river network as these MP load 'pulses' travel downstream with unknown consequences for ecosystem and biotic health and exposure downstream. It is therefore imperative to investigate whether this type of 'pulses of MP' are present at other types of WWTPs and other scales of streams and rivers, and with different combinations of point and non-point sources of MP and to assess their potential effect on local exposure risks.

5.5.4 Implications and future research

WWTPs have previously been referred to as important and steady sources for MP (Bretas Alvim et al., 2020, Murphy et al., 2016, Wu et al., 2022, Yaseen et al., 2022), at this field site, snap-shot sampling was not sufficient to capture the true MP concentration fluctuations in the WWTP outflow and instead of acting as a steady MP source, the WWTP created MP blooms travelling downstream. As this is the first study where the discharge and MP concentrations were compared in a stream where a WWTP acts as the sole MP source, it cannot be excluded that this type of fluctuation also occurs at other WWTP sites and has simply not been noticed due to lack of sampling. Further studies with high-temporal scale at different WWTPs, ideally at sites with negligible upstream water source to avoid dilution effect, are required to gain full understanding of how MP concentration fluctuates in outflow in the course of a single day.

Within the investigated freshwater system, the high variability in both discharge and MP concentrations resulted in a high variability in MP loads downstream of the WWTP. If these changes are not quantified through accurate sampling strategy, this is likely to have consequences on local risk assessments and when estimating any local exposure and the consequent risk for the receiving ecosystem. The results from this study (see Appendix 4: S3 and Figure S7), suggest that in the investigated system it would require five hourly samples / day (Appendix 4: Figure S7), to capture the variability of the MP concentrations at the site. Furthermore, recording accurately the stream discharge is imperative, as this will allow more precise MP load estimations to be calculated, which will enable the transfer from local exposure estimations (MP concentrations at given time) towards more predictive downstream consequences (MP loads). For example, the sub-daily sampling revealed an increase of 276,000 MP h^{-1} within 1 hour. These swift changes in MP loads

to downstream should be included in local risk assessments, as they inherently will affect MP exposures downstream, with the potential for MP 'pulses' having unknown effects on biota and ecosystem health. Previous work has suggested that moving from areas of high to low flow can lead to deposition of MP to the sediment (Tibbets et al., 2018), so these pulses might also lead to accumulation of MP at the lower energy sites at River Blythe.

We recommend that in order to obtain better understanding of the actual contribution of different types of WWTPs to MP concentrations and loads in freshwater streams, and to understand if the MP load 'pulses' observed here occur also at other WWTP sites, introduction of a pre-monitoring campaign/pilot studies could be implemented. This would include discharge, velocity and the MP concentration in the effluent being monitored through the daily outflow pattern in order to understand their variability and thus to determine, the minimum sampling frequency needed to provide a reasonable representation of the MP concentration. This would lead to better planning for the overall study and maximise the effectiveness of the final sampling campaign and can help to avoid the collection of nonrepresentative samples as well as aid in local exposure assessments based on the resulting snap-shot data.

5.6 References

BEN-DAVID, E. A., HABIBI, M., HADDAD, E., HASANIN, M., ANGEL, D. L., BOOTH, A. M. & SABBAH, I. 2021. Microplastic distributions in a domestic wastewater treatment plant: Removal efficiency, seasonal variation and influence of sampling technique. *Science of The Total Environment,* 752**,** 141880.

BERGMANN, M., COLLARD, F., FABRES, J., GABRIELSEN, G. W., PROVENCHER, J. F., ROCHMAN, C. M., VAN SEBILLE, E. & TEKMAN, M. B. 2022. Plastic pollution in the Arctic. *Nature Reviews Earth & Environment,* 3**,** 323-337.

BESSELING, E., WEGNER, A., FOEKEMA, E. M., VAN DEN HEUVEL-GREVE, M. J. & KOELMANS, A. A. 2013. Effects of Microplastic on Fitness and PCB Bioaccumulation by the Lugworm Arenicola marina (L.). *Environmental Science & Technology,* 47**,** 593-600.

BIAN, P., LIU, Y., ZHAO, K., HU, Y., ZHANG, J., KANG, L. & SHEN, W. 2022. Spatial variability of microplastic pollution on surface of rivers in a mountain-plain transitional area: A case study in the Chin Ling-Wei River Plain, China. *Ecotoxicology and Environmental Safety,* 232**,** 113298.

BIGALKE, M., FIEBER, M., FOETISCH, A., REYNES, J. & TOLLAN, P. 2022. Microplastics in agricultural drainage water: A link between terrestrial and aquatic microplastic pollution. *Science of The Total Environment,* 806**,** 150709.

BLACKBURN, K. & GREEN, D. 2022. The potential effects of microplastics on human health: What is known and what is unknown. *Ambio,* 51**,** 518-530.

BLAIR, R. M., WALDRON, S. & GAUCHOTTE-LINDSAY, C. 2019. Average daily flow of microplastics through a tertiary wastewater treatment plant over a ten-month period. *Water Research,* 163**,** 114909.

BÖCK, K., POLT, R. & SCHÜLTING, L. 2018. Ecosystem Services in River Landscapes. *In:* SCHMUTZ, S. & SENDZIMIR, J. (eds.) *Riverine Ecosystem Management: Science for Governing Towards a Sustainable Future.* Cham: Springer International Publishing.

BOOKHAGEN, B. & BURBANK, D. W. 2010. Toward a complete Himalayan hydrological budget: Spatiotemporal distribution of snowmelt and rainfall and their impact on river discharge. *Journal of Geophysical Research: Earth Surface,* 115.

BRENNECKE, D., DUARTE, B., PAIVA, F., CAÇADOR, I. & CANNING-CLODE, J. 2016. Microplastics as vector for heavy metal contamination from the marine environment. *Estuarine, Coastal and Shelf Science,* 178**,** 189-195.

BRETAS ALVIM, C., MENDOZA-ROCA, J. A. & BES-PIÁ, A. 2020. Wastewater treatment plant as microplastics release source – Quantification and identification techniques. *Journal of Environmental Management,* 255**,** 109739.

CARR, S. A., LIU, J. & TESORO, A. G. 2016. Transport and fate of microplastic particles in wastewater treatment plants. *Water Research,* 91**,** 174-182.

CONLEY, K., CLUM, A., DEEPE, J., LANE, H. & BECKINGHAM, B. 2019. Wastewater treatment plants as a source of microplastics to an urban estuary: Removal efficiencies and loading per capita over one year. *Water Research X,* 3**,** 100030.

CORCORAN, P. L., BIESINGER, M. C. & GRIFI, M. 2009. Plastics and beaches: A degrading relationship. *Marine Pollution Bulletin,* 58**,** 80-84.

COWGER, W., GRAY, A. B., GUILINGER, J. J., FONG, B. & WALDSCHLÄGER, K. 2021. Concentration Depth Profiles of Microplastic Particles in River Flow and Implications for Surface Sampling. *Environmental Science & Technology,* 55**,** 6032-6041.

CRISTALDI, A., FIORE, M., ZUCCARELLO, P., OLIVERI CONTI, G., GRASSO, A., NICOLOSI, I., COPAT, C. & FERRANTE, M. 2020. Efficiency of Wastewater Treatment Plants (WWTPs) for Microplastic Removal: A Systematic Review. *International Journal of Environmental Research and Public Health* [Online], 17.

DRUMMOND, J. D., NEL, H. A., PACKMAN, A. I. & KRAUSE, S. 2020. Significance of Hyporheic Exchange for Predicting Microplastic Fate in Rivers. *Environmental Science & Technology Letters,* 7**,** 727-732.

DRUMMOND, J. D., SCHNEIDEWIND, U., LI, A., HOELLEIN, T. J., KRAUSE, S. & PACKMAN, A. I. 2022. Microplastic accumulation in riverbed sediment via hyporheic exchange from headwaters to mainstems. *Science Advances,* 8**,** eabi9305.

FERREIRA, G. V. B., JUSTINO, A. K. S., EDUARDO, L. N., LENOBLE, V., FAUVELLE, V., SCHMIDT, N., JUNIOR, T. V., FRÉDOU, T. & LUCENA-FRÉDOU, F. 2022. Plastic in the inferno: Microplastic contamination in deep-sea cephalopods (Vampyroteuthis infernalis and Abralia veranyi) from the southwestern Atlantic. *Marine Pollution Bulletin,* 174**,** 113309.

GIES, E. A., LENOBLE, J. L., NOËL, M., ETEMADIFAR, A., BISHAY, F., HALL, E. R. & ROSS, P. S. 2018. Retention of microplastics in a major secondary wastewater treatment plant in Vancouver, Canada. *Marine Pollution Bulletin,* 133**,** 553-561.

GRIBOVSZKI, Z., SZILÁGYI, J. & KALICZ, P. 2010. Diurnal fluctuations in shallow groundwater levels and streamflow rates and their interpretation – A review. *Journal of Hydrology,* 385**,** 371-383.

HARTMANN, N. B., HÜFFER, T., THOMPSON, R. C., HASSELLÖV, M., VERSCHOOR, A., DAUGAARD, A. E., RIST, S., KARLSSON, T., BRENNHOLT, N., COLE, M., HERRLING, M. P., HESS, M. C., IVLEVA, N. P., LUSHER, A. L. & WAGNER, M. 2019. Are We Speaking the Same Language? Recommendations for a Definition and Categorization Framework for Plastic Debris. *Environmental Science & Technology,* 53**,** 1039-1047.

IYARE, P. U., OUKI, S. K. & BOND, T. 2020. Microplastics removal in wastewater treatment plants: a critical review. *Environmental Science: Water Research & Technology,* 6**,** 2664-2675.

JOHNSON, A. C., TERNES, T., WILLIAMS, R. J. & SUMPTER, J. P. 2008. Assessing the Concentrations of Polar Organic Microcontaminants from Point Sources in the Aquatic Environment: Measure or Model? *Environmental Science & Technology,* 42**,** 5390-5399.

KELLEHER, L., SCHNEIDEWIND, U., KRAUSE, S., HAVERSON, L., ALLEN, S., ALLEN, D., KUKKOLA, A., MURRAY-HUDSON, M., MASELLI, V. & FRANCHI, F. 2023. Microplastic accumulation in endorheic river basins – The example of the Okavango Panhandle (Botswana). *Science of The Total Environment,* 874**,** 162452.

KRAUSE, S., BARANOV, V., NEL, H. A., DRUMMOND, J. D., KUKKOLA, A., HOELLEIN, T., SAMBROOK SMITH, G. H., LEWANDOWSKI, J., BONET, B., PACKMAN, A. I., SADLER, J., INSHYNA, V., ALLEN, S., ALLEN, D., SIMON, L., MERMILLOD-BLONDIN, F. & LYNCH, I. 2021. Gathering at the top? Environmental controls of

microplastic uptake and biomagnification in freshwater food webs. *Environmental Pollution,* 268**,** 115750.

KUKKOLA, A., KRAUSE, S., LYNCH, I., SAMBROOK SMITH, G. H. & NEL, H. 2021. Nano and microplastic interactions with freshwater biota – Current knowledge, challenges and future solutions. *Environment International,* 152**,** 106504.

KUKKOLA, A., KRAUSE, S., YONAN, Y., KELLEHER, L., SCHNEIDEWIND, U., SMITH, G. H. S., NEL, H. & LYNCH, I. 2023a. Easy and accessible way to calibrate a fluorescence microscope and to create a microplastic identification key. *MethodsX,* 10**,** 102053.

KUKKOLA, A., RUNKEL, R., CHNEIDEWIND, U., MURPHY, S., KELLEHER, L., S SMITH, G. H. S., NEL, H. & LYNCH, I. KRAUSE, S., 2023b. Prevailing impacts of river management on microplastic transport in contrasting US streams requires rethinking of global microplastic flux estimations. *(IN PRESS)*

KUKKOLA, A., RUNKEL, R., CHNEIDEWIND, U., MURPHY, S., KELLEHER, L., S SMITH, G. H. S., NEL, H. & LYNCH, I. KRAUSE, S., 2023b. Prevailing impacts of river management on microplastic transport in contrasting US streams requires rethinking of global microplastic flux estimations. *(IN PRESS)*

KUKKOLA, A. T., SENIOR, G., MAES, T., SILBURN, B., BAKIR, A., KRÖGER, S. & MAYES, A. G. 2022. A large-scale study of microplastic abundance in sediment cores from the UK continental shelf and slope. *Marine Pollution Bulletin,* 178**,** 113554.

LIU, W., ZHANG, J., LIU, H., GUO, X., ZHANG, X., YAO, X., CAO, Z. & ZHANG, T. 2021. A review of the removal of microplastics in global wastewater treatment plants: Characteristics and mechanisms. Environment International, 146, 106277.

LAMBERT, S. & WAGNER, M. 2018. Microplastics Are Contaminants of Emerging Concern in Freshwater Environments: An Overview. *In:* WAGNER, M. & LAMBERT, S. (eds.) *Freshwater Microplastics : Emerging Environmental Contaminants?* Cham: Springer International Publishing.

LARES, M., NCIBI, M. C., SILLANPÄÄ, M. & SILLANPÄÄ, M. 2018. Occurrence, identification and removal of microplastic particles and fibres in conventional activated sludge process and advanced MBR technology. *Water Research,* 133**,** 236-246.

LIU, W., ZHANG, J., LIU, H., GUO, X., ZHANG, X., YAO, X., CAO, Z. & ZHANG, T. 2021. A review of the removal of microplastics in global wastewater treatment plants: Characteristics and mechanisms. *Environment International,* 146**,** 106277.

MAGNI, S., BINELLI, A., PITTURA, L., AVIO, C. G., DELLA TORRE, C., PARENTI, C. C., GORBI, S. & REGOLI, F. 2019. The fate of microplastics in an Italian Wastewater Treatment Plant. *Science of The Total Environment,* 652**,** 602-610.

MAK, C. W., TSANG, Y. Y., LEUNG, M. M.-L., FANG, J. K.-H. & CHAN, K. M. 2020. Microplastics from effluents of sewage treatment works and stormwater discharging into the Victoria Harbor, Hong Kong. *Marine Pollution Bulletin,* 157**,** 111181.

MANI, T., HAUK, A., WALTER, U. & BURKHARDT-HOLM, P. 2015. Microplastics profile along the Rhine River. *Scientific Reports,* 5**,** 17988.

MARGENAT, H., NEL, H.A., STONEDAHL, S.H., KRAUSE, S., SABATER, F., DRUMMOND, J.D. 2021. Hydrologic controls on the accumulation of different sized microplastics in the streambed sediments downstream of a wastewater treatment plant (Catalonia, Spain). *Environmental Research Letters,* 16.

MATEOS-CÁRDENAS, A., O'HALLORAN, J., VAN PELT, F. N. A. M. & JANSEN, M. A. K. 2020. Rapid fragmentation of microplastics by the freshwater amphipod Gammarus duebeni (Lillj.). *Scientific Reports,* 10**,** 12799.

MATO, Y., ISOBE, T., TAKADA, H., KANEHIRO, H., OHTAKE, C. & KAMINUMA, T. 2001. Plastic Resin Pellets as a Transport Medium for Toxic Chemicals in the Marine Environment. *Environmental Science & Technology,* 35**,** 318-324.

MILLER, E., SEDLAK, M., LIN, D., BOX, C., HOLLEMAN, C., ROCHMAN, C. M. & SUTTON, R. 2021. Recommended best practices for collecting, analyzing, and reporting microplastics in environmental media: Lessons learned from comprehensive monitoring of San Francisco Bay. *Journal of Hazardous Materials,* 409**,** 124770.

MINTENIG, S. M., INT-VEEN, I., LÖDER, M. G. J., PRIMPKE, S. & GERDTS, G. 2017. Identification of microplastic in effluents of waste water treatment plants using focal plane array-based micro-Fourier-transform infrared imaging. *Water Research,* 108**,** 365-372.

MUNNO, K., DE FROND, H., O'DONNELL, B. & ROCHMAN, C. M. 2020. Increasing the Accessibility for Characterizing Microplastics: Introducing New Application-Based and Spectral Libraries of Plastic Particles (SLoPP and SLoPP-E). *Analytical Chemistry,* 92**,** 2443-2451.

MURPHY, F., EWINS, C., CARBONNIER, F. & QUINN, B. 2016. Wastewater Treatment Works (WwTW) as a Source of Microplastics in the Aquatic Environment. *Environmental Science & Technology,* 50**,** 5800-5808.

NEL, H., KRAUSE, S., SAMBROOK SMITH, G. H. & LYNCH, I. 2019. Simple yet effective modifications to the operation of the Sediment Isolation Microplastic unit to avoid polyvinyl chloride (PVC) contamination. *MethodsX,* 6**,** 2656-2661.

ORT, C., LAWRENCE, M. G., REUNGOAT, J. & MUELLER, J. F. 2010a. Sampling for PPCPs in Wastewater Systems: Comparison of Different Sampling Modes and Optimization Strategies. *Environmental Science & Technology,* 44**,** 6289-6296.

ORT, C., LAWRENCE, M. G., RIECKERMANN, J. & JOSS, A. 2010b. Sampling for Pharmaceuticals and Personal Care Products (PPCPs) and Illicit Drugs in Wastewater Systems: Are Your Conclusions Valid? A Critical Review. *Environmental Science & Technology,* 44**,** 6024-6035.

RUFFELL, H., PANTOS, O., NORTHCOTT, G. & GAW, S. 2021. Wastewater treatment plant effluents in New Zealand are a significant source of microplastics to the environment. *New Zealand Journal of Marine and Freshwater Research***,** 1-17.

SCHMIDT, C., KUMAR, R., YANG, S. & BÜTTNER, O. 2020. Microplastic particle emission from wastewater treatment plant effluents into river networks in Germany: Loads, spatial patterns of concentrations and potential toxicity. *Science of The Total Environment,* 737**,** 139544.

SUN, J., DAI, X., WANG, Q., VAN LOOSDRECHT, M. C. M. & NI, B.-J. 2019. Microplastics in wastewater treatment plants: Detection, occurrence and removal. *Water Research,* 152**,** 21-37.

TALVITIE, J., MIKOLA, A., KOISTINEN, A. & SETÄLÄ, O. 2017. Solutions to microplastic pollution – Removal of microplastics from wastewater effluent with advanced wastewater treatment technologies. *Water Research,* 123**,** 401-407.

TIBBETTS, J., KRAUSE, S., LYNCH, I. & SAMBROOK SMITH, G. H. 2018. Abundance, Distribution, and Drivers of Microplastic Contamination in Urban River Environments. *Water,* 10**,** 1597

VÁRI, Á., PODSCHUN, S. A., ERŐS, T., HEIN, T., PATAKI, B., IOJĂ, I.-C., ADAMESCU, C. M., GERHARDT, A., GRUBER, T., DEDIĆ, A., ĆIRIĆ, M., GAVRILOVIĆ, B. & BÁLDI, A. 2022. Freshwater systems and ecosystem services: Challenges and chances for cross-fertilization of disciplines. *Ambio,* 51**,** 135-151.

WALDSCHLÄGER, K., BRÜCKNER, M. Z. M., CARNEY ALMROTH, B., HACKNEY, C. R., ADYEL, T. M., ALIMI, O. S., BELONTZ, S. L., COWGER, W., DOYLE, D., GRAY, A., KANE, I., KOOI, M., KRAMER, M., LECHTHALER, S., MICHIE, L., NORDAM, T., POHL, F., RUSSELL, C., THIT, A., UMAR, W., VALERO, D., VARRANI, A., WARRIER, A. K., WOODALL, L. C. & WU, N. 2022. Learning from natural sediments to tackle microplastics challenges: A multidisciplinary perspective. *Earth-Science Reviews,* 228**,** 104021.

WANG, Z., CHEN, M., ZHANG, L., WANG, K., YU, X., ZHENG, Z. & ZHENG, R. 2018. Sorption behaviors of phenanthrene on the microplastics identified in a mariculture farm in Xiangshan Bay, southeastern China. *Science of The Total Environment,* 628-629**,** 1617-1626.

WATKINS, L., SULLIVAN, P. J. & WALTER, M. T. 2019. A case study investigating temporal factors that influence microplastic concentration in streams under different treatment regimes. *Environmental Science and Pollution Research,* 26**,** 21797-21807.

WEISS, L., LUDWIG, W., HEUSSNER, S., CANALS, M., GHIGLIONE, J.-F., ESTOURNEL, C., CONSTANT, M. & KERHERVÉ, P. 2021. The missing ocean plastic sink: Gone with the rivers. *Science,* 373**,** 107-111.

WU, X., ZHAO, X., CHEN, R., LIU, P., LIANG, W., WANG, J., TENG, M., WANG, X. & GAO, S. 2022. Wastewater treatment plants act as essential sources of microplastic formation in aquatic environments: A critical review. *Water Research,* 221**,** 118825.

YANG, L., LI, K., CUI, S., KANG, Y., AN, L. & LEI, K. 2019. Removal of microplastics in municipal sewage from China's largest water reclamation plant. *Water Research,* 155**,** 175-181.

YANG, Y., LIU, W., ZHANG, Z., GROSSART, H.-P. & GADD, G. M. 2020. Microplastics provide new microbial niches in aquatic environments. *Applied Microbiology and Biotechnology,* 104**,** 6501-6511.

YASEEN, A., ASSAD, I., SOFI, M. S., HASHMI, M. Z. & BHAT, S. U. 2022. A global review of microplastics in wastewater treatment plants: Understanding their occurrence, fate and impact. *Environmental Research,* 212**,** 113258.

YUAN, Z., NAG, R. & CUMMINS, E. 2022. Human health concerns regarding microplastics in the aquatic environment - From marine to food systems. *Science of The Total Environment,* 823**,** 153730.

ZIAJAHROMI, S., NEALE, P. A., TELLES SILVEIRA, I., CHUA, A. & LEUSCH, F. D. L. 2021. An audit of microplastic abundance throughout three Australian wastewater treatment plants. *Chemosphere,* 263**,** 128294.

Chapter 6: A tale of two catchments - what makes microplastic move?

Anna Kukkola[a], Uwe Schneidewind[a], Liam Kelleher[a,c], Lee Haverson[a], Greg Sambrook Smith[a], Iseult Lynch[a,c] and Stefan Krause[a,b,c]

[a] School of Geography, Earth and Environmental Sciences, University of Birmingham, Edgbaston, Birmingham B15 2TT, United Kingdom

[b] LEHNA- Laboratoire d'ecologie des hydrosystemes naturels et anthropises, University of Lyon, Darwin C & Forel, 3-6 Rue Raphaël Dubois, 69622 Villeurbanne, France.

[c] Institute of Global Innovation, University of Birmingham B15 2SA, Birmingham. United Kingdom.

6.1 Abstract

Microplastics (MP) are a global concern and developing accurate risk assessments requires understanding of MP sources and their transport mechanisms. This study aimed to identify transport mechanisms in two catchments, one with a well-defined point source (Eastcote Brook, downstream of a sewage treatment works) and the other with an urban diffuse source (Bourn Brook). MP concentrations were determined via fluorescent microscopy following extraction from both sediment and surface water. Despite the point source having a small hydrological catchment, it also exhibited an urban signal, indicating that this site could not be defined by its natural catchment. MP loading was dominated by the point source and was less dependent on the stream discharge, highlighting the point-source and water management activities as the drivers of the

loading in this case. However, at the diffuse source site, discharge and MP load exhibited strong correlation, suggesting hydrometeorological source activation (e.g., rainfall events) as the major driver. The results offer important evidence on how different source types are activated and thus influence MP concentrations and loadings at specific sampling timepoints and provide a necessary first step for better understanding of catchment wide source and MP load assessments.

6.2 Introduction

Microplastics (MP) are historically defined as plastics smaller than 5 mm (Thompson et al., 2004, GESAMP, 2016) or, more recently, smaller than 1 mm (the size definition used here) (Hartmann et al., 2019) and are ubiquitous in all environmental compartments globally, including rivers (Samandra et al., 2022, Kukkola et al., 2022, Bergmann et al., 2022, Campanale et al., 2020, Evangeliou et al., 2020, Yuan et al., 2022). Research into their behavior, transport and effects in freshwater environments has received increased attention over the last decade, yet open questions on their distribution and sources remains (Krause et al., 2021, Ateia et al., 2022, Xu et al., 2020).

River environments are of particular interest, as it is becoming ever more apparent that MP transportation within river networks and environments is far more complex than previously thought (Bank and Hansson, 2022, Horton and Dixon, 2018, Margenat, 2021). Rivers can act both as a source for MP transport from terrestrial sources to the global oceans or as a sink trapping MP for extended timescales, depending on the prevailing hydrodynamic conditions (e.g., settling and resuspension) (Drummond et al., 2022, Drummond et al., 2020, Krause et al., 2021, Hurley et al., 2018, Dhivert et al., 2022). Rivers can also redistribute MP back to the terrestrial environment during either high flow events that re-disperse sediment, such as during severe weather events (Hurley et al 2018), or due to water management, where water is diverted back to the environment

(Kukkola et al., 2023b). MP also can cause adverse effects on freshwater organisms and have detrimental consequences for ecosystem health (Anbumani and Kakkar, 2018, Kukkola et al., 2021, Sun et al., 2021, Triebskorn et al., 2019) making the study of their transport mechanisms, which determines their accumulation sites and vulnerable ecosystems, vital if realistic local risk assessments are to be made.

The development of risk assessments requires quantification of the presence/abundance of MP and assessment of their respective source(s) and transport mechanisms including evaluation of their relevance or relative contribution. On this basis, an extensive understanding of how MP move within river networks can be obtained. This includes the direct mapping of MP contributions from different source-types to identify the controlling transport mechanisms, which contribute to MP release and their potential agglomeration in the river environment. MP (and other pollution) sources are classified into two broad categories: point and non-point (diffuse) sources (Krause et al., 2021, Horton et al., 2017). Point-sources, such as outflow (effluent) from sewage treatment works (WWTP) have been suggested to have more significant local impact than diffuse sources, due to expected higher local concentrations than those resulting from diffuse sources which include runoff from roads and atmospheric deposition (Krause et al., 2021, Horton et al., 2017). However, some evidence suggests that the local MP release estimations from WWTPs may have uncertainty associated with them, depending on sampling frequency (Chapter 5), the site and time of sampling (Cristaldi et al., 2020, Iyare et al., 2020). Further, studies have reported widespread presence of MP in rivers without point-sources present, hinting to the relatively high importance of diffuse MP sources. Close proximity to high anthropogenic activity areas, such as cities and industrial areas has been cited to increase the MP concentrations in rivers (de Carvalho et al., 2021, Peters and Bratton, 2016, Chen et al., 2021), though anecdotally, similar concentrations of MP has been

reported in WWTP outflow (Stanton et al., 2020, Wang et al., 2021), suggesting that the relative significance of these two source types in terms of MP loads downstream are yet to be determined. To further complicate the reliable estimation of MP sources and transport mechanisms, field data for MP transport and the control mechanisms from diffuse sources is severely lacking (Meng et al., 2020, Campanale et al., 2022), with not enough studies quantifying the relative importance of this source-type. By definition, diffuse sources cannot be pinpointed, but rather are the result of the activities occurring in the hydrological catchment of the sampling location at a given time. Delineating the hydrological catchment for the sampling location and comparing the land use within the catchment to the MP distribution has gained attention as a potential way to measure diffuse source activity, though this is typically limited by the resolution of the land use and/or population density data (Bond et al., 2022, Matjašič et al., 2023, Dai et al., 2022). Furthermore, effects of water management activities (e.g., diversion of water for agricultural, or potable water use etc.) are often overlooked, and if these exists within the catchment being studied, the effects of these on the MP signal downstream are not always clear (Kukkola et al., 2023b/Chapter 4). Further, when a point source effects are being measured, this is often done by measuring the relative difference between MP concentrations up/downstream from the WWTP activity, though other sources might exist in the catchment area (e.g., Matjašič et al., 2023, Margenat, 2021, Estahbanati and Fahrenfeld, 2016). No studies currently exist where the sole contribution of point or diffuse source effects on MP concentrations in rivers have been isolated and compared, or the degree to which transport and/or source controls the MP distribution in rivers with well-defined source types.

To begin bridging this knowledge gap and to develop primary mechanistic understanding of how the different potential MP sources in urban catchments with different characteristics may get activated and contribute MP to rivers, we present here a year-long study deploying a paired

catchment approach that compares two contrasting urban river catchments with different MP source characteristics in terms of their surface water MP dynamics. While one of the catchments is characterized by a diverse range of potential sources that are likely to create diffuse inputs into the river network, the other catchment is dominated by a known point-source (an WWTP) as the likely MP source of that river. Our comparative analyses aim to:

1) Establish the temporal dynamics of MP concentrations in the water column and sediment of both river catchments;

2) Evaluate the relative impact of hydrometeorological controls on MP concentrations and loads transported out of the two river catchments;

3) Identify differences in transport behaviors and potential MP signatures at both sites in relation to MP source type

6.3 Materials and methods

6.3.1 Study sites

The two study sites are located in the West Midlands, UK in low-order streams (Figure 6.A1 and 6.A2). The point source study site was located in the Eastcote Brook (henceforth denoted as "EB") stream near Hampton-in-Arden (UK) (latitude: 52.419714, longitude: -1.704480) with a catchment area of 2.1 km^2, (Figure 6.1B) and flowing into the River Blythe. The sampling site was approximately 800 m downstream from a large sized sewage treatment works (WWTP) equipped with a tertiary treatment system and sand filtration (Severn Trent Plc.) and with service population of 63,500. It was considered that all of the stream flow originated from an outflow from the WWTP point source. For further details and justification see Chapter 5. At EB, the dominant land use type was arable and horticulture (41.9%), followed by grassland (32.8%).

The diffuse source sampling site was located at a small urban headwater stream, Bourn Brook (BB), Birmingham, UK (latitude: 52.447108, longitude: -1.931416) with a drainage area of 17.4 km^2 and with a permanent resident population of 76,102 (2011 Census, Office for National Statistics) The stream source is located approximately 4.8 km upstream in a semi-natural woodland area, though at the sampling site urban and suburban land use dominated most of the drainage area with 62.3% of the land use classified as suburban and 10.6% as urban (Figure 6.1C). Several storm sewer systems exist in the drainage area, diverting water from the roads/pavements into the BB (Carstea et al., 2010, Khamis et al., 2017), making this site particularly well suited for diffuse source monitoring, as it is expected that due to the mainly paved catchment characteristics, MP within the catchment will end up in the stream due to runoff.

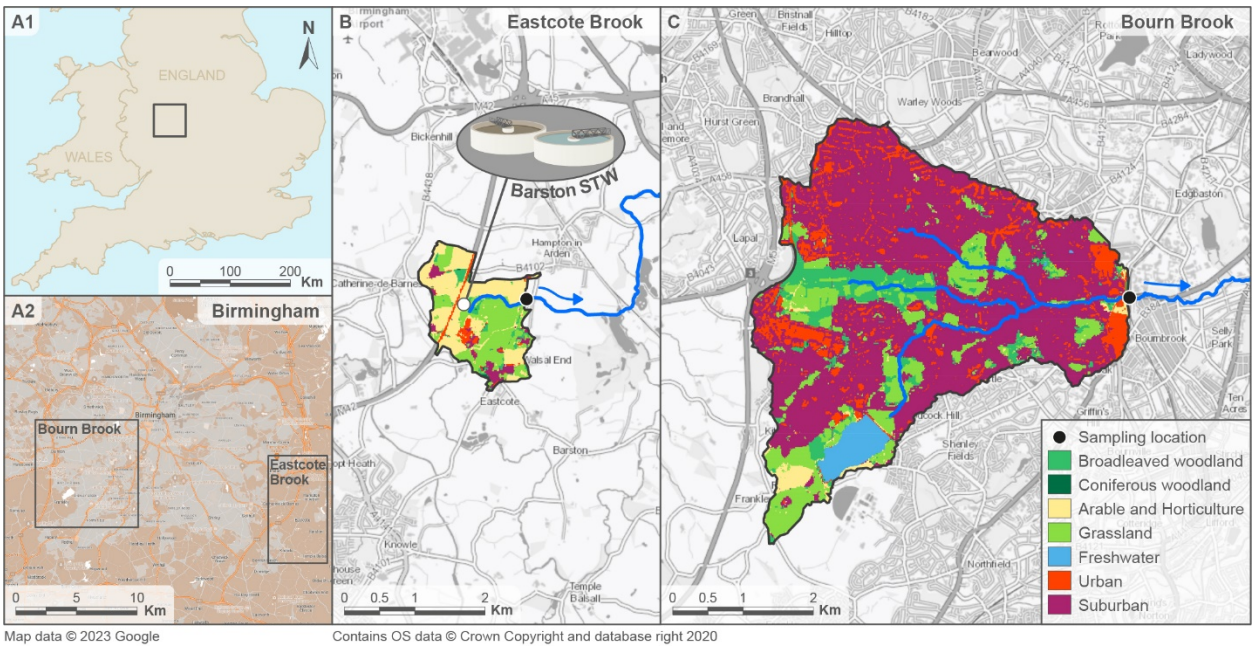


Figure 6.1: Maps showing the sampling locations in the context of the United Kingdom (A1) and the city of Birmingham (A2). Map B shows the point-source EB and map C shows the diffuse

source catchments and the respective land use obtained from the UK Centre for Ecology & Hydrology for 2020.

6.3.2 Field sampling

The sampling was conducted over a one-year period (1.4.2021-31.3.2022) and comprised of 12 monthly samples for both sites, collected during the last two weeks of each month), whereby both sites were visited within 5-day window.

Water sampling followed the protocol described in Kukkola et al., 2023b/Chapter 4, with some modifications: At each sampling occasion, three individual 50 L surface water samples were collected from the centre of the river and filtered in-situ over a 63 µm nylon mesh, from which each of the contents were transferred into a clean 20 mL glass vial using deionised water (DI-water). Additionally, three sediment samples were collected, in a triangular manner, with the central point always being the middle of the stream and the two sides being near the left and right banks (see schematic in Appendix 5: Figure S6.1). For each sediment sample, sediment ~5 cm depth was scooped into a pre-cleaned glass jar, which was only opened under water. All samples (n_{water} = 72, $n_{sediment}$ = 72) were transported immediately to the University of Birmingham where they were stored in the dark in a cold room (+ 6 ℃) before processing.

Additional hydrological parameter included flow velocity to obtain average stream discharge at the time of sampling. Flow velocity was obtained using a Sensa-RC2 (Aqua Data Services Ltd) electromagnetic velocity meter, from a predetermined and marked cross-section of the stream. For each 30 cm distance (beginning of 0, marking the start of the bank), depth measurements were taken and coupled with the average velocity measurement (averaged over 15 s), allowing the total stream discharge to be calculated as follows:

$$\sum Q_x = v_x \left[\frac{b_{n+1} - b_{n-1}}{2}\right] d_x$$

where ***Q*** is the discharge ($m^3 s^{-1}$), ***x*** indicates the sub-section, ***v*** is the flow velocity ($m s^{-1}$), ***b*** is the distance (m) from the initial point of observation, ***n+1*** and ***n-1*** refer to the following and preceding distances ***b,*** and ***d*** is the depth (m).

Rainfall data for BB was obtained from the Birmingham Urban Observatory which collects Netatmo citizen science data and for EB from the Meteorological Office (MET) office for the Coleshill station. The time from last moderate or heavier rain events (defined as > 4.9 mm rain in 24 hours according to MET) was recorded.

6.3.3. Laboratory analysis

6.3.3.1 Sample Preparation, digestion, and staining

The samples were extracted following the methods described in Kukkola et al., (2023b/Chapter 4). Briefly: sediment samples were dried at 50°C until constant weight, after which the three sediment samples from each sampling occasion were combined into a composite and homogenised. Approximately 35g of sediment was then extracted using density separation with a sediment-MP isolation (SMI) unit with $ZnCl_2$ (1.5 g cm^3) in accordance with Nel et al., (2020) and Kukkola et al (2023b/Chapter 4). After density separation had occurred (~18 hours/sample), samples were decanted over a 63 µm sieve and backwashed into 200 ml beakers with approximately 20 mL of 30% H_2O_2. Fenton reagent was used to digest organic matter (OM), and Fe^{2+} (aq) (0.05 M) catalyst was added to the beakers in ratio of 1:10 (Fe^{+2} : H_2O_2) (Margenat et al 2021; Kukkola 2023b/Chapter 4). Samples were covered with loose aluminium foil lids enabling

any heat/gas to escape but preventing airborne contamination and then left for at least 24 h at ambient room temperature.

After digestion, samples were decanted through a 63 µm sieve and backwashed into beakers with DI-water before staining with Nile Red (working concentration of 5 µg mL^{-1}) and left in an orbital shaker at 105 rpm (Grant-bio, PSU-20i) to stain for an hour. The samples were then filtered via a glass vacuum-filtration system onto glass-fibre GF/D filters (Whatmann) and rinsed with DI-water. Yellow goggles and UV-light were used to inspect the beaker and the funnel to ensure all visible particles had been removed. The filters were stored in clean PP Petri dishes with lids closed and dried for 24 h at 50 °C. Surface water samples were processed in an identical way, except for that they were treated individually (no composite was created) and the density separation step was omitted. The overall workflow is shown schematically in Figure 6.2.

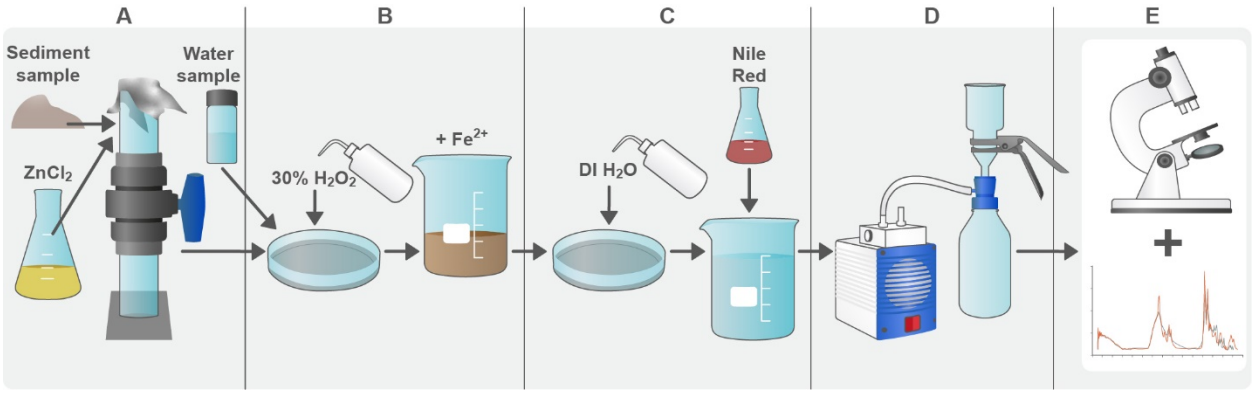


Figure 6.2: Schematic illustration of the sample preparation workflow. A) Density separation (sediment samples only), B) Digestion with Fenton's reagent, C) staining with Nile Red, D) Vacuum filtration and E) Microscopy and spectroscopy and data analysis.

6.3.3.2 Microscopy and MP identification

Fluorescent microscopy followed the methodology and criteria set in (Kukkola et al 2023a, Kukkola et al 2023b/Chapter 4). Briefly: a macro zoom microscope (Olympus MVX-ZB10) equipped with GFP filter cube (excitation filter: 470/40 nm, dichroic mirror: 495 nm high pass, emission filter: 525/50 nm) and with 100W mercury light source was used in fluorescence mode, 12% light intensity on 32x magnification with 50 ms exposure time. Measurements for fluorescence intensity and photographs were taken with a DP74 colour camera using CellSens Software (Olympus). A pre-set fluorescence threshold and identification-key were used to identify all potential MP (Nel et al., 2021: Kukkola et al., 2023a). Each filter was also scanned under bright field mode and non-fluorescence fibres that met the identification criteria were also included, due to Nile Red having difficulties to stain fibres (Kukkola et al., 2023a, Stanton et al., 2019). This inability of Nile Red to reliably stain fibres has been postulated to be related to specific colourants present in fibres (Stanton et al., 2019), or to be result of high proportion of fibres consisting of polymers that stain poorly (such as polyester and polyethylene terephthalate) (Shim et al., 2016; Kukkola et al., 2022), though the underlining mechanism is still unknown.

From the MP identified and counted in fluorescence step, 40% n=161 (EB) and 58% n=209 (BB) were picked from surface water for further chemical verification. These particles were analysed via A Renishaw InVia Qontor Raman microscope equipped with a 785 nm laser following the setup in Kelleher 2023 and Kukkola 2023b. Briefly: For spectral matching, the fingerprint region of 650-1700 cm^{-1} was used and the spectra were exported into a custom Python script (Python 3.9) and peaks were matched to reference libraries using the Pearson correlation coefficient (Kelleher et al., 2023). 70% hit quality index was set as a threshold for positive identification.

6.3.4 QA/QC

Field background samples (n = 24) were collected during the sampling by using glass jars that were left open by the stream bank to identify any air deposition. To combat any contamination from the researchers during sample collection, the same outer layer was worn for each field visit throughout the sampling campaign, and fibre samples from personnel's clothing were taken as controls. Fibres matching these samples were excluded from the analysis.

All solutions were pre-filtered onto GF/D (2.7µm) glass-fibre filters. Equipment was cleaned with detergent and rinsed with DI-water before and between use. Glassware was placed in a sonification bath (GT sonic-D9) for 10 min for further cleaning. Personnel wore 100% cotton laboratory coats and non-synthetic clothes were preferred in the laboratory. Aluminium foil was used to cover samples during procedures. Two procedural blanks were run per surface water extraction batch (n_{total} = 16) using DI-water and one procedural sediment blank in an SMI-unit using clean $ZnCl_2$ (n_{total} = 11). All blanks were analysed following the same criteria as the original samples.

The 12 BB air background samples had 2 particles across the 12 samples, one clear in November 2021 and one clear March 2022. From the 12 EB air samples three contained one clear fragment each, indicating that air deposition was minimal at the sites at the time of collection. From the 11 sediment procedural blanks, one fragment was discovered and from the 16-surface water laboratory blanks no MP were detected. It was deemed that any contamination present would be negligible and extremely random and thus not reliably quantifiable.

From the chemical analysis it was found that 86.3% particles picked from EB were identified as plastics and 100% at BB, suggesting robust identification rate.

6.3.5 Data analysis

All statistics were carried out in RStudio (RStudio, Inc. R Core Team 2022) with significance threshold at $\alpha = 0.05$. All values for MP concentrations in water are reported as mean and standard deviation (SD), sediment concentrations are reported as measured values (MP Kg^{-1} dried sediment). The normality of all data was assessed with Shapiro-Wilk's test and non-parametric tests were applied where statistical assumptions required normal distribution.

When assessing differences between sediment MP concentrations and size distribution on individual sampling days an unpaired two-samples Wilcoxon test was applied. When assessing intra-variability within the datasets, Kruskal-Wallis tests were applied, followed by Dunn-test with the Benjamini-Hochberg Procedure to reduce false discovery rates. To assess any monthly based differences between the two sites, Kruskal-Wallis tests were performed.

When evaluating the effect of the average stream flow velocity, time from the last rainfall and stream discharge on mean size of MP, MP concentration or MP load, Pearson or Spearman rank coefficient was used to assess direction and strength of any correlation observed. Where the assumptions of a linear Regression model were met, a Linear Regression Model was fitted and R^2 and homoscedasticity of residuals was evaluated to further assess the goodness of the fit.

The MP loads were calculated as: $$L = C_t \times \sum Q_t$$

where $\boldsymbol{L}$ is the load (#MP s^{-1}), **C** is the concentration of MP in the surface water (MP L^{-1}), $\boldsymbol{Q}$ is the discharge (m^3 s^{-1}) and $\boldsymbol{t}$ is the time/date of the measurement. MP concentration was scaled to MP per m^3. For hourly load the L is adjusted by multiplying with 60 (seconds to minute) and the product multiplied with 60 (minutes to an hour).

6.4 Results

6.4.1 MP concentration in water column and sediment

MP were detected in all surface water and sediment samples across the two catchments and throughout all monthly sampling time steps over the year. The average MP concentration in surface water at the EB point source was 0.244 ± 0.104 MP L^{-1}, with a range of 0.14 - 0.55 MP L^{-1} and at the diffuse source BB 0.207 ± 0.101 MP L^{-1}, with range of 0.12 - 0.46 MP L^{-1} (Figure 6.3). There was no significant difference between the two sites in terms of their overall MP particle concentrations (chi-squared = 17.3, p = 0.366), however, a pair-wise Wilcoxon test suggested that July 2021 (p = 0.049), October 2021 (p = 0.049) and January 2022 (p = 0.046) exhibited higher MP concentrations in surface water at EB (point source) than at BB (diffuse source), while in February 2022 BB exhibited higher MP concentration (p = 0.049).

Inter date comparison, within each site, indicated that at the EB there was a significant difference in MP concentration in water between the sampling dates (Chi squared = 22.386, p = 0.021), and the Dunn test indicated that the month of July 2021 was significantly different from April (p = 0.038) and December (p = 0.041). At the BB, significant difference was also recorded (chi-squared = 19.878, p = 0.047), with the Dunn-test indicating that the surface water samples from February 2023 were different from all other months, with the exception of June (p = 0.166) and September 2021 (p = 0.626).

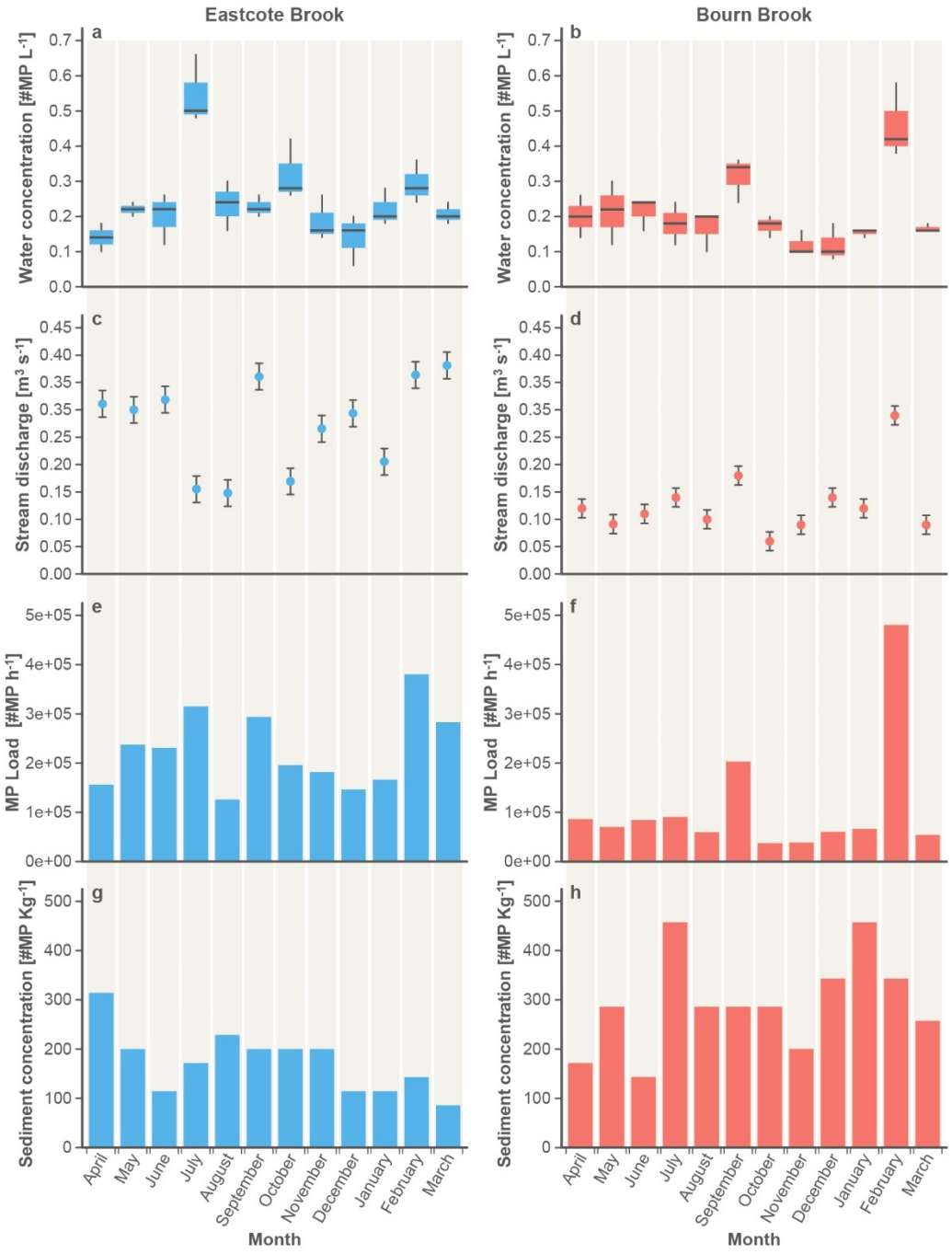


Figure 6.3: Surface water concentrations [#MP L^{-1}] (panels a-b), Stream discharge [m^3 s^{-1}] (panels c-d), MP load per hour [#MP h^{-1}] (panels e-f) and MP concentration in sediments [#MP Kg^{-1}] for Eastcote Brook (left column) and Bourn Brook (right column).

In the sediments, the MP concentration at EB was 174 ± 64 MP Kg^{-1} with a trend of higher concentration observed at BB which averaged 293 ± 98 MP Kg^{-1} (Figure 6.3), though the averages monthly values across the 12-month period were not significantly different (chi-squared = 16.1, p = 0.096). When MP concentration in sediments and MP comcentration in surface water were compared, no correlation was found for EB nor BB (Figure 6.4).

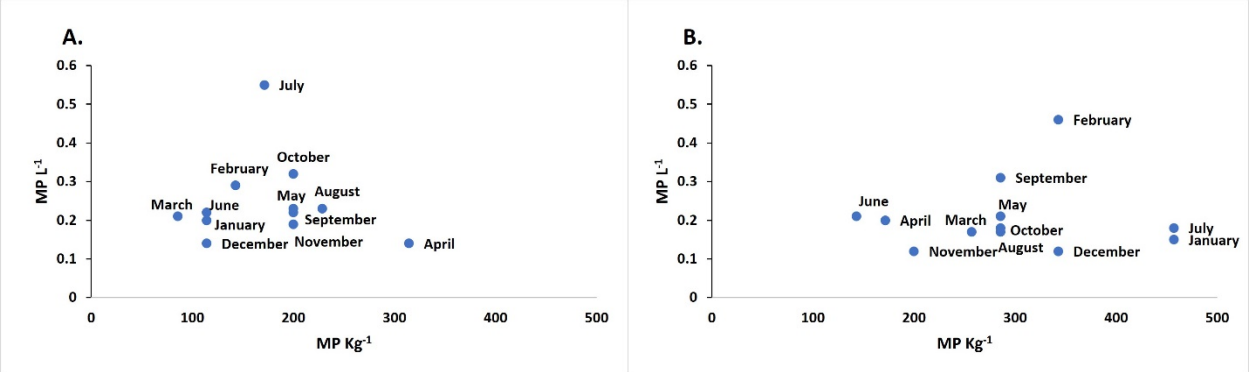


Figure 6.4. Surface water MP concentrations (MP L^{-1}) plotted against sediment MP concentrations (MP Kg^{-1}) for A) Eastcote Brook and B) Bourn Brook

6.4.2 Physical properties of identified MP

In surface water samples, a similar distribution of morphological properties was recorded across both sites: fibers made up 34.5% of total MP and fragments 65.5% at EB, while at BB, 28.7% of all MP were fibers and 71.3% were fragments (Appendix 5: Figure S6.2). No spheres were recorded. The average length of fibers in surface water samples was not significantly different between the two sites (chi-squared = 102.04, p = 0.424), with mean fiber length at EB 1133.2 µm and at BB 1279.5 µm).

The color of the identified fibers was also similar between both sites: Black dominated (38.2% at EB and 28.5% at BB), followed by clear/transparent (19.7% at EB and 27.6% at BB) and blue (17.1% at EB and 11.3% at BB) (Appendix 5: Figure S6.3).

There was no significant difference in the sizes of fragments between the two sites (chi-squared =193.78, p = 0.390) (Figure 6.5). The mean size for fragments at EB was 284.3 µm and 283.7 µm for BB. The dominant color of fragments at both sites was clear/transparent (75.7% at EB and 73.9% at BB). The second most common color recorded at EB was white (6.9%) and at BB was grey (5.7%) (Appendix 5: Figure S6.4).

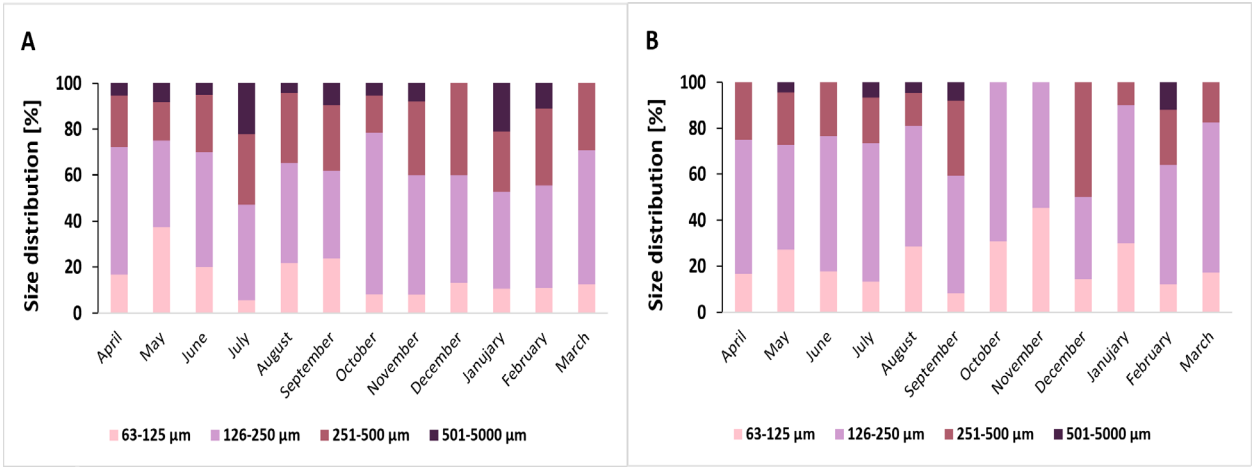


Figure 6.5: Size distribution of fragments in surface water for A) Eastcote Brook (EB) and B) Bourn Brook (BB). The size fraction buckets reflect standard sediment grain sizes.

From the EB sediments, only 0.5% of all MP were fibers (n = 4), with 99.5% being fragments. In BB sediments, fibers made up 17.5% (n = 22) of MP and fragments were 82.5%,

with no spheres found from either site. The average length of fibers was not significantly different between the sites in sediments (chi-squared = 3, p = 0.391), with an average of 1634.8 µm at EB and 1237.1 µm at BB. Blue was the most common color of fibers at EB (50%) and black at BB (30%), with grey and blue both making up 20% of total fibers at BB. Similarly, the mean size of fragments was not significantly different between the sites (chi-squared = 66.29, p = 0.466), with mean sizes of 257.4 µm at EB and 221.2 µm at BB (Figure 6.6). Clear/transparent was the most dominant colour of sediment-extracted fragments, constituting 63.8% of fragments at EB and 83.2% at BB (Appendix 5: Figure S6.5).

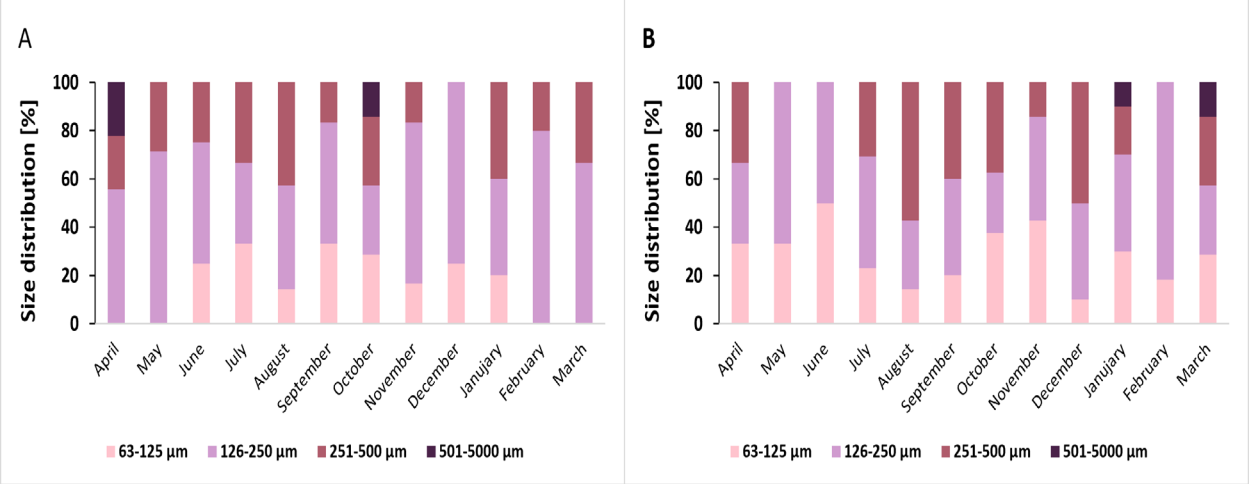


Figure 6.6: The size distribution of MP fragments recovered from sediment samples from A) Eastcote Brook (EB) and B) Bourn Brook (BB).

The mean MP sizes in sediment and overlying water were not correlated at either sampling site (Rs_{EB} = 0.006, p = 0.982, Rs_{BB} = -0.293, p = 0.354) (Figure 6.4). When the MP size distribution between sediments and surface waters were compared individually for each of the sampling dates

by sampling location, with unpaired two-samples Wilcoxon test, a significant difference was recorded only for February 2023 at the BB ($p = 0.007$), with the mean MP size in water being 333.9 µm and that in sediment being 152.6 µm. None of the other sampling dates at either site indicated any significant difference in MP sizes between sediments and surface water.

The chemical composition of MP, however, did differ between the two sites: For fragments, at EB, acrylic made the majority of identified fragments (40%), followed by polylactic acid (PLA) (15%) and Nylon (15%) (Figure 6.7). While the dominant polymers at BB were polyethylene (PE) (22%), followed by Nylon (18%), polyethylene terephthalate (PET) (18%) and polystyrene (PS) (18%). For fibres, the dominant polymer at EB was acrylic (27%), followed by PS (16%), PE (16%), PET (13%) and PLA (11%) (Figure 6.7). At BB, fibres were dominated by PET (26%) and polypropylene (PP) (26%), followed by PE (18%) and nylon (11%) (Figure 6.7).

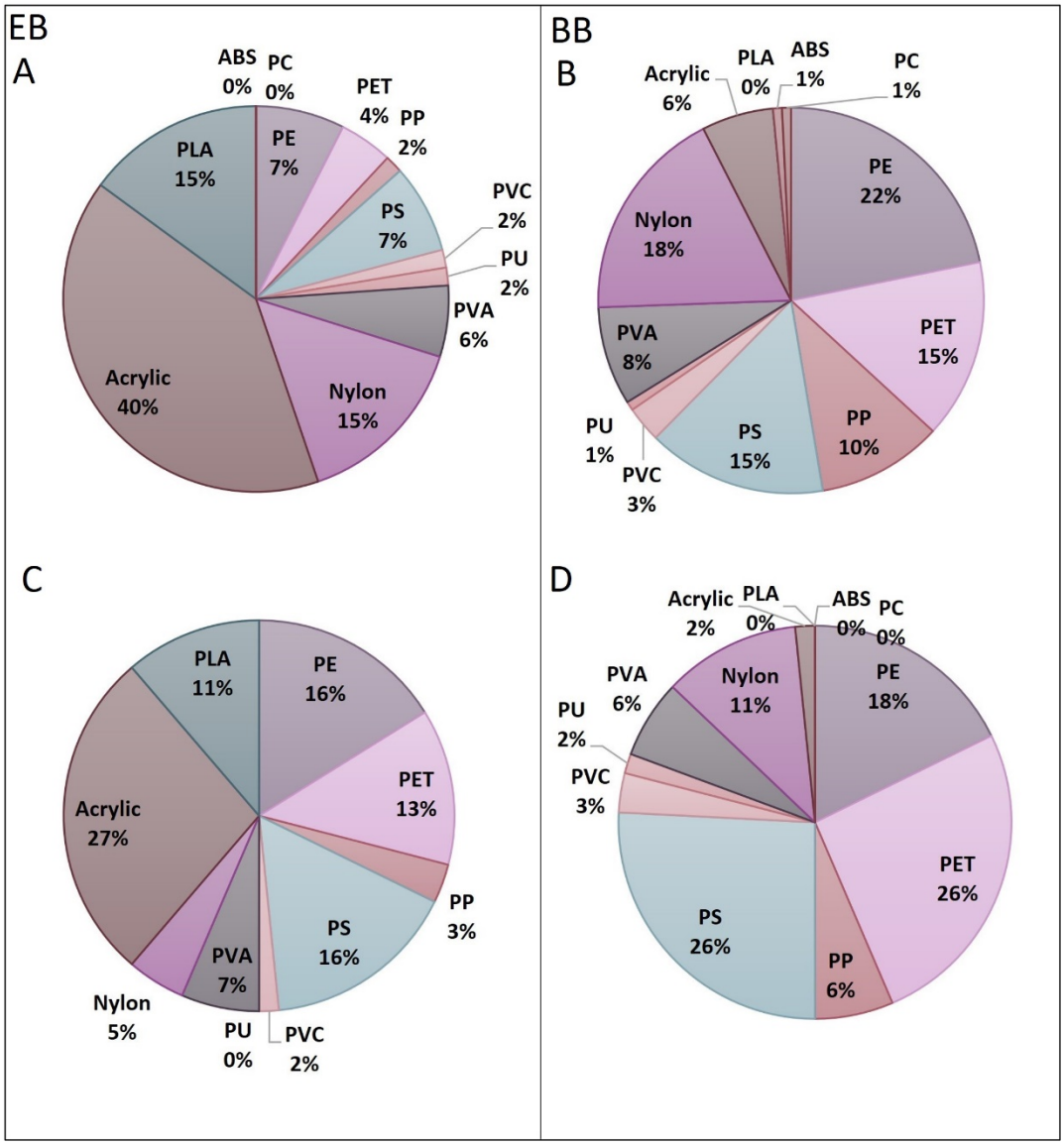


Figure 6.7: Chemical composition of Fragments (A-B) and fibres (C-D) identified at Eastcote Brook (EB) on the left and Bourn brook (BB) on the right.

6.4.3 Flow controls on MP concentrations

Stream discharge was generally lower at the BB than at the EB (Figure 6.3). The range for the EB was between 0.15 m^3 s^{-1} (August 2021) and 0.38 m^3 s^{-1} (March 2022), whereas at the BB the range was between 0.06 m^3 s^{-1} (October 2021) and 0.29 m^3 s^{-1} (February 2022). The annual

average stream discharge at the EB was 0.31 m^3 s^{-1} and 0.12 m^3 s^{-1} at the BB (Figure 6.3). MP concentrations in surface water were weakly correlated with stream discharge at the EB, but this relationship was not significant (Rs = -0.324, p = 0.053) (Figure S6.2), however, MP concentration in surface water was strongly correlated with discharge at BB (Rs = 0.749, p < 0.001) (Appendix 5: Figure S6.6). In sediments, the MP concentration was not correlated with stream discharge at the EB (Rs = -0.257, p = 0.418) or at the BB (Rs = 0.285, p = 0.367) (Appendix 5: Figure S6.7).

The average MP sizes in surface water were correlated with the discharge at the BB (Rs = 0.71, p = 0.009) but not at the EB (Rs = 0.08, p = 0.002) (Appendix 5: Figure S6.8). The average MP sizes in sediment were not correlated with discharge at either EB (Rs = 0.006, p = 0.845) or BB (Rs = 0.017, p = 0.956).

At EB the average MP load (calculated as product of discharge m^3 s^{-1} and MP concentration per m^3 and scaled to one hour) was 224,897 MP h^{-1} and had a range between 124,183 and 384,076 MP h^{-1}, while the average MP load at the BB was 111,014 MP h^{-1} with a range between 37,440 and 480,240 MP h^{-1}. The average load was higher at EB than at BB (Chi-squared = 9.72, p = 0.002) (Figure 6.8). The MP load h^{-1} in surface water was strongly correlated with MP concentration at the BB (p < 0.001, Figure 4A) and stream discharge (p < 0.001, Figure 4B) but this correlation was much weaker and non-significant at the EB (Figure 6.8).

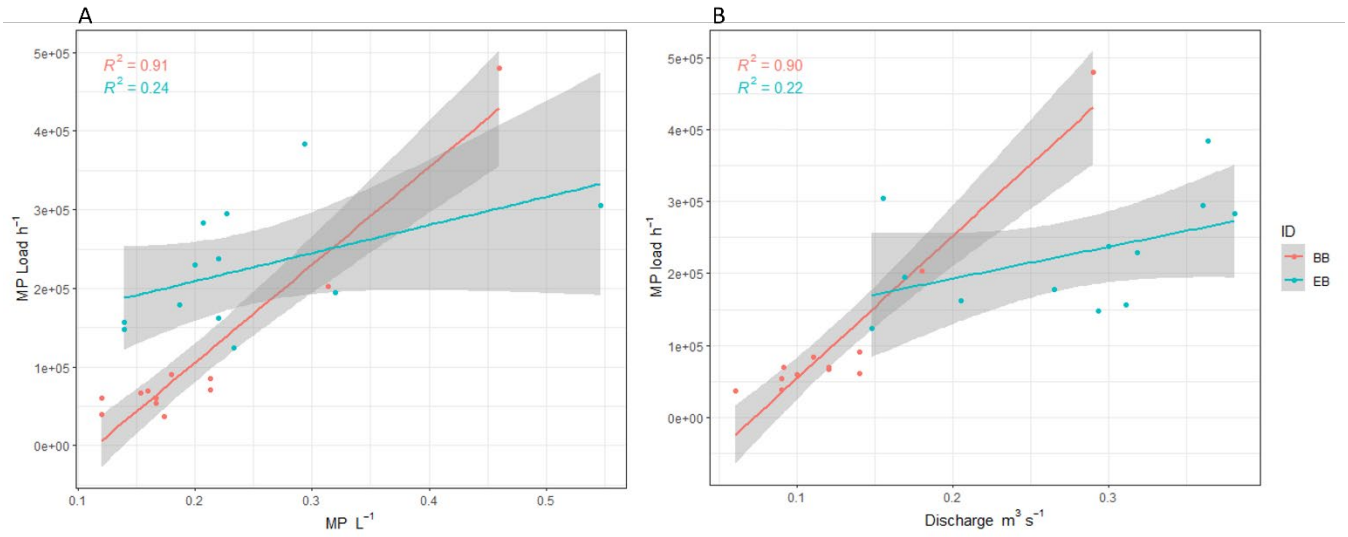


Figure 6.8: A) MP load per hour (MP h^{-1}) plotted against mean MP concentration in surface water, B) MP load (MP h^{-1}) plotted against stream discharge (m^3 s^{-1}) in surface water of Bourn Brook (BB) in red and Eastcote Brook (EB) in blue.

The average stream flow velocity at the sampling location at the EB was 0.146 m s^{-1} (range 0.079 - 0.465 m s^{-1}) and at the BB was 0.176 (range 0.050 - 0.303 m s^{-1}). The average stream velocity did not correlate with MP concentration in surface water at EB (Rs = -.101, p = 0.555), but did exhibit a strong correlation with MP concentration in the surface water at the BB (Rs=.726, $p < 0.001$) (Appendix 5: Figure S6.9). No correlation between average stream velocity and MP concentrations in sediments were found for EB (Rs = .077, p = 0.810) or BB (Rs =.057, p = 0.859) (Appendix 5: Figure S6.10).

MP sizes in surface water did not correlate with average velocity either at EB (Rs =.083, p = 0.002) or BB (Rs =.027, p = 0.659). MP sizes in sediments did not correlate with the average velocity in EB (Rs =.038, p = 0.744) or at BB (Rs =-.108, p = 0.233).

6.4.4 Impact of rain events

There was a weak negative correlation with stream discharge (m^3 s^{-1}) and number of days from the last rain event at the EB (Rs = -.318, p = 0.051) and a negative correlation at the BB (Rs= -.524, p = 0.001), with higher flows recorded closer to rain events at both sites.

There was no correlation between MP concentration in surface water and days from the last rain event at the EB (Rs =.333, p = 0.289). Conversely, a negative correlation was found between the time passed from last rain event and MP concentration in the water column at the BB (Rs = -.459, p = 0.004), however, no correlation between the rain events and MP concentration in sediments was found in samples from the BB (Rs = -.187, p = 0.559). Interestingly, a strong negative correlation was identified at the EB (Rs = -.643, p = 0.024) with higher sediment MP concentrations being recorded closer to rainfall events.

No correlation was found between the MP sizes and rain events in surface water at EB (Rs =.197, p < 0.001) or at BB (Rs =.120, p = 0.021). Only an extremely weak correlation was found between MP sizes in sediments and rain event at EB (Rs=-.236, p < 0.001) and none for samples from the BB (Rs =.015, p = 0.863).

6.5 Discussion

6.5.1 MP concentrations exhibit urban signal at both sampled sites with distinct MP compositions

MP were identified in all samples (surface water and sediment) collected from both locations across the whole temporal scale. The mean surface water MP concentration was 0.244 ±

0.104 MP L^{-1} at EB and 0.207 ± 0.101 MP L^{-1} at BB. Though the concentrations are lower than those reported from high-order rivers, (e.g., 1.6 - 187 MP L^{-1}) (Sekudewicz et al., 2021, Leslie et al., 2017) they are higher than previously reported from low-order streams in Slovenia (0.059 ± 0.016 MP L^{-1} > 150 μm) (Matjašič et al., 2023) and from the River Leen (0.083 ± 0.10 MP L^{-1} >63μm) and River Trent (0.075 ± 0.11 MP L^{-1} > 63μm) in the UK (Stanton et al., 2020). The sampling locations used by Stanton et al., (2020), were lower in anthropogenic activity than our site(s), signifying the effect of urbanization leading to generally higher MP concentrations. This is further supported by a recent study by Kukkola et al. (2023b/Chapter 4) where two catchments with similar hydrogeological properties but different degrees of urbanization were compared, which found that at the catchment with higher urbanization, surface water MP concentrations were roughly twice as high (0.22 ± 0.14 MP L^{-1} > 63 μm) as those determined in the less urbanised neighbouring catchment 0.09 ± 0.05 MP L^{-1} > 63 μm). This implies that the degree of urbanization can have an immediate effect on MP concentrations, even in low-order and headwater streams.

The mean MP concentration in sediment from the EB was 174 ± 64 MP Kg^{-1} and from the BB was 293 ± 98 MP Kg^{-1}. These concentrations are similar to what has been previously reported from urbanised rivers, such as the river Ganga (210.25 ± 124.65 MP Kg^{-1}, > 63 μm) (Sarkar et al., 2019) and the Rhine River (260 ± 100 to 11,070 ± 600 MP Kg^{-1}, > 11 μm) (Mani et al., 2019). They also align with the MP sediment concentrations recorded from the urban part of Boulder Creek, USA 186 ± 80 MP Kg^{-1} (> 63 μm) (Kukkola et al 2023b/Chapter 4) but are higher than those reported from small Auckland streams (9-80 MP Kg^{-1}, > 63 μm) (Dikareva and Simon, 2019). The MP concentrations measured here are, however, much lower than previously reported downstream of a WWTP, where up to 8,400 MP kg^{-1} sediment (> 64 μm) was reported ~600 m

downstream from a WWTP outlet (Margenat et al., 2021), however the WWTP was not the only MP source at the site and thus it is likely that long term accumulation from other sources affected the observed MP concentrations. However, since an insufficient number of studies have measured sediment MP concentrations immediately downstream from WWTPs to date, it is still to be determined if the MP concentrations observed in the present study, are typical ranges.

Despite the hydrological catchment of the EB being only 2.1 km^2 and mostly comprising horticulture land use, the MP concentrations in both compartments (surface water and sediment), exhibited a similar signal to that of the BB whose hydrological catchment is over eight times bigger and is mostly urbanized. This is likely related to the EB catchment having a much wider reach than its actual 'natural' hydrological catchment, as the WWTP releases the treated wastewater of ~62,500 people directly into the brook. Even with high MP removal efficiencies from WWTP of 95 – 99% (Liu et al., 2021, Wu et al., 2022, Shen et al., 2020, Blair et al., 2019), it is expected that some MP will be released in the effluent, especially in the smaller size scale and sewage related polymers (Reddy and Nair, 2022). This was supported by the chemical identification of the MP, which revealed distinct polymer compositions between the two sites: EB had higher occurrence of 'unconventional' polymers, such as acrylic and PLA, while BB had more 'traditional' MP profile, with common polymers, such as PE and PS being more commonly reported (Sun et al., 2019; Talbot and Chang, 2022). Acrylic may be used as flocculant at WWTPs (Arp and Knutsen, 2020; Salehizadeh et al., 2018; Vajihinejad et al., 2019) and in many household detergents (Arp and Knutsen, 2020), while PLA is a biopolymer, that has wide array of uses in sanitation products, such as in wet wipes, due to being perceived as "biodegradable" (Harter et al., 2021; Jem and Tan, 2020). The high presence of these polymers at the EB site therefore seems to indicate unique fingerprint

that can be directly linked to the WWTP. This suggests that it might be possible to use the occurrence of these polymers in higher amounts as signal of existence of WWTP within the catchment. However, further studies are needed to be carried out from the outflow of WWTPs with similar extraction methods, to verify whether these polymers are prominent also within other plant types.

Together these results entail that the MP loading of the EB site and consequently its receiver River Blythe is influenced by far larger area than its 'natural' catchment area, and in fact, such sites cannot be measured by their actual hydrological catchment properties, which are overshadowed by the water management activities and the existence of the point-source, which dominates and controls the MP concentration at this location. This is something that needs to be considered when MP sources and MP fluxes are being estimated at urban areas, when natural flow networks are complemented by anthropogenic water management, as this can lead to misinterpretations of MP hot-spots and skew our understanding of the relative importance of diffuse/point sources if sufficient care to understand the complexities is not taken.

6.5.2 MP load controlled by source at EB and by source activation at BB

Though stream discharge has been previously linked to MP concentrations downstream from WWTPs (Mintenig et al., 2020, Schell et al., 2021, Watkins et al., 2019), no correlation was found between the discharge and MP concentrations or sizes in the surface water or in sediments from the EB. For instance, stream discharge has been linked to higher MP concentration in surface water downstream from WWTPs, with elevated MP concentrations reported for both high stream discharge (55-500 µm) (Schell et al., 2021) and low stream discharge leading (> 335 µm) (Watkins et al., 2019). However, in these studies WWTP effluent contribution to the total flow was either

not assessed or at maximum was reported to contribute only up to 3% of the total volume of the river. In the present study, essentially all the stream discharge was considered to originate from the WWTP, and it is likely that the MP concentrations recorded at the EB were due to fluctuating MP concentration in the WWTP discharge (Chapter 5) and therefore MP concentrations in the surface water and sediment at EB are expected to be driven by the release of MP from this single source (release of effluent), rather than by the discharge (the overall stream flow rate).

The MP load observed at our point source was not correlated with either the stream discharge or with the MP concentration in the surface water (Figure 6.7). The MP load could be determined by both discharge (m^3 s^{-1}) and MP concentration in water, either individually or in tandem, and exhibited high temporal variability at this site. Some months, such as February and March 2022, exhibited high MP loads (Figure 6.3), which coincided with both high stream discharge, as well as high MP concentrations. However, the second highest month in terms of MP load was in July 2021 (305,136 MP h^{-1}) and was purely driven by MP concentration (0.55 MP L^{-1}), as the discharge at this time was the second lowest measured during the year (0.155 m^3 s^{-1}) (Figure 6.3). Rain events, while not being correlated with surface water MP concentrations or MP loads, exhibited weak positive correlation with the stream discharge at the EB (confirming that the effluent releases from the WWTP were the main driver of EB stream discharge) and higher MP concentrations from sediments were recorded closer to rain events. It is possible that during rain events the extremely pronounced water-level change arising from the periodic effluent releases gets muffled, which could lead to more settling taking place during periods of rainfall. This suggests that while the EB site exhibits high diversity in MP loading, this is solely linked to the varied and highly diverse outputs from the WWTP and are thus controlled by water management.

Conversely, at the BB, stream discharge exhibited a strong positive correlation with MP concentration in surface water. MP concentrations in surface water of urban rivers have previously been linked to changes in stream discharge with both low and high flow conditions associated with higher MP concentrations (Chen et al., 2021, Kapp and Yeatman, 2018, Xiong et al., 2019). It has been hypothesized that the increase of MP concentrations during low discharge could reflect the accumulation of MP in slow moving waters (Kapp and Yeatman, 2018, Xiong et al., 2019), however, this type of accumulation during low discharge did not occur at our site. Another hypothesis that has been put forward for increased MP concentrations in surface water during high stream discharge conditions, is that this might reflect the resuspension of MP from the stream sediments due to turbulence from high flow, rather than new MP entering the stream from the catchment due to runoff (Chen et al., 2021). However, here no relationship was observed between the MP concentration in surface water and sediments, nor between the discharge and MP concentration in sediments at BB, suggesting that the increase in MP concentrations in surface water in the BB was the direct result of new MP entering the stream.

The MP loads in surface water were also highly correlated with both the stream discharge and MP concentration, indicating a strong hydrological MP transport mechanism at the BB (Figure 6.7). The data suggest that higher discharges were linked to the time since the last rain event, demonstrating hydrometeorological activation of the MP sources at the BB catchment. This means that during dry periods, MP will accumulate in the paved/urban catchment, and will then be activated during rainfall within the catchment, resulting in their release into the stream as road run-off, resulting in higher stream discharge. This type of source activation and MP concentration increase due to surface run-off has been reported previously (Hitchcock, 2020, Sun et al., 2023,

Cheung et al., 2019, Piñon-Colin et al., 2020) and is supported by the fact that sediment MP concentrations were not correlated with the rain events, nor with the discharge, suggesting that despite high flows and high MP concentrations in the overlaying water, no significant settling nor resuspension occurred at the site and the increased MP in water column was introduced into the stream from, other external sources.

It should be noted that our sampling took place a minimum of 15 hours after the last rain event, suggesting that what was observed at the time of sampling might not have been descriptive of what occurs in the stream during the actual rain events, and that MP loads may have been significantly higher during the rain event. It has previously been shown that the highest MP concentrations during rain events are likely to occur during the rising limb of the hydrograph (Cheung et al., 2019, Sun et al., 2023) as is often the case with other pollutants (Lee et al., 2007). This is likely to be the case at the BB, as the catchment itself is highly urbanized, with 70% of the total area being suburban or urban, and this type of land-use is also linked to higher MP concentrations in its run-off (Piñon-Colin et al., 2020). It is therefore highly likely that during the rain events the MP load might easily rise over 480,000 MP h^{-1} at BB, which was the highest MP load observed in this study, which occurred at BB during the recorded high loading events in February 2022. However, though the rain event signal was captured here, our study was not designed to measure the effects of runoff or rainfall, and therefore further studies would be required at the site to understand and characterize how the MP concentration and MP loads change in relation to rain event type or duration, and whether different events have different mobilization effects on MP.

6.6. Conclusions

A pairwise comparison of two semi-urban streams, one representing a point source (a WWTP) and the other representing a diffuse source (mainly road run-off), over a 12-monthly sampling campaign revealed that both sites exhibited similar MP concentrations in surface water and sediments, with the point source having an urban signature despite its small hydrological catchment size. This suggests that catchment size should be used as an indicator of the sources if water management activities (such as the WWTP) occur within its boundaries. The point source also presented higher MP loading than the diffuse source, which was driven by complex WWTP outputs, where both MP concentration and discharge resulted in high MP loads being transported downstream.

At the diffuse source, dry periods saw relatively stable MP input to the stream. Rain events, by contrast, activated and mobilized additional sources from the catchment, which were then flushed into the stream creating "intense pollution moments" for MP pollution in the stream. The data suggests that, while a point source discharges higher MP pollution loads downstream during dry periods, the diffuse source can become much more important for downstream transport during and after rain events. At the diffuse source site assessed here (the BB), the MP load is directly correlated to both discharge (measured as rainfall amount) and MP concentration and the MP load was much more predictable than that of the point source (the WWTP) in its MP output (to the EB).

These results highlight how complex urban MP sources, and their transport, can be, as one single source can dominate the MP concentration and MP loads in a catchment, whereas hydrometeorological activation mechanisms can also play a crucial part in urban areas leading to bursts of MP input due to source activation. The important message for researchers, policy makers

and those responsible for environment monitoring for MP is the need to fully understand the system being studied, and that mapping of potential MP input sources is not sufficient, as there needs to be fundamental understanding of how these sources are activated and how this affects the downstream transport of MP in the specific catchment context.

Future studies should be conducted with both point and diffuse sources located in the same catchment, and with higher resolution data collected prior during and after rainfall events to determine how MP concentrations and loads respond upstream and immediately downstream from a point source and from diffuse sources to changes in rainfall, as this will allow better understanding of how these two sources contribute to MP loading downstream, when located in close proximity.

6.7 References

ANBUMANI, S. & KAKKAR, P. 2018. Ecotoxicological effects of microplastics on biota: a review. *Environmental Science and Pollution Research,* 25**,** 14373-14396.

ARP, H. P. H. & KNUTSEN, H. 2020. Could We Spare a Moment of the Spotlight for Persistent, Water-Soluble Polymers? Environmental Science & Technology, 54, 3-5.

ATEIA, M., ERSAN, G., ALALM, M. G., BOFFITO, D. C. & KARANFIL, T. 2022. Emerging investigator series: microplastic sources, fate, toxicity, detection, and interactions with micropollutants in aquatic ecosystems – a review of reviews. *Environmental Science: Processes & Impacts,* 24**,** 172-195.

BANK, M. S. & HANSSON, S. V. 2022. The microplastic cycle: An introduction to a complex issue. *Microplastic in the Environment: Pattern and Process***,** 1-16.

BERGMANN, M., COLLARD, F., FABRES, J., GABRIELSEN, G. W., PROVENCHER, J. F., ROCHMAN, C. M., VAN SEBILLE, E. & TEKMAN, M. B. 2022. Plastic pollution in the Arctic. *Nature Reviews Earth & Environment,* 3**,** 323-337.

BLAIR, R. M., WALDRON, S. & GAUCHOTTE-LINDSAY, C. 2019. Average daily flow of microplastics through a tertiary wastewater treatment plant over a ten-month period. *Water Research,* 163**,** 114909.

BOND, C., LI, H. & RATE, A. W. 2022. Land Use Pattern Affects Microplastic Concentrations in Stormwater Drains in Urban Catchments in Perth, Western Australia. *Land* [Online], 11.

CAMPANALE, C., GALAFASSI, S., SAVINO, I., MASSARELLI, C., ANCONA, V., VOLTA, P. & URICCHIO, V. F. 2022. Microplastics pollution in the terrestrial environments: Poorly known diffuse sources and implications for plants. *Science of The Total Environment,* 805**,** 150431.

CAMPANALE, C., STOCK, F., MASSARELLI, C., KOCHLEUS, C., BAGNUOLO, G., REIFFERSCHEID, G. & URICCHIO, V. F. 2020. Microplastics and their possible sources: The example of Ofanto river in southeast Italy. *Environmental Pollution,* 258**,** 113284.

CARSTEA, E. M., BAKER, A., BIEROZA, M. & REYNOLDS, D. 2010. Continuous fluorescence excitation–emission matrix monitoring of river organic matter. *Water Research,* 44**,** 5356-5366.

CHEN, H. L., GIBBINS, C. N., SELVAM, S. B. & TING, K. N. 2021. Spatio-temporal variation of microplastic along a rural to urban transition in a tropical river. *Environmental Pollution,* 289**,** 117895.

CHEUNG, P. K., HUNG, P. L. & FOK, L. 2019. River Microplastic Contamination and Dynamics upon a Rainfall Event in Hong Kong, China. *Environmental Processes,* 6**,** 253-264.

CRISTALDI, A., FIORE, M., ZUCCARELLO, P., OLIVERI CONTI, G., GRASSO, A., NICOLOSI, I., COPAT, C. & FERRANTE, M. 2020. Efficiency of Wastewater Treatment Plants (WWTPs) for Microplastic Removal: A Systematic Review. *International Journal of Environmental Research and Public Health* [Online], 17.

DAI, L., WANG, Z., GUO, T., HU, L., CHEN, Y., CHEN, C., YU, G., MA, L. Q. & CHEN, J. 2022. Pollution characteristics and source analysis of microplastics in the Qiantang River in southeastern China. *Chemosphere,* 293**,** 133576.

DE CARVALHO, A. R., GARCIA, F., RIEM-GALLIANO, L., TUDESQUE, L., ALBIGNAC, M., TER HALLE, A. & CUCHEROUSSET, J. 2021. Urbanization and hydrological conditions drive the spatial and temporal variability of microplastic pollution in the Garonne River. *Science of The Total Environment,* 769**,** 144479.

DHIVERT, E., PHUONG, N. N., MOURIER, B., GROSBOIS, C. & GASPERI, J. 2022. Microplastic trapping in dam reservoirs driven by complex hydrosedimentary processes (Villerest Reservoir, Loire River, France). *Water Research,* 225**,** 119187.

DIKAREVA, N. & SIMON, K. S. 2019. Microplastic pollution in streams spanning an urbanisation gradient. *Environmental Pollution,* 250**,** 292-299.

DRUMMOND, J. D., NEL, H. A., PACKMAN, A. I. & KRAUSE, S. 2020. Significance of Hyporheic Exchange for Predicting Microplastic Fate in Rivers. *Environmental Science & Technology Letters,* 7**,** 727-732.

DRUMMOND, J. D., SCHNEIDEWIND, U., LI, A., HOELLEIN, T. J., KRAUSE, S. & PACKMAN, A. I. 2022. Microplastic accumulation in riverbed sediment via hyporheic exchange from headwaters to mainstems. *Science Advances,* 8**,** eabi9305.

ESTAHBANATI, S. & FAHRENFELD, N. L. 2016. Influence of wastewater treatment plant discharges on microplastic concentrations in surface water. *Chemosphere,* 162**,** 277-284.

EVANGELIOU, N., GRYTHE, H., KLIMONT, Z., HEYES, C., ECKHARDT, S., LOPEZ-APARICIO, S. & STOHL, A. 2020. Atmospheric transport is a major pathway of microplastics to remote regions. *Nature Communications,* 11**,** 3381.

GESAMP 2016. SOURCES, FATE AND EFFECTS OF MICROPLASTICS IN THE MARINE ENVIRONMENT: PART TWO OF A GLOBAL ASSESSMENT. *In:* KERSHAW P.J., A. R., C.M (ed.). GESAMP Working Group 40 2nd phase. London: IMO/FAO/UNESCO-IOC/UNIDO/WMO/IAEA/UN/UNEP/UNDP Joint Group of Experts on the Scientific Aspects of Marine Environmental Protection.

HARTER, T., BERNT, I., WINKLER, S. & HIRN, U. 2021. Reduced dispersibility of flushable wet wipes after wet storage. Scientific Reports, 11, 7942.

HARTMANN, N. B., HÜFFER, T., THOMPSON, R. C., HASSELLÖV, M., VERSCHOOR, A., DAUGAARD, A. E., RIST, S., KARLSSON, T., BRENNHOLT, N., COLE, M., HERRLING, M. P., HESS, M. C., IVLEVA, N. P., LUSHER, A. L. & WAGNER, M. 2019. Are We Speaking the Same Language? Recommendations for a Definition and Categorization Framework for Plastic Debris. *Environmental Science & Technology,* 53**,** 1039-1047.

HITCHCOCK, J. N. 2020. Storm events as key moments of microplastic contamination in aquatic ecosystems. *Science of The Total Environment,* 734**,** 139436.

HORTON, A. A. & DIXON, S. J. 2018. Microplastics: An introduction to environmental transport processes. *WIREs Water,* 5**,** e1268.

HORTON, A. A., WALTON, A., SPURGEON, D. J., LAHIVE, E. & SVENDSEN, C. 2017. Microplastics in freshwater and terrestrial environments: Evaluating the current understanding to identify the knowledge gaps and future research priorities. *Science of The Total Environment,* 586**,** 127-141.

HURLEY, R., WOODWARD, J. & ROTHWELL, J. J. 2018. Microplastic contamination of river beds significantly reduced by catchment-wide flooding. *Nature Geoscience,* 11**,** 251-257.

IYARE, P. U., OUKI, S. K. & BOND, T. 2020. Microplastics removal in wastewater treatment plants: a critical review. *Environmental Science: Water Research & Technology,* 6**,** 2664-2675.

JEM, K. J. & TAN, B. 2020. The development and challenges of poly (lactic acid) and poly (glycolic acid). Advanced Industrial and Engineering Polymer Research, 3, 60-70.

KAPP, K. J. & YEATMAN, E. 2018. Microplastic hotspots in the Snake and Lower Columbia rivers: A journey from the Greater Yellowstone Ecosystem to the Pacific Ocean. *Environmental Pollution,* 241**,** 1082-1090.

KELLEHER, L., SCHNEIDEWIND, U., KRAUSE, S., HAVERSON, L., ALLEN, S., ALLEN, D., KUKKOLA, A., MURRAY-HUDSON, M., MASELLI, V. & FRANCHI, F. 2023. Microplastic accumulation in endorheic river basins – The example of the Okavango Panhandle (Botswana). Science of The Total Environment, 874, 162452.

KHAMIS, K., BRADLEY, C., STEVENS, R. & HANNAH, D. M. 2017. Continuous field estimation of dissolved organic carbon concentration and biochemical oxygen demand using dual-wavelength fluorescence, turbidity and temperature. *Hydrological Processes,* 31**,** 540-555.

KRAUSE, S., BARANOV, V., NEL, H. A., DRUMMOND, J. D., KUKKOLA, A., HOELLEIN, T., SAMBROOK SMITH, G. H., LEWANDOWSKI, J., BONET, B., PACKMAN, A. I., SADLER, J., INSHYNA, V., ALLEN, S., ALLEN, D., SIMON, L., MERMILLOD-BLONDIN, F. & LYNCH, I. 2021. Gathering at the top? Environmental controls of microplastic uptake and biomagnification in freshwater food webs. *Environmental Pollution,* 268**,** 115750.

KUKKOLA, A., KRAUSE, S., LYNCH, I., SAMBROOK SMITH, G. H. & NEL, H. 2021. Nano and microplastic interactions with freshwater biota – Current knowledge, challenges and future solutions. *Environment International,* 152**,** 106504.

KUKKOLA, A., KRAUSE, S., YONAN, Y., KELLEHER, L., SCHNEIDEWIND, U., SMITH, G. H. S., NEL, H. & LYNCH, I. 2023a. Easy and accessible way to calibrate a fluorescence microscope and to create a microplastic identification key. MethodsX, 10, 102053

KUKKOLA, A., RUNKEL, R., CHNEIDEWIND, U., MURPHY, S., KELLEHER, L., S SMITH, G. H. S., NEL, H. & LYNCH, I. KRAUSE, S., 2023b. Prevailing impacts of river management on microplastic transport in contrasting US streams requires rethinking of global microplastic flux estimations. (IN PRESS)

KUKKOLA, A. T., SENIOR, G., MAES, T., SILBURN, B., BAKIR, A., KRÖGER, S. & MAYES, A. G. 2022. A large-scale study of microplastic abundance in sediment cores from the UK continental shelf and slope. *Marine Pollution Bulletin,* 178**,** 113554.

LEE, H., SWAMIKANNU, X., RADULESCU, D., KIM, S.-J. & STENSTROM, M. K. 2007. Design of stormwater monitoring programs. *Water Research,* 41**,** 4186-4196.

LESLIE, H. A., BRANDSMA, S. H., VAN VELZEN, M. J. M. & VETHAAK, A. D. 2017. Microplastics en route: Field measurements in the Dutch river delta and Amsterdam canals, wastewater treatment plants, North Sea sediments and biota. *Environment International,* 101**,** 133-142.

LIU, W., ZHANG, J., LIU, H., GUO, X., ZHANG, X., YAO, X., CAO, Z. & ZHANG, T. 2021. A review of the removal of microplastics in global wastewater treatment plants: Characteristics and mechanisms. *Environment International,* 146**,** 106277.

MANI, T., PRIMPKE, S., LORENZ, C., GERDTS, G. & BURKHARDT-HOLM, P. 2019. Microplastic Pollution in Benthic Midstream Sediments of the Rhine River. *Environmental Science & Technology,* 53**,** 6053-6062.

MARGENAT, H., NEL, H. A., STONEDAHL, S. H., KRAUSE, S., SABATER, F. & DRUMMOND, J. D. 2021. Hydrologic controls on the accumulation of different sized microplastics in the streambed sediments downstream of a wastewater treatment plant (Catalonia, Spain). *Environmental Research Letters,* 16**,** 115012.

MARGENAT, H., NEL, H.A., STONEDAHL, S.H., KRAUSE, S., SABATER, F., DRUMMOND, J.D. 2021. Hydrologic controls on the accumulation of different sized microplastics in the streambed sediments downstream of a wastewater treatment plant (Catalonia, Spain). *Environmental Research Letters,* 16.

MATJAŠIČ, T., MORI, N., HOSTNIK, I., BAJT, O. & KOVAČ VIRŠEK, M. 2023. Microplastic pollution in small rivers along rural–urban gradients: Variations across catchments and between water column and sediments. *Science of The Total Environment,* 858**,** 160043.

MENG, Y., KELLY, F. J. & WRIGHT, S. L. 2020. Advances and challenges of microplastic pollution in freshwater ecosystems: A UK perspective. *Environmental Pollution,* 256**,** 113445.

MINTENIG, S. M., KOOI, M., ERICH, M. W., PRIMPKE, S., REDONDO- HASSELERHARM, P. E., DEKKER, S. C., KOELMANS, A. A. & VAN WEZEL, A. P. 2020. A systems approach to understand microplastic occurrence and variability in Dutch riverine surface waters. *Water Research,* 176**,** 115723.

PETERS, C. A. & BRATTON, S. P. 2016. Urbanization is a major influence on microplastic ingestion by sunfish in the Brazos River Basin, Central Texas, USA. *Environmental Pollution,* 210**,** 380-387.

PIÑON-COLIN, T. D. J., RODRIGUEZ-JIMENEZ, R., ROGEL-HERNANDEZ, E., ALVAREZ-ANDRADE, A. & WAKIDA, F. T. 2020. Microplastics in stormwater runoff in a semiarid region, Tijuana, Mexico. *Science of The Total Environment,* 704**,** 135411.

REDDY, A. S. & NAIR, A. T. 2022. The fate of microplastics in wastewater treatment plants: An overview of source and remediation technologies. *Environmental Technology & Innovation,* 28**,** 102815.

SALEHIZADEH, H., YAN, N. & FARNOOD, R. 2018. Recent advances in polysaccharide bio-based flocculants. Biotechnology Advances, 36, 92-119.

SAMANDRA, S., JOHNSTON, J. M., JAEGER, J. E., SYMONS, B., XIE, S., CURRELL, M., ELLIS, A. V. & CLARKE, B. O. 2022. Microplastic contamination of an unconfined groundwater aquifer in Victoria, Australia. *Science of The Total Environment,* 802**,** 149727.

SARKAR, D. J., DAS SARKAR, S., DAS, B. K., MANNA, R. K., BEHERA, B. K. & SAMANTA, S. 2019. Spatial distribution of meso and microplastics in the sediments of river Ganga at eastern India. *Science of The Total Environment,* 694**,** 133712.

SCHELL, T., HURLEY, R., NIZZETTO, L., RICO, A. & VIGHI, M. 2021. Spatio-temporal distribution of microplastics in a Mediterranean river catchment: The importance of wastewater as an environmental pathway. *Journal of Hazardous Materials,* 420**,** 126481.

SEKUDEWICZ, I., DĄBROWSKA, A. M. & SYCZEWSKI, M. D. 2021. Microplastic pollution in surface water and sediments in the urban section of the Vistula River (Poland). *Science of The Total Environment,* 762**,** 143111.

SHEN, M., SONG, B., ZHU, Y., ZENG, G., ZHANG, Y., YANG, Y., WEN, X., CHEN, M. & YI, H. 2020. Removal of microplastics via drinking water treatment: Current knowledge and future directions. *Chemosphere,* 251**,** 126612.

SHIM, W. J., SONG, Y. K., HONG, S. H. & JANG, M. 2016. Identification and quantification of microplastics using Nile Red staining. Marine Pollution Bulletin, 113, 469-476.

STANTON, T., JOHNSON, M., NATHANAIL, P., GOMES, R. L., NEEDHAM, T. & BURSON, A. 2019. Exploring the Efficacy of Nile Red in Microplastic Quantification: A Costaining Approach. Environmental Science & Technology Letters, 6, 606-611.

STANTON, T., JOHNSON, M., NATHANAIL, P., MACNAUGHTAN, W. & GOMES, R. L. 2020. Freshwater microplastic concentrations vary through both space and time. *Environmental Pollution,* 263**,** 114481.

SUN, J., DAI, X., WANG, Q., VAN LOOSDRECHT, M. C. M. & NI, B.-J. 2019. Microplastics in wastewater treatment plants: Detection, occurrence and removal. Water Research, 152, 21-37.

SUN, T., ZHAN, J., LI, F., JI, C. & WU, H. 2021. Environmentally relevant concentrations of microplastics influence the locomotor activity of aquatic biota. *Journal of Hazardous Materials,* 414**,** 125581.

SUN, X., JIA, Q., YE, J., ZHU, Y., SONG, Z., GUO, Y. & CHEN, H. 2023. Real-time variabilities in microplastic abundance and characteristics of urban surface runoff and sewer overflow in wet weather as impacted by land use and storm factors. *Science of The Total Environment,* 859**,** 160148.

TALBOT, R. & CHANG, H. 2022. Microplastics in freshwater: A global review of factors affecting spatial and temporal variations. Environmental Pollution, 292, 118393.

THOMPSON, R. C., OLSEN, Y., MITCHELL, R. P., DAVIS, A., ROWLAND, S. J., JOHN, A. W. G., MCGONIGLE, D. & RUSSELL, A. E. 2004. Lost at Sea: Where Is All the Plastic? *Science,* 304**,** 838-838.

TRIEBSKORN, R., BRAUNBECK, T., GRUMMT, T., HANSLIK, L., HUPPERTSBERG, S., JEKEL, M., KNEPPER, T. P., KRAIS, S., MÜLLER, Y. K., PITTROFF, M., RUHL, A. S., SCHMIEG, H., SCHÜR, C., STROBEL, C., WAGNER, M., ZUMBÜLTE, N. & KÖHLER, H.-R. 2019. Relevance of nano- and microplastics for freshwater ecosystems: A critical review. *TrAC Trends in Analytical Chemistry,* 110**,** 375-392.

VAJIHINEJAD, V., GUMFEKAR, S. P., BAZOUBANDI, B., ROSTAMI NAJAFABADI, Z. & SOARES, J. B. P. 2019. Water Soluble Polymer Flocculants: Synthesis, Characterization, and Performance Assessment. Macromolecular Materials and Engineering, 304, 1800526.

WANG, T., WANG, J., LEI, Q., ZHAO, Y., WANG, L., WANG, X. & ZHANG, W. 2021. Microplastic pollution in sophisticated urban river systems: Combined influence of land-use types and physicochemical characteristics. *Environmental Pollution,* 287**,** 117604.

WATKINS, L., SULLIVAN, P. J. & WALTER, M. T. 2019. A case study investigating temporal factors that influence microplastic concentration in streams under different treatment regimes. *Environmental Science and Pollution Research,* 26**,** 21797-21807.

WU, X., ZHAO, X., CHEN, R., LIU, P., LIANG, W., WANG, J., TENG, M., WANG, X. & GAO, S. 2022. Wastewater treatment plants act as essential sources of microplastic formation in aquatic environments: A critical review. *Water Research,* 221**,** 118825.

XIONG, X., WU, C., ELSER, J. J., MEI, Z. & HAO, Y. 2019. Occurrence and fate of microplastic debris in middle and lower reaches of the Yangtze River – From inland to the sea. *Science of The Total Environment,* 659**,** 66-73.

XU, C., ZHANG, B., GU, C., SHEN, C., YIN, S., AAMIR, M. & LI, F. 2020. Are we underestimating the sources of microplastic pollution in terrestrial environment? *Journal of Hazardous Materials,* 400**,** 123228.

YUAN, W., CHRISTIE-OLEZA, J. A., XU, E. G., LI, J., ZHANG, H., WANG, W., LIN, L., ZHANG, W. & YANG, Y. 2022. Environmental fate of microplastics in the world's third-largest river: Basin-wide investigation and microplastic community analysis. *Water Research,* 210**,** 118002.

Chapter 7: Conclusions and discussion

The work presented here aimed to uncover some key mechanisms affecting the activation of MP sources, their transport and connectivity and hence, distribution of MP in river systems of different degrees of urbanisation. It therefore developed fast and reliable methodologies for MP detection and quantification and applied the developed methods to samples collected from three different urban river systems. The thesis also includes a comprehensive literature review aiming to understand the requirements that MP effects studies in the laboratory needs to fulfil to reflect more closely field studies, and what type of data field studies need to report to better aid the effect study designs. The work presented in this thesis underlines how important it is to fully characterise the flow regimens and identify any water management operations/structures in the system being studied, prior to and during conducting field work for MP sampling.

The literature synthesis revealed evidence of a significant mismatch between field and laboratory studies in terms of the MP compositions and shapes being studied relative to those actually present in the environment, highlighting a significant gap in our knowledge on how the most common morphology of MP might affect freshwater species. It was found that more comprehensive reporting from the field is required to inform lab-scale ecotoxicity testing. The development of an advanced MP detection method was successful, demonstrating that fluorescence detection limits for Nile Red combined with a pre-set MP identification key, provided a reliable, fast, and transparent tool for basic MP identification and quantification.

For the first research objective, where the aim was to obtain better understanding of the magnitude of impact of the degree of urbanization and water management on MP distribution, it

was found that while the degree of urbanization has a distinct signal in terms of MP concentrations and loads, it is critically important to record stream discharge at the time of sampling, as well as to include sampling of any possible water management constructions present in the river system to understand their impact on the MP loadings. Here, the loading analysis often used for other types of pollutants (e.g., metals) was used to quantify the changes of MP loads between river segments, providing a powerful approach for conducting longitudinal spatial MP source estimations. This approach, when applied to a river segment with a water diversion, also enabled the quantification of MP that is being diverted from the original river system, for agricultural or potable water purposes. It was found that, even in a low-order mountainous stream, over 1.8×10^5 MP were diverted per hour, with likely much higher MP numbers diverted from high order streams, highlighting the importance of measuring not only the MP concentrations, but also the stream discharge when sampling for MP. These results clearly demonstrate that water management can have substantial implications for MP load estimations and should be taken into consideration for quantification of catchment residence times of MP and river network contributions to the oceans. The loading analysis is a valuable tool, that ought to be used in future MP river studies, when MP sources are being estimated, and as such has been made available to the community as part of the resulting manuscript.

For the second research objective, where the effectiveness of snap-shot sampling downstream of sewage treatment works as the only MP source was assessed, a high variability in MP loads was found, which was driven by two different mechanisms, MP concentration in wastewater effluent or variation in stream discharge ($m^3\ s^{-1}$) or a combination of both. Our results point at the fact that MP concentrations in the effluent were not consistent at the site and depending

on the time of the day that sampling has occurred, a significant difference in the annual emission estimations could have been obtained. Notably, sampling at a fixed timepoint on each sampling date (e.g., between 9-11 am) did not address this variability fully, as the sub-daily sampling revealed that the difference could be as much as 214,428 MP in just one hour at these respective times. It was also uncovered that the MP concentration was not correlated with the stream discharge nor MP load. In fact, the observed spatial patterns and temporal dynamics of MP loading were highly complex. Importantly, snap-shot sampling provided to be inadequate in capturing and estimating the annual MP loads, and several samples would be required to be collected per day at this site in order to obtain more accurate understanding of the MP variability and loads. A preliminary study capturing the different parameters that may affect the MP loading should be implemented to determine the optimal sampling frequency needed to provide representative data for extrapolation to annual loadings. This type of reconnaissance campaign should be considered when studies are being planned in different river systems, especially those with water management in place, as without more accurate temporal distribution information, researchers risk over or underestimating the importance of certain sources/locations in relation to their respective MP loading.

For the third research objective, where the different impacts of point and diffuse sources were assessed to determine the mechanisms affecting the relative MP inputs into the streams, it was found that the impact of the investigated point source caused an urban signal, which could override the catchment signal in terms of determining the MP load. The MP load was higher from the point source than that of the diffuse urban sources and was driven by water management. However, the diffuse source was controlled by source activation by hydrometeorological

conditions and exhibited high MP load moments whereby the MP load rose several orders of magnitude due to inputs from road run-off following rain events, indicating that while a point source emits more steadily higher MP loads downstream, storm or rain events can cause the diffuse sources to become higher emitters for the duration of these events. It is important to note that the storm events that created the high MP load moments were observed by chance as the study regimen was not designed to capture the storm events and the capturing of these was coincidental. This raises some questions on whether the sampling reported in the literature, which is often carried out in dry weather, is biased and may have missed (or recorded unknowingly) such increased MP load-moments, as here the system characterization would have been different if the two rain events would not have been captured.

All in all, this thesis exhibits a disconnect between reported field studies and laboratory effect studies with regards to MP types, morphologies, and size. Much work is still needed, especially in ecotoxicity, aiming to include more 'environmentally realistic' MP (such as acrylic, PLA and other polymers, with varied morphologies and sizes) in the effect studies. Efforts should also be made to move towards to understanding the underlying mechanisms of toxicity (leachate vs physical impacts) and as a part of this effort, it is important for field studies to report clearly and comprehensively, not only the number/concentration of MP identified from the environment but also their size, morphology, chemical characteristics and any other physical parameters that could be useful for toxicity studies (e.g., colour as this can be indicative of certain colourants). Collecting and reporting this data can in turn be used by toxicologists in planning MP exposures to increase their environmental relevance, leading into a better understanding of underlying toxicity mechanisms and risk assessments.

Further, this thesis underlines the importance of the study design, as it was found that human impacts, specifically water management, can have a substantial impact on MP distribution and their downstream evolution. There is a risk that if the river catchments being studied are imperfectly characterised without fully understanding their properties, such as flow regimen and source activation, this could lead into under, or overestimation of their MP emission sources, and MP loads and their perceived importance. It is also imperative that future sampling campaigns will try to avoid sampling during only dry and/or sunny weather conditions. Here it was found that organizing sampling times for dry-weather conditions only would have led to underestimations of the diffused source MP loading downstream. This type of data is important, as only by capturing the rain events it was possible to identify that the point source discharged higher MP pollution loads downstream during the dry periods, however the diffused source became much more significant for downstream transport of MP during and after rain events. This speaks volumes for the importance of the pre-characterization of the study systems, and how it is of the utmost importance to collect more representative samples that reflect the anthropogenic and hydrometeorological features of the system. As a result, the key recommendation from this thesis is that effort should be made to understand the temporal and spatial catchment properties of the site being studied, before any sampling regimen is being implemented, as this will lead to a more detailed understanding of the short-to-long term changes driven by hydrological and/or anthropogenic forcings. This type of data will be essential to build an accurate MP pollution baseline, as well as to inform any local and/or regional mitigative legislation and risk assessments.

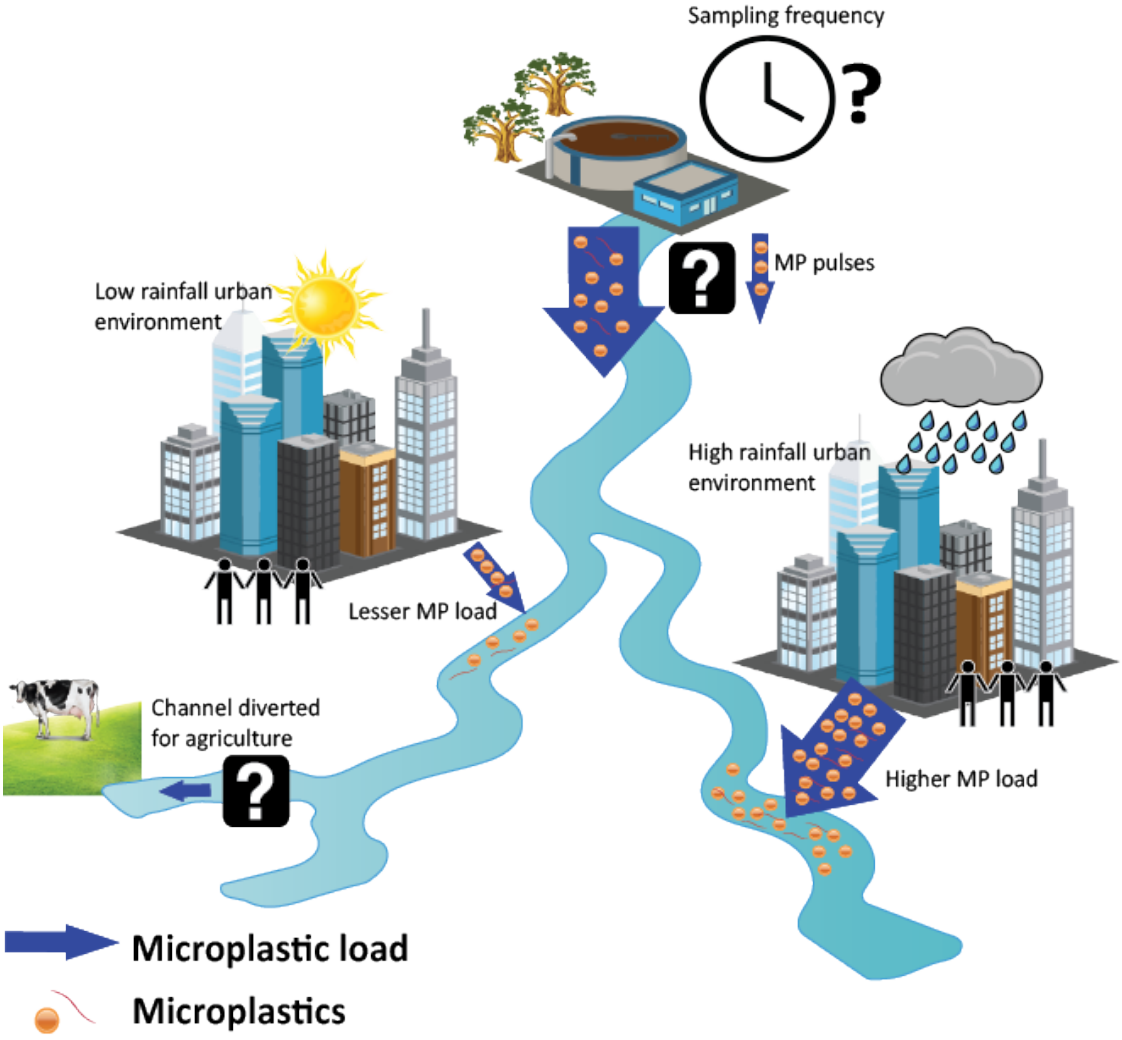


Figure 7.1. Schematic figure presenting a conceptual overview of the main results from this thesis: Urbanization will increase MP concentrations and loadings in river systems, with WWTP as the point source of MP being unpredictable in terms of load amounts downstream ("pulses" of MP travelling downstream) and thus annual MP load estimations could not be calculated based on the MP concentrations determined from snap-shot sampling. Similarly, diversion of water can have influence on MP loading downstream, and as such, loading models that account for abstractions are critical: Water management activities such as diversions need to be accounted for, to obtain a holistic understanding of global MP fluxes. Hydrometeorological source

activation is an important factor for urban catchments with diffuse MP sources being mobilised by rain events. Understanding of the catchment through pre-sampling at high temporal resolution (e.g., hourly for one day) to determine the number of samples needed to be representative of the variability in MP concentrations and loads at the specific site is a key recommendation from this thesis, such as via a pre-sampling campaign to estimate variance.

APPENDIX 1

The raw results of the Wilcoxon Rank Sum tests with multiple comparisons for different system settings for each different plastic types are provided. The intersection of vertical and horizontal settings shows the pairwise comparison between the setting types and the corresponding p-value. The codes on the rows & columns correspond to the settings used for imaging: **2xLi12)** 20x magnification with light intensity 12 and 50 ms exposure time, **2xLi25)** 20x magnification with light intensity 25 and 50 ms exposure time, **3.2xLi12)** 32x magnification, light intensity 12, and 50 ms exposure time, **5xLi12)** 50x magnification, light intensity 12 and 50 ms exposure time and **5xLi25)**, 50x magnification, light intensity 25 with 50 ms exposure time.

Expended polystyrene (EPS)

	2xLi12	2xLi25	3.2xli12	5xLi12
2xLi25	5.1e-05	-	-	-
3.2xli12	5.8e-06	1.00000	-	-
5xLi12	4.3e-06	0.11368	0.11368	-
5xLi25	1.3e-07	0.00028	0.00037	0.11368

High-density polyethylene, HDPE

	2xLi12	2xLi25	3.2xli12	5xLi12
2xLi25	0.0875	-	-	-
3.2xli12	0.0031	0.2234	-	-
5xLi12	0.0875	0.7437	0.4641	-
5xLi25	8.8e-05	0.0142	0.0780	0.0875

High-density polyethylene from a milk bottle, HDPE_milk

	2xLi12	2xLi25	3.2xli12	5xLi12
2xLi25	0.63	-	-	-
3.2xli12	0.57	0.57	-	-
5xLi12	0.65	0.57	0.97	-
5xLi25	0.65	0.57	0.65	0.97

Polyamide-6 fragment, PA-6_frag

	2xLi12	2xLi25	3.2xli12	5xLi12
2xLi25	0.012	-	-	-
3.2xli12	0.769	0.769	-	-
5xLi12	0.769	0.769	0.875	-
5xLi25	6.5e-05	0.058	0.769	0.582

Polyethylene red colour, PE_red

	2xLi12	2xLi25	3.2xli12	5xLi12
2xLi25	0.27107	-	-	-
3.2xli12	0.90246	0.48477	-	-
5xLi12	0.00065	0.00328	0.00234	-
5xLi25	0.00021	0.00021	0.00021	0.00195

Polyethylene terephthalate, PET

	2xLi12	2xLi25	3.2xli12	5xLi12
2xLi25	0.9296	-	-	-
3.2xli12	1.0000	1.0000	-	-
5xLi12	2.9e-06	8.3e-06	5.6e-05	-
5xLi25	6.4e-08	6.4e-08	8.3e-06	0.0064

Polylactic acid, PLA

	2xLi12	2xLi25	3.2xli12	5xLi12
2xLi25	0.32297	-	-	-
3.2xli12	0.06897	0.78509	-	-
5xLi12	0.00030	0.06089	0.03077	-
5xLi25	1.5e-06	0.00034	0.00074	0.02847

Polypropylene blue coloured, PP_blue

	2xLi12	2xLi25	3.2xli12	5xLi12
2xLi25	1.00000	-	-	-
3.2xli12	0.63369	0.37149	-	-
5xLi12	0.01816	0.35714	0.03847	-
5xLi25	0.00068	0.20833	0.00068	0.11106

Polypropylene grey coloured, PP_grey

	2xLi12	2xLi25	3.2xli12	5xLi12
2xLi25	0.0973	-	-	-
3.2xli12	0.0925	0.0214	-	-
5xLi12	0.1126	1.0000	0.0014	-
5xLi25	1.3e-07	4.2e-05	1.5e-07	7.0e-05

Polypropylene white coloured, PP_white

	2xLi12	2xLi25	3.2xli12	5xLi12
2xLi25	0.79	-	-	-
3.2xli12	0.62	0.53	-	-

5xLi12	0.53	0.87	0.53	-
5xLi25	0.53	0.86	0.53	0.97

Expanded polystyrene, PS_exp

	2xLi12	2xLi25	3.2xli12	5xLi12
2xLi25	0.80000	-	-	-
3.2xli12	0.07348	0.8000	-	-
5xLi12	0.03752	0.8000	0.8000	-
5xLi25	1.3e-07	0.20833	0.04091	0.00036

Polystyrene orange coloured, PS_orange

	2xLi12	2xLi25	3.2xli12	5xLi12
2xLi25	0.129	-	-	-
3.2xli12	0.853	0.910	-	-
5xLi12	0.514	0.098	0.514	-
5xLi25	0.862	0.129	0.910	0.910

Polyvinyl chloride rigid, PVC_rigid

	2xLi12	2xLi25	3.2xli12	5xLi12
2xLi25	0.014	-	-	-
3.2xli12	0.713	0.033	-	-
5xLi12	3.9e-05	0.024	8.6e-05	-
5xLi25	1.3e-07	8.8e-05	2.6e-07	0.129

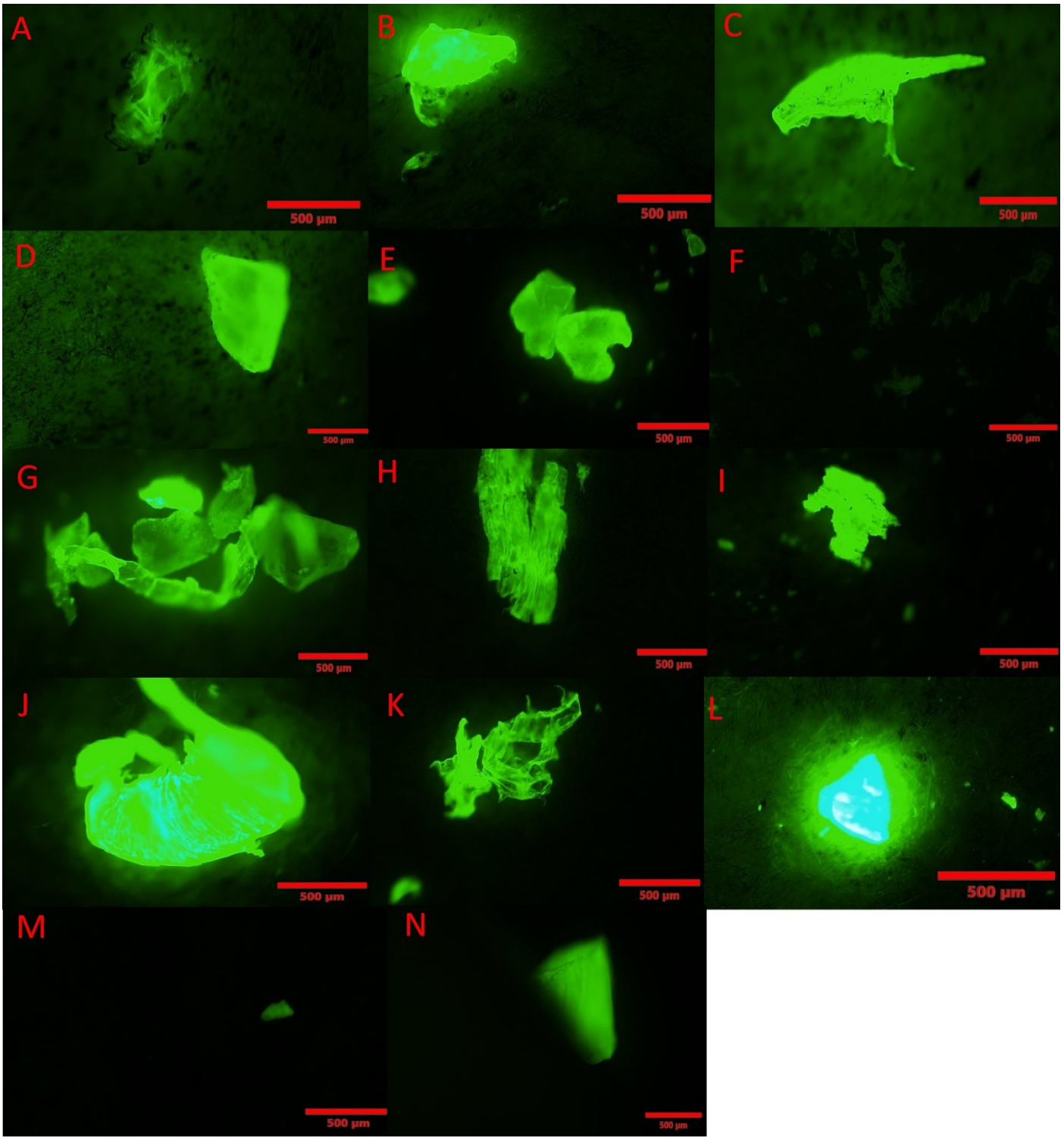


Figure S2.1: Plastic standards photographed under 32x magnification, Light intensity 12 and with 50 ms exposure time. Plastics are: A) expanded polystyrene (EPS), B) high density polyethylene

(HDPE), C) high density polyethylene (HDPE) from a milk bottle, D) polyamide-6 (PA-6), E) polyethylene (PE), F) polyethylene terephthalate (PET), G) polylactic acid (PLA), H) blue polypropylene (PP), I) grey polypropylene (PP), J) white polypropylene (PP), K) polystyrene (PS), L) orange polystyrene (PS), M) rigid polyvinyl chloride (PVC), N) soft polyvinyl chloride (PVC).

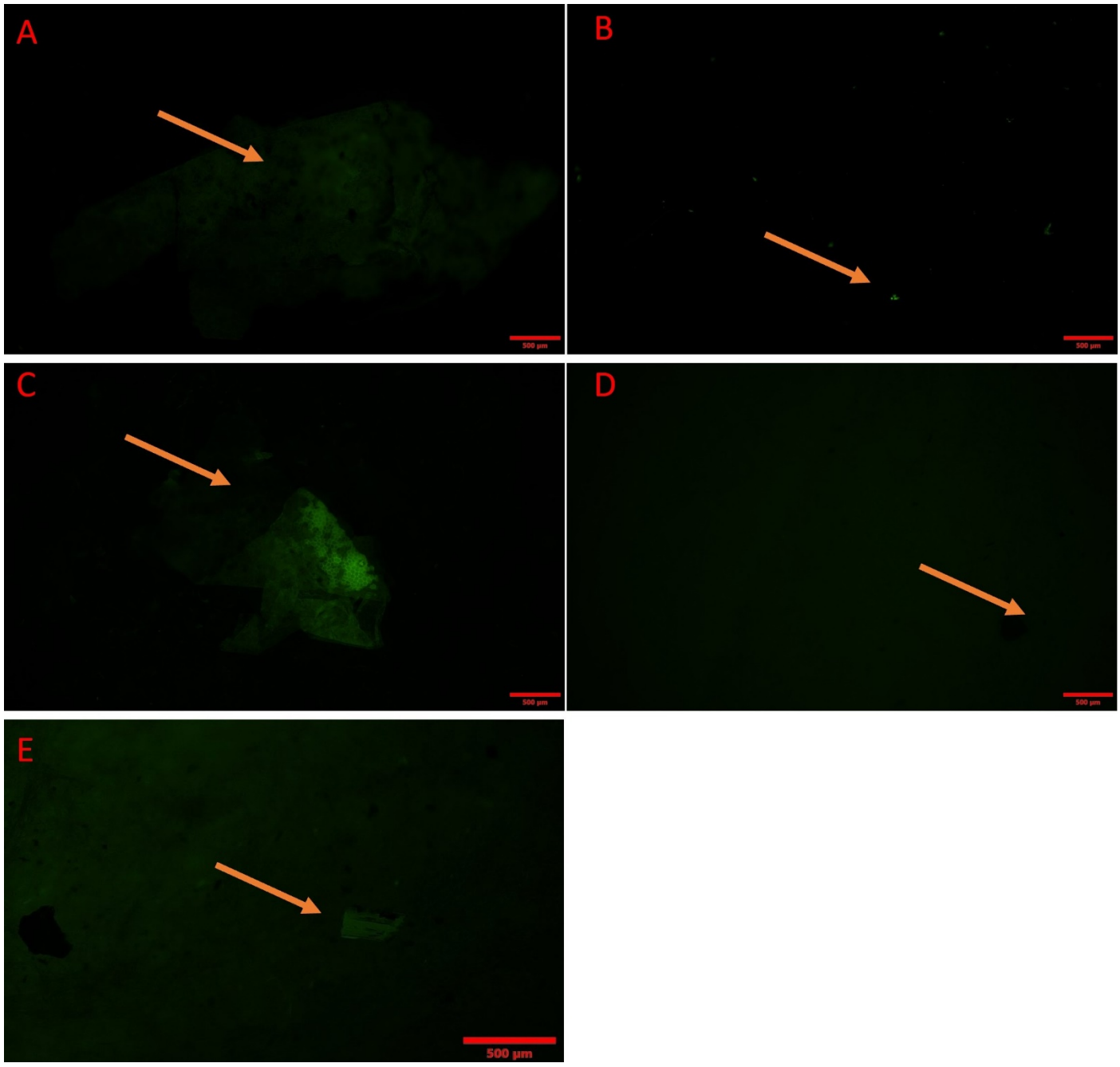


Figure S2.2: False positives photographed under 32x magnification, light intensity 12 and 50 ms exposure time. A) Birch, B) Chitosan, C) Maple, D) Sand, E) Wood. Orange arrows indicate the locations of the particles of interest.

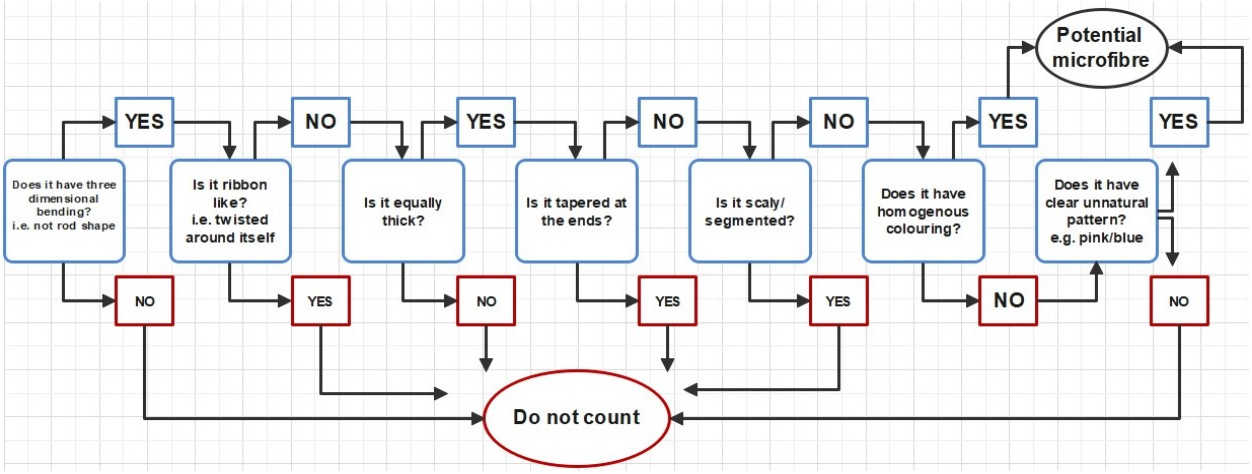


Figure S2.3: Identification key for fluorescent and non-fluorescent microplastic fibres. It is suggested that each filter should be also scanned under bright field mode for non-fluorescent fibres, as they stain poorly and may lead to false negatives if not included in the final count.

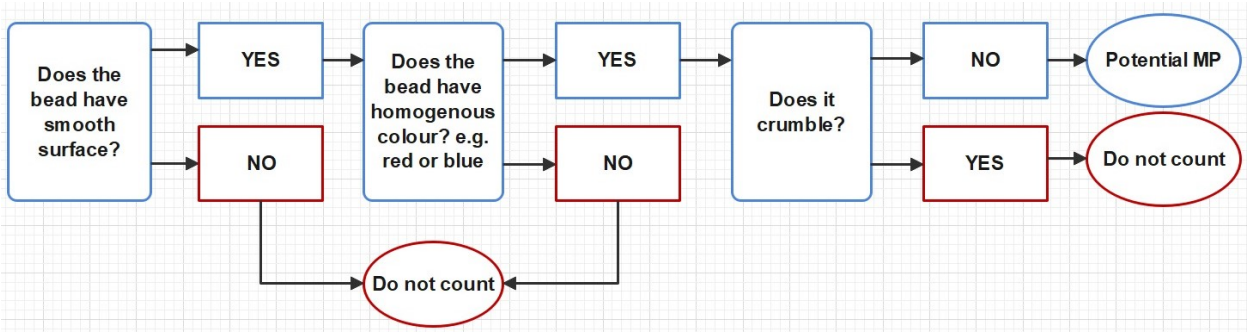


Figure S2.4: Identification key for microplastic spheres/beads. In our studies we found that eggs which do not have a clear cell structure (typically excluded with the general identification key shown in Figure 5) can exhibit bright fluorescence. However, when poked with a needle/fine forceps they crumble or are filled with fluid, making identification easy.

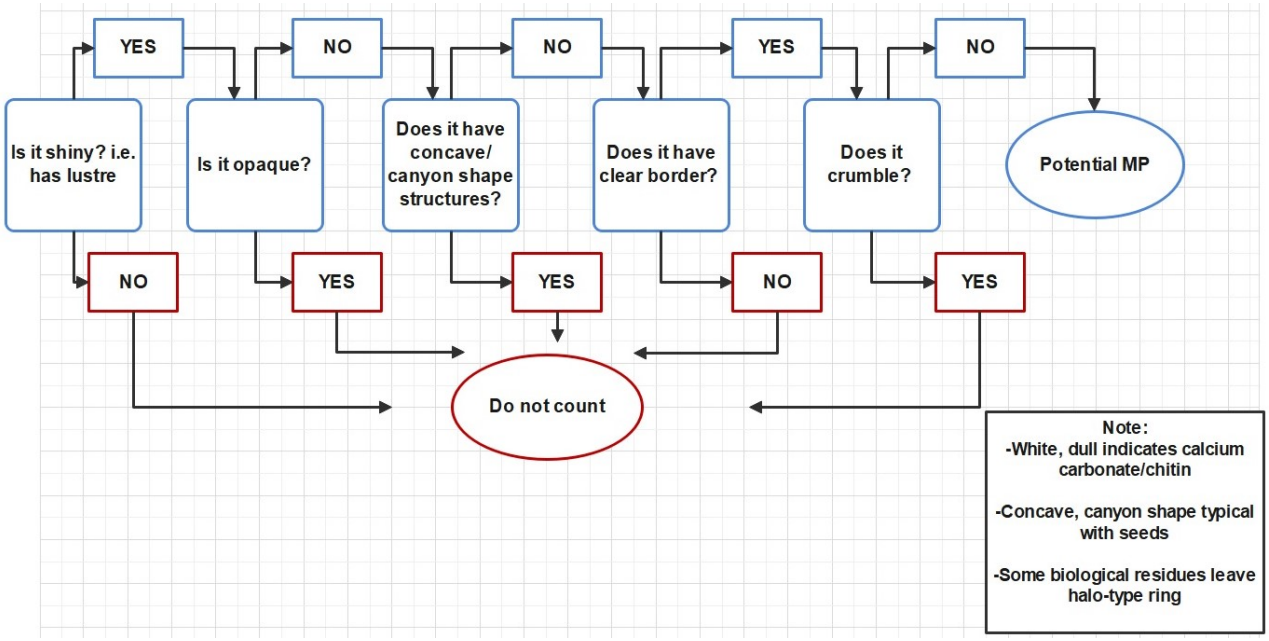


Figure S2.5: Identification key for microplastic fragments including films. Many seeds can exhibit bright fluorescence, with no clear cell structure, but they can be identified by their concave structure, or they may resemble a canyon.

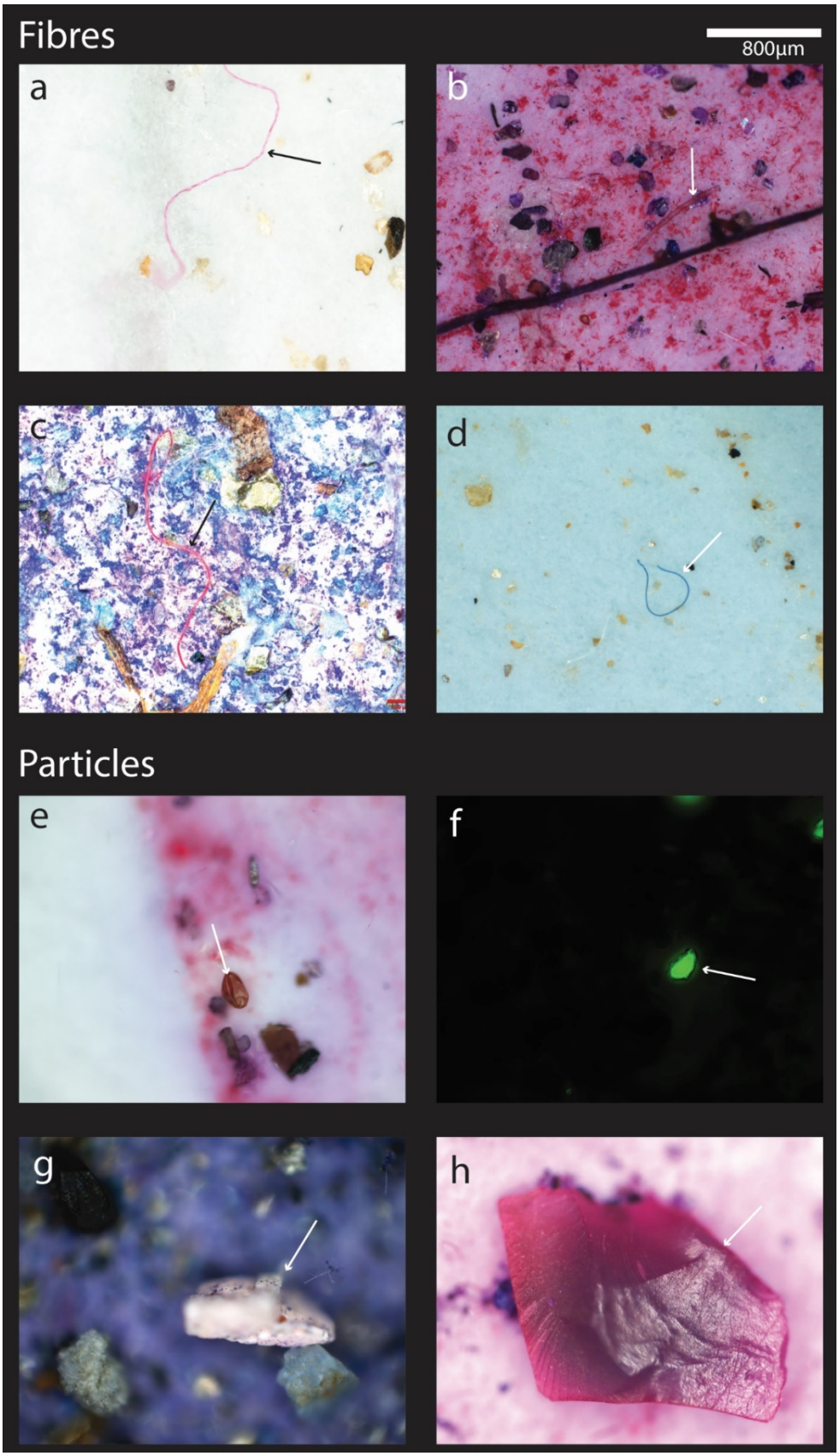

Fibres
800µm
a
b
c
d
Particles
e
f
g
h

Figure S2.6: Photographs taken in bright field and fluorescent light modes showing features described in Figures 2.3-2.5 above. a) Ribbon-like natural fibre. b) Natural fibre with unequal thickness. c) & d) Fibres positively identified as microplastic. e) Particle identified as being a seed due to its concave structure. f) False positive particle showing pale "halo" in fluorescent light. g) Particle of calcium carbonate/chitin with dull, crumbly surface texture. h) Particle positively identified as microplastic. All of the particles have been stained in DI-water containing 5µg mL^{-1} Nile Red.

APPENDIX 2

Table S3.1: The laboratory and field based studies included in this review and the species identified to interact with nano and/or microplastics, the dominant shape of plastic used/found, dominant polymer type(s) and sizing method.

		Laboratory studies						Field studies					
Trophic level	**Biota group**	**Reference**	**Species**	**Dominant shape of MP**	**Dominant polymer**	**Size**	**Sizing method**	**Reference**	**Species**	**Dominant shape of MP**	**Dominant polymer**	**Size**	**Sizing method**
Primary producer decomposers and/or transformers	**Microbes** 20 studies 13 lab, 7 field study	Eckert, Di Cesare et al. 2018	several	Square	PS	4 × 4 mm × 0.1 mm	Punch maker (RW home, Renz, Germany)	McCormick, Hoellein et al. 2014	several	Fibres	NA	0.33-2 mm	Stacked sieves
		Kleinteich, Seidenstickker et al. 2018	several	Particles	PE	212-250 µm	Information from manufacturer	McCormick, Hoellein et al. 2016	several	Pellets, fibres and fragments	PP, PE, PS	0.33 - 4.75 mm	Stacked sieves
		Hossain, Jiang et al. 2019	several	Disk	HDPE, LDPE, PP, PS	4.5 mm	A hole-puncher	Hoellein, McCormick et al. 2017	several	Fibres	PP, PS, PE	0.33 - 4.75 mm	Stacked sieves
		Miao, Guo et al. 2019	several	Particles	PS	129 ± 34	DLS	Kettner, Oberbeckmann et al. 2019 *controlled	several	Particles	PE, HDPE,PS	3-5 mm	Manufacturer information
		Miao, Hou et al. 2019	several	Particles	PS	11.2 ± 2.13, 1.35 ± 2.45 and 635 ± 135, 129 ± 34, 135 ± 16 nm	DLS	Ram and Kumar, 2020	several	NA	NA	75 µm-4 mm	Visual identification and SEM

		Miao, Wang et al. 2019	*several*	*Particles*	*PP, PE*	*3-4 mm*	*Manufacturer information*	*Li et al., 2020b*	*Several*	*Fibres*	*PP, PS, PE*	*0.1-1 mm*	*Stereo microscope*
		Parrish and Fahrenfeld 2019	*several*	*Particles*	*PS, PE*	*PS: 106-125 and 355-425 µm PE: 125-250 µm and 250-500 µm*	*Manufacturer information*	*Tavşanoğlu et al., 2020*	*Several*	*Fibres*	*PET and PET-PVCblend polymer*	*100 and 330-µm*	*Mesh size*
		Gong, Yang et al. 2019	*several*	*Particles*	*LDPE*	*1 and 5 mm*	*Manufacturer information*						
		Kelly et al., 2020	*several*	*Fragments and Particles*	*PE*	*0.25-1mm*	*Not stated*						
		Fringer et al., 2020	*Shewanella oneidensis*	*Particles*	*PS*	*160 nm*	*STEM–EDX*						
		Wang et al., 2020a	*several*	*Fragments*	*PE,PP*	*NA*	*NA*						
		Wang et al., 2020b	*several*	*Fragments*	*Tire wear*	*120, 136, 102 µm*	*Masterisizer*						
		Ramsperger et al., 2020	*several*	*Fragments*	*PA, PET,PVC*	*<500, 1-4000 µm*	*Manufacturer information and Sieving*						

	Algae and blue-green bacteria *Included in 22 studies, 22 laboratory, 0 field studies*	*Besseling, Wang, Lürling, & Koelmans, 2014*	*Scenedesmus obliquus*	*Particles*	*PS*	*~70 nm*	*SEM*						
		Lagarde, Olivier et al. 2016	*Chlamydomas reinhardtii*	*Fragments*	*PP, HDPE*	*400-1000 µm*	*Sieving*	*-*					
		Sjollema, Redondo-Hasselerharm et al. 2016	*Chorella vulgaris*	*Particles*	*PS*	*0.05, 0.5 and 6 µm*	*Manufacturer information*	*-*					
		Mao, Ai et al. 2018	*Chlorella pyrenoidosa*	*Particles*	*PS*	*0.1 and 1.0 µm*	*SEM, DLS*	*-*					
		Zhang, Qu et al. 2018	*Microcystis aeruginosa*	*Particles*	*PS*	*200 nm*	*DLS*	*-*					
		Chae, Kim et al. 2018	*Chlamydomonas reinhardtii*	*Particles*	*PS*	*60.39 nm*	*DLS*	*-*					
		Cunha, Faria et al. 2019	*1. Microcystis panniformis 2. Scenedesmus sp.*	*Fragments*	*PMMA, PS*	*<106 µm and 106-250 µm*	*Sieving*	*-*					
		Liu, Wang et al. 2019	*Scenedesmus obliquus*	*Particles*	*PS*	*50-100 nm*	*DLS*	*-*					
		Luo, Xiang et al. 2019	*Chlorella vulgaris*	*Sheets*	*PUR*	*3 x 3 mm*	*Not stated*	*-*					
		Wu, Guo et al. 2019	*1. Chlorella*			*64-236,*		*-*					

			pyrenoidosa 2. Microcystis flos-aquae	*Particles*	*PP, PVC*	*111 - 216 um*	*Mastersizer*						
		Capolupo et al., 2020	*Raphidocelis subcapitata*	*Leachate experiment*	*car tire, PP, PET, PS ,PVC*	*NA*	*Leachate experiment*						
		Baudrimont et al., 2020	*Scenedemus subspicatus*	*Fragments*	*PE*	*<0.45 µm*	*Filter pore size followed by TOC*						
		Feng et al., 2020	*Microcystis aeruginosa*	*Particles*	*PS*	*50 nm*	*TEM*						
		Li et al., 2020	*Chlamydomonas reinhardtii*	*Particles*	*PS*	*300-600 nm*	*FE-SEM*						
		Wang et al., 2020	*Chlorella pyrenoidosa*	*Particles*	*PS*	*600 nm*	*DLS*						
		Guschina et al., 2020	*Chlorella sorokiniana*	*Fragments*	*PS*	*<70 µm*	*Sieving and macro imaging system*						
		Xiao et al., 2020	*Euglena gracilis*	*Particles*	*PS*	*0.1 and 5 µm*	*DLS*						
		Déniel et al., 2020	*Chlamydomonas reinhardtii*	*Fragments*	*PS*	*158 nm*	*DLS*						
		Liao et al., 2020	*Euglena gracilis*	*Particles*	*PS*	*05.4 nm and 5.02 µm*	*TEM and DLS*						

		Zheng et al., 2020	*Microcystis aeruginosa*	*Particles*	*PS*	*60 nm*	*Manufacturer information*						
		Tunali et al., 2020	*Chlorella vulgaris*	*Particles*	*PS*	*0.5 µm*	*Manufacturer information*						
		Wang et al., 2020	*Chlamydomonas reinhardtii*	*Particles*	*PVC*	*1.02 m^2/g, and 0.49 m^2/g*	*BET*						
	Vascular plants *Included in 4 studies: 4 laboratory, 0 field studies*	*Kalčíková, Žgajnar Gotvajn et al. 2017*	*Lemna minor*	*Irregular*	*PE*	*71.30 ± 34.29 µm 96.00 ± 69.99 µm*	*SEM, light microscope*						
		Mateos-Cárdenas, Scott et al. 2019	*Lemna minor*	*Particles*	*PE*	*10-45 µm*	*Manufacturer information*						
		Dovidat, Brinkmann et al. 2020	*Spirodela polyrhiza*	*Particles*	*PS*	*50 nm and 500 nm*	*Manufacturer information*						
		Kalčíková et al., 2020	*Lemna minor*	*Fragments*	*PE*	*180.5 ± 118.7 µm*	*FE-SEM*						

Primary consumers													
	Cladocerans *Included in 43 studies: 43 laboratory, 0 field studies*	*Imhof, Ivleva et al. 2013*	*Daphnia magna*	*Fragments*	*PMMA*	*29.5 ± 26 µm*	*Fluorescence microscope*						
		Panko, Kreider et al. 2013	*Ceriodaphnia dubia*	*Fragments*	*Road and tire wear*	*<150 µm*	*Sieving*						
		Besseling, Wang, Lürling, & Koelmans, 2014	*Daphnia magna*	*Particles*	*PS*	*~70 nm*	*SEM*						
		Mattsson, Ekvall et al. 2015	*Daphnia magna*	*Particles*	*PS*	*24.7 ± 0.2 and 27.5 nm*	*DLS*						
		Ma, Huang et al. 2016	*Daphnia magna*	*Particles*	*PS*	*25-75,480 - 520 nm, 5-7, 8-12 and 11-16 µm*	*TEM*						
		Jemec, Horvat et al. 2016	*Daphnia magna*	*Fibres*	*PET*	*60-1400 µm*	*Optical microscopy and SEM*						

		Ogonowski, Schür et al. 2016	*Daphnia magna*	*Particles and fragments*	*Cospheric proprietary and PE*	*1-5 µm and 2.6 ± 1.8 µm*	*Laser particle counter*						
		Rehse, Kloas et al. 2016	*Daphnia magna*	*Particles*	*PE*	*1-4 µm and 90-106 µm*	*Stereomicroscope*						
		Scherer, Brennholt et al. 2018	*Daphnia magna*	*Particles*	*PS*	*1, 10 and 90 µm*	*Manufacturer information*						
		Ziajahromi, Kumar et al. 2017	*Ceriodaphnia dubia*	*Fibres and Particles*	*PET, PE*	*280 ± 50 µm, 1-4 µm*	*Fluorescent microscope*						
		Mattsson, Johnson et al. 2017	*Daphnia magna*	*Particles*	*PS*	*53 and 180 nm*	*DLS*						
		Imhof, Rusek et al. 2017	*Daphnia magna*	*Fragments*	*MIX A: PA, polycarbonate, PET, PVC MIX B: Acrylonitrile-burtdiene-styrene terpolymer, plasticized PVC,*	*~40 µm*	*Sieving*						

					polyoxymethylene homopolymer and styrenea crylonitrile) copolymer								
		Rist, Baun, & Hartmann, 2017	Daphnia magna	Particles	PS	100 nm and 2 µm	DLS and particles counter						
		Rehse, Kloas et al. 2018	Daphnia magna	Fragments	PA	15-20 µm	Manufacturer information						
		Aljaibachi and Callaghan 2018	Daphnia magna	Particles	PS	2 µm	Manufacturer information						
		Chae, Kim et al. 2018	Daphnia magna	Particles	PS	60.39 nm	DLS						
		Martins and Guilherminо 2018	Daphnia magna	Particles	Cospheric proprietary	1-5 µm	Manufacturer information						
		Pacheco, Martins et al. 2018	Daphnia magna	Particles	Cospheric proprietary	1-5 µm	Manufacturer information and microscopy						
		Jaikumar, Baas et al. 2018	1. Daphnia magna 2. Daphnia pulex	Particles,	Cospheric proprietary and PE	1-5 µm and 1-10 µm	Manufacturer informat						

			3. Ceriodaphnia dubia	fragments			ion and sieving						
		Canniff and Hoang 2018	Daphnia magna	Particles	PE	63-75 µm	Manufacturer information						
		Liu, Cai et al. 2018	Daphnia pulex	Particles	PS	71.18 nm	TEM						
		Liu, Yu et al. 2019	Daphnia pulex	Particles	PS	75 nm	DLS						
		Tang, Wang et al. 2019	Daphnia magna	Particles	PS	1.25 µm	Manufacturer information						
		Jaikumar, Brun et al. 2019	1. Daphnia magna 2. Daphnia pulex 3. Ceriodaphnia dubia	Particles, fragments	Cospheric proprietary and PE	1-5 µm and 1-10 µm	TEM						
		Bosker, Olthof et al. 2019	Daphnia magna	Particles	PS	1-5 µm	Manufacturer information						
		Colomer, Müller et al. 2019	Daphnia magna	Particles	PS	2.5-30 µm	Manufacturer information						
		De Felice, Sabatini et al. 2019	Daphnia magna	Particles	PS	1 and 10um	Manufacturer information						
		Renzi, Grazioli et al. 2019	Daphnia magna	Fragments	PP, PE, PVC, PVC/PE	10-100 µm	Sieving, microscopy						
		Saavedra, Stoll et al. 2019	Daphnia magna	Particles	PS	226.4	DLS						

						±8.6 nm							
		Reynolds, Giltrap et al. 2019	Daphnia magna	Particles	PS	100 ± 10 nm	DLS						
		Schrank, Trotter et al. 2019	Daphnia magna	Fragments	PVC	10-60 µm	Stereo microscope						
		Sadler, Brunner et al. 2019	Daphnia magna	Particles	PS	575 ± 18.9 nm	Confocal microscopy						
		Taipale, Peltomaa et al. 2019	Daphnia magna	Fragments	PE	<20 µm	Microscopy						
		Trestrail et al., 2020	Daphnia magna	Fragments	PF	170.4 ± 147.5 µm	SEM and Light microscopy						
		Aljaibachi et al., 2020	Daphnia magna	Particles	PS	15 µm	Epi-fluorescent microscope						
		Liu et al., 2020	Daphnia pulex	Particles	PS	75 nm	TEM and DLS						
		Elizalde-Velázquez et al., 2020	Daphnia magna	Particles	PS	5.46 µm	SEM						
		Kelpsiene et al., 2020	Daphnia magna	Particles	PS	26, 53 and 62 nm	DLS						
		Felten et al., 2020	Daphnia magna	Particles	PE	1-4 µm	Manufacturer information						
		Kalčíková et al., 2020	Daphnia magna	Fragments	PE	180.5 ± 118.	Diffraction analyser						

						7 µm							
		Xu et al., 2020	*Daphnia magna*	*Particles*	*PS and PE, PET, PP, PE,PA for secondary*	*20 nm and 300 nm-17 µm*	*DLS*						
		Hanslik et al., 2020	*Daphnia magna*	*Particles*	*PMMA*	*48 µm*	*Manufacturer information*						
		Abdolahpur Monikh et al., 2020	*Daphnia magna*	*Particles*	*PS, PE*	*730 ± 45 nm, 320 ± 28 nm and 410 ± 85 nm*	*TEM and NTA*						
	Crustaceans *Included in 19 studies: 16 laboratory, 3 field studies*	*Panko, Kreider et al. 2013*	*Hyalella azteca*	*Fragments*	*Road and tire wear*	*<150 µm*	*Sieving*	**Lv, Zhou et al. 2019*	*Procambarus clarkii*	*Fibres*	*PE, PP*	*<1 mm*	*Dissecting microscope*
		Imhof, Ivleva et al. 2013	*Gammarus pulex, Notodromas monacha*	*Fragments*	*PMMA*	*29.5 ± 26 µm*	*Fluorescence microscope*	*Iannilli et al., 2020*	*Cryptorchestia garbinii*	*Fragments*	*PA,PE*	*~ 55 µm*	*Infrared microscope*
		Au, Bruce et al. 2015	*Hyalella azteca*	*Particles, fibres*	*PE, PP*	*10-27 µm,*	*Laser Measuring Microscope*	*Nan et al., 2020*	*Paratya australiensis*	*Fibres*	*Rayon, PET*	*0.19-4.2*	*Stereo microscope and*

						20-75 µm						1 mm	image J
		Blarer and Burkhardt-Holm 2016	Gammarus fossarum	Particles, fibres	PS, PA	1.6 µm, 500 × 20 µm	Manufacturer information						
		Scherer, Brennholt et al. 2017	Gammarus pulex	Particles	PS	1, 10 and 90 µm	Fluorescence microscopy						
		Straub, Hirsch et al. 2017	Gammarus fossarum	Fragments	PHB and PMMA	32-63, 63-125 and 125-250 µm	Sieving						
		Redondo-Hasselerharm, de Ruijter et al. 2018	Gammarus pulex	Fragments	Car tire	~66 µm	Sieving and Mastersizer						
		Weber, Scherer et al. 2018	Gammarus pulex	Fragments	PET	10-150 µm	Sieving and SEM						
		Redondo-Hasselerharm, Falahudin et al. 2018	Gammarus pulex, Hyalella azteca, Asellus aquaticus	Fragments	PS	20-500 µm	Mastersizer						
		Khan, Halle et al. 2019	Hyalella azteca	Fragments	Tire rubber	<500 µm	Sieving						
		Saavedra, Stoll et al. 2019	Thamnocephalus platyurus	Particles	PS	226.4 ±8.6 nm	DLS						

		Mateos-Cárdenas, Scott et al. 2019	*Gammarus duebeni*	*Particles*	*PE*	*10-45 µm*	*Manufacturer information*						
		Yardy and Callaghan, 2020	*Gammarus pulex*	*Fibres*	*Acrylic*	*200-500 µm*	*Not stated*						
		Bartonitz et al., 2020	*Gammarus roeseli*	*Particles*	*PA*	*40-63 µm*	*Sieving*						
		Mateos-Cárdenas et al., 2020	*Gammarus duebeni*	*Particles*	*PE*	*10-45 µm*	*SEM*						
		Li et al., 2020	*Macrobrachium nipponense*	*Particles*	*PS*	*71.18 nm*	*TEM*						
	Gastropods *Included in 8 studies: 6 laboratory, 2 field studies*	*Kratina, Watts et al. 2019*	*Gammarus pulex*	*Particles*	*PMMA*	*40.2 µm*	*Manufacturer information*	*Akindele, Ehlers et al. 2019*	*1. Lanistes varicus 2. Melanoides tuberculata 3. Theodoxus fluviatilis*	*Fibres*	*PE, PA, PP*	*NA*	*Digital microscope*
		Imhof, Ivleva et al. 2013	*Potamopyrgus antipodarum*	*Fragments*	*PMMA*	*29.5 ± 26 µm*	*Fluorescence microscope*	*Xu et al., 2020*	*Bellamya aeruginosa*	*Fibres*	*PVAc, PS, PA, PET*	*50-810 µm*	*Optical microscope*
		Imhof and Laforsch 2016	*Potamopyrgus antipodarum*	*Fragments*	*PA, PET, polycarbonate, PS, PVC*	*118 ± 105 µm*	*Digital image analysis system*						
		Horton et al., 2020	*Lymnaea stagnalis*	*Fragments*	*PA*	*13-19 µm*	*Coulter Counter*						
		Trestrail et al., 2020	*Physa acuta*	*Fragments*	*PF*	*170.4 ± 147.*	*SEM and light*						

						5 µm	*microscopy*						
		Qu et al., 2020	*Cipangopaludina cathayensis*	*Particles*	*PS*	*700 nm*	*Manufacturer information*						
	***Dipterans** Included in 13 studies: 11 laboartory, 2 field studies*	*Scherer, Brennholt et al. 2017*	*Physella acuta*	*Particles*	*PS*	*1, 10 and 90 µm*	*Fluorescence microscopy*	*Nel, Dalu et al. 2018*	*Chironomus spp*	*NA*	*NA*	*NA*	*Dissecting microscope*
		Panko, Kreider et al. 2013	*Chironomus dilutus*	*Fragments*	*Road and tire wear*	*<150 µm*	*Sieving*	*Akindele et al., 2020*	*1.Chironomus sp. 2.L. viridis 3.Siphlonurus sp*	*Fibres*	*PET,PP*	*NA*	*Digital microscope*
		Scherer, Brennholt et al. 2017	*Chironomus riparius*	*Particles*	*PS*	*1, 10 and 90 µm*	*Fluorescence microscopy*						
		Al-Jaibachi, Cuthbert et al. 2018	*Culex pipiens*	*Particles*	*PS*	*2 and 15 µm*	*Manufacturer information*						
		Cuthbert, Al-Jaibachi et al. 2019	*1. Chaoborus flavicans 2. Culex pipiens*	*Particles*	*PS*	*2 µm*	*Manufacturer information*						
		Al-Jaibachi, Cuthbert et al. 2019	*Culex pipiens*	*Particles*	*PS*	*2 ± 0.2 and 15.4 5 ± 1.1µm*	*Epi-fluorescent microscope*						

		Ziajahromi, Kumar et al. 2019	*Chironomus tepperi*	*Particles*	*PE*	*10-27 µm*	*Manufacturer information*						
		Silva, Silva et al. 2019	*Chironomus riparius*	*Fragments*	*PE*	*32-63, 63-250 and 125-500 µm*	*Sieving*						
		Scherer et al., 2020	*Chironomus riparius*	*Particles*	*PVC*	*<50 µm*	*Coulter Counter*						
		Khosrovyan and Kahru, 2020	*Chironomus riparius*	*Fragments*	*PA*	*10-180 µm*	*Nikon 1270 imaging software*						
		Hanslik et al., 2020	*Chironomus riparius*	*Particles*	*PMMA*	*48 µm*	*Manufacturer information*						
	***Bivalves** included in 21 studies: 14 laboratory, 7 field studies*	*Rochman, Parnis et al. 2017*	*Corbicula fluminea*	*Fragments*	*PET, PE PVC, PS*	*198, 209 169 and 179 µm*	*Custom Processing Services*	*Su, Xue et al. 2016*	*Corbicula fluminea*	*Fibres*	*cellophane, PET, PP*	*333 - 1000 µm*	*Stereo microscope*
		Guilhermino, Vieira et al. 2018	*Corbicula fluminea*	*Particles*	*Cospheric proprietary*	*1-5 µm diameter*	*Manufacturer information*	*Su, Cai et al. 2018*	*Corbicula fluminea*	*Fibres*	*PP, PET*	*0.021-4.02 mm*	*Microscopy*
		Magni, Gagné et al. 2018	*Dreissena polymorpha*	*Particles*	*PS*	*1 and 10 µm*	*Manufacturer information*	*Domogalla-Urbansky, Anger et al. 2019 (controlled field-based study)*	*Unio pictorum*	*NA*	*PVC, PP*	*6-80 µm*	*Confocal Raman Microscope*

		Oliveira, Barboza et al. 2018	Corbicula fluminea	Particles	Cospheric proprietary	1-5 µm diameter	Manufacturer information and Microscopy	Schessl, Johns et al. 2019	Dreissena polymorpha and D. bugensis	None found	NA	NA	Dissecting microscope
		Li, Su et al. 2019	Corbicula fluminea	Fibres	PEA, PET, AC, PA), RA, PVA	5-100, 100-250, 250-500, 500-1000 and 1000-5000 µm	LUMOS µ-FT-IR	Berglund, Fogelberg et al. 2019	Anodonta anatina	Fibres	NA	NA	Light microscopy
		Magni, Della Torre et al. 2019	Dreissena polymorpha	Particles	PS	1 and 10 µm	Confocal microscopy	Baldwin et al., 2020	Dreissena bugensis and Corbicula fluminea	Fibres	NA	NA	Stereoscope
		Merzel, Purser et al. 2019	Dreissena rostrformis bugensis	Particles	PS	200, 1000 and 2000 nm	AFM-IR	Wardlaw and Prosser, 2020	Lasmigona costata	Fragments	Polypropylene-co-ethylene, PP	21-298 µm	Filtering screens and stereomicroscope
		Baudrimont et al., 2020	Corbicula fluminea	Fragments	PE	<0.45 µm	Filtration and total organic carbon measurements						
		Auclair et al., 2020	Elliptio complanata	Particles	PS	50 nm	Manufacturer information						

		Pedersen et al., 2020	*Dreissena bugensis*	*Particles*	*PE*	*10-45 µm*	*Manufacturer information*						
		Weber et al., 2020	*Dreissena polymorpha*	*Fragments*	*PS*	*2-60 µm*	*Sieving and Coulter Counter*						
		Magni et al., 2020	*Dreissena polymorpha*	*Fragments*	*PVC, Mater-Bi®*	*56 ± 35 µm and 41 ± 36 µm*	*DLS*						
		Webb et al., 2020	*Perna canaliculus*	*Particles*	*PE*	*38-45 µm*	*Manufacturer information*						
		Facchetti et al., 2020	*Unio elongatulus*	*Particles*	*PVC(platinum octaethylporphyrin doped)*	*62 ± 1, 120 ± 5, and 380 ± 80 µm*	*Masterisizer*						
	Annelids *Included in 7 studies: 6 laboratory, 1 field studies*	*Imhof, Ivleva et al. 2013*	*Lumbriculus variegatus*	*Fragments*	*PMMA*	*29.5 ± 26 µm*	*Fluorescence microscope*	*Hurley, Woodward et al. 2017*	*Tubifex tubifex*	*Fibres*	*PS, PE, PP*	*847 ± 673 µm*	*Stereo Zoom Microscope*
		Scherer, Brennholt et al. 2017	*Lumbriculus variegatus*	*Particles*	*PS*	*1, 10 and 90 µm*	*Fluorescence microscopy*						
		Redondo-Hasselerharm, de	*Tubifex spp.*		*Car tire*								

		Ruijter et al. 2018		*Fragments*		*~66 µm*	*Mastersizer*						
		Redondo-Hasselerharm, Falahudin et al. 2018	*Lumbriculus variegatus*	*Fragments*	*PS*	*20-500 µm*	*Mastersizer*						
		Scopetani et al., 2020	*Tubifex tubifex*	*Particles*	*PE*	*10 µm*	*Manufacturer information*						
		Castro et al., 2020	*Allonais inaequalis*	*Particles*	*PE*	*40-48 µm*	*Light microscopy*						
	Others *Included in 11 studies: 10 Laboratory, 1 field studies*	*Imhof, Ivleva et al. 2013*	*Notodromas monacha*	*Fragments*	*PMMA*	*29.5 ± 26 µm*	*Fluorescence microscope*	*Windsor, Tilley et al. 2019*	*Baetidae, Heptageniidae and Hydropsychidae*	*NA*	*NA*	*0.5-5mm*	*Light microscopy, bright- and dark-field spectroscopy*
		Fueser, Mueller et al. 2019	*Caenorhabditis elegan, Panagrolaimus thienemanni, Plectus acuminatus, Poikilolaimus regenfussi and Acrobeloides nanus*	*Particles*	*PS*	*0.47 ± 0.01, 0.91 ± 0.01, 3.00 ± 0.15, 6.10 ± 0.24*	*Fluorescence microscope*						

						and 10.10 ± 0.71 µm							
		Murphy and Quinn 2018	Hydra attenuata	Flakes	PE	<400 µm	Sieving						
		Gambino et al. 2020	Dugesia japonica	Particles and fibres	PE and PET	1-10, 10-27 and 6, 30 um	Microscopy						
		Shang et al., 2020	Caenorhabditis elegans	Particles	PS	1 and 5 µm	SEM						
		López-Rojo et al., 2020	Sericostoma pyrenaicum	Particles	PS	10 µm	Manufacturer information						
		Ehlers et al., 2020	Lepidostoma basale	Fragments	PVC,PET	200-500 µm	Sieving						
		Banaee et al., 2020	Emys orbicularis	Particles	PE	<0.2 mm	Manufacturer information						
		Fueser et al., 2020	Nematodes, rotifers,crustaceans	Particles	PS	0.47 ± 0.01, 0.91 ± 0.01, 3.00 ± 0.15	Fluorescence microscope						

						, 6.10 ± 0.24 and 10.10 ± 0.71 µm							
		Drago et al., 2020	*Brachionus calyciflorus*	*Particles*	*PS*	*1.03, 3.06, and 5.73 µm*	*Manufacturer information*						
Secondary consumers													
	Amphibians *Included in 7 studies: 5 laboratory, 2 field studies*	*Hu, Su et al. 2016*	*Xenopus tropicalis*	*Particles*	*PS*	*1 and 10 µm*	*Manufacturer information*	*Hu, Chernick et al. 2018*	*Microhyla ornata, Rana limnochari, and Pelophylax nigromaculatus and/or toads (Bufo gargarizans)*	*Fibres*	*PES, PP, PE*	*<0.5 -2 mm*	*Stereo microscope*
		De Felice, Bacchetta et al. 2018	*Amphibian Xenopus laevis*	*Particles*	*PS*	*2.75 ± 0.09 µm*	*SEM*	*Kolenda et al., 2020*	*1.Bufo bufo 2.Rana temporaria 3.Pelophylax esculentus complex 4.Pelobates fuscus 5.Hyla arborea*	*Fibres*	*PA, Polyisoprene*	*0.5-2.2 mm*	*Stereo microscope*
		Araújo et al., 2020	*Physalaemus cuvieri*		*PE*	*35.46 ±*	*SEM*						

				Particles		*18.17 µm*							
		Boyero et al., 2020	*Alytes obstetricans*	*Particles*	*PS*	*10 µm*	*Manufacturer information*						
		Araújo and Malafaia, 2020	*Physalaemus cuvieri*	*Particles*	*PE*	*35.46 µm ± 18.17 µm*	*SEM*						
	Fish *Included in 90 studies: 45 laboratory, 45 field studies*	*Oliveira, Ribeiro et al. 2013*	*Pomatoschistus microps*	*Particles*	*PE*	*1-5 µm*	*Manufacturer information*	*Sanchez, Bender et al. 2014*	*Gobio Gobio*	*Fibres*	*NA*	*NA*	*Dissecting microscope*
		Panko, Kreider et al. 2013	*Pimephales promelas*	*Fragments*	*Road and tire wear*	*<150 µm*	*Sieving*	*Phillips and Bonner 2015*	*44 species*	*Film, Fibres*	*PP, PET, PMMA, PS, PA*	*73 ± 98.6 μm^2 160 ± 245 μm^2*	*Dissecting microscope and FT-IR*
		Khan, Syberg et al. 2015	*Danio rerio*	*Particles*	*PE*	*59 ± 19 µm*	*Microscopy*	*Faure, Demars et al. 2015*	*1. Alburnus alburnus 2. Perca fluviatilis 3. Rutilus rutilus 4. Leuciscus leuciscus*	*Fibres, fragments*	*PE,PP*	*NA (reported as weight)*	*Stereo microscope, FT-IR*
		Mattsson, Ekvall et al. 2015	*Carassius carassius*	*Particles*	*PS*	*24.7 ± 0.2*	*DLS*	*Peters and Bratton 2016*	*1. Lepomis macrochirus*	*Fibres*	*NA*	*NA*	

						and 27.5 nm			2. Lepomis megalotis				Stereo micro scope
		Batel, Linti et al. 2016	Danio rerio	Particles	Cospheric propriet ary, PE	1-5 µm and 10-20 um	Manufacturer information	Biginagwa, Mayoma et al. 2016	1. Lates niloticus 2. Oreochromisniloticus	NA	PE, PUR PET, polyethylene/polypropylene co-polymer and silicone rubber	>0.5mm	Dissection micro scope
		Fonte, Ferreira et al. 2016	Pomatoschistus microps	Particles	PE	1-5 µm	Manufacturer information	Pazos, Maiztegui et al. 2017	11 species	Fibres	NA	0.06 - 4.7 mm	Stereo micro scope
		Karami, Romano et al. 2016	Clarias gariepinus	Fragments	LDPE	<60 µm	Masterizer	Campbell, Williamson et al. 2017	1. Esox lucius 2. Catostomus commersoni 3. Notropis atherinoides 4. Pimephales promelas 5. Eucalia inconstans	Fibres, fragments	NA	NA	Dissection micro scope
		Lu, Zhang et al. 2016	Danio rerio	Particles	PS	70 nm, 5 µm, and 20 µm	DLS, fluorescence microscopy	Roch and Brinker 2017	1. Neogobius melanostomus 2. Barbus barbus	Fragments	NA	264 - 2907 µm	Dissecting micro scope
		Wardrop, Shimeta et al. 2016	Melanotaenia fluviatilis	Fragments	PE		Microscopy	Vendel, Bessa et al. 2017	69 species	Fibres	NA	NA	Stereo scopic

						10-700 µm							micro scope
		Mattsson, Johnson et al. 2017	Carassius carassius	Particles	PS	53 nm and 180 nm	DLS	Zhang, Xiong et al. 2017	13 species	Fibres, sheets	PE,PA	0.3-1.8 mm	Stereo scopic micro scope
		Karami, Groman et al. 2017	Danio rerio	Fragments	LDPE	~10.9 µm	Masterizer	Jabeen, Su et al. 2017	1. Cyprinus carpio 2. Carassius auratus 3. Hypophthalmichthys molitrix 4. Pseudorasbora parva 5. Megalobrama amblycephala 6. Hemiculter bleekeri	Fibres	Cellophane, PE, PET	0.04-5 mm	Stereo micro scope
		Rochman, Parnis et al. 2017	Acipenser transmontanus	Fragments	PET, PE PVC, PS	198, 209, 169 and 179 µm	Custom Processing Services	Silva-Cavalcanti, Silva et al. 2017	Hoplosternum littorale	Fibres	NA	NA	Dissecting micro scope
		Wagner, Wang et al. 2017	Oryzias latipes	Fragments	PVC, PE, PP, PS, PET	100-2000 µm	Custom Processing Services and FTIR	McGoran, Clark et al. 2017	1. Platichthys flesus 2. Osmerus eperlanus	Fibres	PA, PET, AC,PE polyester-nylon mix	NA	Dissecting micro scope

		Ravit et al. 2017	Danio rerio	Fragments	PE, PP, polyethylene-vinyl acetate copolymer	<2mm	Sieving	Xiong, Zhang et al. 2018	Gymnocypris przewalskii	Fibres	PE, PS, PA, PP	NA	Stereo microscope
		Chae, Kim et al. 2018	1. Oryzias sinensis 2. Zacco temminckii	Particles	PS	60.39 nm	DLS	Horton, Jürgens et al. 2018	Rutilus rutilus	Fibres, fragments	PE, PP, PET	NA	Binocular microscope
		Wen, Zhang et al. 2018	Symphysodon aequifasciatus	Particles	PE	70-88 µm	DLS	McNeish, Kim et al. 2018	11 species	Fibres	PE, polyacrylonitrile, polyacetal, polyvinyl acetate	<1.5 mm	Dissecting microscopes
		Lei, Wu et al. 2018	Danio rerio	Fragments Particles	PA, PE, PP, PVC and PS	~70 µm And 0.1, 1, 5 µm	Sieving and microscopy and DLS	Collard, Gasperi et al. 2018	Squalius cephalus	Fibres, fragments	PET,PP,PAN	147-567 µm	Stereo microscope
		Ding, Zhang et al. 2018	Oreochromis niloticus	Particles	PS	0.1 µm	TEM	Andrade, Winemiller et al. 2019	16 species	Fibres	PE,PVC, PA, PP	1-15 mm	Stereo microscope
		Malinich, Chou et al. 2018	Pimephales promelas	Particles	PE	425-500 µm 180-212 µm	Manufacturer information	Slootmaekers, Catarci Carteny et al. 2019	Gobio gobio	Foam	EVA, PP, PET, PVC	<2 mm	Stereo microscope and macroscope
		LeMoine, Kelleher et al. 2018	Danio rerio	Particles	PE	10-45 µm	Manufacturer information	Lv, Zhou et al. 2019	Monopterus albus	Fibres	PE,PP	<1 mm	Microscopy, dissecting microscope
		Jabeen, Li et al. 2018	Carassius auratus			0.7-5.0 mm,		Yuan, Liu et al. 2019	Carassius auratus				Dissecting

				Fibres, fragments, pellets	*EVA, PS, PA*	*2.5-3.0 mm, 4.9-5.0 mm*	*Raman Microscope*			*Fibres*	*PP, PE*	*< 0.5 mm*	*microscope*
		Zhang, Ding et al. 2019	*Oreochromis niloticus*	*Particles*	*PS*	*0.1 µm*	*SEM*	*Su, Nan et al. 2019*	*Gambusia holbrooki*	*Fibres*	*PET, RA, PA*	*0.09-4.86 mm*	*Stereomicroscope*
		Kim, Chae et al. 2019	*Danio rerio*	*Particles*	*PE*	*247.5 ± 14.4 µm*	*Microscopy*	*Ryan, Watkins et al. 2019*	*Alosa aestivalis*	*Fibres*	*NA*	*0.335-5.0 mm*	*Dissecting microscope*
		Liu, Wang et al. 2019	*Danio rerio*	*Particles*	*PS*	*50-100 nm*	*TEM*	*Roch, Walter et al. 2019*	*22 species*	*Fragments, fibres*	*NA*	*<5 mm*	*Dissecting microscope*
		Qiang and Cheng 2019	*Danio rerio*	*Particles*	*PS*	*1 µm*	*Fluorescence microscope and DLS*	*Blettler, Garello et al. 2019*	*Prochilodus lineatus*	*NA*	*NA*	*0.5-3 mm*	*Dissecting microscope*
		Trevisan, Voy et al. 2019	*Danio rerio*	*Particles*	*PS*	*44 nm*	*DLS*	*Zheng, Fan et al. 2019*	*1.Hypophthalmichthys molitrix. 2.Ctenopharyngodon idella 3.Megalobrama hoffmanni 4.Squaliobarbus curriculus 5.Cirrhinus molitorella 6.Cyprinus carpio 7.Carassius gibelio 8.Coptodon*	*Fibres, fragments*	*PET, PE*	*1-5 mm*	*Stereomicroscope and binocular microscope*

									zillii 9.Channa maculata				
		Limonta, Mancia et al. 2019	Danio rerio	Fragments	HDPE, PS	90% <90 µm	Manufacturer information	Urbanski et al., 2020	Prochilodus lineatus	NA	NA	0.18-12.3 mm	Stereo microscope
		Parenti, Ghilardi et al. 2019	Danio rerio	Particles	PS	0.5 µm	Confocal microscopy and DLS	Hurt et al., 2020	1.Dorosoma cepedianum 2. Micropterus salmoides	NA	NA	NA	Stereo microscope
		Mbedzi et al., 2020	Tilapia sparrmanii	Particles	PE	125 µm	Manufacturer information	Kuśmierek and Popiołek, 2020	1.Gobio gobio 2.Rutilus rutilus	Fibres	NA	0.5-5 mm	Stereo microscope
		Malafaia et al., 2020	Danio rerio	Particles	PE	38.26 ± 15.64 µm	SEM	Kasamesiri and Thaimuangphol, 2020	1.Mystus bocourti 2.Puntioplites proctozysron 3.Henicorhynchus siamensis 4.Laides longibarbis 5.Labiobarbus siamensis 6.Cyclocheilichthys repasson 7.Hemibagrus spilopterus 8.Labeo chrysophekadion	Fibres	NA	0.03-3.84 mm	Stereo microscope

		Hamed et al., 2020	Oreochromis niloticus	Particles	Not given	>100 nm	Manufacturer information	Park et al., 2020	1.Cyrinus carpio 2.Carassius cuvieri 3.Lepomis macrochirus 4.Micropterus salmoides 5.Silurus asotus 6.Channa argus	Fragments	PFTE, PE and rayon	0.3-0.6 mm	FTIR Microscopy
		Trestrail et al., 2020	Danio rerio	Fragments	PF	170.4 ± 147.5 µm	SEM and Light microscopy	Baldwin et al., 2020	1.Morone saxatilis 2.Cyprinus carpio	Fibres	NA	NA	Stereoscope
		Roch et al., 2020	1.Oncorhynchus mykiss 2.Thymallus thymallus 3.Cyprinus carpio 4.Carassius carassius	Fragments	PE,PP, PS,EPS, PET,PVC	1-2 mm	Not stated	Adeogun et al., 2020	1.Coptodon zillii 2.Oreochromis niloticus 3.Sarotherodon melanotheron 4.Chrysichthys nigrodigitatus 5.Lates niloticus 6.Parachanna obscura 7.Hemichromis fasiatus 8.Hepsetus odoe	Not separately stated-assumed particles/fragments	NA	124 µm - 1.53 mm	Stereoscope
		Roda et al., 2020	Prochilodus lineatus					Khan et al., 2020	1.Oreochromis niloticus				

				Particles	PE	10-90 µm	Manufacturer information		2.Bagrus bayad	Fibres	PE, PET, PP	NA	Dissection microscope
		Elizalde-Velázquez et al., 2020	Pimephales promelas	Particles	PS	5.46 µm	SEM	Sembiring et al., 2020	Chanos chanos	Fragments	PP,PE	1000-5000 µm	Microscope and an FTIR spectroscopy
		Xia et al., 2020	Cyprinus carpio	Particles	PVC	~100-200 µm	SEM	Li et al., 2020	1.Hemiculter leucisculus 2.Hypophthalmichthys molitrix 3.Carassius auratus 4.Cyprinus carpio	Fibres	PET,PP	<1-3 mm	Microscopy
		Yu et al., 2020	Danio rerio	Particles	PE	100-400 µm	DLS and SEM	Adu-Boahen et al., 2020	24 species	Fragments	NA	NA	Stereomicroscope
		Boyle et al., 2020	Danio rerio	Fragments	PVC, HDPE and PET	~200 µm	Sieving, light microscopy	Tien et al., 2020	1.Oreochromis niloticus niloticus 2.Pterygoplichthys pardalis 3.Leiognathus equulus 4.Carassius auratus auratus 5.Pomadasys argenteus	Fibres	PP, PA and PE	50-297-5000 µm	Compound light microscope
		Brandts et al., 2020	Danio rerio	Particles	PS	65.1 ±	DLS	Wang et al., 2020	15 species	Fragments	NA		Sievin g

						0.6 nm						<0.5 mm	
		Assas et al., 2020	1.Oryzias latipes 2. Oryzias javanicus	Particles	PS	2 µm	Fluorescence microscopy	Merga et al., 2020	1.Clarias gariepinus 2.Cyprinus carpio 3.Carassius carassius 4.Oreochromis niloticus	Fragments	PE,PP	0.2-5 mm	Stereo microscope
		Kurchaba et al., 2020	Danio rerio	Particles	PE	10-45 µm	Manufacturer information	Ribeiro-Brasil et al., 2020	14 species	Fibres	NA	<1 mm and 1.1 – 5.0 mm	Stereo microscope
		Hanslik et al., 2020	Danio rerio	Particles	PMMA	48 µm	Manufacturer information	Garcia et al., 2020	1.Oreochromis niloticus 2.Prochilodus magdalenae 3.Pimelodus grosskopfii	Fragments/films	PET,PES, and PE	NA	Stereo microscope
		Pedersen et al., 2020	Danio rerio	Particles	PS	42 nm and 194 nm	Fluorescent microscope	O'Connor et al., 2020	Salmo trutta	Fibres	EVA,EPDM,PVF	350 µm to ≤ 5 mm	Stereo microscope
		da Costa Araújo et al., 2020	1.Poecilia reticulat2. Danio rerio	Particles	PE	35.46 µm ± 18.17 µm	Microscopy and SEM	Bosshart et al., 2020	Neogobius melanostomus	NA	Not detected	>300 µm	Stereo microscope
		Qiang et al., 2020	Danio rerio					Park et al., 2020	1.Cyprinus carpio 2.Carassius auratus				

				Particles	*PS*	*1 µm*	*Fluorescence microscope*		*3.Pseudogobio esocinus 4.Micropterus salmoides 5.Zacco platypus.*	*Fragment*	*PE,PET*	*0.1-0.3 mm*	*Microscopy FT-IR microscopy*
	Birds *Included in 7 studies: 0 laboratory, 7 field studies*	-	-					*English, Robertson et al. 2015*	*1. Anas rubripes 2. Anas platyrhynchos*	*NA*	*NA*	*0.5-5 mm*	*Microscopy*
		-	-					*Faure, Demars et al. 2015*	*1. Ardea cinerea 2. Cygnus olor 3. Anas platyrhynchos*	*Fragments, foam*	*PE,PP*	*NA*	*Stereomicroscope, FT-IR*
		-	-					*Holland, Mallory et al. 2016*	*18 species*	*Fragments*	*NA*	*50 µm to 5 mm*	*Dissecting microscope*
		-	-					*Gil-Delgado, Guijarro et al. 2017*	*1. Fulica atra 2. Anas platyrhynchos 3. Tadorna tadorna*	*Fragments, fibres*	*NA*	*1.38-2.33mm, 1.64-2.43mm*	*Binocular magnifying glass*
		-	-					*Reynolds and Ryan 2018*	*1. Anas erythrorhyncha 2. Anas smithii*				

									3. Anas undulata 3. Dendrocygna viduata 4. Alopochen aegyptiaca 5. Plectropterus gambensis	*Fibres*	*NA*	*NA*	*Microscopy*
								D'Souza et al., 2020	*Cinclus cinclus*	*Fibres*	*PVA,PET*	*0.5-5 mm*	*light, infrared and bright- and dark-field microscopy*
								Winkler et al., 2020	*Alcedo atthis*	*Fibres*	*PET,PE,PUR,PP*	*63 µm-3.09 mm*	*Stereomicroscope, SEM-EDS*

APPENDIX 3

Table S4.1. Hydrological and physical properties of sampling locations.

[km^2, square kilometres; $m^3\ s^{-1}$, cubic meters per second; $m\ s^{-1}$, meters per second; m, meters; km, kilometres; g, grams; MP, microplastic; Kg, kilograms; L, litres]

ID	*Latitude*	*Longitude*	*Size of catchment km^2*	*Discharge $m^3\ s^{-1}$*	*Average velocity $m\ s^{-1}$*	*Distance from reservoir (s) (m)*	*sediment weight (g) A*	*B*	*MP per Kg^{-1}*	*MP L^{-1}*
B1	39.981	-105.454	106.708	0.29	0.252	3719	35.89	35.27	182	0.12
B3	40.004	-105.407	114.737	0.23	0.261	9711	35.60	35.89	98	0.12
B9	40.006	-105.330	264.179	0.40	0.201	18150	36.05	36.28	97	0.04
B10	40.014	-105.325	269.359	0.45	0.272	19676	35.44	35.36	141	0.17
B12	40.012	-105.304	336.699	0.50	0.319	22266	35.20	35.69	253	0.26
B15	40.013	-105.295	336.699	0.40	0.158	23322	36.92	35.27	209	0.28

B17	40.014	-105.284	341.879	0.46	0.276	24286	35.22	35.33	170	0.25
B19	40.014	-105.280	352.239	0.49	0.256	24678	36.00	35.75	279	0.28
B24	40.010	-105.265	352.239	0.12	0.137	26073	33.31	35.18	309	0.62
B27	40.011	-105.254	352.239	0.14	0.140	27097	35.88	35.35	140	0.26
B28.5	40.015	-105.242	360.009	0.14	0.130	28272	35.87	35.98	195	0.16
B33	40.038	-105.212	745.917	0.24	0.115	32777	35.27	35.79	183	0.26
B34	40.052	-105.178	790.000	0.54	NA	36721	34.89	35.97	169	0.1
S1	39.938	-105.348	241.905	2.48	0.471	1515	35.78	35.42	98	0.16
S4	39.932	-105.281	48.174	0.18	0.324	12319	35.97	35.83	167	0.02
S6	39.935	-105.271	50.764	0.25	0.170	13354	35.67	35.81	139	0.06
S9	39.953	-105.241	68.894	0.29	0.437	17352	35.12	35.73	155	0.04
S11	39.959	-105.233	76.664	0.29	0.238	18454	35.28	35.42	139	0.08

S13	39.985	-105.221	87.024	0.30	0.158	21952	36.11	35.56	168	0.12
S14	40.014	-105.216	87.024	0.06	0.048	23848	30.75	36.66	107	0.14
S15	40.014	-105.215	105.154	0.08	0.159	25630	35.60	34.09	171	0.16

S4.1 Microplastic extraction

Sediment samples were oven dried at 50 °C until constant weight was achieved, before being homogenized. Sediment-Microplastic Isolation (SMI) units and $ZnCl_2$ (density = 1.5 g cm^{-3}) was used for density separation (Coppock et al., 2017; Nel et al., 2019), with approximately 35 g (Table S4.1) of sediment transferred to the SMI unit with 750 mL of $ZnCl_2$ and stirred at low speed using a magnetic stirrer before being left to settle overnight. The supernatant was then collected by decanting the SMI units over a 63 µm sieve, after which the upper part of the unit was removed and rinsed through the sieve (Nel et al., 2019). The contents of the sieve were rinsed into 250-mL glass beakers, using 30% H_2O_2, before Fe^{2+} (aq) (0.05 M) was added as a catalyst (ratio of 1:10) to facilitate organic matter oxidation (Margenat et al., 2021; Masura, et al. 2015). Samples were covered with loose aluminium foil lids enabling any heat/gas to escape but preventing airborne contamination and then left for at least 24 h at ambient room temperature.

After digestion had ceased, samples were decanted through a 63 µm sieve and backwashed into beakers with DI-water before staining with Nile Red (5µg mL^{-1}). Staining occurred over a one-

hour period, throughout which beakers were gently shaken repeatedly. Samples were then filtered onto glass-fibre GF/D filters (Whatman, 47 mm diameter, 2.7 µm pore size) using a glass vacuum-filtration system and a vacuum pump. The funnel of the filtration system was rinsed with DI-water to ensure no particles had adhered to the sides. Yellow goggles and UV-light were used to inspect sample beakers and the filtration system to ensure all visible particles had been collected. GF/D filters were then transferred into pre-labelled clean polypropylene (PP) Petri dishes and dried for 24 h at 50 °C (Nel et al., 2021). Surface water samples were also extracted following the above procedure but without using density separation with $ZnCl_2$.

S4.2 Fluorescence microscopy

GF/D Filters were observed with a macro zoom microscope (Olympus MVX-ZB10) equipped with a 1 x 0.25 N objective (MVPLAPO 1X, Olympus), U-M49002XL green fluorescent protein (GFP) filter cube (excitation filter: 470/40 nm, dichroic mirror: 495 nm high pass, emission filter: 525/50 nm) and a 100 W mercury apo lamp light source. Samples were observed under 12% light intensity on 32x magnification with 50 ms exposure time (see Kukkola et al., 2023 for details of how this was optimized and how to perform similar optimization for other microscopes). Measurements of fluorescence intensity and photographs were taken with a DP74 colour camera using CellSens Software (Olympus). A set threshold of 100 fluorescence a.u. (arbitrary units) was used to identify putative MP. This threshold was chosen by a validation experiment (For details see below). Each putative MP was also observed under bright field (Ring light, with 45 LED bulbs), with a magnification of 63x and had to meet pre-set selection criteria to be identified as MP (see decision key in Kukkola et al., 2023 for details). Further, as one of the main limitations of Nile Red is that it does not stain (polar) polymers such as Polyamide (PA) and polyethylene terephthalate (PET)

very well, each filter was scanned under bright field mode and all non-fluorescent fibres that met the pre-determined identification criteria were also included in the count. The parameters captured at this step contained: longest ferret diameter, area, colour, and morphology. These physical parameters are important to record, as evidence exists that visual predators (specifically) are prone to take up certain morphologies and colours and laboratory experiments have shown that different sizes and morphologies may have different ecotoxicological impacts on biota (Kukkola et al., 2021). Recording these parameters can aid in the planning of environmentally ore realistic ecotoxicity exposures in laboratory studies and are important to be included in the results. To aid MP identification and to ensure consistency, a morphology specific MP identification key was produced. This key was constructed by combination of reviewing existing literature and by the researcher's own expertise, and is described in Kukkola et al., 2023.

S4.3 Raman spectroscopy acquisition settings

44% of particles identified as MP in fluorescent counting step were selected for further chemical verification. The particles and fibres were transferred with fine-tip stainless steel tweezers into glass vials with DI-water, before filtered onto Anodiscs (0.2 µm, Whatman) for Raman spectroscopy analysis.

A Renishaw InVia Qontor Raman microscope equipped with a 785 nm laser was used with the following configurations: 20x objective, slit width 65 µm, 1200 l/mm, spatial resolution < 1µm and a spectral resolution <1 cm^{-1}, laser intensity 10% of the system (approximately 15 mW), 10 accumulations of 1s exposures were repeated 3 times per particle. Cosmic ray removal and baseline subtraction (polynomial fitting) was applied directly from WiRE 5.2. No data smoothing or transformation was carried out. For spectral matching, the fingerprint region of 650-1700 cm^{-1} was

used. The pre-processed spectra were exported into Spectragryph v1.2.15 for spectral matching using the Pearson correlation coefficient for the fingerprint region to reference libraries. The spectral library consisted of the SLOPP, SLOPP-E (Munno et al., 2020) and in-house built reference libraries. Hit Quality Index of 65% was applied to positively identify MP.

S4.4 QA/QC

Field background samples (n = 4, one per sampling day) were collected using empty glass jars that were opened during sampling and closed between sampling points. These samples helped to account for any atmospheric deposition. Samples were transported to the University of Birmingham for further analysis, where they were stored in a cold, dark room (+6 °C) before processing. Sequential replicates (a second surface water sample collected immediately after the first) were also obtained at two locations to assess sampling variability. Relative percentage differences in MP concentrations for the two replicates are 24% (Site B17) and 35% (Site B10).

Laboratory working surfaces were cleaned prior to and after sample handling with 70% ethanol. Extraction equipment was frequently cleaned with detergent and rinsed with DI-water before and between usage. Glassware was used where feasible, and beakers were placed in a DI-water sonification bath for 20 min for further cleaning. Personnel wore 100% cotton laboratory coats and reduced synthetic clothing where possible. Nitril gloves were worn when handling samples. During procedures aluminium foil was used to cover the processes and all equipment to reduce any airborne contamination in the lab. All solutions used were pre-filtered onto GF/D (0.47 μm) glass-fibre filters and procedural blanks were run parallel to extraction batches for both

sediment (n=13) and water (n=8) using either $ZnCl_2$ or DI-water and analysed following the same criteria as for the samples.

For testing the extraction efficiency of the method used here, a single-blinded spiking experiment was set up. Kids play sand that had been muffled at 500 ℃ for 6 hours was pre examined with TGA-FTIR-GCMS to confirm that no MP contamination was present. Then a researcher added a known number of mixtures of five different polymers (PE, PLA, PP, PS, PVC) between sizes 100 to 2000 µm into four cups containing 35 g of sand. These polymers were specifically chosen to represent the full spectrum from very low pixel brightness (PB) to high PB. Counts were done by a different researcher, with no prior knowledge regarding the types or numbers of polymers used for spiking. The sand samples were extracted as described in sections S1 above and Raw results are presented in the Table S4.2. The researcher counting the filters noted down that there seemed to be fluorescent particles in sample ID 2 that has rolled under the filter but did not include these in the final count.

Table S4.2. Results for positive blank spiking experiment

ID	Spiked	Count	Recovery %
1	12	15	125
2	27	21	77.7
3	10	10	100
4	6	6	100

Laboratory contamination was found in two of the thirteen sediment procedural blanks (one fragment each) and none in any of the water procedural blanks. No synthetic fibres were recorded in any of the procedural blanks. From the field background samples, only the one collected on 15th of October contained one pink fragment and one brown fibre. Given that this exposure was cumulative across seven separate sites, the background atmospheric deposition during the sampling event was deemed negligible. Recovery rates from the spiking experiments ranged between 77.7 and 125% with a mean of 100.06%. This suggests that the method used here is robust for MP isolation and detection and no data transformation had to be made.

S4.5 Reclassification of land cover categories

Land cover categories were obtained utilizing the USGS National Land Cover Database (NLCD) 2019 dataset, which contains official land cover data for the USA (2019) with a resolution of 30 x 30 m. The original 20 land cover classes from the USGS data set were reclassified into 9 general categories (e.g., all developed land covers were classified to "Urban" and all sub-groups of forests were grouped) (Table S4.3). Open water/wetlands were later excluded from the analysis, due to this being a methodological artefact of how NLCD 2019 classified wetlands, leading to 9 categories.

Table S4.3. The land classification according to NLCD 2019 and the new classification

NLCD Number	*NLCD 2019 category*	*new numbers*	*Combined NLCD numbers*	*new land cover category for this study*
0	Unclassified			

11	open water	1	**11,90,95**	Water/wetland (Excluded)
12	perennial ice snow	2	**12**	perennial ice snow
21	developed, open space	3	**21,22,23,24**	Urban
22	developed, low intensity	4	**31**	Barren land
23	developed, medium intensity	5	**41,42,43**	Forest
24	developed, high intensity	6	**51,52,73,74**	shrub/scrub
31	barren land (rock/sand)	7	**71,72**	grassland
41	Deciduous forest	8	**81**	pastry-hay
42	evergreen forest	9	**82**	cultivated crops
43	mixed forest			
51	dwarf scrub			
52	shrub/scrub			
71	grassland/herbaceous			
72	sedge/herbaceous			
73	lichens			
74	moss			
81	pasture/hay			
82	cultivated crops			

90	woody wetland
95	emergent herbaceous wetlands

S4.6. Chemical properties of MP

Based on the analysed 206 particles, the most common polymer type system-wide in surface water was polyester (PEST) (50%) followed by polypropylene (PP) (19%), polyethylene terephthalate (PET) (12%) and polyethylene (PE) (7%) (Figure S4.1). The most dominant polymer in sediments was PET (36%) followed by PP (21%), polyvinyl chloride (PVC) (15%), PEST (11%), and polyamide (PA) (9%). 10 spectra were missing, due to fibres transferred to the anodisc forming a fibre ball from which spectra were as difficult to obtain, and 34 spectra were unidentified/burned.

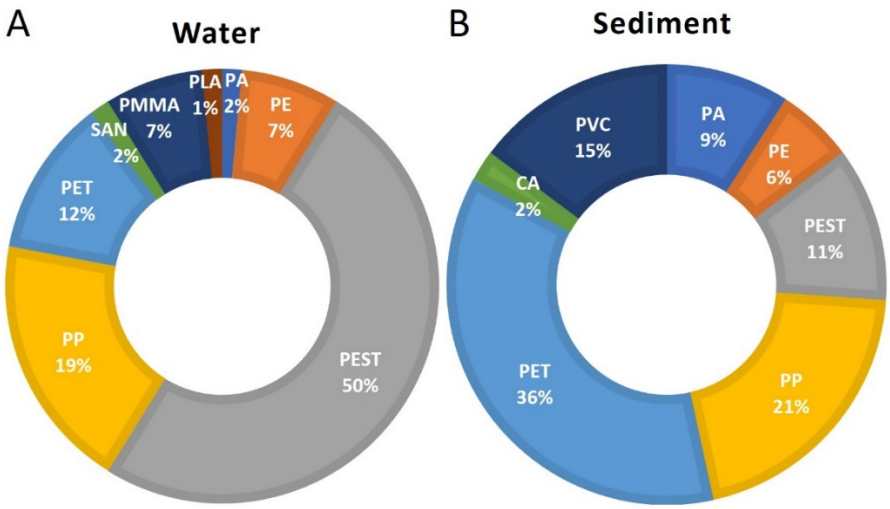


Figure S4.1: The chemical composition of MP in A) water and B) sediments. Abbreviations for polymers: PEST-polyester, PP-polypropylene, PET-polyethylene terephthalate, SAN-styrene acrylonitrile, PMMA-poly(methyl methacrylate), PLA-polylactic acid, PA-polyamide, PE-polyethylene, CA-cellulose acetate, PVC-polyvinyl chloride.

Light density polymers and fibres were more common in surface water, whereas high-density polymer fragments were mostly found in sediment. The most abundant plastic type in surface water was PEST and PET fibres, followed by PP and PE particles, which are some of the most common light plastic types in use (PlasticsEurope, 2020). PEST is the most frequently reported fibre type and is considered to originate from synthetic fabrics (Alam et al., 2019; Cordova et al., 2022; Zaki et al., 2021). Their deposition in the river is likely through either atmospheric input, which has been previously reported for this area and the adjacent Upper Colorado River Basin (Reynolds et al., 2022; Wetherbee et al., 2019), or from recreational activities, where clothes can shed fibres directly to the environment.

This could potentially imply that the fate of MP is not only related to their density, but also to their morphology. For example, fibres may stay suspended longer because of surface tension and their elongated morphology (Nguyen et al., 2022). For denser plastics, such as polyvinyl chloride (PVC) which was only recovered from sediments as fragments, it is plausible that the lower surface-to-volume ratio causes them to settle more quickly. This may have implications for exposure and risk scenarios, especially as PVC and its additives are considered to pose a relatively high risk for biota compared to other lighter polymers (Meng et al., 2021; Xu et al., 2018).

The fraction of fibres in the present study was lower than previously reported from freshwater systems, both in surface water and sediment (as reviewed by: Li et al., 2020; Yang et al., 2021), where up to 90% of MP were reportedly fibres. Different ratios between fibres and fragments may be due to the variation in methodologies applied, as it has been shown that fibres are more readily identified under bright light observation (Lenz et al., 2015), which was used in most previously

reported studies. Nile Red, used here, has been found to identify small MP with a strong reliability (Kukkola et al., 2023; Nel et al., 2021; Yaranal et al., 2021), which could lead different ratios between fibres and fragments. The low incidence of fibres could also reflect the low anthropogenic presence in the mountainous portion of the catchments, where population densities are relatively low (Barber et al., 2006). Fibres were more prevalent in surface water than in sediments, which is consistent with other studies (Lin et al., 2018; Scherer et al., 2020). This is likely due to lower settling rates for elongated fibres (Nguyen et al., 2022), as well as their fragmentation once settled into sediments, which was supported by the presence of PEST fragments in the sediments.

Table S4.4. Spearman correlation coefficients and p values for microplastic particle size (maximum Feret length) and hydrological forcings. BC – Boulder Creek, SBC – South Boulder Creek.

Hydrological forcing mechanism	***BC Rs & p-value (n=71)***	***SBC Rs & p-value (n=20)***	***BC and SBC Rs & p-value (n=91)***
flow velocity ($m\ s^{-1}$)/ water	Rs -.088, p=0.475	Rs .118, p=0.630	Rs=-.063, p=0.565
river slope (m/m) /water	Rs -.065, p=0.585	Rs .681, p<0.05	Rs-.012, p=0.908
discharge ($m^3\ s^{-1}$) /water	Rs -.105, p=0.383	Rs .561, p<0.05	Rs=.059, p=0.577
flow velocity ($m\ s^{-1}$) /sediment	Rs -.153, p=0.077	Rs -.108, p=0.359	Rs-.173, p=0.012

river slope (m/m) /sediment	Rs -.105, p=0.208	Rs -.142, p=0.226	Rs -.032, p= 0.638
discharge (m^3 s^{-1}) /sediment	Rs -.089, p=0.285	Rs -.120, p=0.306	Rs-.059, p=0.377

Table S4.5. Spearman correlation coefficients and p values for microplastic counts in water and sediments with hydrological factors. BC – Boulder Creek, SBC – South Boulder Creek.

Hydrological forcing mechanism	***BC Rs & p-value***	***SBC Rs & p-value***	***BC and SBC Rs & p-value***
flow velocity (m s^{-1})/ water	Rs=-.088, p =0.762	Rs= -.280, p=0.509	Rs=-.314, p= 0.176
river slope (m/m) /water	Rs= -.288, p=0.339	Rs=.514, p=0.191	Rs=-.074, p= 0.748
discharge (m^3 s^{-1}) /water	Rs= -.066, p= 0.829	Rs=.023, p= 0.955	Rs= -.314, p= 0.176
flow velocity (m s^{-1}) /sediment	Rs= .045, p=0.834	Rs=.145, p=0.577	Rs=-.108, p= 0.498
river slope (m/m) /sediment	Rs= -.098, p=0.747	Rs= -.285, p=0.492	Rs=-.312, p<0.05

discharge (m^3 s^{-1}) /sediment	Rs=.186, p=0.362	Rs=-.066, p=0.799	Rs= 0.096, p= 0.537

References

ALAM, F. C., SEMBIRING, E., MUNTALIF, B. S. & SUENDO, V. 2019. Microplastic distribution in surface water and sediment river around slum and industrial area (case study: Ciwalengke River, Majalaya district, Indonesia). *Chemosphere,* 224**,** 637-645.

BARBER, L. B., MURPHY, S. F., VERPLANCK, P. L., SANDSTROM, M. W., TAYLOR, H. E. & FURLONG, E. T. 2006. Chemical Loading into Surface Water along a Hydrological, Biogeochemical, and Land Use Gradient: A Holistic Watershed Approach. *Environmental Science & Technology,* 40**,** 475-486.

COPPOCK, R. L., COLE, M., LINDEQUE, P. K., QUEIRÓS, A. M. & GALLOWAY, T. S. 2017. A small-scale, portable method for extracting microplastics from marine sediments. *Environmental Pollution,* 230**,** 829-837.

CORDOVA, M. R., NURHATI, I. S., SHIOMOTO, A., HATANAKA, K., SAVILLE, R. & RIANI, E. 2022. Spatiotemporal macro debris and microplastic variations linked to domestic waste and textile industry in the supercritical Citarum River, Indonesia. *Marine Pollution Bulletin,* 175**,** 113338.

KUKKOLA, A., KRAUSE, S., YONAN, Y., KELLEHER, L., SCHNEIDEWIND, U., SMITH, G. H. S., NEL, H. & LYNCH, I. 2023. Easy and accessible way to calibrate a fluorescence microscope and to create a microplastic identification key. *MethodsX,* 10**,** 102053

LENZ, R., ENDERS, K., STEDMON, C. A., MACKENZIE, D. M. A. & NIELSEN, T. G. 2015. A critical assessment of visual identification of marine microplastic using Raman spectroscopy for analysis improvement. *Marine Pollution Bulletin,* 100**,** 82-91.

LI, C., BUSQUETS, R. & CAMPOS, L. C. 2020. Assessment of microplastics in freshwater systems: A review. *Science of The Total Environment,* 707**,** 135578.

LIN, L., ZUO, L.-Z., PENG, J.-P., CAI, L.-Q., FOK, L., YAN, Y., LI, H.-X. & XU, X.-R. 2018. Occurrence and distribution of microplastics in an urban river: A case study in the Pearl River along Guangzhou City, China. *Science of The Total Environment,* 644**,** 375-381.

MASURA, J., et al. 2015. Laboratory methods for the analysis of microplastics in the marine environment: recommendations for quantifying synthetic particles in waters and sediments. NOAA Technical Memorandum NOS-OR&R-48

MENG, J., XU, B., LIU, F., LI, W., SY, N., ZHOU, X. & YAN, B. 2021. Effects of chemical and natural ageing on the release of potentially toxic metal additives in commercial PVC microplastics. *Chemosphere,* 283**,** 131274.

MUNNO, K., DE FROND, H., O'DONNELL, B. & ROCHMAN, C. M. 2020. Increasing the Accessibility for Characterizing Microplastics: Introducing New Application-Based and Spectral Libraries of Plastic Particles (SLoPP and SLoPP-E). *Analytical Chemistry,* 92**,** 2443-2451.

NEL, H., KRAUSE, S., SAMBROOK SMITH, G. H. & LYNCH, I. 2019. Simple yet effective modifications to the operation of the Sediment Isolation Microplastic unit to avoid polyvinyl chloride (PVC) contamination. *MethodsX,* 6**,** 2656-2661.

NEL, H. A., CHETWYND, A. J., KELLEHER, L., LYNCH, I., MANSFIELD, I., MARGENAT, H., ONOJA, S., GOLDBERG OPPENHEIMER, P., SAMBROOK SMITH, G. H. &

KRAUSE, S. 2021. Detection limits are central to improve reporting standards when using Nile red for microplastic quantification. *Chemosphere,* 263**,** 127953.

NGUYEN, T. H., KIEU-LE, T.-C., TANG, F. H. M. & MAGGI, F. 2022. Controlling factors of microplastic fibre settling through a water column. *Science of The Total Environment,* 838**,** 156011.

PLASTICSEUROPE 2020. Plastics the facts - 2020.

REYNOLDS, R. L., GOLDSTEIN, H. L., KOKALY, R. F. & DERRY, J. 2022. Microplastic particles in dust-on-snow, Upper Colorado River Basin, Colorado Rocky Mountains, 2013–16. *Open-File Report.* Reston, VA.

SCHERER, C., WEBER, A., STOCK, F., VURUSIC, S., EGERCI, H., KOCHLEUS, C., ARENDT, N., FOELDI, C., DIERKES, G., WAGNER, M., BRENNHOLT, N. & REIFFERSCHEID, G. 2020. Comparative assessment of microplastics in water and sediment of a large European river. *Science of The Total Environment,* 738**,** 139866.

WETHERBEE, G. A., BALDWIN, A. K. & RANVILLE, J. F. 2019. It is raining plastic. *Open-File Report.* Reston, VA.

XU, P., PENG, G., SU, L., GAO, Y., GAO, L. & LI, D. 2018. Microplastic risk assessment in surface waters: A case study in the Changjiang Estuary, China. *Marine Pollution Bulletin,* 133**,** 647-654.

YANG, L., ZHANG, Y., KANG, S., WANG, Z. & WU, C. 2021. Microplastics in freshwater sediment: A review on methods, occurrence, and sources. *Science of The Total Environment,* 754**,** 141948.

YARANAL, N. A., SUBBIAH, S. & MOHANTY, K. 2021. Identification, extraction of microplastics from edible salts and its removal from contaminated seawater. *Environmental Technology & Innovation,* 21**,** 101253.

ZAKI, M. R. M., ZAID, S. H. M., ZAINUDDIN, A. H. & ARIS, A. Z. 2021. Microplastic pollution in tropical estuary gastropods: Abundance, distribution and potential sources of Klang River estuary, Malaysia. *Marine Pollution Bulletin,* 162**,** 111866.

APPENDIX 4

Table S5.3: Details on average microplastic (MP) concentration [MP L^{-1}] obtained from the triplicate samples, the stream discharge [m^3 s^{-1}] and MP loads [MP h^{-1}].

Sampling Date	***Sampling time***	***Stream discharge [m^3 s^{-1}]***	***Average MP con. [MP L]***	***Average MP con. [MP m^3]***	***MP load [MP h^{-1}]***
30/04/2021	10	0.31	0.14	140.0	156719
24/05/2021	10	0.30	0.22	220.0	237579
22/06/2021	10	0.32	0.20	200.0	229409
26/07/2021	9	0.16	0.55	546.7	305136
18/08/2021	9	0.15	0.23	233.3	124183
29/09/2021	10	0.36	0.23	226.7	294381
28/10/2021	9	0.17	0.32	320.0	194951
30/11/2021	10	0.27	0.19	186.7	178339
15/12/2021	11	0.29	0.14	140.0	147927
26/01/2022	11	0.21	0.22	220.0	162466
23/02/2022	11	0.36	0.29	293.3	384076
23/03/2022	10	0.38	0.21	206.7	283596
02/06/2021	10	0.38	0.21	78.4	282092
08/06/2021	10	0.39	0.21	80.9	291260
15/06/2021	10 *from sub-daily	0.30	0.31	313.3	337838
22/06/2021	10	0.32	0.20	63.7	229409
02/07/2021	10	0.32	0.40	127.4	458819
09/07/2021	10	0.32	0.47	148.5	534581
15/07/2021	10	0.30	0.63	187.7	675677
26/07/2021	9	0.16	0.55	84.8	305136
15/06/2021	9	0.14	0.23	233.3	120312
15/06/2021	10	0.30	0.31	313.3	337838
15/06/2021	11	0.18	0.17	166.7	108936
15/06/2021	12	0.21	0.23	233.3	174185
15/06/2021	13	0.30	0.22	220.0	238941
15/06/2021	14	0.34	0.22	220.0	270924
15/06/2021	15	0.14	0.22	220.0	107201
15/06/2021	16	0.21	0.11	113.3	85691
15/06/2021	17	0.29	0.22	220.0	231622
15/06/2021	18	0.21	0.33	326.7	246993

15/06/2021	19	0.33	0.21	206.7	245086
15/06/2021	20	0.09	0.27	266.7	85922
16/06/2021	9	0.20	0.15	146.7	106182
16/06/2021	10	0.22	0.18	180.0	141604
16/06/2021	11	0.30	0.17	173.3	189925
16/06/2021	12	0.26	0.21	206.7	190083
16/06/2021	13	0.25	0.22	220.0	196441
16/06/2021	14	0.19	0.17	173.3	119060
16/06/2021	15	0.20	0.14	140.0	101806
16/06/2021	16	0.26	0.29	286.7	273200
16/06/2021	17	0.20	0.15	146.7	107907
16/06/2021	18	0.31	0.24	240.0	268647
16/06/2021	19	0.33	0.15	146.7	172830
16/06/2021	20	0.22	0.31	306.7	241250
19/06/2021	9	0.40	0.14	141.2	205067
19/06/2021	10	0.33	0.13	127.5	151182
19/06/2021	11	0.40	0.14	141.2	205067
19/06/2021	12	0.16	0.08	81.8	47283
19/06/2021	13	0.38	0.14	136.4	184433
19/06/2021	14	0.21	0.10	101.7	77535
19/06/2021	15	0.38	0.14	138.0	191258
19/06/2021	16	0.11	0.07	66.1	26438
19/06/2021	17	0.30	0.12	121.6	132017
19/06/2021	18	0.34	0.14	141.4	171757
19/06/2021	19	0.32	0.13	125.6	144723
19/06/2021	20	0.34	0.15	148.8	182938
20/06/2021	9	0.38	0.15	151.4	205789
20/06/2021	10	0.36	0.13	133.0	170951
20/06/2021	11	0.43	0.16	162.5	250130
20/06/2021	12	0.32	0.13	125.6	144723
20/06/2021	13	0.32	0.13	130.4	151323
20/06/2021	14	0.33	0.13	127.5	151182
20/06/2021	15	0.38	0.15	152.6	211342
20/06/2021	16	0.29	0.12	119.5	125777
20/06/2021	17	0.42	0.16	157.8	238319
20/06/2021	18	0.38	0.14	138.0	191258
20/06/2021	19	0.21	0.10	98.5	75071
20/06/2021	20	0.40	0.14	141.2	205067

S5.1: Fluorescence microscopy - microscope configuration

Each filter was observed under fluorescence mode with a Macro zoom microscope (Olympus MVX-ZB10) equipped with 1 x 0.25 N objective (MVPLAPO 1X, Olympus), U-M49002XL GFP filter cube (excitation filter: 470/40 nm, dichroic mirror: 495 nm high pass, emission filter: 525/50 nm) and 130 W U-HGLGPS mercury apo lamp light source. Samples were observed under 12% light intensity on 32x magnification with 50 ms exposure time.

S5.2: Raman configuration

For MP identification, a 5x objective was used, with slit width 65 µm, 1200l/mm, spatial resolution <1 µm and a spectral resolution < 1cm^{-1}, laser intensity 10% of the system (approximately 15 mW), 3 accumulations of 5s exposures per MP particle. Cosmic ray removal and baseline subtraction (adaptive polynomial fitting) and smoothing (Savitsky-Golay filter with interval 10 and polynomial order 3) was applied using Spectragryph v1.2.16.1.

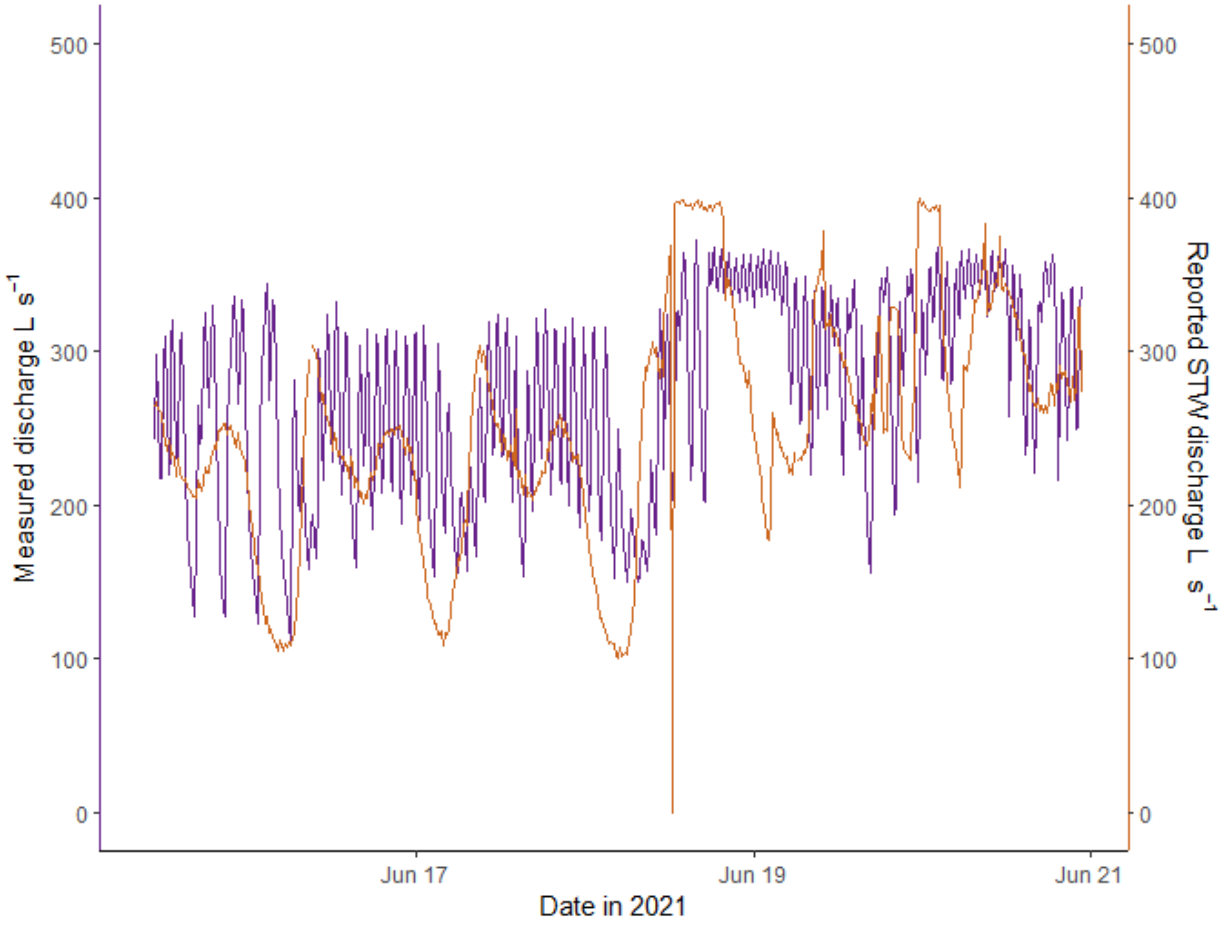


Figure S5.1:15-minute interval hydrograph comparing reported WWTP outflow and the level of stream discharge at the sampling location reported in L s^{-1} (data obtained as an EA request from Barston WWTP and provided as a spreadsheet by Mr Jack Morris). The stream discharge data is based on the Solinist level logger data inserted *in situ*.

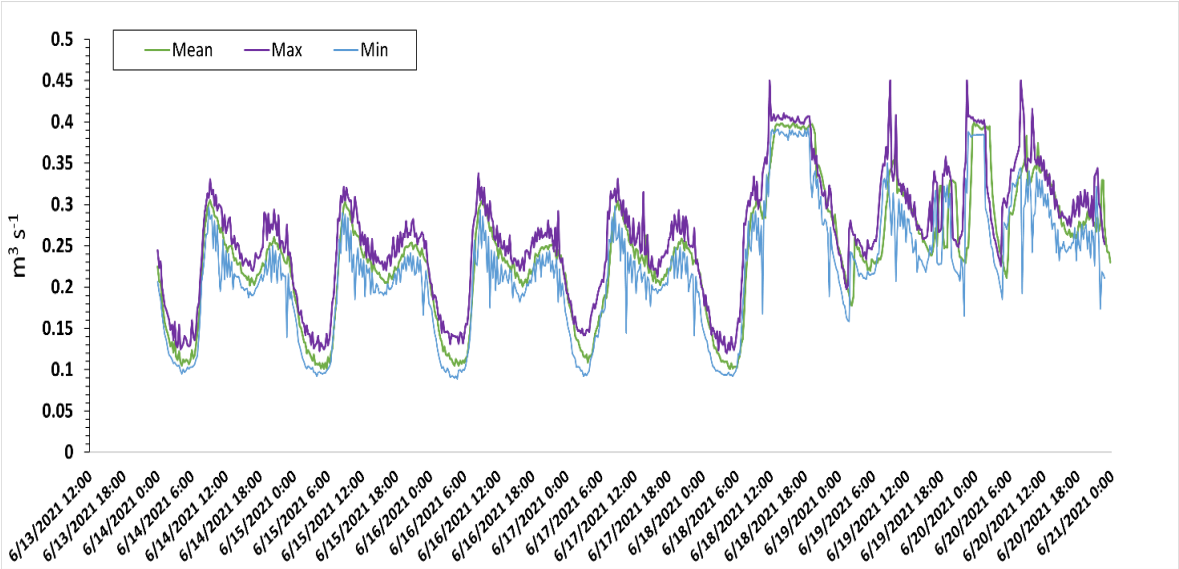


Figure S5.2. Outflow data for 15-minute intervals reported by Barston WWTP for the period of 14th June – 20th June 2021. Mean flow (green), maximum flow (purple) and minimum flow (blue) reported in 15 min intervals.

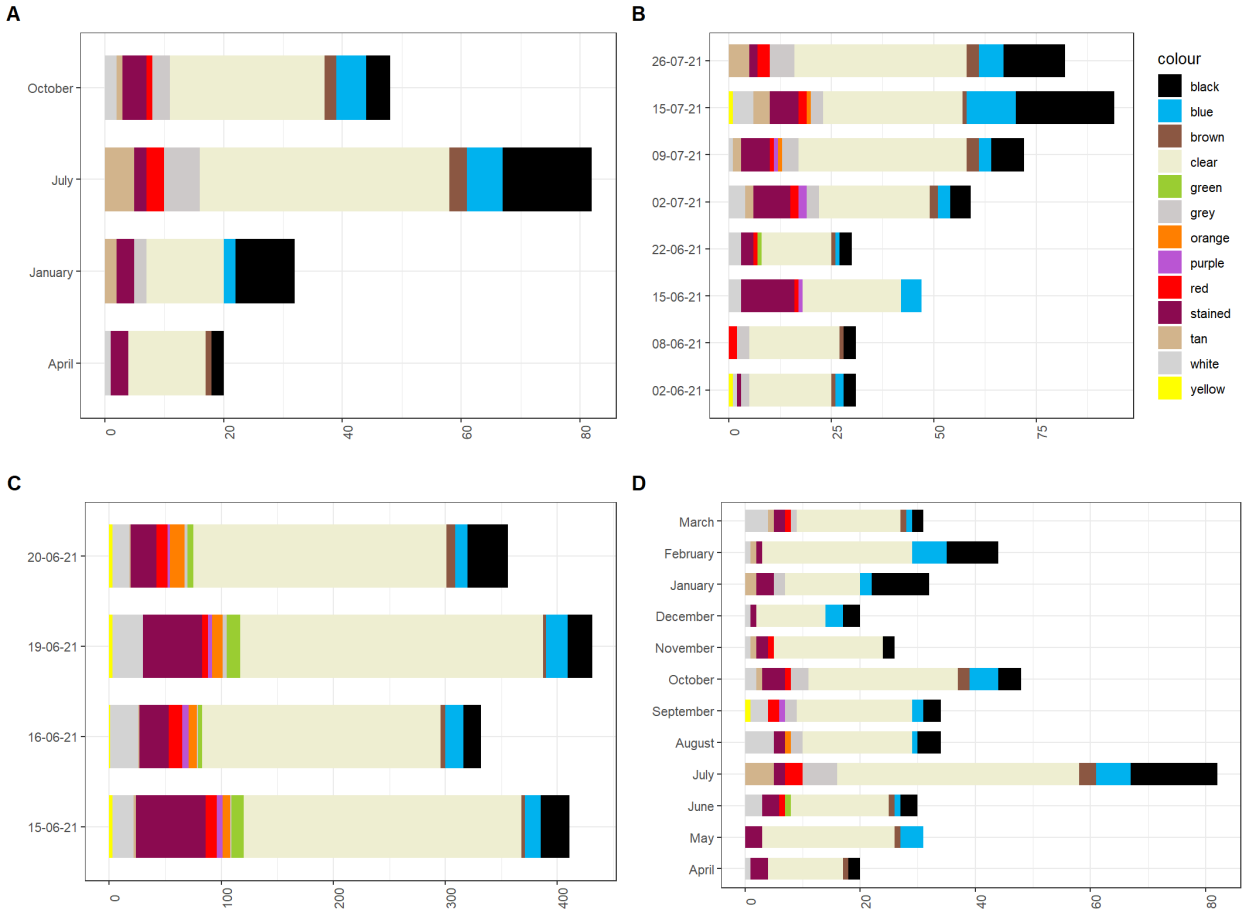


Figure S5.3: The respective colours of MP extracted from the samples for: A) 4-seasons, B) 8-weekly, C) Daily (12 x hourly samples per day over 4 days) and D) 12-monthly sampling.

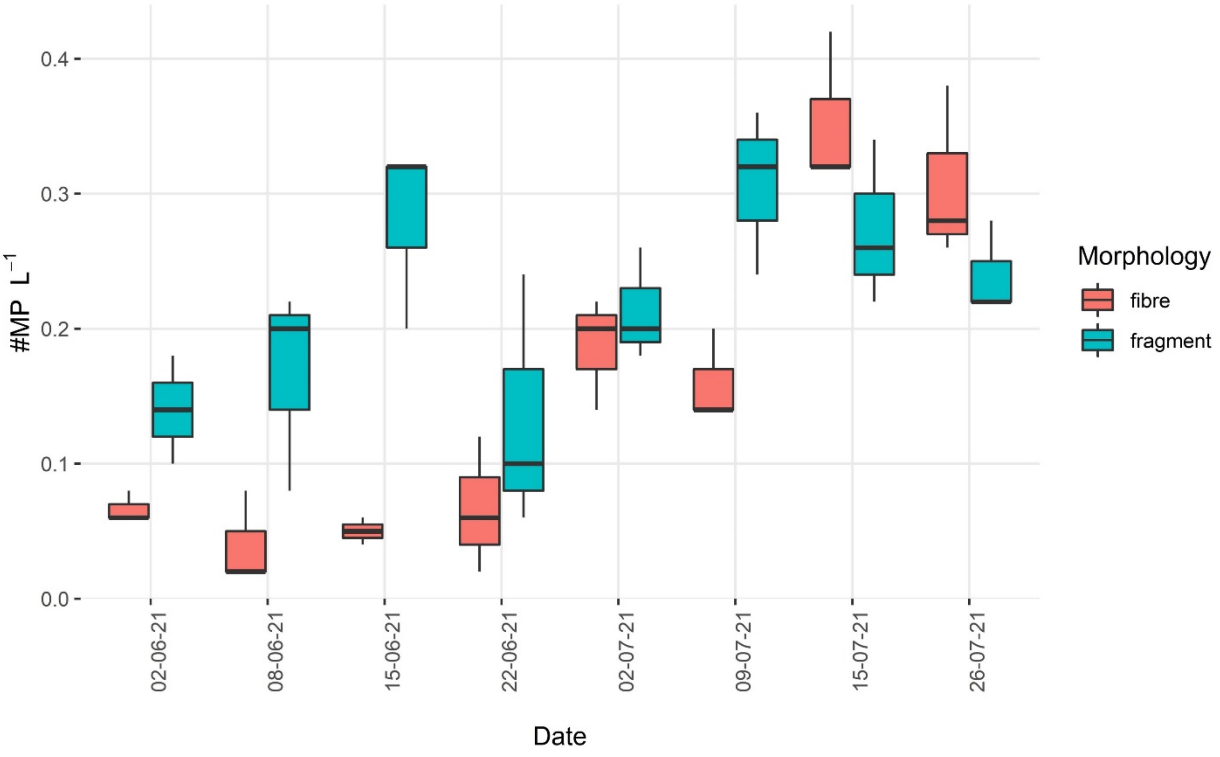


Figure S5.4: The relative fraction and abundance of fragments and fibres extracted from the water column samples for the 8-week sampling campaign.

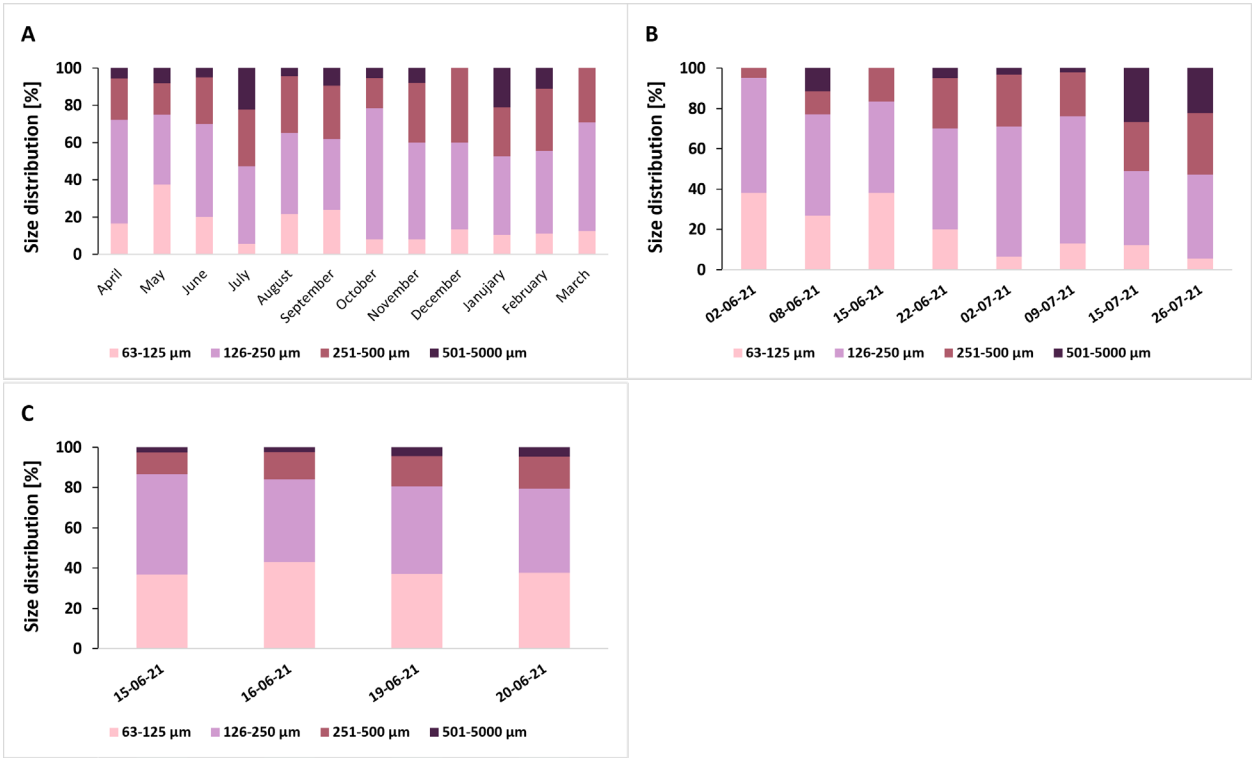


Figure S5.5: The size ranges of the MP fragments extracted from the samples for: A) 12-monthly sampling, B) 8-weekly sampling and C) for sub-daily as a summary. The size fraction buckets reflect standard sediment grain sizes between very find sand and coarse sand.

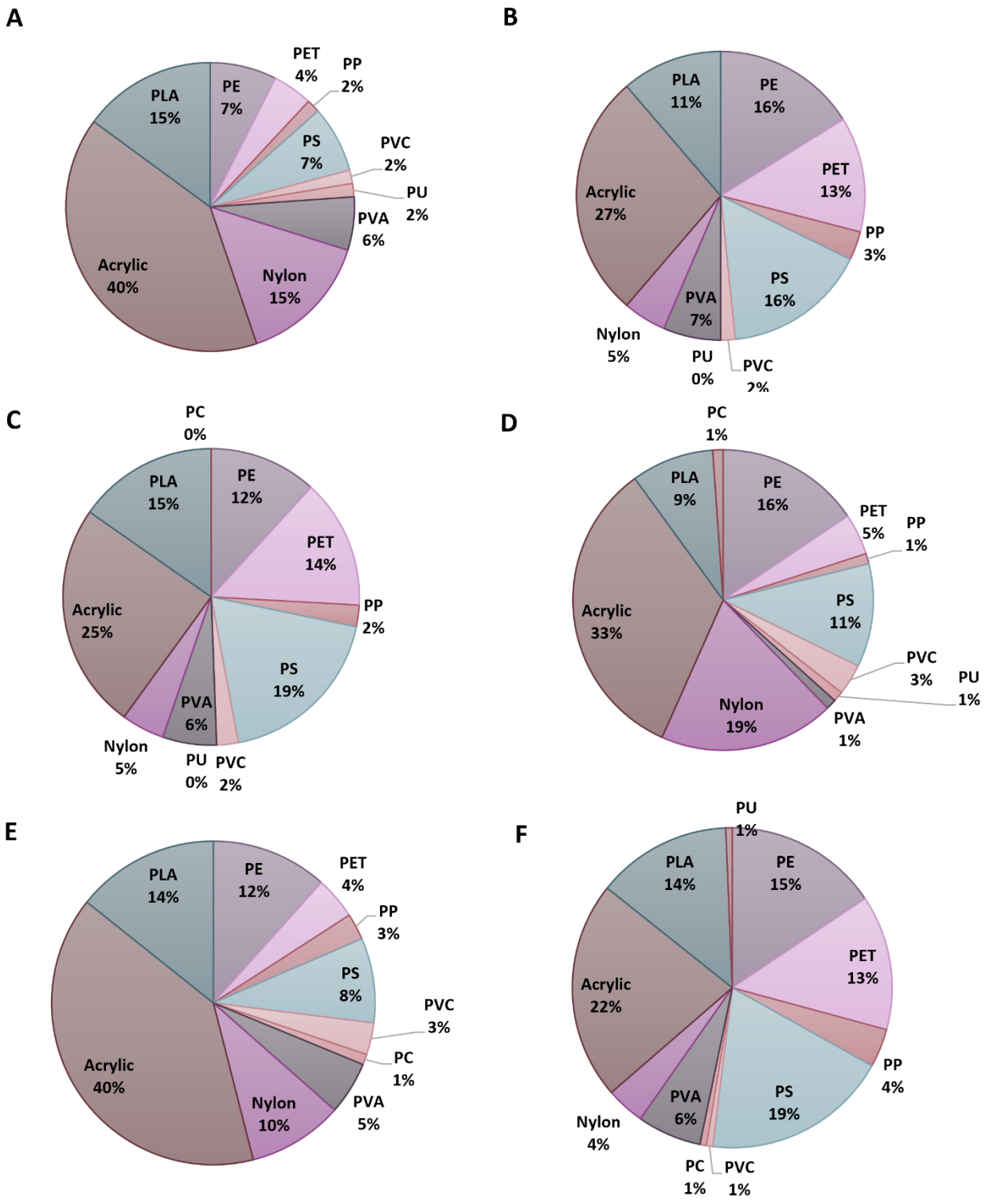

A
PLA 15%
PE 7%
PET 4%
PP 2%
PS 7%
PVC 2%
PU 2%
PVA 6%
Nylon 15%
Acrylic 40%
B
PLA 11%
PE 16%
PET 13%
PP 3%
PS 16%
PVA 7%
Nylon 5%
PU 0%
PVC 2%
Acrylic 27%
C
PC 0%
PLA 15%
PE 12%
PET 14%
PP 2%
PS 19%
PVA 6%
Nylon 5%
PU 0%
PVC 2%
Acrylic 25%
D
PC 1%
PLA 9%
PE 16%
PET 5%
PP 1%
PS 11%
PVC 3%
PU 1%
PVA 1%
Nylon 19%
Acrylic 33%
E
PLA 14%
PE 12%
PET 4%
PP 3%
PS 8%
PVC 3%
PC 1%
PVA 5%
Nylon 10%
Acrylic 40%
F
PU 1%
PLA 14%
PE 15%
PET 13%
PP 4%
PS 19%
PVA 6%
Nylon 4%
PC 1%
PVC 1%
Acrylic 22%

Figure S5.6: The detailed breakdown of polymer types extracted from the samples over the 12-months monthly sampling period: A) Fragments (n = 75), B) fibres (n = 64); over the 8-week weekly sampling campaign: C) Fragments (n = 80) and D) fibres (n = 90); and over the four sub-daily (12 x hourly samples) pooled together E) fragments (n = 186) and B) fibres (n = 154).

S5.3. Assessing coefficient of variation for sub-daily MP concentrations

To further assess and understand the variability of the collected hourly MP samples, and to assess how many hourly samples may be needed to characterize the in-stream MP concentration and achieve values close to the daily average (i.e., the mean of the 12 hourly samples per day), we determined all unique combinations of 3, 5, 8, and 10 samples for each of the four 12-hour sampling days. For each of these unique combinations we computed the mean value and then compared these values to the actual daily average (12 samples). To better represent the variation of these combinations of different mean values, we calculated the coefficient of variation (CV) for each of the combinations as follows: (Standard Deviation of CVs divided by the mean) *100%. Higher CV values suggest higher variability and dispersion of the population around the population mean. This allowed us to visualise the dispersion of the means for the unique combinations and their respective range.

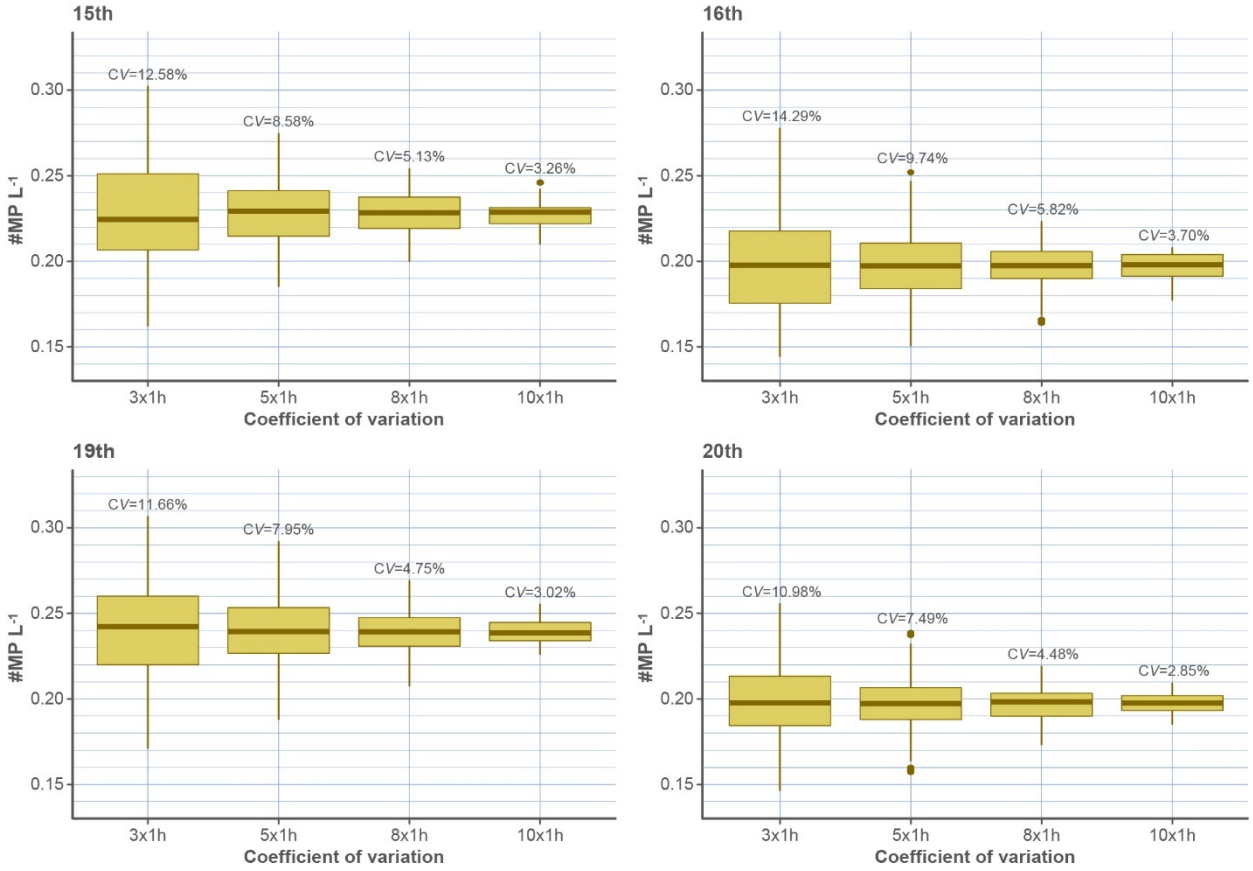


Figure S5.7: The coefficient variation of MP concentration means for all randomly chosen 3x1h, 5x1h and 10x1h combinations for each of the sub-daily sampling days. Larger CV values indicate a higher dispersion level around the mean.

APPENDIX 5

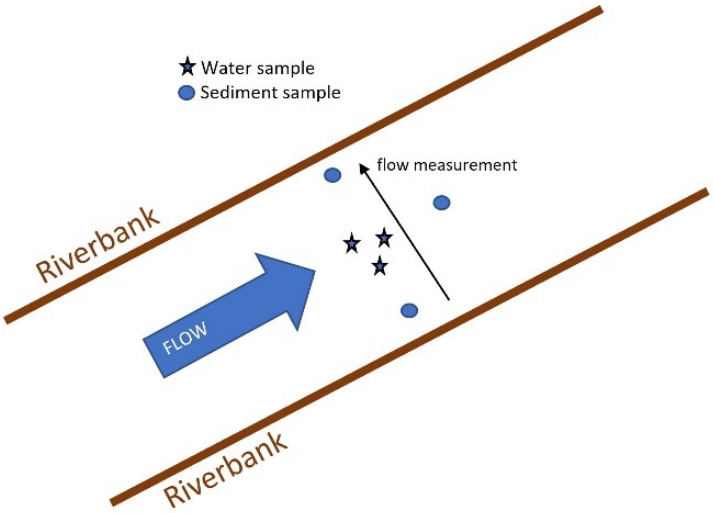


Figure S6.1: Schematic figure illustrating the spatial distribution of the sediment sample collection in relation to the river corridor, and flow velocity measurements.

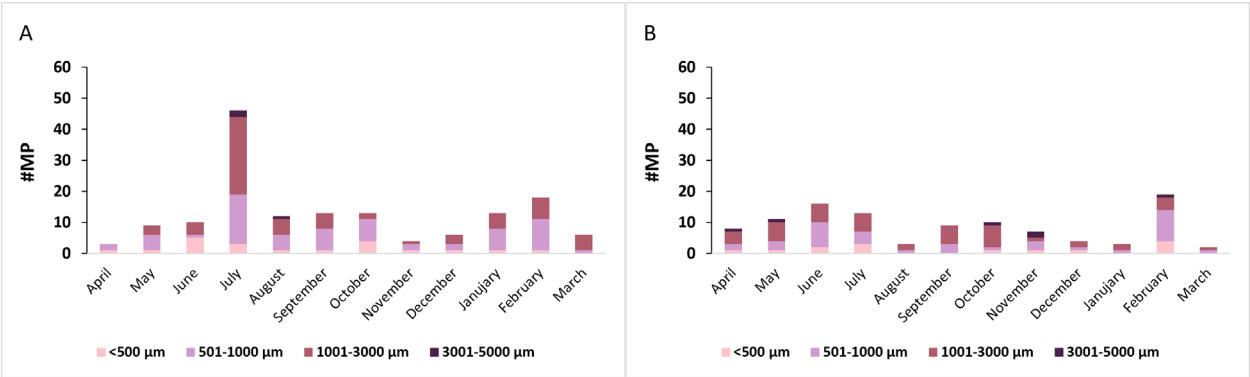


Figure S6.2: The distribution of MP fibre sizes in surface waters at A) Eastcote brook and B) Bourn Brook

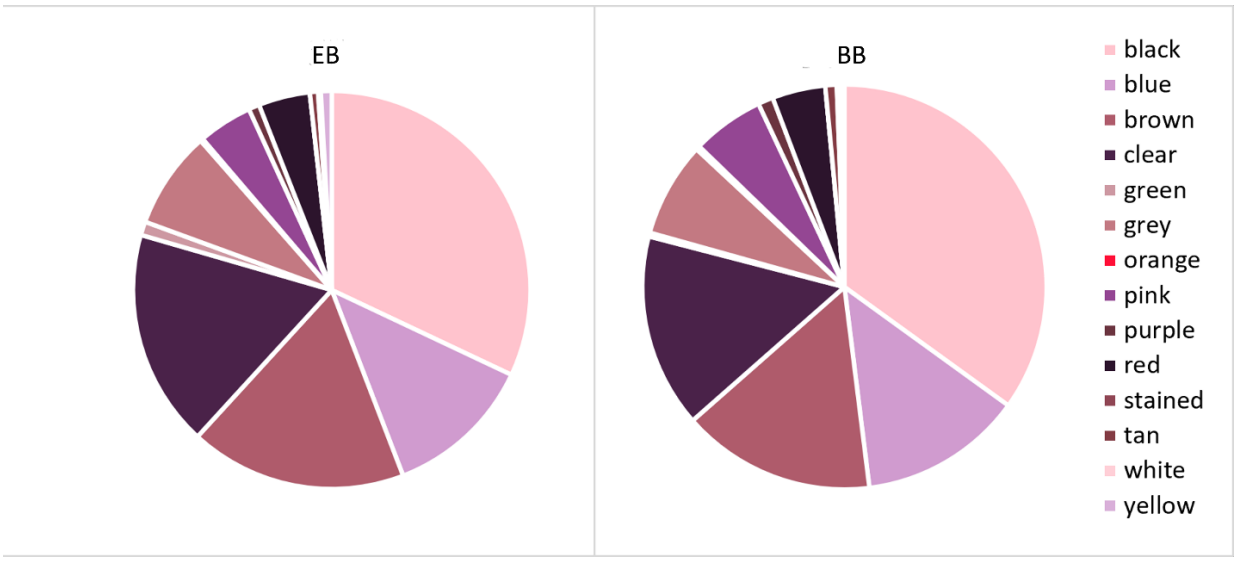


Figure S6.3: Distribution of the fibre colours in surface water from Eastcote Brook (EB) and Bourn Brook (BB)

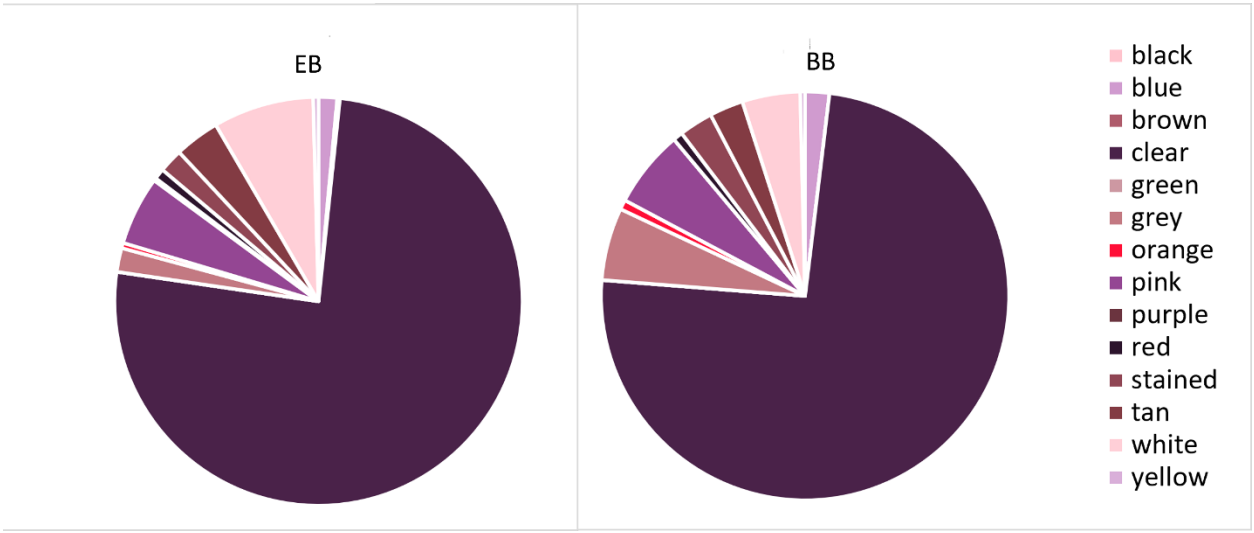


Figure S6.4: Distribution of The Fragment colour breakdown in surface water from Eastcote Brook (EB) and Bourn Brook (BB)

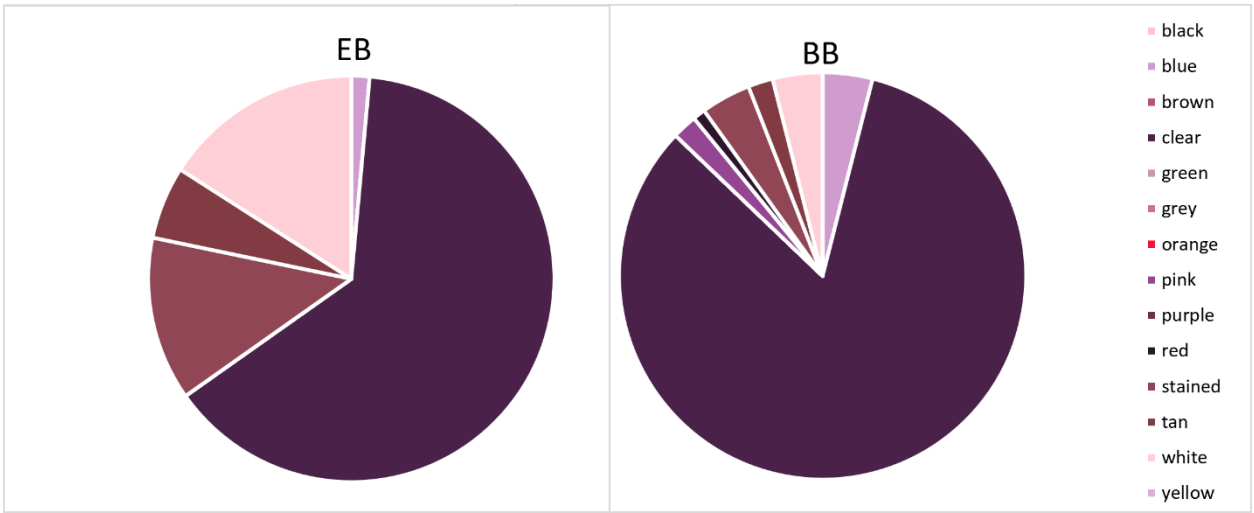


Figure S6.5: The distribution of fragment colours in sediments from Eastcote Brook (EB) and Bourn Brook (BB)

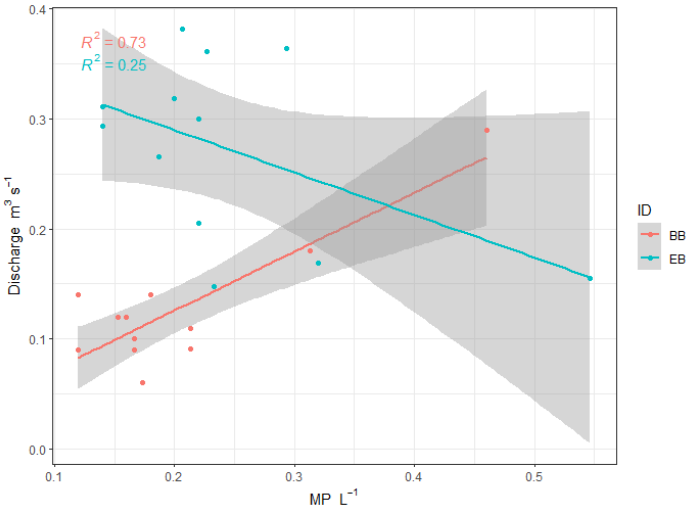


Figure S6.6: The stream discharge (m^3 s^{-1}) plotted against MP concentration in surface water (MP L^{-1}). Red indicates Bourn Brook (BB) and blue Eastcote Brook (EB).

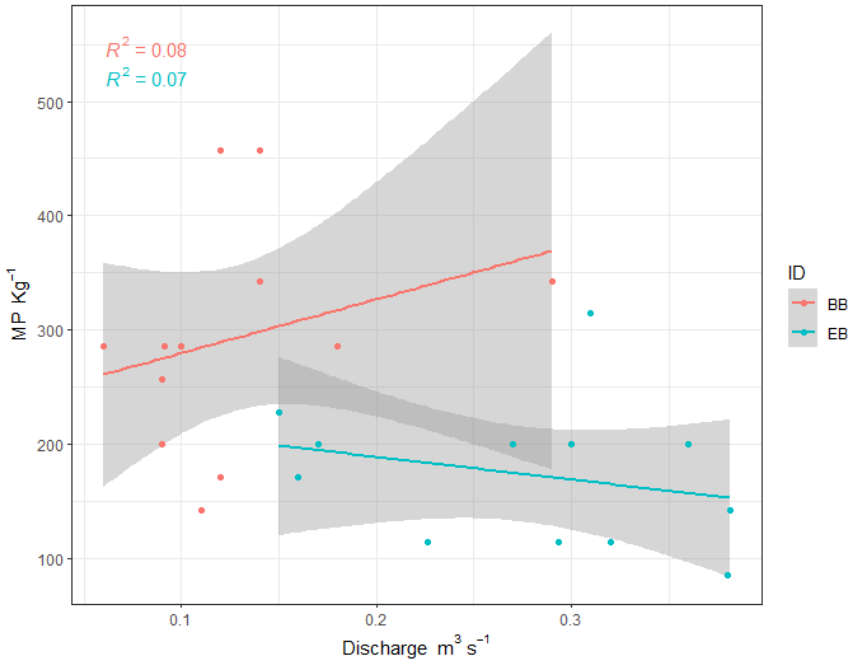


Figure S6.7: The stream discharge (m^3 s^{-1}) plotted against MP concentration in sediments (MP Kg^{-1}). Red indicates Bourn Brook (BB) and blue Eastcote Brook (EB).

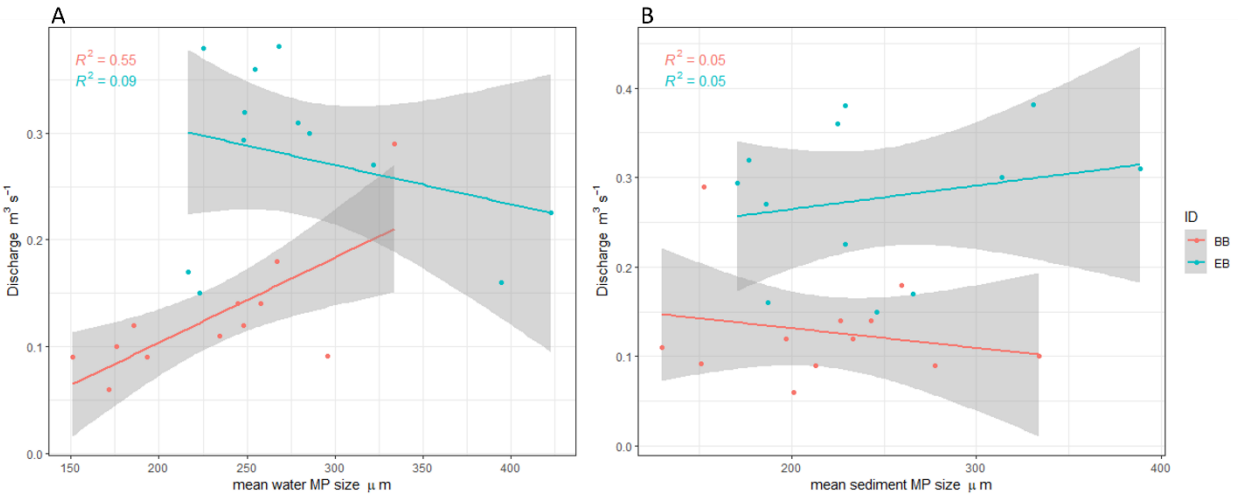


Figure S6.8: The average MP size plotted against discharge (m^3 s^{-1}) for A) in surface waters and B) in sediments. Red indicates Bourn Brook (BB) and blue Eastcote Brook (EB).

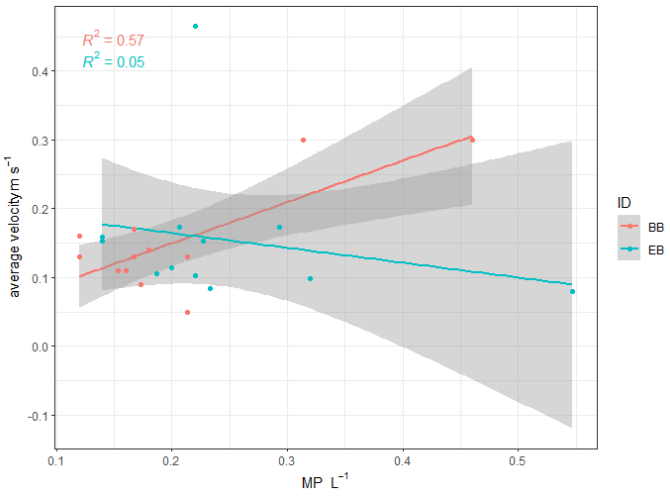


Figure S6.9: The average stream velocity (m s^{-1}) plotted against MP concentration in surface water (MP L^{-1}). Red indicates Bourn Brook (BB) and blue Eastcote Brook (EB).

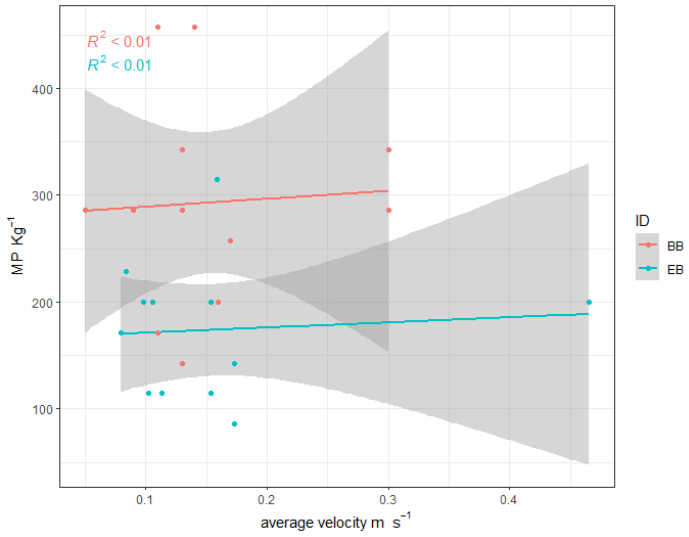


Figure S6.10: The average stream velocity (m s^{-1}) plotted against MP concentration in sediments (MP Kg^{-1}). Red indicates Bourn Brook (BB) and blue Eastcote Brook (EB).